DROUGHTS: OCCURRENCE, EVOLUTION AND IMPACTS OVER INDIA

Ph.D. Thesis

By
VIKAS POONIA

DEPARTMENT OF CIVIL ENGINEERING
INDIAN INSTITUTE OF TECHNOLOGY INDORE

NOVEMBER 2021

DROUGHTS: OCCURRENCE, EVOLUTION AND IMPACTS OVER INDIA

A THESIS

Submitted in partial fulfillment of the requirements for the award of the degree
of
DOCTOR OF PHILOSOPHY

by
VIKAS POONIA

DEPARTMENT OF CIVIL ENGINEERING

INDIAN INSTITUTE OF TECHNOLOGY INDORE

NOVEMBER 2021

INDIAN INSTITUTE OF TECHNOLOGY INDORE

I hereby certify that the work which is being presented in the thesis entitled **DROUGHTS: OCCURRENCE, EVOLUTION AND IMPACTS OVER INDIA** in the partial fulfillment of the requirements for the award of the degree of **DOCTOR OF PHILOSOPHY** and submitted in the **DEPARTMENT OF CIVIL ENGINEERING, Indian Institute of Technology Indore**, is an authentic record of my own work carried out during the time period from December, 2018 to November, 2021 under the supervision of Dr. Manish Kumar Goyal, Associate Professor, Department of Civil Engineering, Indian Institute of Technology Indore.

The matter presented in this thesis has not been submitted by me for the award of any other degree of this or any other institute.

VPoonia
08/11/2021

signature of the student with date
VIKAS POONIA

This is to certify that the above statement made by the candidate is correct to the best of my knowledge.

Manish

Signature of Thesis Supervisor with date
Dr. Manish Kumar Goyal

VIKAS POONIA has successfully given his Ph.D. Oral Examination held on **28 January 2022**

Manish

Signature of Thesis Supervisor with date
Dr. Manish Kumar Goyal 28 Jan 2022

ACKNOWLEDGEMENTS

First and foremost, I would like to place on record my sincere thanks and a deep sense of gratitude to my thesis supervisor Dr. Manish Kumar Goyal, Associate Professor, Department of Civil Engineering, Indian Institute of Technology Indore for his invaluable guidance and full hand cooperation throughout all aspects of this research work. He plays a magnificent role in transforming my research career. His energetic and enthusiastic nature always helped me to be on track in the research work. His vision and planning are admirable. I am thankful for his technical suggestions, valuable comments on basic concepts, and technical writing of papers.

I am grateful to Dr. Lalit Borana, Dr. Guru Prakash, and Dr. Pritee Sharma for their valuable inputs and progress evaluation during the completion of the research work. Their technical inputs and valuable ideas have greatly helped me in shaping this thesis.

I want to express my gratitude and acknowledgement to Prof. Neelesh Kumar Jain, Director, Indian Institute of Technology Indore for providing me the opportunity to explore my research capabilities at the Indian Institute of Technology Indore. Also, I take this opportunity to thank Dr. Sandeep Chaudhary and Dr. Neelima Satyam for their support and valuable time at the institute for administrative purposes.

I am thankful to my mother, Smt. Indrawati Devi, and Father Shri Gulab Singh Poonia for unconditional support. Without their faith in me, I would not have been able to carry out this study. My mother helped a lot to support me during my doctorate journey and motivated me in my good and bad times. I am thankful to my elder sisters Suman Poonia and Kavita Poonia and my younger brother Vikram Poonia for throughout motivation during my Ph.D. work. I want to thank my wife, Rachana to give unconditional support and love in this journey. She always keeps herself available to help and support me. My son, Vihaan Poonia, always gives me positive energy during my hard times. The time spent with him keeps me away from the work stress and keeps me afresh and receptive for infinite learning every new morning. This thesis was not possible without the help and support of my family members especially my mother and my son.

Special thanks to Dr. Jew Das and Dr. Srinidhi Jha for providing crucial inputs during my research work. I am thankful to my lab-mates Saket, Nikhil, Shivam Singh, Shivukumar, and Vijay Jain for their cooperation and support. I am grateful to the entire scientific staff of the Department of Civil Engineering who have always been helpful to me.

Finally, I am thankful to all who directly or indirectly contributed, helped and supported me.

Dedicated to
my family

ABSTRACT

Novel approaches to assess the occurrence, distribution, trend, concurrence, and evolution of major drought types are required to understand their implications on terrestrial ecosystems especially agricultural productivity. The complexity of the drought phenomenon, intricate ecosystem-drought interactions, and interdependence of the drought characteristics make the drought assessment a challenging task. In addition to traditional droughts, flash drought is a newly discovered extreme event that has rapid intensification without sufficient early warning. Such flash drought poses a great threat to terrestrial ecosystems. The ecosystem resistance and vegetation adaptation to flash droughts are significantly dependent upon the accurate estimation of flash drought events and their interaction with ecosystem metrics such as GPP, NPP, and LAI. Therefore, in context of climate change, a better understanding of the droughts in terms of their occurrence, trend, concurrence, evolution as well as joint dependence of drought characteristics is important to investigate the implications on terrestrial ecosystem. This thesis presents the study carried out to deliver a comprehensive assessment of drought conditions over India and their implications on the terrestrial ecosystem.

The initial part of the thesis is devoted to explain the drought from multi-perspectives such as severity, distribution, trends, concurrence, and evolution. The investigation is carried out using the most widely used drought indices (SPI, SRI, SSI, and VCI) to monitor different drought types over 24 major river basins of India. The results show that hydrological and soil moisture droughts were observed to be more influential as compared to the meteorological and vegetation droughts in most of the river basins of India. Further, approximately 82% of concurrent droughts include soil moisture drought. This suggests that the soil moisture is more influencing rather than precipitation in the study area.

The assessment of drought characteristics is approached from a joint dependence perspective in the second part. A copula based bivariate probabilistic analysis of drought characteristics across Indian river basins is carried out. It was observed that Southern Indian river basins have a higher exceedance probability and smaller joint return period compared to the Western river basins of India. This suggests that drought events in Western and Central India are more severe and longer whereas the ones in the south Indian river basins are more frequent but less severe.

In the third part, flash drought identification and its impact on the regional terrestrial ecosystem was investigated. To account for terrestrial ecosystem, gross primary productivity (GPP) from MODIS was used to quantify the response of ecosystem to flash droughts in India. It was found that GPP responds to more than 95% of the flash droughts across India, with the highest response frequency occurring over Ganga basin and southern India while the lowest response across northeastern India. The discrepancies in the response frequency are majorly attributed to different vegetation resilience conditions across different parts of the country.

The final part of the study is aimed to understand the impact of climate change on crop water requirement and productivity of major crops in Sikkim. The investigation is carried out using two crop models i.e., AquaCrop and CROPWAT in order to estimate crop yield and crop water requirement, respectively. From the investigation, an increase in the mean percentage change in the crop yield was observed over Sikkim during 2021 2099. This can be attributed to the suitable temperature profile, increase in the CO2 concentration, high elevation of the study area. The CWR and CIR investigation also suggests an increase in the CWR towards the end of the twenty-first century for rice and wheat over West and South Sikkim with respect to the baseline period.

LIST OF PUBLICATIONS

Journal papers published

- **Poonia, Vikas,** Goyal, M.K., Jha, S., Dubey, S (2022). "Terrestrial Ecosystem Response to Flash Droughts over India." ***Journal of Hydrology***, 605, 127402. ***(Impact Factor: 5.722)***
- **Poonia, Vikas,** Jha, S., Goyal, M.K., (2021). "Copula based analysis of meteorological, hydrological and agricultural drought characteristics across Indian river basins." ***International Journal of Climatology***, 1-16. ***(Impact Factor: 4.069)***
- **Poonia, Vikas,** Goyal, M.K., Gupta, B.B., Gupta, A.K., Jha, S., Das, J. (2021). "Drought occurrence in different river basins of India and blockchain technology-based framework for disaster management." ***Journal of Cleaner Production***, 127737. ***(Impact Factor: 9.297)***
- **Poonia, Vikas,** Das, J., Goyal, M.K., (2021). "Impact of climate change on crop water and irrigation requirements over eastern Himalayan region." ***Stochastic Environmental Research and Risk Assessment. (Impact Factor: 3.379)***
- Kumar, N., **Poonia, Vikas,** Gupta, B.B., Goyal, M.K., (2021). "A novel framework for risk assessment and resilience of critical infrastructure towards climate change." ***Technological Forecasting and Social Change***, 165, 120532. ***(Impact Factor: 8.593)***
- Das, J., **Poonia, Vikas**, Jha, S., Goyal, M. K. (2020). "Understanding the climate change impact on crop yield over Eastern Himalayan Region: ascertaining GCM and scenario uncertainty." ***Theoretical and Applied Climatology,*** 142, 467-482. ***(Impact Factor: 3.179)***

Book chapters published

- **Poonia, Vikas,** Goyal, M.K., Madramootoo, C.A., Gupta, A.K., Saraswat, C. (2020), "Impact of COVID-19 on agro-food industry and transitions towards food security", Chapter 12 in ***Integrated Risk of Pandemic: Covid19 Impacts, Resilience and Recommendations***, Publisher: Springer, Singapore. https://doi.org/10.1007/978-981-15-7679-9_12

TABLE OF CONTENTS

LIST OF FIGURES

LIST OF TABLES

NOMENCLATURE

θ	Copula parameter
μ_{GPP}	Mean of GPP time series
σ_{GPP}	Standard deviation of GPP time series
Δ	Slope of vapour pressure curve
γ	Psychrometric constant
α	Shape parameter of the Gamma distribution
β	Scale parameter of the Gamma distribution
μ	Location parameter of the Gaussian distribution
σ	Scale parameter of the Gaussian distribution
$\bar{Y}_0$	Mean observed yield
$*$	Bias-corrected
B	Biomass
C	Copula function
C	Performance Index
CC	Canopy cover
CC^*	Adjusted green canopy cover
CC_0	Initial canopy cover

CC_X	Maximum canopy cover
C_F	Frank copula
C_G	Gumbel copula
CO_2	Carbon dioxide
con	Control period
C_P	Plackett copula
Do	Abnormally Dry
D1	Moderate Drought
D2	Severe Drought
D3	Extreme Drought
D4	Exceptional Drought
E	Soil evaporation
E(L)	Expected drought interarrival time
e_a	Actual vapor pressure
e_s	Saturation vapor pressure
ET_0	Reference evapotranspiration
ET_c	Crop evapotranspiration
F	Cumulative distribution function

$F_D(d)$	Marginal distribution of drought duration
f_{HI}	Adjustment factor
$F_S(s)$	Marginal distribution of drought severity
fut	Future
G	Ground heat flux
GPP_{SA}	Standardized anomalies of GPP
HI_0	Reference Harvest Index
K_c	Crop coefficient
K_S	Stress coefficient
K_{sat}	Saturated hydraulic conductivity
K_{Sb}	Stress indicator of cold temperature for biomass
L	Interarrival time
M	Monthly
N	Normal distribution
$NDVI_{max}$	Maximum normalized difference vegetation index
$NDVI_{min}$	Minimum normalized difference vegetation index
obs	Observed
P	Precipitation

$P_{effective}$	Effective rainfall
R^2	Coefficient of determination
RCP4.5	Stabilized emission scenario
RCP8.5	Extreme emission scenario
R_n	Net radiation
S	Slope
S_n	Cumulative severity
SPI-12	Standardized precipitation index at 12-month scale
SPI_n	Cumulative summation of standardized precipitation index
T	Temperature
T_D	Univariate return period
T_{max}	Absolute maximum temperature
T_{min}	Absolute minimum temperature
T_r	Crop transpiration
U_2	Wind speed at 2-m height
WP^*	Normalized water productivity
Y_o	Observed yield
Y_s	Simulated yield

ACRONYMS

ACCESS1.0	Australian Community Climate and Earth-System Simulator version 1.0
AIC	Akaike's Information Criteria
ANLIB	Area of North Ladakh not draining into Indus basin
BIC	Bayesian Information Criteria
CCI	Climate Change Initiative
CCSM4	Community Climate System Model, version 4
CDC	Canopy Decline Coefficient
CDF	Cumulative Distribution Function
CGC	Canopy Growth Coefficient
CIR	Crop Irrigation Requirement
CNRM-CM5	Centre National de Recherches Météorologiques Coupled Global Climate Model, version 5
CORDEX	Coordinated Regional Climate Downscaling Experiment
CWR	Crop Water Requirement
DEM	Digital Elevation Map

ECMWF	European Centre for Medium-Range Weather Forecasts
EFRGKB	East flowing rivers between Godavari and Krishna basins
EFRKPB	East flowing rivers between Krishna and Pennar basins
EFRMGB	East flowing rivers between Mahanadi and Godavari basins
EFRPCB	East flowing rivers between Pennar and Cauvery basins
EFRSCB	East flowing rivers between Subernrekha and Cauvery basins
EOS	Earth Observing System
ERA	European Reanalysis
ES	East Sikkim
ESA	European Space Agency
ET	Evapotranspiration
FAO	Food and Agriculture Organization
FC	Field Capacity
GCM	Global Climate Model
GDD	Growing Degree Days

GIMMS	Global Inventory Monitoring and Modeling System
GLDAS 2	Global Land Data Assimilation System version 2
GPP	Gross Primary Productivity
HI	Harvest Index
IDW	Inverse Distance Weighted
IMD	India Meteorological Department
IMDAA	Indian Monsoon Data Assimilation And Analysis
KS	Kolmogorov-Smirnov
LAI	Leaf Area Index
MBE	Mean Bias Error
MERRA-2	Modern-Era Retrospective analysis for Research and Applications
MK	Mann Kendall
MODIS	Moderate Resolution Imaging Spectroradiometer
MPI-ESM-LR	Max Planck Institute for Meteorology Earth System Model LR
MRFB	Minor rivers flowing into Bangladesh

MRFM	Minor rivers flowing into Myanmar
NASA	National Aeronautics and Space Administration
NCEP/NCAR	National Center for Environmental Prediction/National Center for Atmospheric Research
NDVI	Normalized Difference Vegetation Index
NPP	Net Primary Productivity
PDF	Probability Density Function
PDSI	Palmer Drought Severity Index
PWP	Permanent Wilting Point
RCP	Representative Concentration Pathways
RMSE	Root Mean Squared Error
SM	Soil Moisture
SPI	Standardized Precipitation Index
SRI	Standardized Runoff Index
SS	South Sikkim
SSI	Standardized Soil Moisture Index
SWSI	Surface Water Supply Index
TAW	Total Available Water

TC	Triple Collocation
uWUE	Underlying Water Use Efficiency
VCI	Vegetation Condition Index
VPD	Vapour Pressure Deficit
WG	Western Ghats
WMO	World Meteorological Organization
WP	Water productivity
WRIS	Water Resources Information System
WS	West Sikkim
WUE	Water Use Efficiency

Chapter 1

Introduction

1.1 Climate change

The climate is generally defined as the average weather conditions such as temperature, precipitation, or wind for a particular region and time, usually taken over 30-years. This particular period of time could range from months to hundreds, thousands, and millions of years. Broadly, the climate is the statistical accounting of the climate system. The climate system is an interactive system consisting of five major elements- the land, atmosphere, biosphere, cryosphere, and hydrosphere. This climate system is continuously changing due to various external and internal forcings. The direct impact of human induced activities on the climate system is considered an external forcing. Several chemical, physical and biological interaction processes occur among the several elements of the climate system, making the system very complex. Climate variability refers to the variations in the average state of climatic variables at various spatial and temporal scales. These variations are usually deviations from the average over a given scale of time (month, season, or year). Whereas, climate change is a statistically significant deviation from the average state over a more extended period, preferably decades.

Climate forcing is the physical process of affecting the climate on the Earth through a number of forcing factors. These factors are specifically known as forcings because they drive the climate to change, and it is important to note that these forcings exist outside of the existing climate system. The climate system includes the hydrosphere, land surface, the cryosphere, the biosphere, and atmosphere. Examples of some of the most important types of forcings include: variations in solar radiation levels, volcanic eruptions, changing albedo, and changing levels of greenhouse gases in the atmosphere. Each of these are considered external forcings because these events change independently of the climate, perhaps as a result of changes in solar activity or human-caused fossil fuel combustion. The human and natural climatic forcings cause internal alterations in several components of the climate system of the Earth. The feedbacks which are generated by these are responsible, either for the intensifying or impairing the forcings. However, it is important to note that different components of the climate system respond differently to these forcings. This response time could range from hours to years for the different components such as ocean surface, atmosphere, land, ice, and vegetation. Likewise, the response time for the glaciers, ice sheets, and deep oceans to exhibit the changes due to forcings can be 100 to 1000 years (Trenberth et al., 1996). Hence, the Earth's climate system can take hours to centuries to respond to external forcing's.

The major reason, as suggested by the Fifth assessment report (AR5) affecting the climate system, has been the increasing concentration of the greenhouse gases causing global warming (IPCC, 2014). The impacts of global warming can already be observed in the natural and human systems, which are of high interest. Climate change is generally defined as the alteration in the mean and/ or the variability in its properties for a long period of time (usually taken over 30-years). This change is mainly attributed to a number of natural and anthropogenic factors. The natural factors may include solar radiation variations, change in Earth's orbit, ocean current changes, volcanic eruptions, and multiple internal variabilities. The major anthropogenic activity which defines the course of climate change has been burning of fossil fuels leading to an increase in greenhouse gas emissions. In this context, the IPCC's AR5 stated that 1983 to 2012, was most likely, the warmest 30 years' period over the last 1400 years, particularly in the Northern Hemisphere. On average, the study of global temperature data set reveals that Earth in 2012 is 0.85 ℃ warmer as compared to 1880 (IPCC, 2014).

1.2 Drought under changing climate

Climate change has attracted much attention in the research community as changing climate conditions have led to changes in the frequency, duration, intensity, and severity of droughts. This changing climate can also alter atmospheric rivers, which in turn disrupt precipitation patterns. A combination of warmer temperatures and shifting atmospheric rivers can potentially devastate the water supply that may contribute to drought conditions. There are several other ways climate change may contribute to drought. For example, longer dry spells and warmer temperatures can contribute to drought conditions. Droughts are likely to be more severe, frequent, and longer lasting than they have been in recent decades under changing climate (Ault, 2020). The climate variability results in a period of precipitation deficit, which is generally driven by the natural climate cycles. If the precipitation deficit sustains for some time (over a scale of weeks/months depending on the climate), it leads to reduction in soil water content, streamflow, and reservoir storage. The water availability is also influenced by other climatic variables such as temperature and evapotranspiration. The reduced surface water and soil water adversely affect food production, hydropower generation, and industrial activities leading to socioeconomic droughts. The interactions between these variables in highly complicated because of the intricacies in land surface processes and human influences. Due to the complexity of the drought phenomenon, it is very difficult to define the onset and end of the drought which leads to poor estimation. It causes massive economical, environmental, and social consequences all over the world (Soľáková et al., 2014). In general, developing countries like India, where the agricultural sector provides livelihood to a large section of the population (Gadgil and Gadgil, 2006) are likely to suffer more economic losses due to such events (Russo et al., 2015). Countries with an increasing trend of drought events tend to be at a higher risk of damage. Proper assessment and estimation of drought events are necessary for policymakers and drought managers for deciding risk reduction strategies. Therefore, it is very important to understand different drought types and their characteristics for drought assessment.

1.2.1 Drought types

Primarily, droughts are defined as a deficit of precipitation over a longer period of time (generally a season or more), resulting in water scarcity. Drought is usually defined as a "creeping phenomenon" as it slowly impacts several sectors of the economy and operates on different time scales. As a complicated phenomenon and slow developmental nature, drought has multiple manifestations and is commonly classified into several types: meteorological, agricultural, hydrological, and socioeconomic drought (Zhong et al., 2019). Details of meteorological, agricultural, hydrological, and socioeconomic drought are presented below:

Meteorological Drought: The occurrence of any drought type is started with the severe persistence of rainfall shortage over a period of time say season or more (Mishra and Desai, 2005). Meteorological drought is defined based on precipitation deficit compared to normal conditions (Keyantash and Dracup, 2002) and it represents the period of lesser precipitation compared to long-term average (normal) precipitation at a place or region**.** Precipitation has been commonly used for meteorological drought analysis (Mishra and Singh, 2010). Definitions of meteorological drought should be region-specific, as the atmospheric situations that result in deficiencies of precipitation are highly region-specific. It is the simplest form of drought, however, it might be transformed to severe drought if the dry period extends for a longer period, as it is the initial stage of all other drought types. Hence, monitoring meteorological drought at an earlier stage could be used as early warning information for decision-makers and the community.

Agricultural Drought: When meteorological drought continues for some period, particularly in the crop growing period, it may lead to agricultural drought. Agriculture drought is the condition of reduced moisture in the top layers of soil to the level that it is not sufficient to support the crops. The water deficiency from meteorological or hydrological sources declines the water availability for crop production. In addition to precipitation deficit, soil moisture deficit also plays a very vital role in defining agricultural drought severity. Hence, agricultural drought indicates the period with decreasing soil moisture content and resulting to crop failure. Due to high water holding capacity, some crops are more resistant to such droughts, while others are not and become highly vulnerable to drought.

Hydrological Drought: When meteorological drought continues for a longer period, resulting in streamflow and groundwater reduction, drying up of lakes, rivers, reservoirs (Hayes et al., 2012). Hydrological drought is often related to a period with insufficient subsurface and surface water resources for established water uses. Surface water availability is the important deciding factor in case of hydrological drought; hence, streamflow is globally employed to develop a hydrological drought index (Clausen and Pearson 1995). Also, it is important to note that hydrological measurements are not the first indicators of drought due to time lag among precipitation and water shortage in lakes, rivers, reservoirs, and streams.

Socio-Economic Drought: Socio-economic drought is associated with the impact of drought events on socioeconomic activities instead of spatio-temporal characteristics of drought (AMS, 2004). It is related to demand and supply of economic goods and it occurs when demand surpasses the supply of economic goods due to scarcity in water supply (Zhao et al., 2019). This drought may occur either from meteorological, agricultural, or hydrological drought or their combined effects for an extended-term (Ziolkowska, 2016). This drought occurs when physical water storage affects individually or collectively. Hydropower deficit and water supply shortage are examples of such drought.

Flash Drought: Flash drought is a recently identified extreme event characterized by its rapid intensification and sudden onset (Otkin et al., 2018). Flash droughts are strongly related to high evapotranspiration, low soil moisture content, and intense heat (Pendergrass et al., 2020). The sudden onset allows limited time for planning and preparation, causing destructive impacts on the terrestrial ecosystem and agriculture due to insufficient early warnings. Due to rapid intensification and high evapotranspiration (ET), flash drought causes quick soil moisture depletion, which results in vegetation stress (Otkin et al., 2018).

In recent years, researchers have defined other classes of droughts such as ecological drought (Crausbay et al., 2017), groundwater drought (Pathak and Dodamani, 2019), or anthropogenic drought (AghaKouchak et al., 2021). The ecological drought is characterized by the water stress across the ecosystems due to widespread water deficit. The groundwater drought is the period of fallen groundwater levels such that the fall in level causes substantial water availability issues. Each type of drought starts off with a persistent precipitation deficit and the responses of different elements of hydrologic cycles lead to propagation of droughts from one class to another.

1.2.2 Drought characteristics

Droughts have several characteristics, for example, drought frequency, duration, areal and temporal extent, concurrence, and its evolution. These characteristics are described below:

Drought frequency: Drought frequency is defined as the number of drought events in a decade or given period.

Drought mean duration: It is defined as the ratio of total drought duration to the total number of droughts.

Spatial extent: The areal or spatial extent can be determined as the ratio of the number of grid cells experiencing drought to the total grid cell of the study area.

Temporal extent: It denotes the count of years for which each grid cell faces drought conditions in the given period.

Drought concurrence: When two or more than two drought types occur simultaneously.

Drought evolution: The drought evolution process indicates the evolution of one drought type into another drought type.

1.3 Drought assessment

As discussed, the drought-related risks posing potential loss of property and lives have increased over the past. Researchers and policymakers around the globe agree that current adaptation and mitigation policies might not be sufficient to deal with the implications of drought events. Therefore, a comprehensive drought assessment is required for minimizing the possible damage. In order to monitor drought conditions, past research suggested the use of drought indices as the simplest approach. Drought indices are quantitative measures based on physical and/or empirical approaches to investigate different drought properties either qualitatively or quantitatively (Hayes, 2006). Generally, drought indices integrate several meteorological and hydrological components like runoff, evapotranspiration, rainfall, temperature, and others into an individual number leading to a complete portrait of decision making. The drought indices are majorly categorized into four categories: meteorological, agricultural, hydrological drought indices, and remote sensing data-derived drought indices (Sumanta Das, 2013). It is important to note that a single drought definition does not work in all conditions, and that's the major reason why the resource planners, policymakers, and others have more difficulty in planning for drought than they do for other natural calamities. Nowadays, most of policymakers now rely on mathematic drought indices to decide when to start performing drought mitigation strategies.

It should be also noted that most of the drought indices that had been developed were regionally based and some drought indices are better suited than others for specific uses (Redmond, 2002; Hayes, 2006; Mishra and

Singh, 2010). Therefore, a review of the existing drought indices is necessary before adopting any of the existing drought indices to use in areas/catchments outside those areas for which they were originally developed. At the same time, in order to quantify, characterize and monitor drought events each drought index has its own strength and weakness (Dai, 2011; Jain et al., 2015; Mishra and Singh, 2010). In order to monitor drought condition, researchers used various drought indices, for example, an surface water supply index, SWSI (Shafer and Dezman, 1982); Palmer standardized precipitation index, SPI (McKee et al., 1993); standardized soil moisture index, SSI (Hao and AghaKouchak, 2013); vegetation condition index, VCI (Kogan, 1995). Details of some of the well-known drought indices which have been used in this thesis are presented below.

Standardized Precipitation Index (SPI): Standard precipitation index (SPI) is a globally used index because it is very simple to calculate, requires modest data and is comparable over a range of climatic zones (McKee et al., 1993). SPI computation is dependent on one input i.e., precipitation accumulations, and hence it is easy to calculate as compared to other drought indices. It has greater spatial consistency, therefore, a more recommendable drought index as compared to other drought indices. In SPI computation, initially raw precipitation data is fitted into gamma type distribution and then further transformed to a standard normal distribution (Tsakiris and Pangalou, 2009). Usually, a negative SPI indicates the drought condition while a positive value indicates the end of the drought. Therefore, SPI has been chosen for the present study.

The cumulative density function of Gamma distribution is $G_x(x)$ in Eq. (1.1):

$$\int_0^x g_x(x)\, dx = \frac{1}{\beta^{\varepsilon}\Gamma(\xi)} \int_0^x x^{\hat{\xi}-1}\, e^{-x/\hat{\beta}} \mathrm{dx}, \qquad (1.1)$$

where $g_x(x)$ is Gamma PDF, β is the scale parameter and α is a shape parameter of Gamma distribution.

$\Gamma(\xi)$ is the Gamma function and given as

$\Gamma(\xi) = \int_0^x t^{\xi-1} e^{-t} dt$ for $\xi>0$.

SPI index can be computed by Eq. (1.2) if the precipitation raw data is fitted into the log-normal distribution with variance $\sigma^2{}_y$ and mean μ_y as:

$$SPI = \frac{\ln(x) - \mu_y}{\sigma_y} \tag{1.2}$$

where ln(x) is log-normal transformed precipitation series.

Standardized Runoff Index (SRI): SRI is a hydrological drought index that was developed by Shukla and Wood (2008) using runoff data. For SRI computation, stream records of a specific region are fitted in appropriate distribution. After this, Probability Density Function and Cumulative Distribution Function are processed, and further, it is converted to a standardized normal deviate with zero mean and unit variance which finally results in Standardized Runoff Index. For SRI calculation, details can be obtained from (Hao et al., 2014; Shukla and Wood, 2008; Vicente-Serrano et al., 2012).

Vegetation Condition Index (VCI): VCI is an index derived from remotely sensed information to represent agricultural drought. It compares the current Normalized Difference Vegetation Index (NDVI) to the range of values observed in the same period in former years. It is capable to separate short-term weather-related fluctuations from long-term ecological changes. Bad and good vegetation situation is given by the low and high value of VCI, respectively. Drought severity classification is utilized to categorize droughts given by Kogan (1995).

VCI can be calculated by applying the following Eq. (1.3):

$$VCI = \frac{NDVI_i - NDVI_{min}}{NDVI_{max} - NDVI_{min}} \times 100 \tag{1.3}$$

Where,

VCI = Vegetation Condition Index

$NDVI_i$ = Index of the current month

$NDVI_{max}$ and $NDVI_{min}$ = Maximum and minimum NDVI of every pixel for each month.

Standardized Soil Moisture Index (SSI): SSI is an agricultural drought index that was developed by Bergman (1988) considering soil moisture data. For SSI computation, soil moisture data of a specific location is fitted in appropriate distribution. After this, Probability Density Function and Cumulative Distribution Function are computed, and it is converted to a standardized normal deviate with zero mean and unit variance which finally results in standardized soil moisture index. For SSI computation, details can be obtained from (Lloyd-Hughes and Saunders, 2002; Yao et al., 2018).

1.4 Limitations and gaps in approaches for drought assessment

An ideal comprehensive drought assessment approach must focus on all major drought types and their interaction. Moreover, it is essential to understand the drought from multi-perspectives such as severity, trends, distribution, duration as well as their complex interaction. However, most of the previous studies have focused on individual drought types, for example, meteorological drought, especially in India. None of them underlines a systematic and comprehensive analysis of the occurrence, distribution, and trend of multiple drought types simultaneously. Moreover, the concurrence and evolution between meteorological, hydrological, and agricultural drought are still unclear over India. Importantly, drought is a multivariate phenomenon, hence, modeling the drought characteristics through multivariate technique is more suitable as significant correlation is not obtained during univariate analysis (Chen et al., 2013). In addition to traditional droughts, flash droughts are newly discovered extreme events that have quick onset and rapid intensification characteristics. The sudden onset of flash drought allows limited time for planning and preparation, causing destructive impacts on the terrestrial ecosystem and agriculture due to insufficient early warnings (Gerken et al., 2018; Liu et al., 2020; Yuan et al., 2018). Due to rapid intensification and high evapotranspiration (ET), flash drought causes quick soil moisture depletion, which results in vegetation stress (Otkin et al., 2018). Such droughts are strongly related to high evapotranspiration, low soil moisture content, and intense heat (Pendergrass et al., 2020; Wang et al., 2016). Recently, flash droughts have occurred frequently, for example, northern USA in 2017 (Gerken et al., 2018), southern Africa in 2015 (Yuan et al., 2018), southern China in 2013 (Yuan et al., 2015), central USA in 2012 (Hoerling et al., 2014). Recently, a study by Yuan et al., (2019) found significant increasing trends flash drought frequency over China in the warming and changing climate. The increasing frequency may impose a higher risk on the ecosystem, crop production, water security, human mortality, vegetation health, and environmental sustainability (Vazifehkhah et al., 2019). Such events could hasten atmospheric carbon dioxide concentrations and reduce carbon uptake. However, how the regional terrestrial carbon dynamics respond to flash droughts is still unknown, especially in India. As we know that India is a very vast and climatologically diverse country having high spatio-temporal variability, therefore, a comprehensive study is required to understand the significant relationship among multiple drought types. Therefore, in the context of climate change, a better understanding of the droughts in terms of their occurrence, trend, concurrence, evolution as well as joint dependence of drought characteristics is necessary. Moreover, flash drought identification and its impact on the terrestrial ecosystem are also important to understand. In light of the above discussion, the following research gaps were identified:

- More comprehensive approach for the assessment of multiple drought types in the context of concurrence and evolution is required.

- Conventional analyses of the drought characteristics involve univariate approaches which are often inadequate to incorporate the complexity.
- How the regional terrestrial ecosystems respond to flash droughts in India remains unknown.
- Dearth of comprehensive approach for the assessment of crop yield and crop water requirement at the regional scale in the hilly terrain of Himalayas under climate change.

1.5 Objectives of the study

The objectives of the study are as follows:

- Assessment of the distribution, trend, concurrence, and evolution of major drought types in India.
- Probabilistic analysis of meteorological, hydrological, and agricultural drought characteristics across Indian river basins in India.
- Terrestrial Ecosystem Response to Flash Droughts over India.
- Understanding the impact of climate change on crop yield and crop water requirement of major crops in Sikkim, Himalayan region of northeast India.

1.6 Organization of the thesis

Literature relevant to various aspects of climate change, drought assessment, drought characteristics, the impact of flash drought on terrestrial ecosystem, and the impact of climate change on crop productivity and crop water requirements are concisely reviewed in Chapter 2.

Chapter 3 discusses the detailed theory, methodology, results, and discussion obtained from the first objective, i.e., assessment of the distribution, trend, concurrence, and evolution of major drought types in

India. The study has been done by analyzing the major drought types for 24 major river basins of India.

Chapter 4 describes the copula based probabilistic analysis of meteorological, hydrological, and agricultural drought characteristics across Indian river basins. Exceedance probability and joint return period are estimated and characterized on the river basin scale.

Chapter 5 presents the seasonal distribution of flash drought and the response of terrestrial ecosystem to flash droughts over India. The flash drought identification on monsoon and non-monsoon scale have been carried out.

Chapter 6 describes the estimation of crop yield and crop water requirement under changing climate over the eastern Himalayan region of India. Further, uncertainty analysis and sensitivity analysis have been carried out.

Chapter 7 summarizes the discussion and conclusion of the entire research work, limitations of the study and future scope of the research work.

Chapter 2

Literature review

2.1 Introduction

Droughts are undoubtedly one of the most catastrophic hydroclimatic events that occur around the globe every year. The subsequent sections in the chapter explain the drought characterization from multi-perspectives, probabilistic analysis of drought characteristics, importance of flash drought identification and their impact on terrestrial ecosystem, and understanding the climate change implication on crop water requirement and crop productivity. The chapter concludes with an outlook that explains the outputs of literature review in the context of the thesis objectives.

2.2 Drought characterization

In general, drought is defined as an event of lesser availability of water resources to meet the environment, human or industrial demands over a significantly extended period, such as months, seasons, or longer (Wilhite, 2000). There is a general perception that droughts occur only in the regions of low precipitation (i.e., arid climate); however, aridity (long term dryness) and droughts (short term dryness) are two different phenomena. Former is a permanent climatic characteristic of a place having less long-term rainfall, whereas the latter is a temporary condition of significantly low rainfall compared to normal. Therefore, droughts are not limited to arid climates but occur in all climates, including low and high rainfall receiving regions of the world. Nagarajan, (2003) observed drought as one of the complex natural hazards as it is very difficult to evaluate the onset and termination of drought event. Hagman et al., (1984) describe drought as the most unpredictable yet least understood natural calamity. Droughts are mostly defined as the inadequacy of rainfall (meteorological drought), streamflow (hydrological drought), vegetation, and soil moisture (agricultural drought), individually or in combination (Dracup et al., 1980; Goyal et al., 2017; Hisdal and Tallaksen, 2000). The National Commission on Agriculture (1976) in India classified 3 types of droughts, specifically, meteorological, agricultural, and hydrological droughts. Meteorological, hydrological and agricultural droughts are defined in terms of the shortage of rainfall, streamflow, and soil moisture individually or together respectively (Bhuiyan et al., 2006; Goyal et al., 2017; Muhammad et al., 2020). Recent literature shows that agricultural drought can be further classified into two droughts i.e., soil moisture and vegetation drought. The categorization is done because analyzing soil moisture and vegetation drought individually is better rather than a multi-variate drought index, because the former gives a more detailed view on changes in environment variables than the latter one. Moreover, both vegetation conditions (Kogan, 1995) and soil moisture (Yang et al., 2017) are closely linked to agricultural droughts and are widely used for agricultural drought characterization. This new approach provides a refined view of drought occurrence. Recently, a new drought called groundwater drought is added as a fourth category (Mishra and Singh 2010).

Since, there is no single definition of drought (Hao and AghaKouchak, 2013), however, the best means to examine the drought occurrence is by the use of drought indices (Stagge et al., 2015). Many researchers used several indices based on their applicability such as standardized precipitation index, SPI (McKee et al., 1993); surface water supply index, SWSI (Shafer and Dezman, 1982), standardized runoff index SRI (Shukla and Wood, 2008), Standardised Hydrological Index (SHI) (Panu and Sharma, 2009), vegetation condition index, VCI (Kogan, 1995) and standardized soil moisture index, SSI (Hao and AghaKouchak, 2013) to define droughts. Each drought index has its own merits and demerits. However, no single drought index can fully describe the drought distribution, intensity, severity, and complexity (Joshi et al., 2016). Over the last century, hydrologists around the world have put substantial efforts to improve the monitoring and prediction of droughts through the development of new drought indices and prediction models.

The outputs from the drought studies based on drought indices suggest that more than half of the earth's land surface is susceptible to drought conditions (Mishra and Singh, 2010). Some of the long-term and highest-impact droughts struck the Amazon Basin (2010), East Africa (2004 and 2005), Australia (2002, and others) with adverse impacts (Sivakumar, 2013). Mishra and Singh, (2010) stated that India has reported a drought event at least once in every three years in the last five decades. The spatial and temporal characteristics of droughts are preconditions and the basis for examining drought occurrence and its impact. Shah and Mishra, (2014) carried out an analysis regarding drought characteristics and found that the drought intensity, spatial extent, and frequency have increasing trend due to increase in air temperature and erratic summer monsoon. From the aspect of drought distribution and trend, Mallya et al., (2015) identified a robust trend of increasing drought severity and frequency over the Indian monsoon region during the period 1972–2004. Several past studies have witnessed variations in drought trends, spatiotemporal patterns, and frequencies in different parts of the World (Ganguli and Reddy, 2014; Goyal and Sharma, 2016; Joshi et al., 2016; Kumar et al., 2021; Mishra et al., 2014; Thomas et al., 2015). To better understand drought concurrence, some studies have attracted more attention towards occurrence of two drought indices for characterizing the drought concurrence. Further, some studies have used various methods for investigating drought evolution process. These methods could be either linear regression or time lag correlation (Zhang et al., 2017). Therefore, it is essential to understand the drought from multi-perspectives such as severity, trends, distribution, duration as well as their complex interaction (Zhang et al., 2017).

The previously mentioned studies discussed the trend of past drought occurrence. Understanding the evolution of future droughts in a changing climate is of great importance in terms of risk assessment and implementation of efficient adaptation measures. The general circulation models (GCMs) are one of such sources which can be used to understand the future propagation of meteorological drought. It is considered that the arid regions will be more drier and wet will be more wetter in the changing climate. The uneven distribution of precipitation changes is expected to enhance the frequency and severity of drought in many regions. Several regional studies performed on various parts of the world invariably reported the increase drought events in changing climatic conditions (Chen and Sun, 2017; Lee et al., 2018; Nam et al., 2015; Naumann et al., 2018; Spinoni et al., 2018; Trenberth et al., 2014). For example, Trenberth et al., (2014) reported that the rise in temperature due to global warming had led to alteration in characteristics of droughts such as frequency and intensity of droughts. Similarly, based on the projections of climate models, Dai, (2011) reported increase in aridity in various regions of the world over the 21st century. Thilakarathne and Sridhar, (2017) analyzed the drought over Lower Mekong Basin and found that more intense and severe droughts are prevalent in the changing climate. Tam et al., (2019) projected the meteorological droughts using 29 GCMs in Canada and observed increasing trend of drought frequency over Prairies, and South-west Canada. Moreover, Indian sub-continent also witness increase in drought frequency in the changing climate (Ahmed et al., 2018; Bisht et al., 2019). Thus, exploring drought characteristics is important for enhancing the level of drought alleviating and monitoring the effects of drought.

2.3 Probabilistic assessment of drought characteristics

The last section of the chapter discussed the univariate analysis of drought characteristics i.e., separate analysis of drought duration, and drought severity, etc. In this section, probabilistic assessment of drought characteristics has been discussed. Drought severity and duration are the two important characteristics used for drought characterization. Moreover, Dracup et al., (1980) identified drought duration and severity as defining characteristics of a drought event. Here, drought duration indicates the period during which the rainfall deficit occurs whereas severity indicates the cumulative rainfall deficit below a particular threshold. There are several methods that allow us to estimate the probabilistic assessment of the drought characteristics, such as stochastic methods, parametric and non-parametric approaches. The concept of the parametric method involves fitting specific distributions to given returns. This approach is also known as the percentile-based approach or the return period method (Hobaek et al., 2015). The main disadvantage of this method is that the estimated returns are incapable of incorporating the tail behaviour, often asymptotic, and cannot be used to produce estimates beyond the sample range. Further, the stochastic approaches produce recurrent conditions which yield return periods based on the random traction from probabilistic projections (Goldstein et al., 2003). Also, these methods consider the Gaussian case; therefore, they do not accommodate the tail complexities. The EVT methods have been formulated particularly to incorporate the tail behaviour of the data (Naveau et al., 2005).

Drought is a multi-variate phenomenon, therefore, modeling the drought characteristics through multivariate technique is more suitable. This is because several probabilistic methods have been developed in the past to examine drought properties, however, significant correlation is not obtained in univariate analysis. Therefore, it is better to adopt a multivariate approach and develop the joint dependence structure to describe the interconnection among drought characteristics. Most of the multivariate distributions are derived from univariate ones and involve several disadvantages (Salvadori and De Michele, 2004), such as marginal distribution needs to be the same. Additionally, complex mathematical derivations are essential for parameter estimations (Shiau, 2006) and based on assumption of stationarity (Das and Umamahesh, 2017). To overcome such limitations, Copula is a promising way to assess joint dependence between random variables (Sklar, 1959).

Copulas are advantageous in modeling joint dependence because they are independent of equality of marginal distribution or normality of variables (Zhang and Singh, 2007). Copulas are widely used in various fields such as climate studies (Jhong and Tung, 2018; Yin et al., 2018), hydrology (Y. D. Chen et al., 2016; Zhang et al., 2012), medical (Emura and Chen, 2018; Winkelmann, 2012), signal processing (Iyengar et al., 2009), finance (Chiou and Tsay, 2008; Ning, 2010). In case of hydro-climatic events, copula provides a robust methodology, for example, soil moisture and precipitation (AghaKouchak, 2015), extreme events and vegetation drought (Jha et al., 2019), groundwater and precipitation (Reddy and Ganguli, 2013), volume and peak flow (Favre et al., 2004). Firstly, Shiau, (2006) applied copula functions to bivariate frequency investigation of drought severity and duration. Further, Lee et al., (2013) explored the applicability of copula in drought characteristics (duration and severity) and found that the joint probabilistic approach offers greater versatility in the estimation of drought characteristics. The bivariate copula based approach accounts for the dependence among drought severity and duration and allows their marginal distributions to belong to different families (Mishra and Singh, 2011). There are several other studies that incorporate the copula-based approach in hydrological studies (De Michele and Salvadori, 2003; Grimaldi and Serinaldi, 2006; Zhang et al., 2013; Gómez et al., 2017; Bracken et al., 2018; Goswami et al., 2018; Ribeiro et al., 2020; Thilakarathne and Sridhar, 2017; Vazifehkhah et al., 2019). Recently, the joint behavior of drought duration and severity was modelled using Copula approach, and it was concluded that the method is more suitable for quantifying the dependence between drought characteristics (Sahana et al., 2020). This multivariate investigation can help policymakers to incorporate effective drought risk management and drought mitigation plans.

2.4 Flash drought and its impact on terrestrial ecosystem

The above two sections of the chapter discussed conventional droughts i.e., meteorological, hydrological, and agricultural droughts. Conventional droughts are generally defined as a slowly growing climate phenomenon, taking a few months or years to attain its spatial extent and maximum intensity (Otkin et al., 2013, 2021c; Yuan et al., 2017). In addition to these drought types, a new kind of rapidly growing drought termed as “flash drought” has come into the scientific dictionary in recent years. Therefore, in this section, flash droughts and their impact on the terrestrial ecosystem have been discussed. Flash drought is a recently recognized extreme event characterized by its sudden onset and rapid intensification (Yuan et al., 2019). The sudden onset allows limited time for planning and preparation, causing destructive impacts on the terrestrial ecosystem and agriculture due to insufficient early warnings (Gerken et al., 2018; Liu et al., 2020; Yuan et al., 2018). Due to rapid intensification and high evapotranspiration (ET), flash drought causes quick soil moisture depletion, which results in vegetation stress (Otkin et al., 2018). Flash droughts are strongly related to high evapotranspiration, low soil moisture content, and intense heat (Pendergrass et al., 2020; Wang et al., 2016). However, flash droughts are hard to monitor and predict (Pendergrass et al., 2020). There are several methods available to investigate flash drought events. For instance, considering the precipitation-deficit-driven and heat wave-driven (Mo and Lettenmaier, 2016, 2015) which focuses the role of temperature anomalies, deriving flash drought events from the soil moisture percentile drop based approaches (Ford and Labosier, 2017) focuses on the rate of change in soil moisture, utilizing the standardized evaporative stress ratio (Basara et al., 2019; Christian et al., 2020, 2019) or utilizing multivariate products like Quick Drought Response Index (QuickDRI) hybrid satellite-based maps (Chen et al., 2019) to estimate the flash drought events.

Recently, flash droughts have occurred frequently, for example, northern USA in 2017 (Gerken et al., 2018), southeastern United States in 2016 (Otkin et al., 2018), southern Africa in 2015 (Yuan et al., 2018), southern China in 2013 (Yuan et al., 2015), central USA in 2012 (Hoerling et al., 2014). During the year 2013, southern China experienced its most terrible drought and heatwave of the last century (Yuan et al., 2016). The rapid intensification of drought significantly minimized carbon uptake (> 100 Tg C) in China. The outputs from these studies suggest that it is very crucial to understand that how different ecosystems respond under flash drought conditions to predict the future atmospheric CO_2 concentrations and terrestrial carbon sink, as well as to provide recommendations for drought mitigation and prevention policies. Moreover, understanding the future patterns of flash drought events is also important for proper risk estimation. In view of this, Yuan et al., (2019) estimated future flash drought events and found significant increasing trend of flash drought frequency over China in the warming and changing climate. Moreover, Mishra et al., (2021) carried out flash drought identification over India for the projected climate and found an increasing trend in the frequency of flash drought events. The increasing frequency may impose a higher risk on the ecosystem, crop production, water security, human mortality, vegetation health, and environmental sustainability (Vazifehkhah et al., 2019).

Apart from the flash drought identification, understanding the impact of drought over productivity of the terrestrial ecosystem is also equally important because it influences food security and others (Jha et al., 2019; Thomey, M.L. et al., 2011). Drought also affects the carbon cycle by changing the physiological behavior comprising vegetation respiration and photosynthesis. Zhao and Running, (2010) showed that satellite images are widely used to examine the ecological influences of drought as it provides a local understanding of terrestrial vegetation conditions (Running et al., 2004). High-resolution vegetation datasets obtained from MODIS are extensively used to control the changes in vegetation characteristics (Sharma and Goyal, 2018a; Wolf et al., 2016). These products offer global gross primary productivity (GPP) (Running et al., 2004) and are widely used in several regional as well as global studies (Anav et al., 2015; Zhao and Running, 2010). Moreover, Flack-Prain et al. (2019) showed that vegetation productivity shows distinct responses to drought from vegetation structural and physiological viewpoints. GPP and NPP are effective indicators for carbon fluxes and ecosystem functioning from physiological and ecological processes (Cao and Woodward, 1998). Otkin et al., (2016) examined that how vegetation conditions and soil moisture evolve during the extreme flash drought event of 2012 across the U.S. and witnessed a significant response of vegetation conditions to the drought. In the summer of 2013, enormous carbon loss is observed through satellite observations and eddy covariance (Yuan et al., 2016).

The previously mentioned studies discussed the response of the terrestrial ecosystem to flash drought events. Moreover, understanding the response of water use efficiency(WUE) to flash drought is also crucial. The ecosystem water use efficiency (WUE) is computed by dividing the carbon uptake by evapotranspiration (Cheng et al., 2017; Xiao et al., 2013), which controls vegetation productivity in a dry environment (Mu et al., 2011). The hydrometeorological parameters also play a crucial part in spatio-temporal variation in WUE via influencing carbon assimilation, transpiration, and evaporation (Sharma and Goyal, 2018a). The response of water use efficiency differs among different ecosystems (Gang et al., 2016; Guo et al., 2019) and droughts with different severity and duration (Liu et al., 2015; Ma et al., 2019). Guo et al., (2019) assessed the response of WUE to the flash drought conditions in China. They found that lower water use efficiency was observed in northwestern China during droughts, whereas WUE was increased over South China and Northeast China. Further, Zhang et al., (2020) suggest to assess the response of the terrestrial ecosystem to flash droughts. Moreover, they also suggest to incorporate two important parameters i.e., response time and response frequency of flash drought due to their variability over different regions. Regarding the investigation of WUE during flash droughts, few global studies have been carried out across the world (Guo et al., 2019; Xie et al., 2016; Zhang and Yuan, 2020).

2.5 Climate change impact on crop water requirement and crop productivity

With the increase in greenhouse gas concentration, climate change has emerged as a paramount concern worldwide in the context of socioeconomic, environmental, and agricultural sustainability. According to IPCC (2013), the increase in the global average temperature is recorded about 0.6^{o}C, and based on the future projections under different scenarios it is likely to increase by 1 to 5^{o}C by end of this century. Over long-term, the climate variability is likely to affect agriculture in various ways, including the crop productivity, crop water requirement, etc. (Todisco and Vergni, 2008). With the twin pressure of climate change and population growth, the demand of crop commodities has increased substantially (Mall et al., 2017), and it is expected that the global agricultural productivity needs to be doubled by 2050 to fulfill the increasing demand (Ray et al., 2013). An estimate from FAO (2016) reports that to fulfil the demand of food in 2050, the annual production of crops and livestock will need to be increased by 60% as compared to 2006 production globally. Moreover, the increase in the concentration of the CO_2 and global warming are expected to alter the future global agricultural productivity by change in plant growth (Eyshi Rezaei et al., 2015), respiration (Peng et al., 2004), photosynthesis (Wang et al., 2011), and transpiration (Crawford et al., 2012). This, in turn, can increase water stress and consequently, food security (Tao et al., 2003). For instance, investigations have shown that crop yield at global scale is likely to be reduced (e.g., rice by 3.2%, wheat by 6.0%, soybean by 3.1%, maize by 7.4%) (Zhao et al., 2017). In this sense, agrarian countries are going to be affected substantially due to the adverse consequences of climate change. Therefore, in the prevailing adverse consequences of climate change, impact assessment on agricultural productivity in changing climate has gained popularity. Hence, recent studies aim at the climate change impact assessment on crop productivity and crop water requirement. For example, Lin (2011) stated that due to the spatio-temporal variability of precipitation, and accessibility of resources such as water, biodiversity, land, and terrestrial resources, climate change is likely to affect the agricultural productivity and food security. Hence, researchers from all corners of the globe have attempted to investigate the climate change impact using crop simulation models on different crops productivity.

Past research indicates that crop models are widely used for crop simulations worldwide. Moreover, crop models enable to analyze and modify the crop growth effectively and subsequently, the yield under changing climate. Due to the projected climate change under various emission scenarios during the mid or late 21st century, it is going to affect productivity negatively over many regions, while individual locations may benefit. For instance, a study by Lobell et al. (2008) using 20 climate models under three different scenarios and climate projections for 2030 revealed negative impacts on several crops over South Asia and Southern Africa without proper adaptation priorities. Schlenker and Roberts (2009) estimated that yields are expected to decrease by 30–46% and 63-82% over U.S. before 2100 under the slowest (B1) scenario and the most rapid warming scenario (A1FI), respectively. Further, Oort and Zwart, (2018) also observed a decrease in crop (rice) yield i.e., 24% decrease under RCP 8.5 scenario over Africa. However, Lobell and Gourdji (2012) stated that with the increase in the CO_2 concentration the global yield is expected to increase roughly by 1.8% per decade, and simultaneously the crop yield may decrease without any effective adaptation roughly by 1.5% per decade. In addition to crop productivity, climate change also impacts crop water requirement and irrigation requirement negatively as well as positively over many regions. Future quantification of spatio-temporal variability of crop water requirement (CWR) and irrigation requirement (IR) can improve water management efficiency. In an effort to analyse the future CWR and IR, limited studies have been carried out by the researchers from various parts of the world and the examples include but are not limited to, De Silva et al. (2007), Droogers (2004), Shen et al. (2013), Shrestha et al. (2013), Song et al. (2018), Tubiello et al. (2000), Zhou et al. (2017), among others.

Apart from this, past research also indicates that the future projections of crop yield are simulated using the meteorological outputs from Global Climate Models (GCMs) under different emission scenarios. Das and Umamahesh (2018) suggest that it is essential to determine the uncertainty associated with the climate models and their scenarios while projecting for the future. The GCM uncertainty has been attributed to model structure, parameterization, resolution, model simulations, and initial conditions for different realizations (Clark et al., 2016). Höllermann and Evers (2017) suggest that it is important to account uncertainty information about foreseen climate scenarios for better adaptation measures. In this sense, past studies adopted different techniques namely, such as sensitivity analysis (Hofer, 1999), imprecise probability (Beer et al., 2013), Bayesian analysis (Das and Umamahesh, 2018), and others to assess the uncertainty in the climate change studies. Recent research widely adopted the possibility theory for uncertainty analysis via allocating possibility distribution to the GCMs and emission scenarios according to the ability in modeling the recent past under climate forcing. This method is inexpensive, simple, and assists in addressing partially information and knowledge (Mujumdar and Ghosh, 2008).

2.6 Conclusions

An overview of drought characterization, probabilistic and multivariate approaches to investigate drought characteristics, the flash drought identification and its impact on terrestrial ecosystem, and climate change impact on crop production has been presented in this chapter. The discussions about drought characterization suggest that it is crucial to understand the drought from multi-perspectives such as severity, trends, distribution, duration as well as their complex interaction. Moreover, evolution and concurrence of meteorological, hydrological and agricultural droughts are of significant importance during drought analysis. Future studies suggest that droughts are likely to be more severe, frequent, and longer lasting than they have been in recent decades under changing climate. Further, the literature review discussed the advantages of Copula in modeling the drought characteristics. The studies suggest that Copula is one of the most reliable tool to model joint dependence between random variables. Further, the concept of flash drought and its impact in the context of terrestrial ecosystem was discussed in the third section. The literature review indicates that flash drought is a recently identified extreme event characterized by its rapid intensification and sudden onset. Due to rapid intensification and high evapotranspiration, flash drought causes quick soil moisture depletion, which results in vegetation stress and possess great threat to terrestrial ecosystem. Further, the climate change impact assessment in the context of crop productivity and crop water requirement was discussed in the last section. The literature review indicates that adverse impact of climate change is going to affect every aspect of the ecosystem in the hilly terrain of the Himalayan region. Moreover, uncertainty analysis is also crucial for analyzing the most possible GCM and scenario through possibilistic approach. Therefore, the thesis, addressing the gaps pointed out in the literature review, aims to assess the drought characteristics and flash drought identification using an advanced multivariate probabilistic approach and rapid intensification approach, respectively.

Chapter 3

Occurrence, Concurrence, and Evolution of Meteorological, Hydrological and Agricultural Droughts over River Basins of India

3.1 Introduction

Drought is a large-scale and recurring phenomenon with random and unpredictable characteristics (X. C. Yuan et al., 2017; Zhang and Zhang, 2016). It causes massive economical, environmental, and social consequences all over the world (Soľáková et al., 2014). In general, droughts are categorized into three categories i.e., meteorological, hydrological, and agricultural droughts (National Commission on Agriculture, 1976). The present study further classified the agricultural drought into soil moisture and vegetation drought. In order to monitor drought condition, researchers used various drought indices for example, standardized soil moisture index, SSI (Hao and AghaKouchak, 2013), standardized precipitation index, SPI (McKee et al., 1993), etc. Each drought index has its own merits and demerits.

India has faced frequent and severe drought (once in every three years) in the last few decades and stands as one of the most vulnerable drought-prone countries in the world (Mishra and Singh, 2010). Several past studies have also witnessed variations in drought trends, spatiotemporal patterns, and frequencies in different parts of India (Goyal and Sharma, 2016; Thomas et al., 2015). Hence, it is crucial to recognize the drought from several perceptions such as severity, trends, distribution, duration as well as their complex interaction (Zhang et al. 2017).

From the literature review, it was observed that most of the previous studies have focused on individual drought types, specifically meteorological drought in India. None of them underlines a systematic and comprehensive investigation of the trends, distribution, severity, and durationof multiple drought types simultaneously, especially in India. Moreover, the concurrence and evolution between meteorological, hydrological, and agricultural drought are still unclear (Mallya et al., 2015; Yadav et al., 2015). To bridge this knowledge gap, we provide a first comprehensive approach to investigate multiple droughts in terms of their occurrence, distribution, trend, concurrence, and evolution to evaluate the implications of droughts in India. The present analysis is performed using high-resolution ($0.5^0 \times 0.5^0$) precipitation, soil moisture, runoff, and vegetation data series over India.

3.2 Data and methodology

3.2.1 Study area and data

Figure 3.1 describes the river basin ID, location, and nomenclature. Each river basin of India has different spatio-temporal variability in its rainfall pattern, for example, the lowest rainfall received by the western parts of India whereas the highest by northern parts. Therefore, all 25 major river basins of India were chosen as the study area. Due to the human interface, drought based on one input such as precipitation or soil moisture is not enough to accurately capture the drought condition. Therefore, the present study adopted a comprehensive approach to carry out this study in all river basins of India.

In this study, monthly gridded datasets of precipitation, NDVI, soil moisture, and runoff during the period 1982-2013 were analyzed. The precipitation data is obtained at a spatial resolution (0.5°×0.5°) from the India Meteorological Department 4 (IMD-4) data set (Pai et al., 2014). IMD precipitation dataset is advised to use because it is capable to detect the Indian climatic conditions efficiently (Mishra et al., 2014).

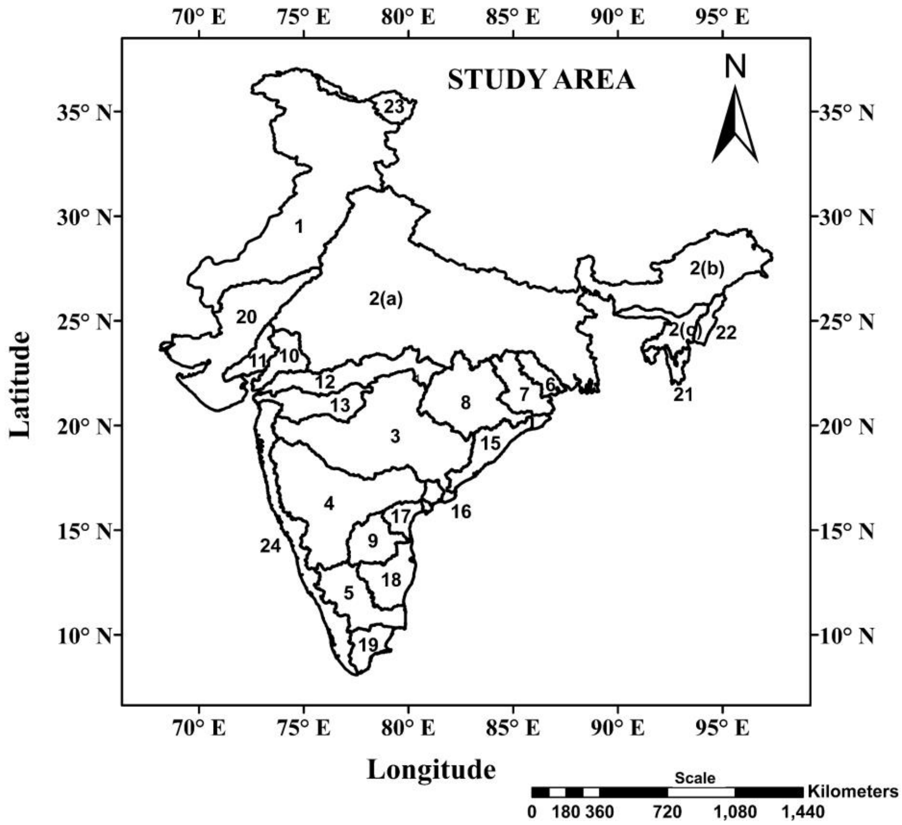

Figure 3.1. Major river basins in India. Source: Watershed Atlas of India (India-WRIS 2012). The details of basin IDs are: 1-Indus, 2(a)-Ganga, 2(b)-Brahmaputra, 2(c)-Barak, 3-Godavari, 4-Krishna, 5-Cauvery, 6-Subernrekha, 7-Brahmani and Baitarani, 8 Mahanadi, 9-Pennar, 10-Mahi, 11-Sabarmati, 12-Narmada, 13- Tapi, 15-East flowing rivers between Mahanadi and Godavari basins (EFRMGB), 16- East flowing rivers between Godavari and Krishna basins (EFRGKB),17- East flowing rivers between Krishna and Pennar basins (EFRKPB),18- East flowing rivers between Pennar and Cauvery basins (EFRPCB), 19-East flowing rivers between Subernrekha and Cauvery basins (EFRSCB), 20-Luni, 21-Minor rivers flowing into Bangladesh (MRFB), 22- Minor rivers flowing into Myanmar (MRFM), 23- Area of North Ladakh not draining into Indus basin (ANLIB), 24- Western Ghats (WG).

Soil and runoff data are obtained from the reanalysis product i.e., MERRA-2 for the 1982-2013 period. Mean monthly and time average soil moisture and runoff data series are available at a resolution of $1/2^0$ to $2/3^0$. The datasets can be accessed from https://gmao.gsfc.nasa.gov/reanalysis/MERRA-2/data_access/. MEERA-2 dataset is recommended as more realistic datasets to detect soil moisture and runoff variability and can signify better interactions between various physical processes and surface landscape (Molod et al., 2015). It is assumed that the reanalysis dataset provides comparable results as these datasets are widely used for various hydrology and climate related investigations. However, these datasets have several uncertainties due to various data sources, data assimilation, and model's simulation (Hodges et al., 2011). Thus, it is suggested to assess the data quality before investigating the climate of the study area (Lin et al., 2014).

NDVI is deemed as a suitable and appropriate factor for investigating the vegetation drought (Zhao et al., 2018). NDVI dataset was obtained from the GIMMS-NDVI with a bi-weekly period and spatial resolution of 1/12°×1/12° and can be accessed from https://nex.nasa.gov/nex/projects/1349. GIMMS-NDVI datasets were available on a 15 day temporal scale and hence, it is average to a monthly dataset. It is essential to note that the NDVI, soil moisture, runoff data are regridded with help of an inverse distance weighted (IDW) interpolation method to a 0.5°×0.5° resolution.

3.2.2 Methods

In the present investigation, standardized precipitation index (SPI), standardized soil moisture index (SSI), vegetation condition index (VCI), and standardized runoff index (SRI) indices were selected for monitoring all major drought types in our study area. The drought indices i.e., SPI, SRI, SSI, and VCI were computed using monthly data of precipitation, runoff, soil moisture, and NDVI datasets, respectively. Moreover, the study investigates the spatio-temporal distribution of droughts, individually and concurrently. These concurrent droughts are computed by accounting drought indices values collectively. Further drought trend analysis is performed based on their mean duration, mean spatial extent, and frequency. Moreover, the evolutionary process which explains the evolution of one drought type into another type is also examined. Figure 3.2. shows the detailed methodology of the present study.

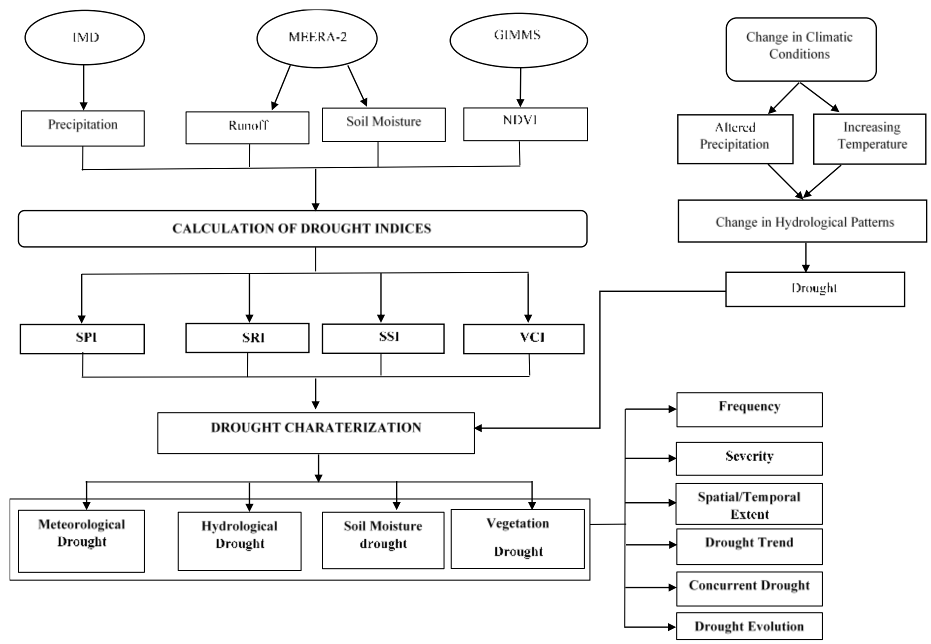

Figure 3.2 Flow chart for the methodology of drought characterization.

3.2.2.1 Computation of drought indices

The SPI method is presented by McKee *et al.*, (1993), which only requires precipitation data for estimation and can be used for both rainy and dry seasons. Typically, negative SPI indicates drought conditions whereas positive SPI refers to the ending of the drought. The raw rainfall data are consistently fitted to gamma or a Pearson Type III distribution and then changed to a normal distribution. SRI and SSI drought indices are used to estimate hydrological and soil moisture drought considering runoff and soil moisture data as input, respectively. For their computation, streamflow/soil moisture data of specific regions are fitted in an appropriate distribution. After that, the cumulative distribution function (CDF), as well as probability density function (PDF) is processed and changed to standardized normal deviation having unit variance and zero mean, and thus finally resulted in SRI/SSI. For SRI calculation, details can be obtained from (Hao et al., 2014; Shukla and Wood, 2008; Vicente-Serrano et al., 2012), and for SSI, details can be obtained from (Lloyd-Hughes and Saunders, 2002; Yao et al., 2018).

The cumulative density function of Gamma distribution is $G_x(x)$ in Eq. (3.1):

$$\int_0^x g_x(x)\,dx = \frac{1}{\beta^{\varepsilon}\Gamma(\xi)} \int_0^x x^{\hat{\xi}-1}\, e^{-x/\hat{\beta}} dx, \tag{3.1}$$

where $g_x(x)$ is Gamma PDF, β is the scale parameter and α is a shape parameter of Gamma distribution.

$\Gamma(\xi)$ is the Gamma function and given as

$\Gamma(\xi) = \int_0^x t^{\xi-1}\, e^{-t} dt$ for $\xi>0$.

SPI index can be computed by Eq. (3.2) if the precipitation raw data is fitted into the log-normal distribution with variance ${\sigma^2}_y$ and mean μ_y as:

$$\mathrm{SPI} = \frac{\ln(x) - \mu_y}{\sigma_y} \tag{3.2}$$

where ln(x) is log-normal transformed precipitation series.

VCI is used to characterize vegetation droughts using NDVI datasets. A higher value of the VCI index signifies good vegetation conditions and vice-versa. VCI can be calculated by applying the following Eq. (3.3):

$$\mathrm{VCI} = \frac{NDVI_i - NDVI_{min}}{NDVI_{max} - NDVI_{min}} \times 100 \tag{3.3}$$

Where,

VCI = Vegetation Condition Index

$NDVI_i$ = Index of the current month

$NDVI_{max}$ and $NDVI_{min}$ = Maximum and minimum NDVI of every pixel for each month.

Since VCI is determined in %, therefore VCI lies between 50-100% shows better than average state of vegetation while VCI from 50 to 35% shows drought condition and VCI under 35% demonstrates severe drought condition (Kogan, 1995). Additionally, specific thresholds were defined to categorize drought severity (see Table 3.1).

Table 3.1 Drought severities as per different drought indices as defined in Svoboda et al., (2002).

Drought Severity	SPI, SRI, and SSI	VCI	Category
Exceptional Drought	-2.00 or Less	0.00 to 0.05	D4
Extreme Drought	-1.60 to -1.99	0.15 to 0.06	D3
Severe Drought	-1.30 to -1.59	0.25 to 0.16	D2
Moderate Drought	-0.80 to -1.29	0.35 to 0.26	D1
Abnormally Dry	-0.50 to -0.79	0.45 to 0.36	D0

3.2.2.2 Temporal extent, duration, frequency, and areal extent of droughts

In the preliminary stage, the occurrence of meteorological, vegetation, soil moisture, and hydrological droughts are computed through SPI, VCI, SSI, and SRI drought indices, respectively. Further, concurrent droughts are determined in the same month by considering drought indices value collectively. Moreover, the frequency of drought is termed as the number of drought events in a decade. However, in the present investigation, we have calculated frequency as the number of drought events in eleven years in order to divide the total time period (1982-2013) into three equal parts.

The temporal extent denotes the count of years for which each grid cell faces drought conditions in the given period or month during 1982-2013. In case of concurrent drought, it can be determined by accounting for the multi-drought occurrence within the same time, such as the temporal extent of meteorological and vegetation drought can be determined by counting the grids witnessed both droughts in the same month. Mean duration is defined as the ratio of total duration time to the number of drought concurrence during the given period. The areal or spatial extent can be determined as the ratio of the number of grid cells experiencing drought to the total grid cell of the study area. The areal extent denotes the study area (in %) under drought conditions.

3.2.2.3 Drought evolution

The drought evolution process indicates the evolution of one drought type into another drought type, for example, meteorological drought to hydrological drought, further leads to soil moisture drought, and lastly to vegetation drought (National Weather Service, 2006). The drought evolution process plays a vital role to analyse the water shortage transformation in several drought studies. However, most of the research does not incorporate the drought evolution process. The present study adopted a linear regression approach to describe the relationship between the evolution process between all major drought types.

3.3 Results and discussion

3.3.1 Drought occurrence during 1982-2013

The occurrence of historical droughts was computed using four major drought indices i.e., SPI, SRI, SSI, and VCI. In the initial analysis, the top droughts by the maximum areal extent and/or level of severity were shown for major drought types (Figure 3.3 (a &b) and 3.4 (a &b)).

In case of drought severity, the soil moisture and hydrological droughts are usually observed to be more influential as compared to other drought types.

However, in the case of the Tapi and Mahi river basins, vegetation and soil moisture droughts are more extreme and influential as compared to meteorological and hydrological droughts.

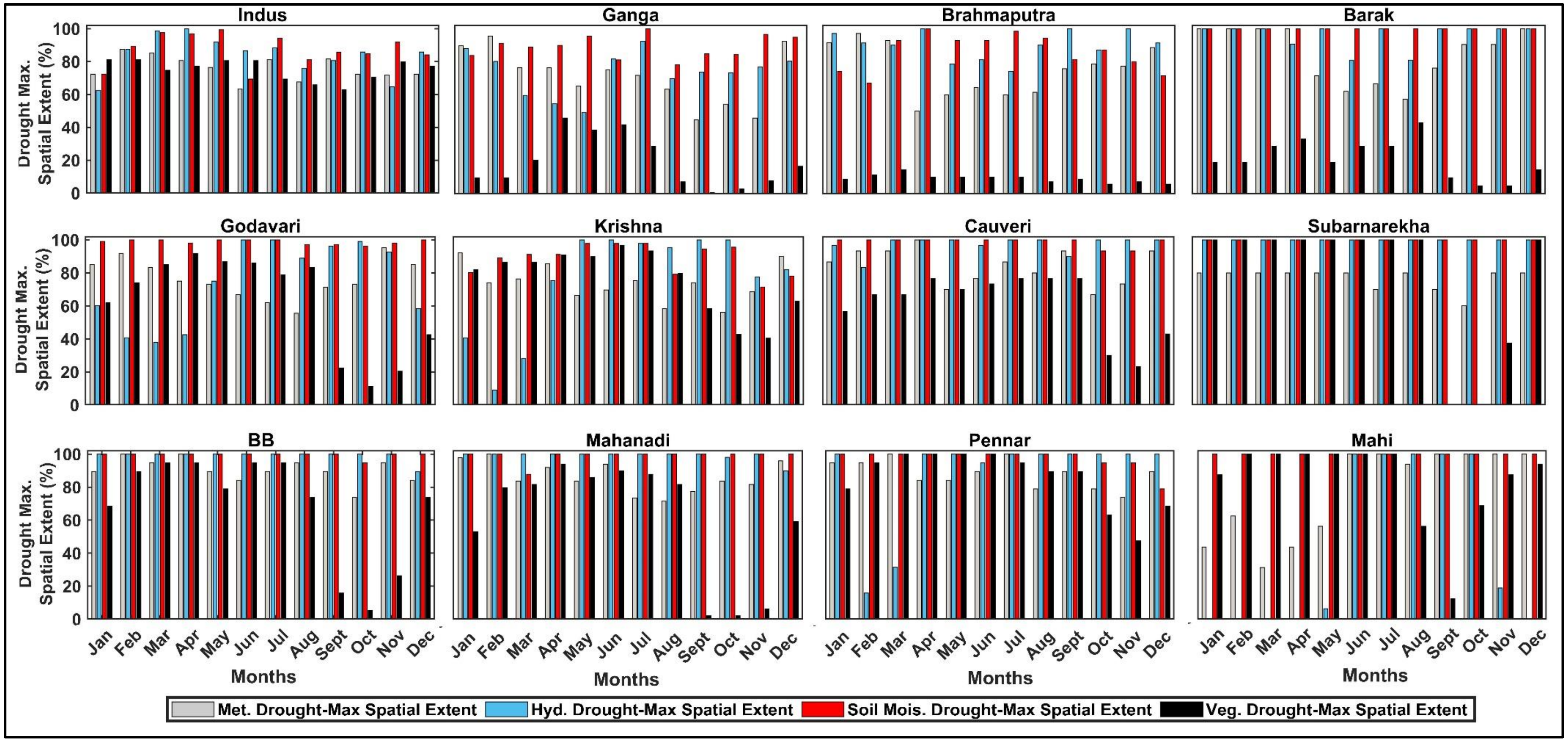

Figure 3.3 (a) Top meteorological, hydrological, soil moisture and vegetation droughts based on spatial extent (%) for all basins of India for every month in 1982-2013.

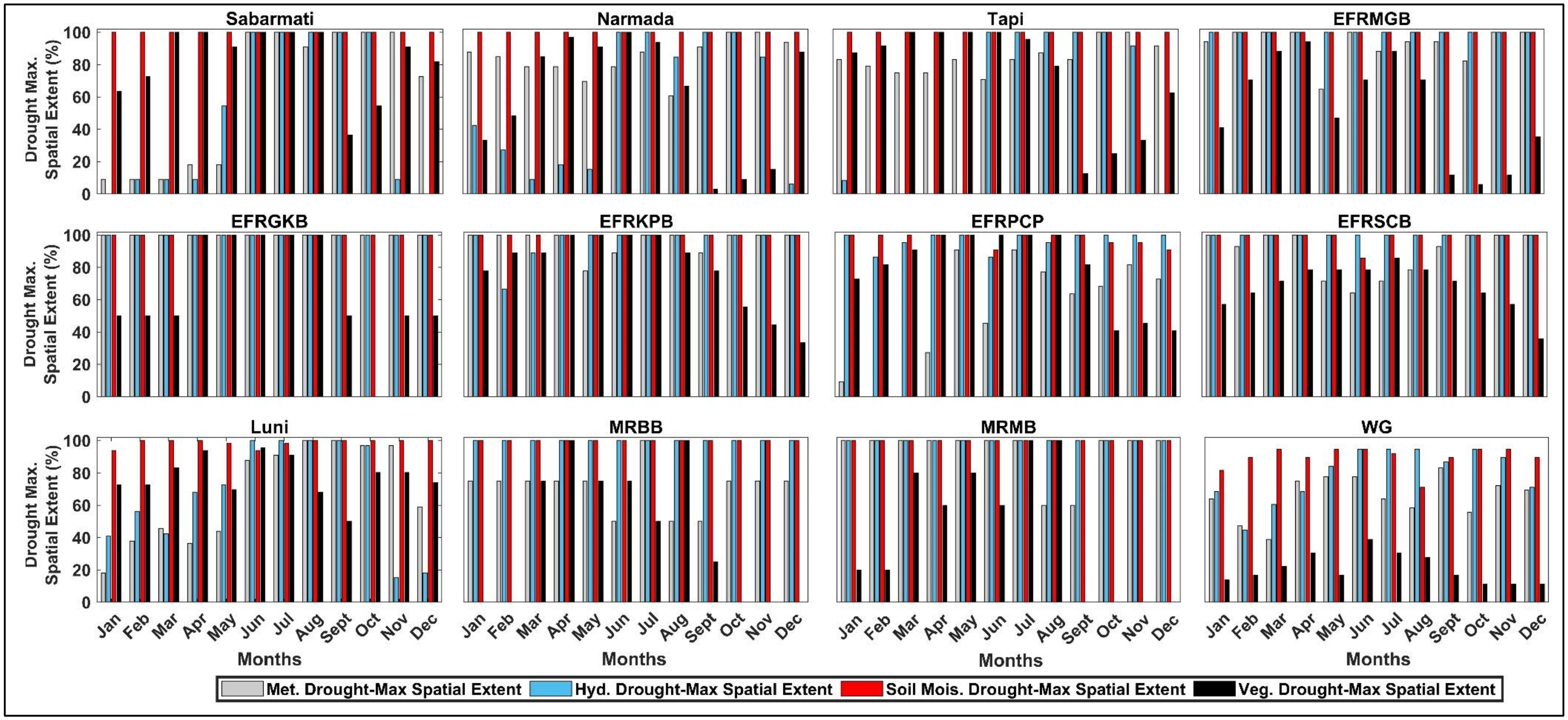

Figure 3.3 (b) Top meteorological, hydrological, soil moisture and vegetation droughts based on spatial extent (%) for all basins of India for every month in 1982-2013.

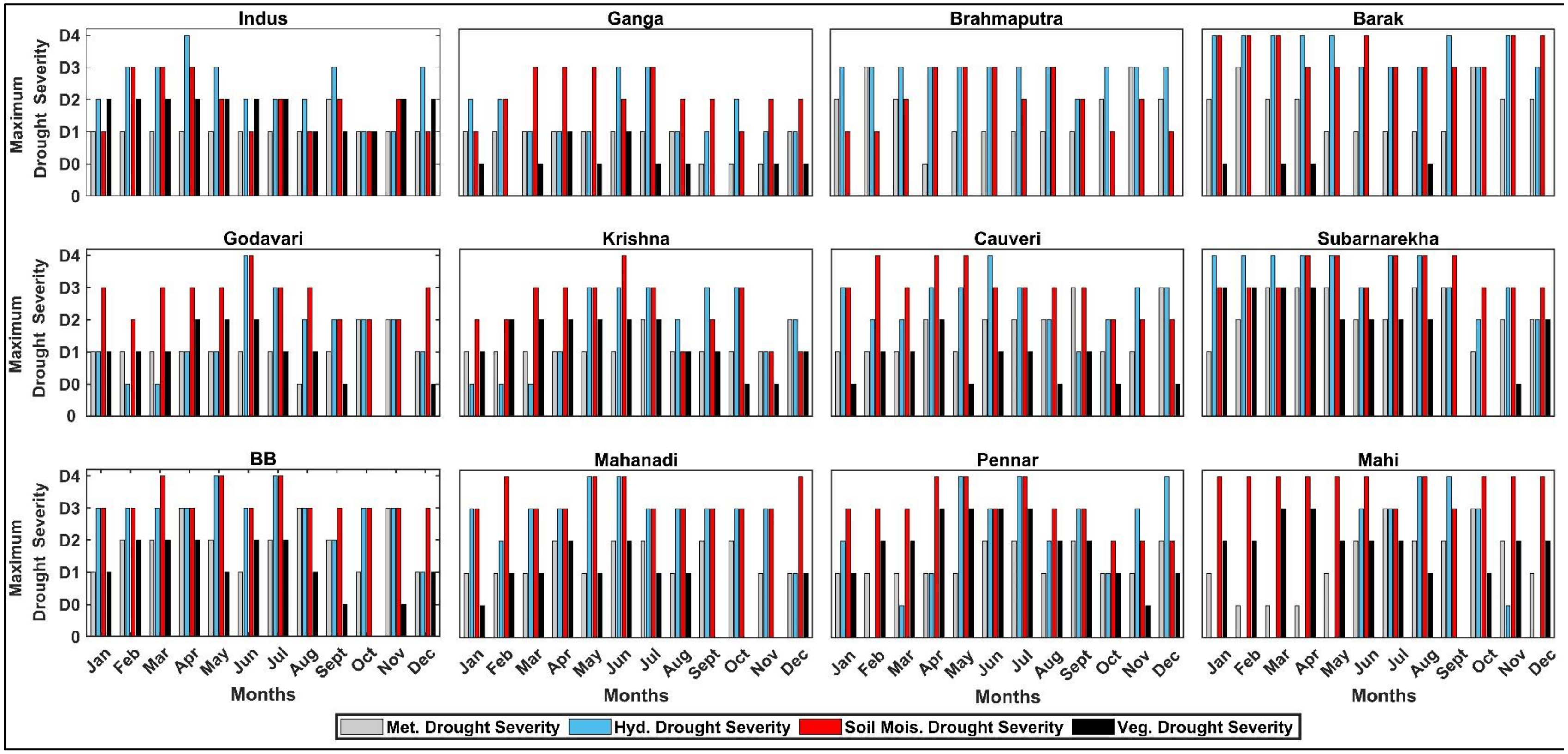

Figure 3.4 (a) Top meteorological, hydrological, soil moisture and vegetation droughts based on severity estimated using domain mean drought indices for all basins of India for every month in 1982-2013.

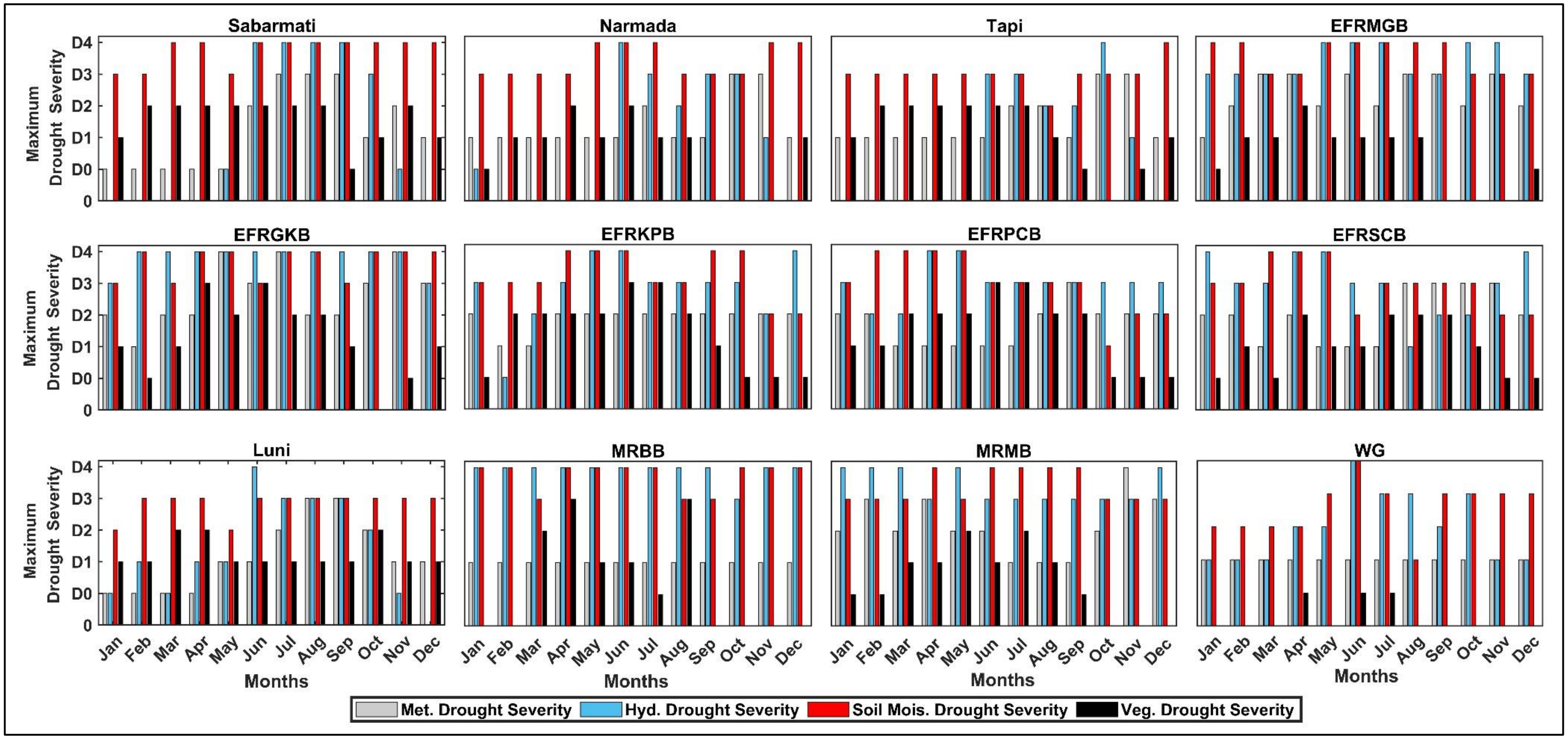

Figure 3.4 (b) Top meteorological, hydrological, soil moisture and vegetation droughts based on severity estimated using domain mean drought indices for all basins of India for every month in 1982-2013.

In terms of the areal extent, similar results were observed in most of the river basins of the study area. Mahi, Sabarmati, and Luni basin have a high likelihood of vegetation drought in low moisture conditions (Jha et al., 2019). Moreover, the investigation also suggests that meteorological droughts are majorly characterized by moderate and severe drought i.e., D1 and D2 severity in the majority of the river basins of India. A similar finding was observed in Pai *et al.,* (2017) where they found moderate and severe droughts in India during the period 1901-2010.

3.3.2 Temporal extent of drought

Figure 3.5 presents the temporal extent of drought given the severity$\geq D_1$ for each month for the period 1982-2013. Investigation suggests that meteorological droughts mostly occur from December to April in major of the river basins in India. This may be due to a rainfall deficit in the given period. Whereas the soil moisture and hydrological droughts show no or very less significant monthly variation in their temporal extent, ranges from 5 to 8 drought years.

Unlike the three droughts, the temporal extent of vegetation drought presents the heterogeneous distribution, similar was found in Jha et al., (2019). Vegetation drought shows significant variation in their temporal extent, as averaged variation ranges from 9 to 19 drought years. Investigation demonstrates that vegetation droughts are mostly appeared from March to July and meteorological drought from December to April, whereas soil moisture and hydrological droughts present insignificant monthly differences in temporal extent. Further, April to July are perceived as drought-prone months and might not suitable for better crop production during these months.

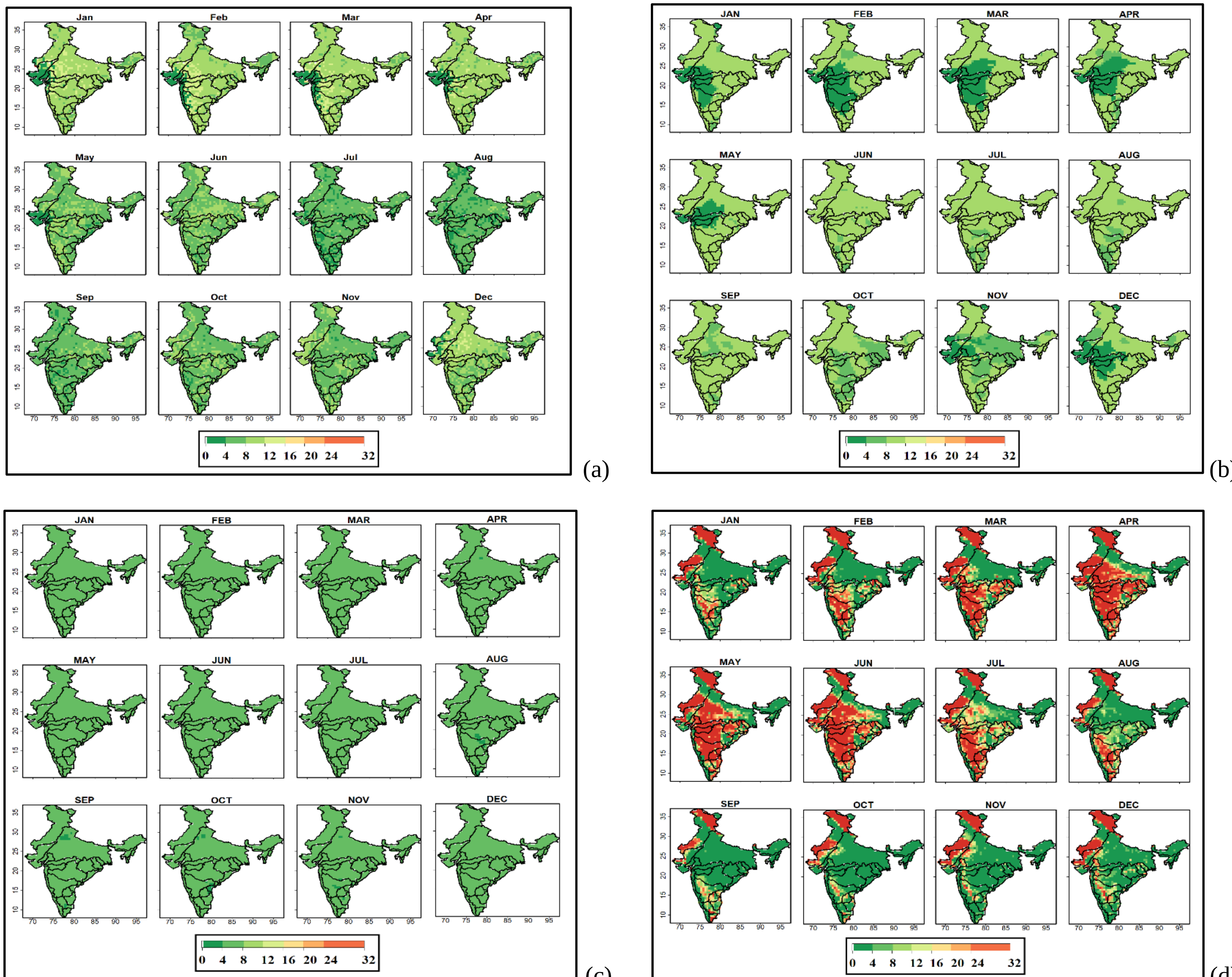

Figure 3.5 Temporal extent of all four drought types ((a) meteorological, (b) hydrological, (c) soil moisture and (d) vegetation) for the study area.

3.3.3 Drought trend analysis

The drought trend is analyzed in terms of mean duration, frequency, and mean areal extent for three-time periods, i.e., 1982-1992, 1993-2003, and 2004-2013 to detect the trend pattern on a decadal basis. However, in the present study, we have taken 11 year's time windows instead of a decadal period.

3.3.3.1 Drought mean duration

In case of drought mean duration (Figure 3.6), the mean duration for meteorological drought shows longer drought duration i.e., from 2.2 months to 2.3 months per drought events from 1982-1992 to 2004-2013. Whereas soil moisture, hydrological and vegetation drought presents a decreasing trend of mean duration from 3 months to 1 month, 4 months to 2months, and 6 months to 4 months from 1982-1992 to 2004-2013, respectively. In terms of moisture drought, a 50% sharp decrease in mean drought duration was witnesses. Further, the MRMB and Cauveri basin witnesses the highest decreasing duration trend for soil moisture and hydrological drought respectively while the Mahi basin exhibit for vegetation and meteorological drought. Investigation suggests that the mean duration of vegetation drought varies from 1 to 4 months while for soil moisture, hydrological and meteorological droughts, it fluctuates from 1 to 2 months. Further, the overall mean duration results suggest that the study area witnesses more frequent "flash droughts" events rather than year-long droughts. Additionally, Eastern India, Mahanadi, the Northern part of India, Brahmani and Baitarani basin, and the Indo-Gangetic plains exhibit the upward drought duration trend of meteorological drought from 1982-1992 to 2004-2013. Recent studies also observed similar results in terms of drought mean duration (Ganguli and Reddy, 2014).

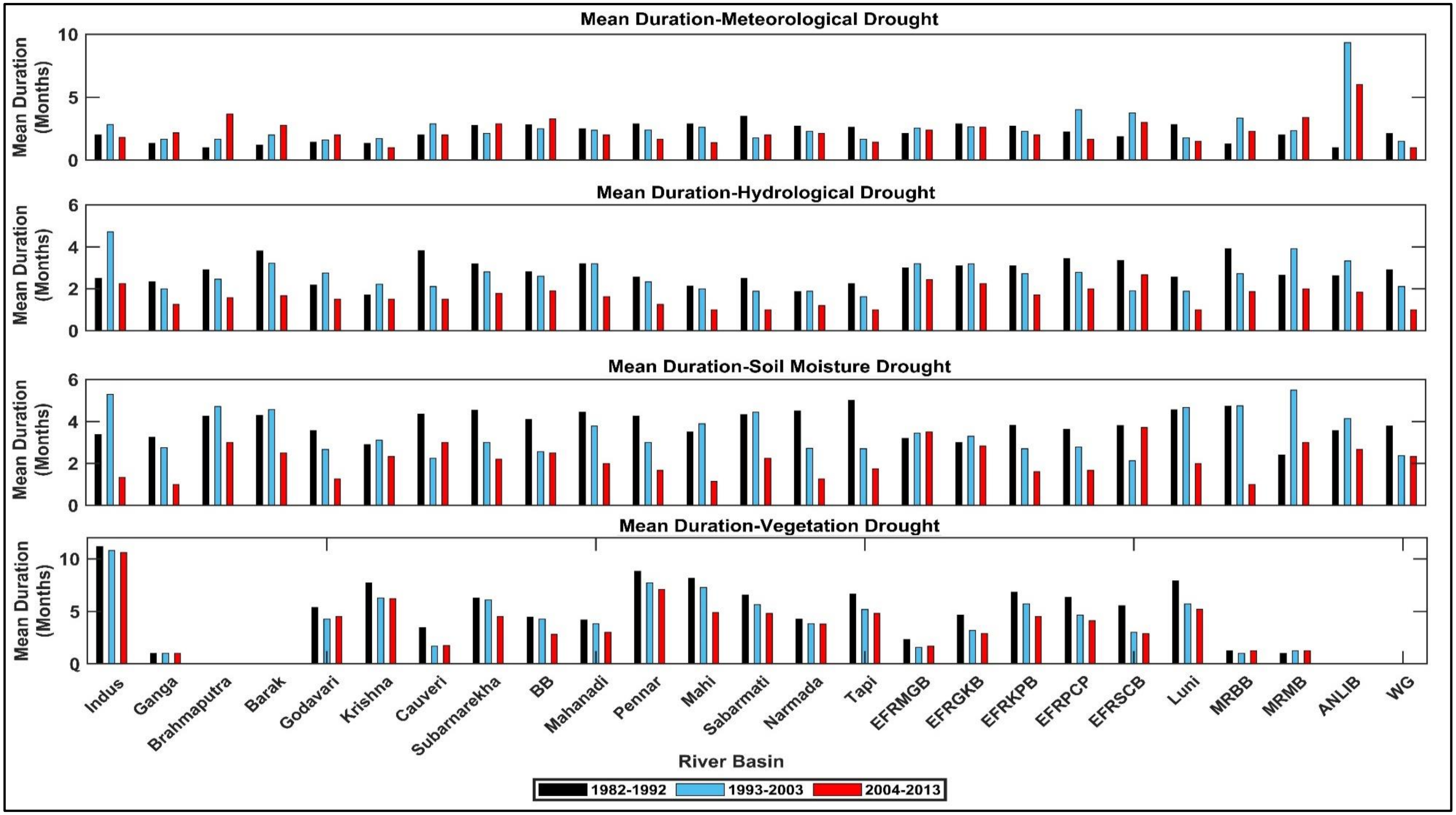

Figure 3.6 Mean Duration (in months) of all four drought types calculated using drought indices during 1982-92, 1993-2003 and 2004-2013.

3.3.3.2 Drought areal extent

Regarding areal extent (see Figure 3.7), the area under meteorological drought shows an upward trend ranges from 3.2% to 4.14% whereas soil moisture, hydrological and vegetation drought presents downward trend ranges from 2.7% to 3.08%, 7.09% to 4.53%, and 10.22% to 7.75% during 1982-1992 to 2004-2013 respectively. The areal extent of meteorological, vegetation, soil moisture, and hydrological drought varies from 0.19% to 30%, 0.1% to 82%, 0.8% to 36.7%, and 1.3% to 25.6%, respectively. Moreover, the Ganga basin witnesses the highest decreasing trend in soil moisture and hydrological drought whereas the highest increasing trend for meteorological drought. The highest decreasing trend in vegetation and meteorological drought was observed for the Krishna river basin. Further, Eastern India, Cauveri, Western part, and Indo-Gangetic plains of India exhibits the upward trend in meteorological drought from 1982-1192 to 2004-2013. Ganguli and Reddy, (2014) and Mallya et al., (2015) also found similar results in terms of drought duration and drought frequency.

3.3.3.3 Drought frequency

From the perception of the frequency, soil moisture, hydrological and vegetation droughts exhibit a decreasing trend while meteorological droughts show an increasing trend from 1982-1992 to 2004-2013 in all river basins of the study area. The frequency of meteorological drought increasing from 15 drought events (1982-92) to 19 drought events (1993-2003) and then decreases to 15 drought events (2004-2013). While the frequency of vegetation, soil moisture, and hydrological droughts decreases from 59 to 38 drought events, 37 to 9 drought events, and 27 to 10 drought events during 1982-1992 to 2004-2013, respectively (Figure 3.8). Das et al., (2019) also observed similar results in terms of drought frequency. Investigation suggests an increase in rainfall anomaly with insignificant anomalies of vegetation, soil moisture, and runoff.

Figure 3.7 Mean Areal Extent (in %) of all four drought types calculated using of drought indices during 1982-92, 1993-2003 and 2004-2013 respectively.

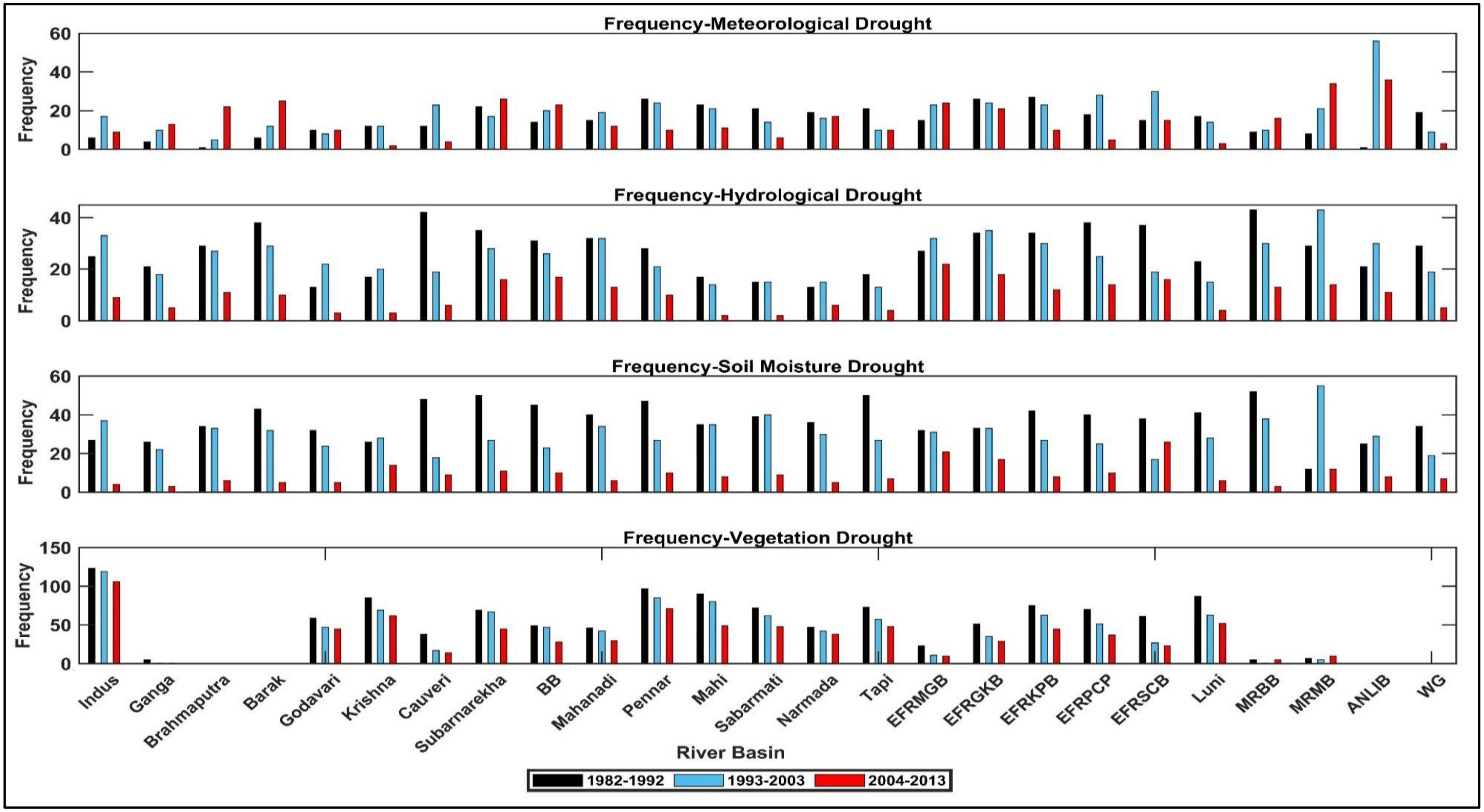

Figure 3.8 Frequency (no. of droughts per 11 years) of all four drought types calculated using domain averaged drought indices (SPI, SRI, SSI, and VCI) during 1982-92, 1993-2003 and 2004-2013 respectively.

Moreover, the highest decreasing trend of the frequency of vegetation drought is witnessed in the Mahi basin. Moreover, the Mahanadi, Northern part of India, Eastern India, Brahmani, and Baitarni basin and the Indo-Gangetic plains show the increasing trend of frequency for meteorological drought during 1982-1992 to 2004-2013. Mishra et al., (2014) and Mallya *et al.*, (2015) also found similar results in terms of drought frequency.

Based on drought trend analysis in terms of mean duration, areal extent, and frequency, it was observed that nearly 10 river basins show continuous, larger area and frequent meteorological drought whereas vegetation, soil moisture, and hydrological droughts exhibited a smaller duration, areal extent, and frequency.

3.3.4 Drought concurrence

Further to individual drought examination, concurrent droughts are also examined in terms of their temporal distribution and types. Concurrent drought calculation is discussed and explained in the methodology section. Investigation suggests that at least 30 concurrent droughts occurred in all 25 river basins of India during the 1982-2013 period (Table 3.2). Interestingly, it was observed that two-drought-based conjunctions range from 38% to 88% of concurrent droughts. Moreover, 82% of concurrent droughts are consists of soil moisture droughts in 16 basins of India. This suggests not only frequent soil moisture droughts but also shows the important role of soil moisture than precipitation in the study region. It suggests that the vegetation ecosystem faces a more frightening situation in near future in India. More than 85 concurrent droughts are witnessed by the Pennar, Indus, EFRKPB, and Subarnarekha basins in 26 to 29 years, as these river basins come into the category of water scarce. March, April, June, and July months are termed as multi-drought prone months with more than 40% of concurrent droughts. In November and December, the Ganga basin witnesses no concurrent drought while ANLIB basin observed no concurrent drought in January.

Table 3.2 Regional droughts for every month during 1982-2013 for all major river basins of India.

Parameters / Basins	No. of concurrent drought	Two-drought based conjunctions (%)	Parameters / Basins	No. of concurrent drought	Two-drought based conjunctions (%)
Indus	**100** droughts in **26** years	50	**Narmada**	**65** droughts in **27** years	72
Ganga	**31** droughts in **20** years	71	**Tapi**	**74** droughts in **24** years	69
Brahma.	**38** droughts in **20** years	82	**EFRMGB**	**78** droughts in **28** years	58
Barak	**60** droughts in **22** years	87	**EFRGKB**	**80** droughts in **28** years	48
Godavari	**52** droughts in **22** years	65	**EFRKPB**	**86** droughts in **27** years	48
Krishna	**62** droughts in **25** years	63	**EFRPCP**	**81** droughts in **27** years	65
Cauveri	**70** droughts in **24** years	68	**EFRSCB**	**82** droughts in **26** years	65
Subarna.	**98** droughts in **28** years	56	**Luni**	**69** droughts in **22** years	67
BB	**77** droughts in **26** years	48	**MRBB**	**65** droughts in **21** years	88
Mahanadi	**69** droughts in **25** years	38	**MRMB**	**62** droughts in **24** years	65
Pennar	**107** droughts in **29** years	61	**ANLIB**	**37** droughts in **13** years	57
Mahi	**80** droughts in **26** years	61	**WG**	**38** droughts in **16** years	86
Sabarmati	**73** droughts in **22** years	58			

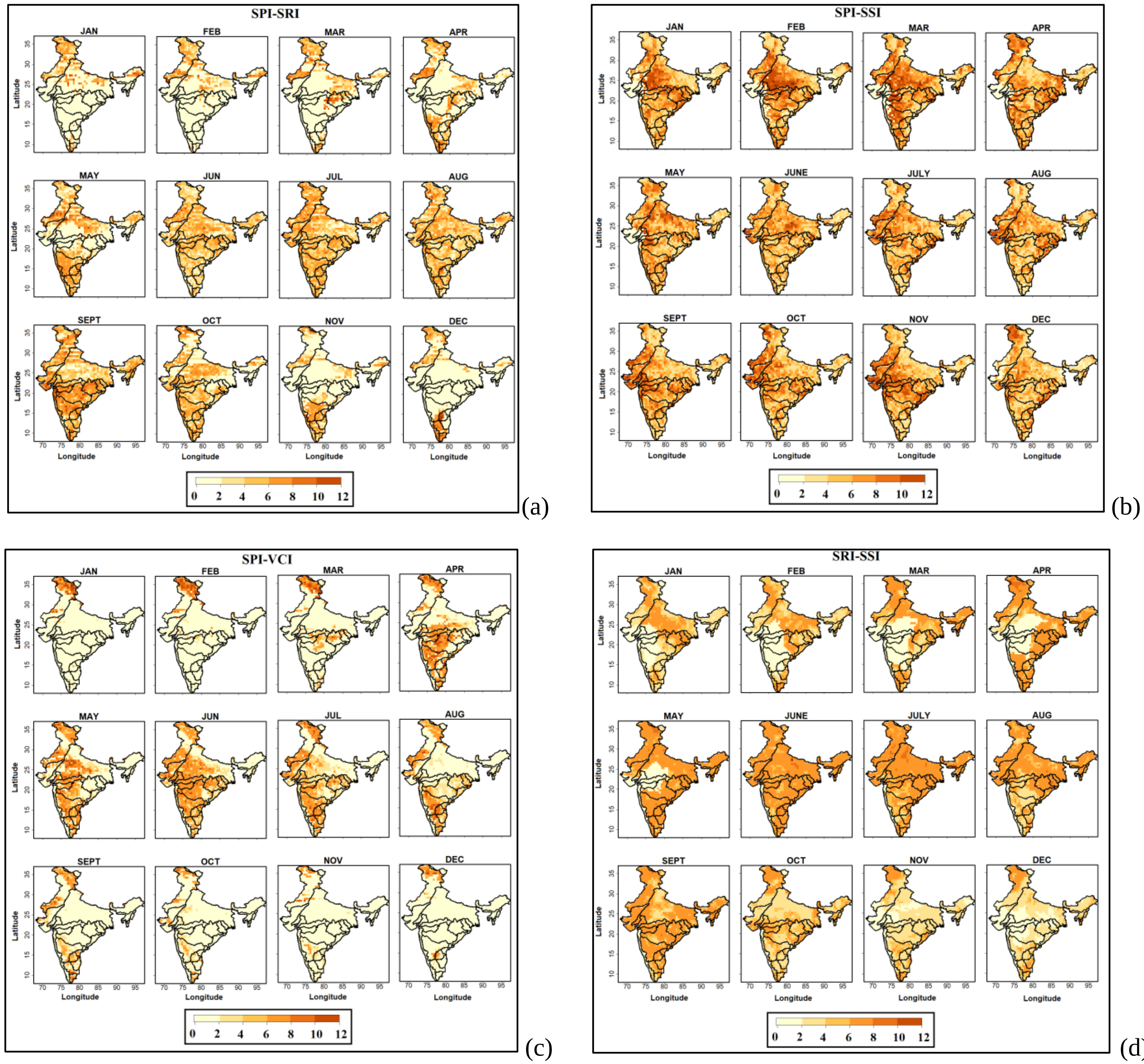

Figure 3.9 Temporal extent of concurrent droughts (figure a to d) for every month during the period 1982-2013.

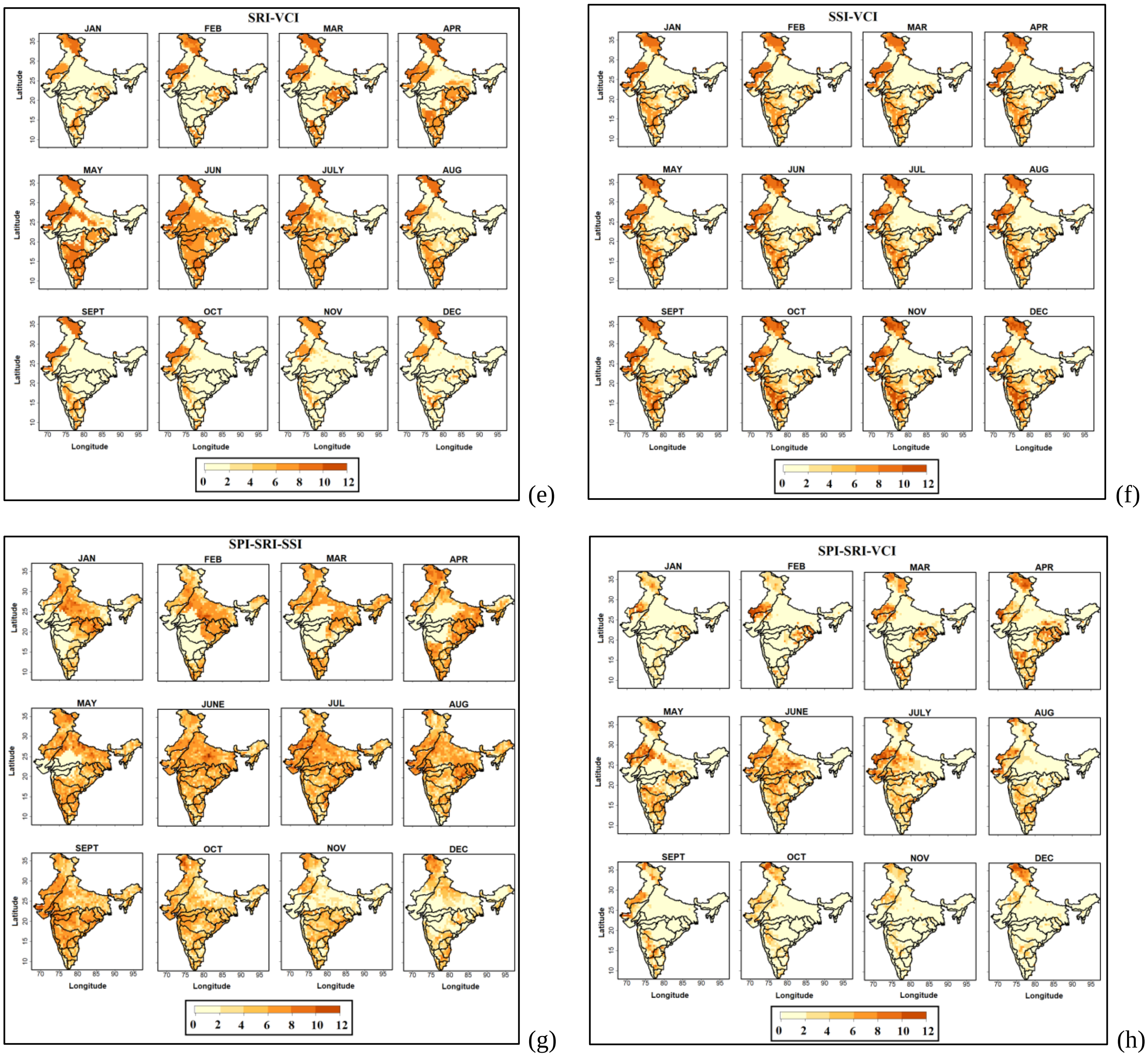

Figure 3.9 Temporal extent of concurrent droughts (figure e to h) for every month during the period 1982-2013.

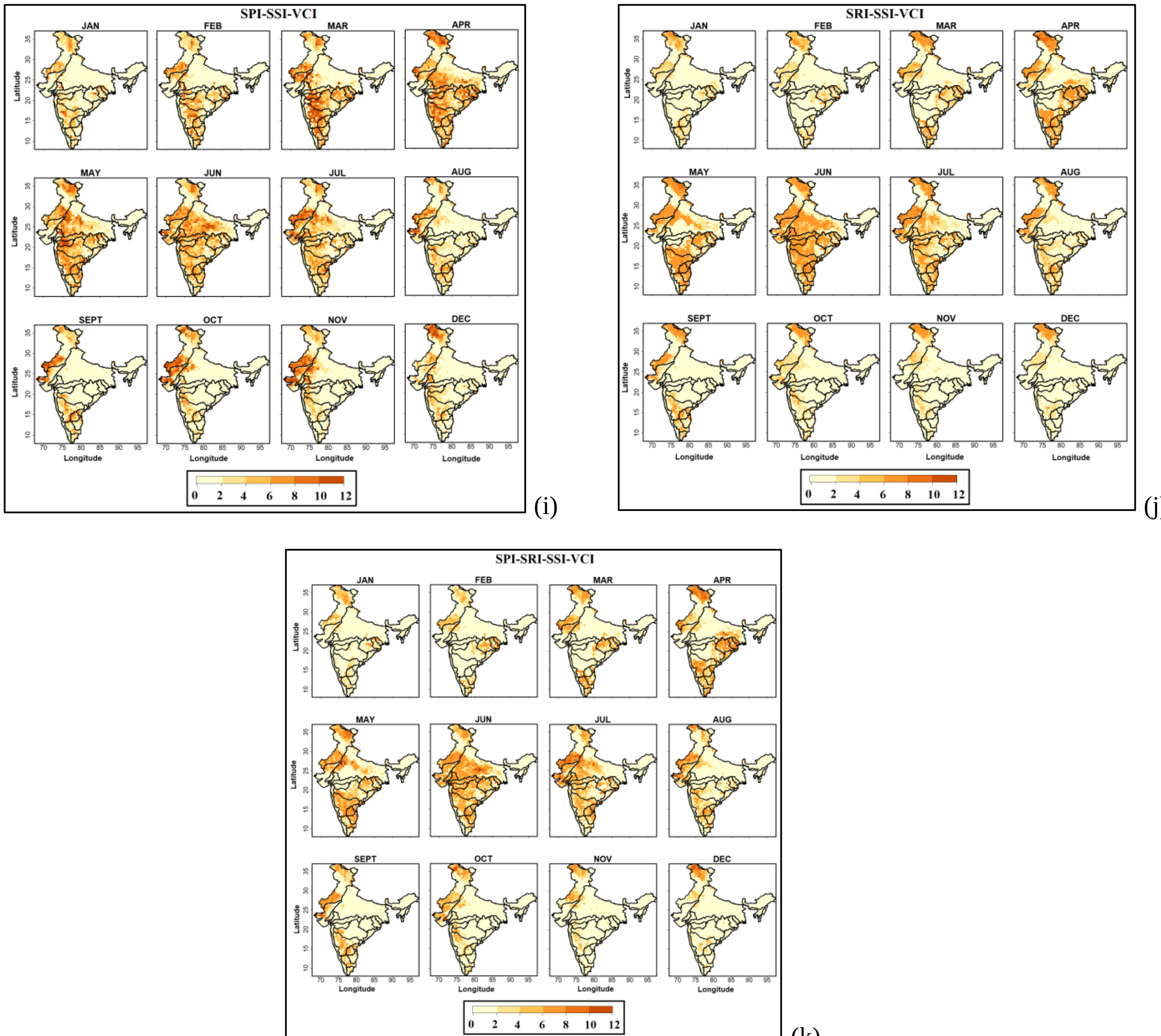

Figure 3.9 Temporal extent of concurrent droughts (figure i to k) for every month during the period 1982-2013.

Figure 3.9 presents the temporal extent of concurrent droughts, where it varies from one to twelve. Combinations such as vegetation- hydrological drought, soil moisture-vegetation drought, and hydrological-soil moisture drought were highly observed combinations. April, May, June, and July are perceived as the most significant months for drought concurrence.

3.3.5 Drought evolution

Figure 3.10 presents the relationship between domain-mean monthly drought indices. The R^2 value demonstrates that 33% of soil moisture and 23% of hydrological variability is due to precipitation anomalies. Interestingly, 50% of soil moisture variability is attributed to the runoff of the study region. Moreover, the Pennar, Subarnarekha, EFRSCB, Krishna, Ganga and Godavari basin illustrate a better coefficient of determination in comparison to other river basins. Additionally, the ANLIB and MRBB basins show a low R^2 value which implies that the soil of the study area achieves maximum soil moisture through runoff only. In case of the Ganga basin, it was observed that there are 42 months of hydrological drought whereas only 20 months with hydrological combined with soil moisture droughts. This indicates that the occurrence of hydrological drought combined with soil moisture drought is about 110% less than the individual hydrological drought. Moreover, the Luni, Western Ghats, ANLIB, Brahmaputra, and Ganga basins observed that hydrological with soil moisture drought is at least 110% less than the hydrological drought. It means irrigation is widely practiced for agricultural activities in the study area. The Open Government Data, India claims that more than 40% of the irrigation rate is practiced in the Indo-Gangetic plane during 2009-2010. Moreover, Annual-Report, 2013-2014 claims that more than 89% of groundwater is used for irrigation purposes in India. Therefore, it is suggested to adopt rapid drought mitigation strategies and policies as soon as the occurrence of meteorological drought in the study area.

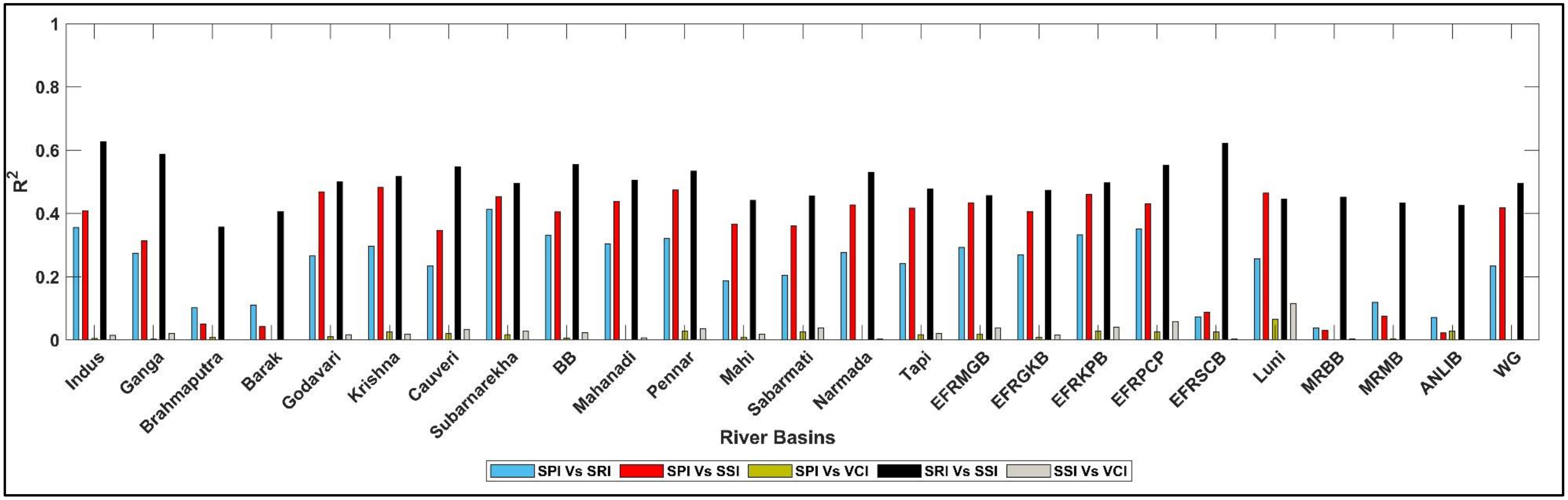

Figure 3.10 Relationship (coefficient of determination (R^2)) between domain-mean monthly [SPI-SRI], [SPI-VCI], [SRI-SSI], [SPI-SSI], and [SSI-VCI].

3.4 Conclusions

Drought is a persistent and recurrent phenomenon that can cause large impacts on the economy, environment, and several important sectors of society. It is very important to understand the impact of all drought types at the regional and national scale and to figure out mitigation measures and adaptation strategies for droughts. Hence, the present study investigates the various drought characteristics occurring in different parts of the country. The main outcomes of present study can be summarized as:

The preliminary examination suggests that hydrological and soil moisture drought severity reaches up to D3 and D4, while meteorological and vegetation drought reaches only up to D1 and S2 severity levels. This simply illustrates that soil moisture and hydrological droughts were more impactful and influential in terms of severity, moreover, similar was observed in terms of spatial extent. The drought trend analysis outcomes imply that meteorological drought has a shorter mean duration and low frequency but with a larger areal extent, which is consistent with past research (Mallya et al., 2015). These outcomes will lead to challenges to agricultural productivity in the arid regions and hence, irrigation is the only possible way to stabilize food production (Leng et al., 2015). Unlike meteorological drought, the other three droughts were relieved by shorter duration, smaller areal extent, and less frequency. Further, temporal extent investigation suggests that insignificant variation is observed for soil moisture and hydrological droughts. Heterogeneous distribution was observed in the temporal extent of vegetation drought in contrast to other drought types. Further, April to July are perceived as drought-prone months and might not suitable for better crop production during these months.

Additionally, investigation of concurrent drought concludes that the majority of the concurrent droughts are made of two drought-based conjunctions. Moreover, it was observed that more than 82% of concurrent droughts are soil moisture drought. This shows the importance of soil moisture more than precipitation in the study area. Results of temporal extent concurrent droughts suggest that concurrent drought years range from 1 to 12. Out of eleven kinds of conjunctions of concurrent droughts, only three conjunctions i.e., hydrological-soil moisture, vegetation-soil moisture, hydrological-vegetation droughts were observed as compared to others. Finally, the drought evolution process demonstrates 50% of soil moisture variability is due to the runoff of the study area. It means runoff is the main source of water for the soil in the study area. Intriguingly, the occurrence of hydrological drought combined with soil moisture drought is 110% less than the individual hydrological drought indicates the role of irrigation and its practice in the study region.

In this study, the hydrological and soil moisture drought is evaluated using reanalysis datasets. However, it is suggested to compare such datasets with observed datasets for exact physical behaviors and performance in drought characterization in the study region (Lin et al., 2014). Moreover, the copula-based analysis may also be helpful to study the drought evolution process and the relationship among different droughts. The present study enables a new approach to investigate drought from several perspectives over India and provide information for drought mitigation and adaptation strategies.

Chapter 4

Copula based analysis of drought characteristics over India

4.1 Introduction

Drought is a large-scale phenomenon due to prolonged deficiency in precipitation levels. Dracup et al., (1980) recognized drought severity and duration as crucial characteristics of a drought event. Here, drought duration indicates the time in which the rainfall deficit occurs whereas severity indicates the aggregate rainfall deficit below a particular threshold. Several probabilistic methods have been developed in the past to examine drought characteristics; however, a significant correlation is not obtained during univariate analysis (Chen et al., 2013). Therefore, it is better to implement a multivariate technique for investigating the joint dependence of drought characteristics and obtain the join probability to describe the duration-severity interaction (Kao and Govindaraju, 2010). However, most of the multivariate techniques are derived from univariate approaches but offers several disadvantages (Michele and Salvadori, 2003), such as the same marginal distribution, complex mathematical derivations, etc.

To overcome such limitations, Copula is a promising way to assess multivariable probability distribution (Sklar, 1959). Copulas are advantageous in modeling joint dependence because they are independent of equality of marginal distribution or normality of variables (Zhang and Singh, 2007). The copula-based approach has been used widely for studying hydro-climatic events, for example, soil moisture and precipitation (AghaKouchak, 2015), extreme events and vegetation drought (Jha et al. 2019), groundwater and precipitation (Reddy and Ganguli 2013), volume and peak flow (Favre et al., 2004), drought duration and severity (Nabaei et al., 2019).

In this study, we used a bivariate copula-based approach to understand the joint dependence of drought characteristics for meteorological, hydrological, and agricultural droughts. In this regard, three types of bivariate copulas (Gumbel, Frank, and Plackett) are estimated for modeling and the best fit copula is selected over 1162 grid points of India. Further, the joint dependence of drought characteristics are analyzed to infer important properties in terms of exceedance probability and return period.

4.2 Data and methodology

4.2.1 Study area and data

In the present analysis, 24 major river basins (as per India-WRIS (2014) classification) of India are selected as a study area. Figure 4.1 describes the river basin ID, location, and nomenclature. India is a climatologically diverse country having high spatial and temporal variability in terms of precipitation and temperature, for example, the maximum precipitation is received by the northern part of the country whereas the lowest is received by the western part of the country. Therefore, all 24 major river basins are important for the drought investigation.

In this study, monthly gridded datasets of precipitation, soil moisture, and runoff during the period 1982-2013 were analyzed. The precipitation data is obtained at a spatial resolution (0.5°×0.5°) from IMD-4 data set (Pai et al., 2014). These datasets were prepared with the use of daily precipitation records over India. IMD data is considered as more accurate dataset for drought analysis (Mishra et al., 2014) as it efficiently captures the temporal and spatial variability of precipitation in India.

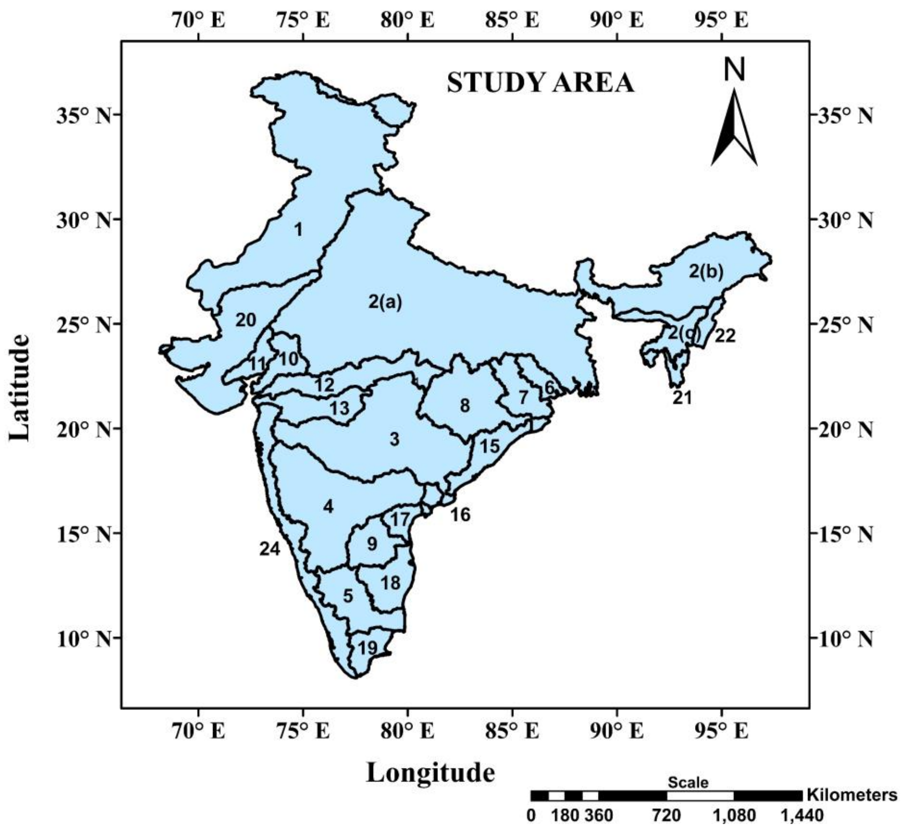

Figure 4.1. Major river basins in India. Source: Watershed Atlas of India (India-WRIS 2012).

Runoff and soil moisture datasets were extracted from the MERRA-2 developed by NASA (available at https://gmao.gsfc.nasa.gov/reanalysis/MERRA-2/data_access/). MERRA-2 is the global reanalysis product to integrate observations of surface landscape and aerosols (Molod et al., 2015). Soil moisture and runoff datasets are extracted for the period 1982-2013 with spatial resolution $1/2^0$ to $2/3^0$. Further, runoff and soil moisture datasets were regridded to 0.5°×0.5° using Inverse-distance Weighting (IDW) method. IDW method is the most widely used method for the approximation of missing data in hydrology.

4.2.2 Methods

Most widely drought indices i.e., standardized precipitation index (SPI), standardized runoff index (SRI) and standardized soil moisture index (SSI) were chosen for defining meteorological, hydrological and soil moisture drought, respectively. In this study, 12-month time scale drought indices are used. Since drought is a multivariate and complex phenomenon, therefore, more efficient techniques (e.g. copula) are required to understand the interrelationship between drought characteristics (Jha et al. 2019; Das et al. 2020). Hence, a copula-based approach is used to perform bivariate distribution. Initially, trend analysis of the drought characteristics is carried out using the MK test at a 5% significance level during the period 1982-2013. However, this trend investigation also recommends that a more effective approach is required to comprehend the drought situation in India. Hence, different copulas were used to build a joint dependence structure among drought characteristics using monthly precipitation (meteorological), runoff (hydrological), and soil moisture (agricultural) data at each grid point in India. Then, the best-fit copula function was selected using the log-likelihood method (Island, 2016). Further, the best copula parameter and best copula were selected based on AIC and BIC values (Cong and Brady, 2012). Finally, based on different copulas, some bivariate probabilistic approaches, for example, exceedance joint return period and probabilities were investigated. Moreover, the conditional approach is also applied to probability and return periods. The methodology of the study is described in Figure 4.2.

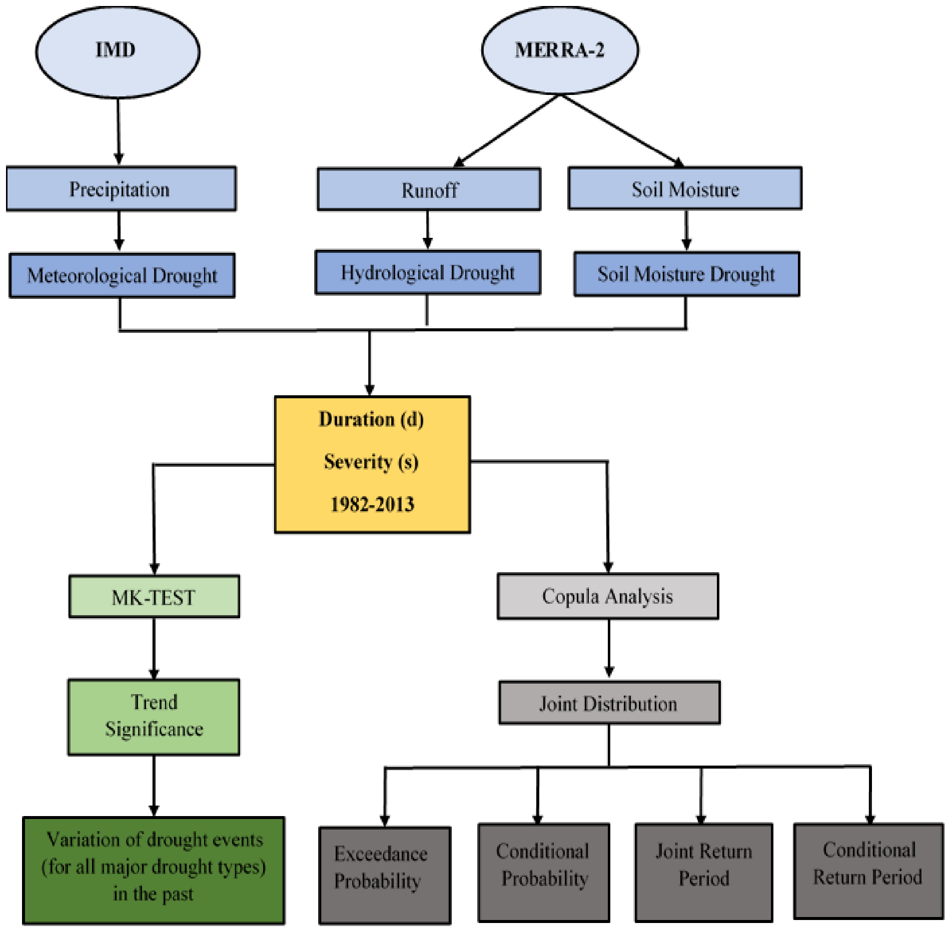

Figure 4.2 Methodological flowchart.

4.2.2.1 Drought characteristics

From the literature review, various drought identification approaches are observed for example, percentile method, discrete Markov process, run analysis, and many more. However, the run theory is widely used in drought analysis and engineering practice (Yevjevich, 1969). Several recent studies have utilized run analysis approach in the evaluation of drought characteristics (Ganguli and Reddy, 2012; Mishra et al., 2009). Here, run analysis approach is used for the computation of the drought duration and severity. In the case of meteorological drought, drought duration (d) can be described as the number of consecutive months in which SPI is less than zero (Shiau, 2006). Within a drought duration (d), the severity (s) can be described as the cumulative summation of negative SPIs during the drought event, which can be expressed as Eq. (4.1):

$$s_n = -\sum_{n=1}^{d} SPI_n \tag{4.1}$$

Additionally, in this study, SRI and SSI values are used instead of SPI in case of hydrological and soil moisture drought respectively. These two important drought parameters i.e., duration and severity (d & s) are strongly correlated and can be modeled using various distributions (Chang and Stenson, 1990). As different points in a single river basin might have different rainfall characteristics, hence, might follow different distributions.

Figure 4.3 illustrates the drought characteristics using the SPI time-series and drought events. Interarrival time (L) indicates the time between the commencement of one drought to the commencement of the next drought event.

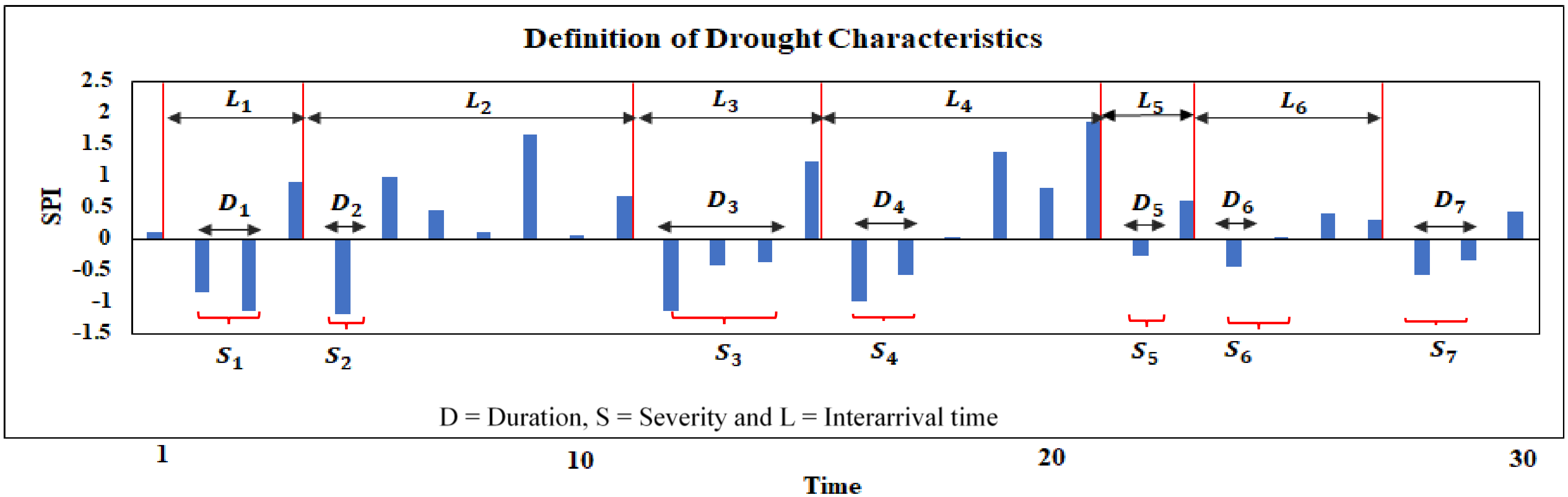

Figure 4.3 Definition of drought characteristics.

4.2.2.2 Trend analysis of drought characteristics

In the present investigation, the trend analysis is performed for the drought severity and drought duration for all three drought types using the MK test at a 5% significance level during the period 1982-2013. The outcomes of MK test were categorized based on Z statistics: significantly increasing (when $Z \geq 1.96$), increasing ($1.96 < Z > 0$), no trend ($Z=0$), decreasing ($0 < Z > -1.96$), and significantly decreasing trend ($Z \leq (-1.96)$) (Dai, 2013; Mallya et al., 2015). The MK test is very useful in trend analysis as it shows accurate results especially in hydrologic and climatic data (Mann, 1945; Mishra and Cherkauer, 2010).

4.2.2.3 Copula based bivariate probabilistic model

Bivariate analysis is incorporated in the present study to determine the joint dependence among drought characteristics. The copula-based technique is used which provides a robust way to formulate a bivariate distribution. Sklar's Theorem states that a multivariate distribution $F(x_1, x_2 \dots x_n)$ can be expressed by a Copula as Eq. 4.2:

$$F(x_1, x_2, \dots . x_n) = C\left[F_{X_1}(x_1), F_{X_2}(x_2) \dots F_{X_n}(x_n)\right] = C(u_1, u_2 \dots u_n) \qquad (4.2)$$

Where $F_{x_i}\ (x_i)$, denoted by u_i in the copula-definition represents the CDF of i^{th} variable. Elliptical copulas such as t and Gaussian have various properties of the multivariate Gaussian distribution (Renard and Lang, 2007; Sraj et al., 2015). Another widely used copula families are the Archimedean copulas (Frank, Clayton, Gumbel) which offer great flexibility in data modeling with inconsistent dependencies (Grimaldi and Serinaldi, 2006).

In the present analysis, three copulas i.e., Gumbel, Frank, and Plackett copula are selected. Gumbel and Frank copula are the most extensively applied copula because they provide more flexibility in data modeling. The above-mentioned copulas offer several benefits. Firstly, they provide more flexibility in developing the joint dependence structure of data. Secondly, these single parameter copulas enable flexible as well as straightforward modelling of the dependence between variables (Ganguli and Reddy 2014). Thirdly, they are capable of modeling positively and negatively correlated random variables (Uttarwar et al., 2020).

Importantly, it is important to initially find the appropriate marginal distribution of data before proceeding to model the joint distributions. In this study, the drought characteristics were fit with five marginal distributions (normal, log-normal, exponential, gamma and Weibull distributions), then the best fit distribution was obtained employing K-S (the Kolmogorov-Smirnov test). Once the best fit marginals were estimated, the copula parameters for the three copula types were obtained. Further, these three copulas (Gumbel, Frank, and Plackett) were tested and the best copula parameters and copula were selected based on two model performance indices, Bayesian Information Criterion and Akaike Information Criterion. The BIC and AIC are widely used in quantifying the comparative performance of models (Jha et al. 2019; Das et al. 2020). Eventually, the joint behavior of different sets of drought characteristics was analyzed to infer important properties in terms of exceedance probability and return periods.

The parameters and structure of the above-mentioned copulas are presented concisely in Eqs. 4.3, 4.4 and 4.5. Please refer Sadegh et al. (2017) for more details.

Gumbel Copula:

$$C_G(u, v) = \exp\{-[(-\ln(u))^{\theta} + (-\ln(u))^{\theta}]^{1/\theta}\} \tag{4.3}$$

Plackett Copula:

$$C_P(u, v) = \frac{1+(\theta-1)(u+v)-\sqrt{[1+(\theta-1)(u+v)]^2-4\theta(\theta-1)uv}}{2(\theta-1)} \tag{4.4}$$

Frank Copula:

$$C_F(u, v) = -\frac{1}{\theta} \ln \left[1 + \frac{(\exp(-\theta_u)-1)(\exp(-\theta_v)-1)}{\exp(-\theta)-1}\right] \quad (4.5)$$

Where θ is copula parameter and parameter range of Gumbel, Plackett and Frank copulas are $[1,\infty)$, $\theta \in (0, \infty)$, and $\theta \in R$ 0, respectively (Das et al., 2020a). Figure 4.4 gives the overview of the copula methodology. The Copula based analysis was done by developing code in MATLAB and the plots were prepared using R studio.

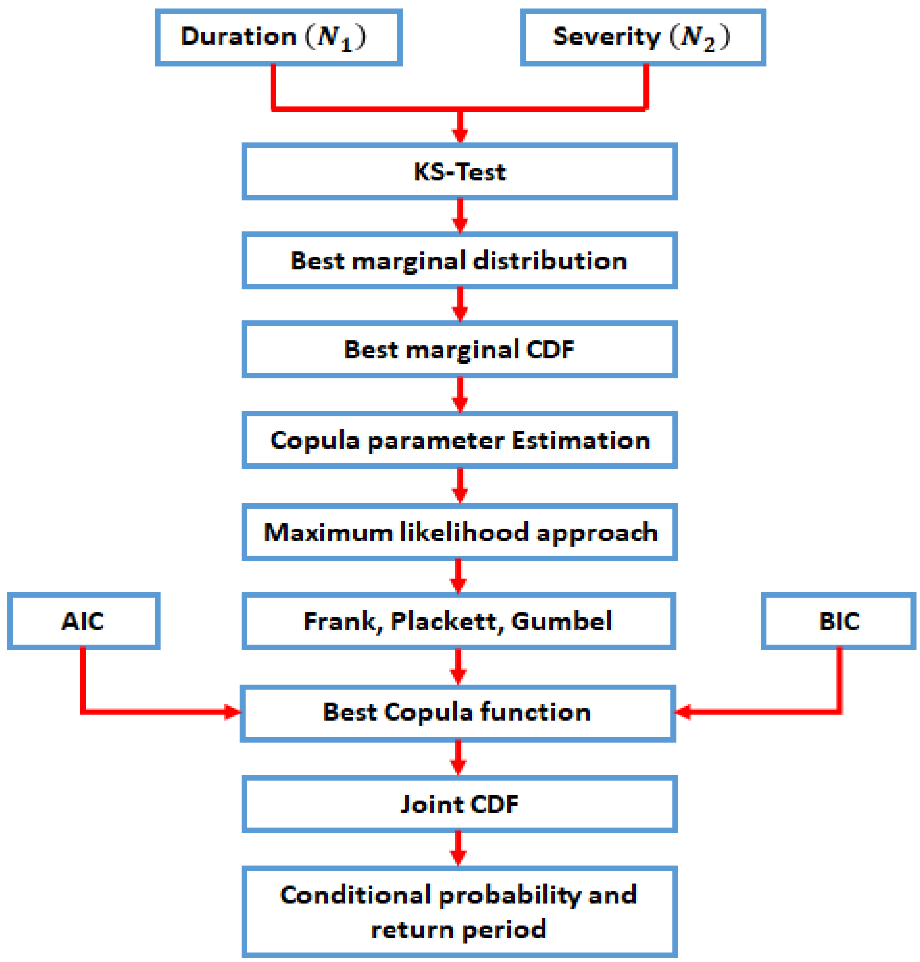

Figure 4.4 Flow chart of the copula-based methodology.

4.2.2.4 Probabilistic analysis

The copula-based joint dependence of drought characteristics is very helpful to derive some significant information about drought management. For example, the probability that both the drought characteristics i.e., severity and duration concurrently exceed specific thresholds is considered a crucial situation for a water distribution systems. In this study, the exceedance probability is computed which can be described as the probability where both drought duration as well as severity surpass a particular threshold. In the current analysis, exceedance probability is computed at the thresholds of 25^{th},50^{th},75^{th} and 95^{th} percentile values of drought variables for all 24 major river basins of India.

The exceedance probability cannot be achieved through a separate analysis of drought characteristics; however, it can be easily obtained through copulas (Eq. 4.6).

$$P(D \geq d, S \geq s) = 1 - F_D(d) - F_S(s) + C(F_D(d), F_S(s)) \tag{4.6}$$

Similarly, computation of conditional probabilities can be done using bivariate drought distribution. This is crucial to estimate the probability of drought duration provided that the drought severity passing a certain threshold s'. The equation for conditional drought duration distribution can be expressed as Eq. 4.7 (Shiau, 2006):

$$P(D \leq d \mid S \geq s') = \frac{P(D \geq d,\ S \leq s')}{P(S \geq s')} = \frac{F_D(d) - F_{D,S}(d, s')}{1 - F_S(s')}$$

$$= \frac{F_D(d) - C(F_D(d), F_S(s'))}{1 - F_S(s')} \tag{4.7}$$

Similarly, Eq. 4.8 presents the equation for conditional drought severity distribution provided the duration exceeding a specific threshold d'.

$$P(S \leq s \mid D \geq d') = \frac{F_S(s) - C(F_D(d'), F_S(s))}{1 - F_D(d')} \tag{4.8}$$

These conditional probabilities were computed for drought characteristics in the present analysis.

4.2.2.5 Return period analysis

Evaluation of the return period plays a crucial role in water management. Eq. 4.9 represents the univariate return period as derived by Shiau and Shen, (2001) as:

$$T_D = \frac{E(L)}{(1-F_D(d))} \tag{4.9}$$

where E (L) is the expected drought interarrival time. Similarly, in case of drought severity, it can be expressed as Eq. (4.10):

$$T_S = \frac{E(L)}{(1-F_S(s))} \tag{4.10}$$

where T_D and T_s are the expected return period of duration and severity respectively.

In the present analysis, the bivariate return period is also computed for two conditions: (a) AND return period where both drought severity as well as duration exceed a certain value (*S* ≥ *s* and *D* ≥ *d)* (Eq. 4.11); (b) OR return period where either severity and duration exceeding a specific value (*S* ≥ *s* or *D* ≥ *d)* (Eq. 4.12). Both are expressed below as (Shiau, 2006):

$$\mathrm{T_{DS}} = \frac{\mathrm{E(L)}}{\mathrm{P(D \geq d,\ \ S \geq s)}} = \frac{\mathrm{E(L)}}{1-\mathrm{F_D(d)}-\mathrm{F_S(s)}+\mathrm{C(F_D(d)\ ,F_S(s))}} \tag{4.11}$$

$$\mathrm{T'_{DS}} = \frac{\mathrm{E(L)}}{\mathrm{P(D \geq d, or\ \ S \geq s)}} = \frac{\mathrm{E(L)}}{1-\mathrm{C(F_D(d)\ ,F_S(s))}} \tag{4.12}$$

Where T_{DS} and T'_{DS} represents the AND & OR joint return period, respectively.

Moreover, the joint return periods may also be expressed for conditional situations. The joint return period of drought duration provided drought severity exceeding a specific threshold and vice-versa as defined in Eqs. 4.13 and 4.14, respectively.

$$\mathrm{T_{D|S \geq s}} = \frac{\mathrm{T_S}}{\mathrm{P(D \geq d,\ \ S \geq s)}} = \frac{\mathrm{E(L)}}{1-\ \mathrm{F_S(s)}} \times \frac{1}{1-\mathrm{F_D(d)}-\mathrm{F_S(s)}+\mathrm{F_{DS}(d,s)}}$$

$$= \frac{1}{[1-\ \mathrm{F_S(s)}]\times[1-\mathrm{F_D(d)}-\mathrm{F_S(s)}+\mathrm{C(F_D(d)\ ,F_S(s))}]} \tag{4.13}$$

$$T_{S|D\geq d} = \frac{T_D}{P(D\geq d,\ S\geq s)} = \frac{E(L)}{1-\ F_D(d)} \times \frac{1}{1-F_D(d)-F_S(s)+F_{DS}(d,s)}$$

$$= \frac{1}{[1-\ F_D(d)]\times[1-F_D(d)-F_S(s)+C(F_D(d),F_S(s))]} \tag{4.14}$$

where $T_{S|D\geq d}$ and $T_{D|S\geq S}$ represents the conditional return period for S (given $D \geq d$) and D (given $S \geq s$), respectively. These conditional return periods were also computed for drought characteristics in the present analysis.

4.3 Results and discussion

4.3.1 Identification of drought characteristics and their trend analysis

Before progressing to the probabilistic modelling, we computed the mean drought characteristics i.e., mean drought duration and mean drought severity from observed meteorological, hydrological, and soil moisture droughts defined by SPI, SRI, and SSI respectively (Figure 4.5 (a&b)). From the investigation, it was found that the mean severity and mean duration of soil moisture and hydrological drought are higher in the western river basins and some parts of the Brahmaputra basin. Reduction in light precipitation days made western river basins more vulnerable to drought conditions because these reductions were more severe in north-eastern and western parts of India (Mishra, A. & Liu, 2014). Mundetia and Sharma, (2014) also suggest that the Western part of India particularly Rajasthan has high rainfall variability and thus, vulnerable to drought. However, the mean severity and mean duration of meteorological drought are higher in the eastern part of the country. In this regard, Mishra and Liu, (2014) have suggested that the northeastern part of India observed an increase in prolonged droughts per decade. The preliminary investigation suggests that the separate analysis of drought severity and duration provides a limited assessment of drought characteristics; therefore, it is better to adopt a multivariate approach and develop the joint dependence structure to describe the interconnection among drought characteristics.

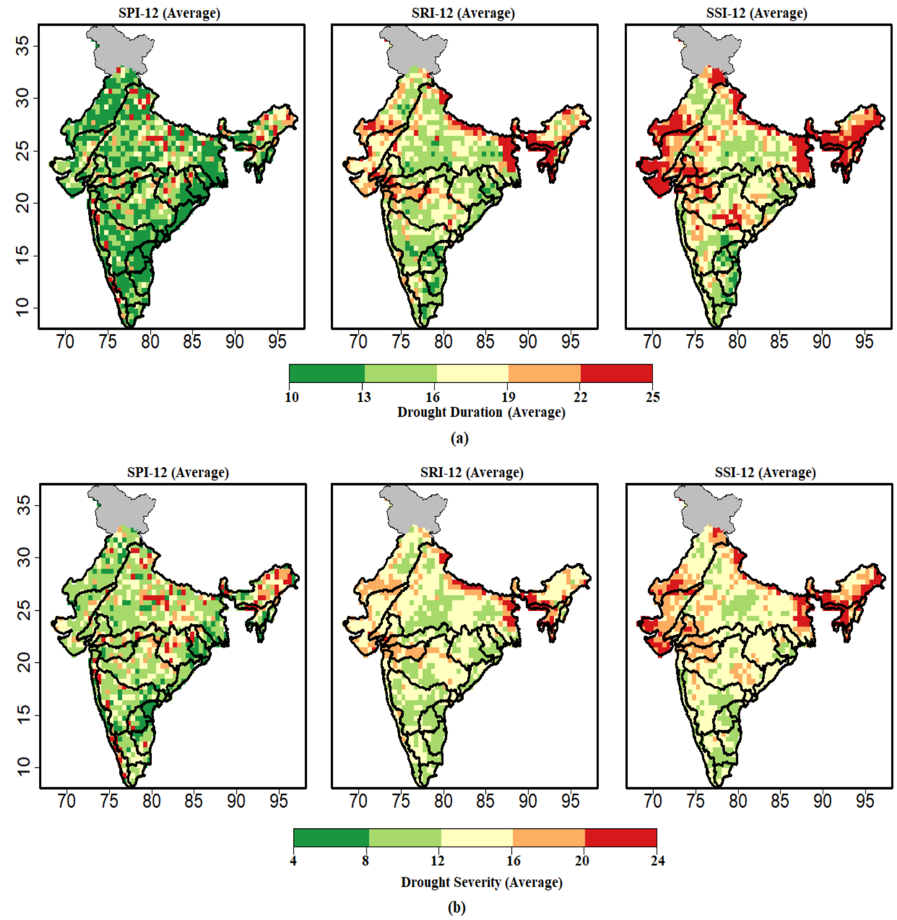

Figure 4.5 Basin wise mean (a) drought duration and (b) drought severity during the period 1982-2013.

Trend analysis is carried out for the drought characteristics of all three drought types using a non-parametric Mann Kendall (MK) test. The outcomes of the MK test were categorized based on Z statistics: significantly increasing (when $Z \geq 1.96$), increasing ($1.96 < Z > 0$), no trend ($Z=0$), decreasing ($0 < Z > -1.96$), and significantly decreasing trend ($Z \leq (-1.96)$). The duration and severity trend results imply no significant decrease or increase in the majority of the study area for all three drought types (Figure 4.5(c)). This random variability of drought properties (duration and severity) makes it difficult to interpret their joint dependence in the trend analysis. Hence, the trend analysis outcomes recommend that a more effective approach is required to comprehend the drought situation in India.

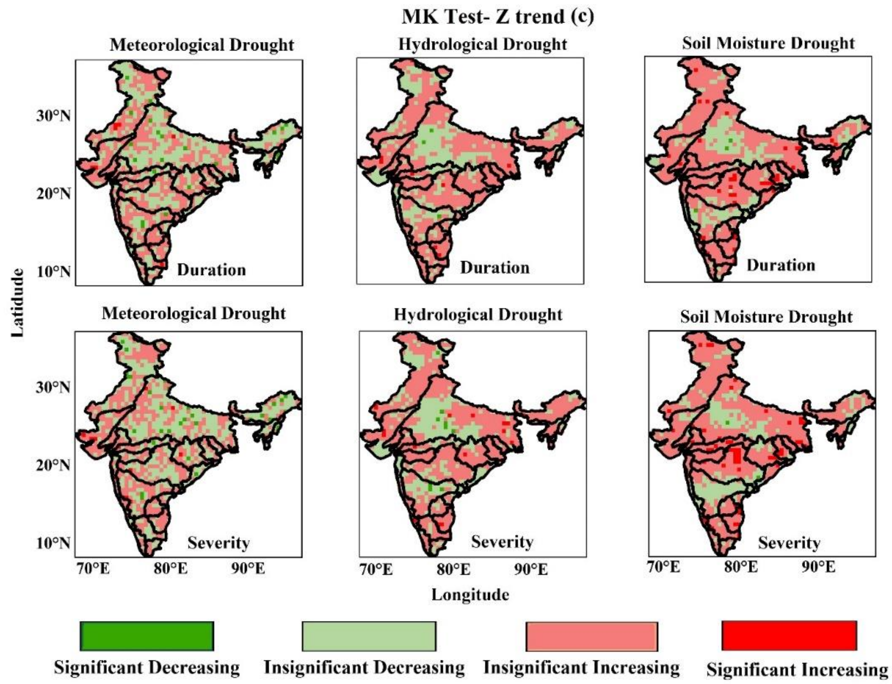

Figure 4.5 (c) Trend analysis of drought duration and severity during the period 1982-2013.

4.3.2 Bivariate analysis of exceedance probability

In the present analysis, we have used several types of distribution, out of which the best one is chosen. Past investigations have used several statistical tests such as KS test, chi-squared test, and many more. However, in the present analysis, AIC is selected as it avoids model overfitting. Further, marginal distributions are determined for both drought duration and severity during 1982-2013. As the best fit marginal distribution is selected, the next step is the selection of the best copula function through maximum likelihood function. Further, the best copula and best copula parameters are computed based on AIC and BIC values. The computation of the best copula, as well as its parameter, plays a vital role in the computation of joint return period and exceedance probability in the present analysis.

Once the joint probabilities are obtained, the exceedance probability is computed (using Eq. 4.6) for different thresholds of drought characteristics at each grid point in India. Figure 4.6a shows exceedance probability for meteorological, hydrological, and soil moisture drought characteristics, where drought duration and drought severity simultaneously exceed 50^{th} percentile values (See Figure 4.6b for 25^{th}, 75^{th} and 95^{th} percentile). To understand the drought occurrence, here, the 50^{th} percentile value results are discussed as they can provide better information. Results show that most of the basins in the country were susceptible to meteorological drought conditions (Figure 4.6a).

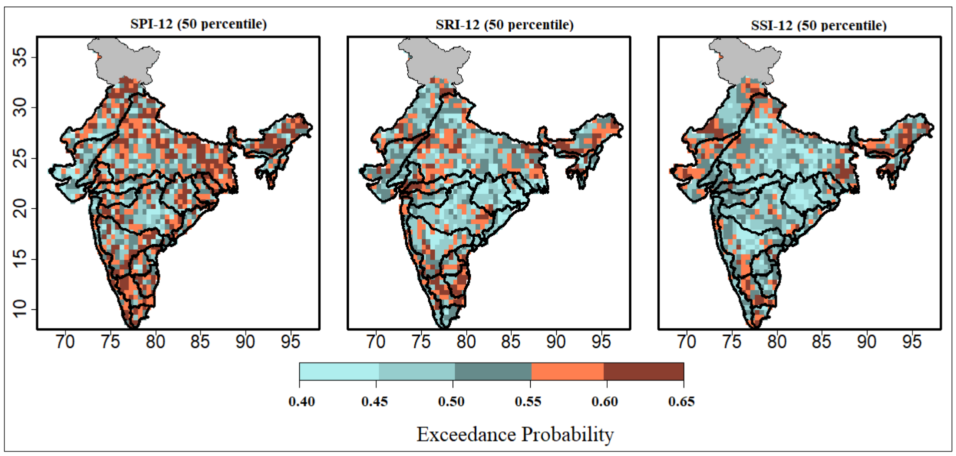

Figure 4.6 (a) Spatial exceedance probability at drought duration and severity exceeding their 50^{th}percentile value for meteorological (SPI-12), hydrological (SRI-12) and soil moisture drought (SSI-12).

A high likelihood of meteorological drought indicates that precipitation shortage is the major risk to the river basins of India. An almost complete study area demonstrated excessive chances of meteorological drought in case of lower exceedance probability scenarios (25^{th} percentile). This might be due to significant decreasing trends of seasonal and annual rainfall while increasing trends of average temperature (Pingale et al., 2014). Kumar et al., (2013) also suggest a general increase in the moderate meteorological droughts during the recent decades.

Moreover, in the case of hydrological drought, Eastern India, some parts of the Western region of India, and the Southern part including EFRKPB, EFRPCB, and Pennar river basins are found to be more vulnerable. During the higher exceedance probability scenario (i.e., 75^{th} percentile), Subernrekha, Mahanadi, Krishna, and Brahmani & Baitarani river basins are found to be more susceptible to both hydrological and soil moisture droughts which is unclear from the univariate analysis. The prolonged precipitation deficit and high temperature would result in soil moisture depletion leading to soil moisture droughts in the Southern part of India and the Western region and similar was found in Pingale et al., (2014). Mishra et al., (2014) also suggested that the majority of the above-mentioned regions of India have chances of increased soil moisture-based droughts during 1980-2008. Hence, results of exceeding probabilities (multivariate analysis) illustrate that the river basins in Central India (Tapi, Narmada) and Southern India (Cauveri, Pennar, EFRSCB, EFRPCB) are witnessing drought persistence. The occurrence of persistent droughts is common in the southern region of India (Amrit et al., 2018). Regions like Central Maharashtra and Southern coast of India are also highlighted for witnessing regional droughts during recent decades (Mallya et al., 2015). Results obtained from simultaneous exceedance of a certain threshold of drought characteristics are much useful and important as compared to the separate investigation of drought severity and duration.

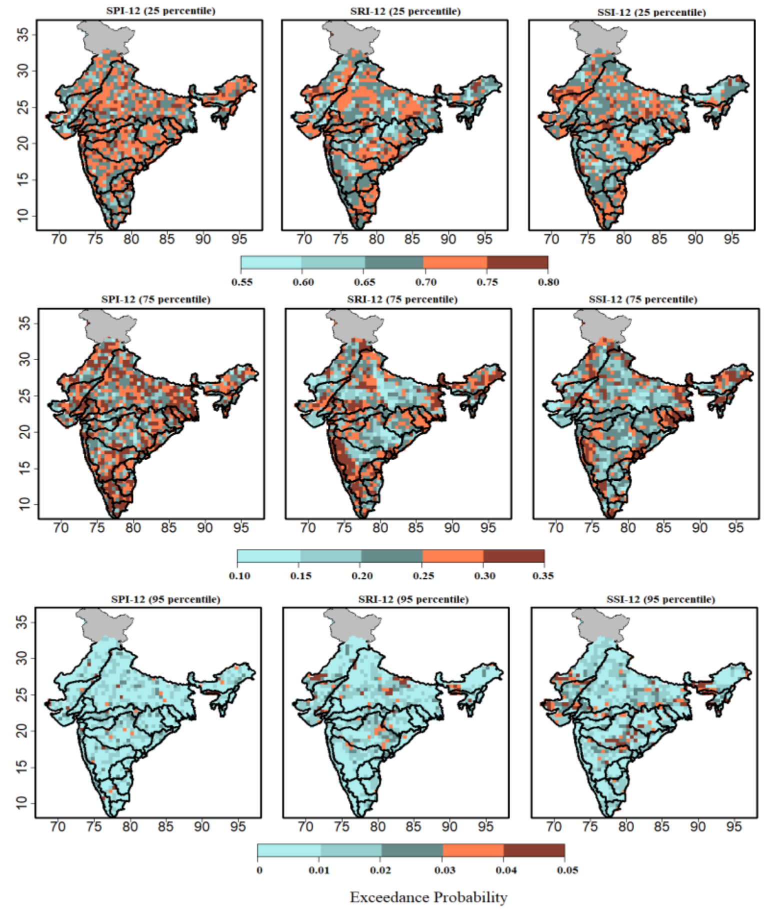

Figure 4.6 (b) Exceedance probabilities 25^{th}, 75^{th} and 95^{th} percentile values for meteorological (SPI-12), hydrological (SRI-12) and soil moisture drought (SSI-12).

4.3.3 Conditional probability of drought characteristics

The conditional probabilities can be easily computed using Eq. 4.7 and 4.8 at 25^{th},50^{th} and 75^{th} percentile values of drought duration and severity at each grid points in India. Figure 4.7a presents conditional probability at 50^{th} percentile of drought duration where drought severity exceeding thresholds of 50^{th} percentile values respectively. However, the conditional probability at 25^{th}, $50^{th}$and 75^{th} percentile of drought duration where severity exceeding several thresholds of 25^{th},50^{th} and 75^{th} percentile values are shown in Figure 4.7 (b), (c), and (d), respectively. In case of meteorological drought (Figure 4.7a), river basins like Tapi, Godavari, and Western region (Luni and Sabarmati basins) of India show higher conditional probability at 50^{th} percentile. High rainfall variability and severe reduction in light precipitation days made western India vulnerable to drought events (Mishra, A. & Liu, 2014; Mundetia and Sharma, 2014). Similarly, in terms of hydrological drought, river basins of Sothern India including Krishna, BB, EFRMGB, EFRGKB, EFRKPB, and Mahanadi river basins are found to be more susceptible to drought conditions at 50^{th} percentile. However, for the same duration, increase in severity (75^{th} percentile) showed very low likelihood of hydrological drought to all river basins of India except southern India. This suggests that hydrological drought is not severe over India except southern India. In case of soil moisture drought, Southern India (Pennar, EFRGKB, EFRKPB), Subarnarekha and the Western Ghats are more susceptible for drought conditions at 50^{th} percentile. Recently, Jha et al., (2019) also suggest that more than 50% of 16 river basins of India have low soil moisture and can be affected by droughts easily. The results from the present analysis indicate that for all drought types, the river basins in Southern India (Cauveri, Pennar, EFRSCB, EFRPCB) and Western part (Luni and Sabarmati) of India are showing high conditional probability and hence, more susceptible to drought, similar was found in Mallya et al., (2015) and Amrit et al., (2018). Results of conditional probabilities using bivariate drought distribution provide a deep understanding of the drought in India for given thresholds of drought duration and severity rather than univariate analysis.

However, the conditional probability at 25^{th}, $50^{th}$and 75^{th} percentile of drought severity where duration exceeding several thresholds of 25^{th},50^{th} and 75^{th} percentile values are shown in Figure 4.7 (e-g), respectively.

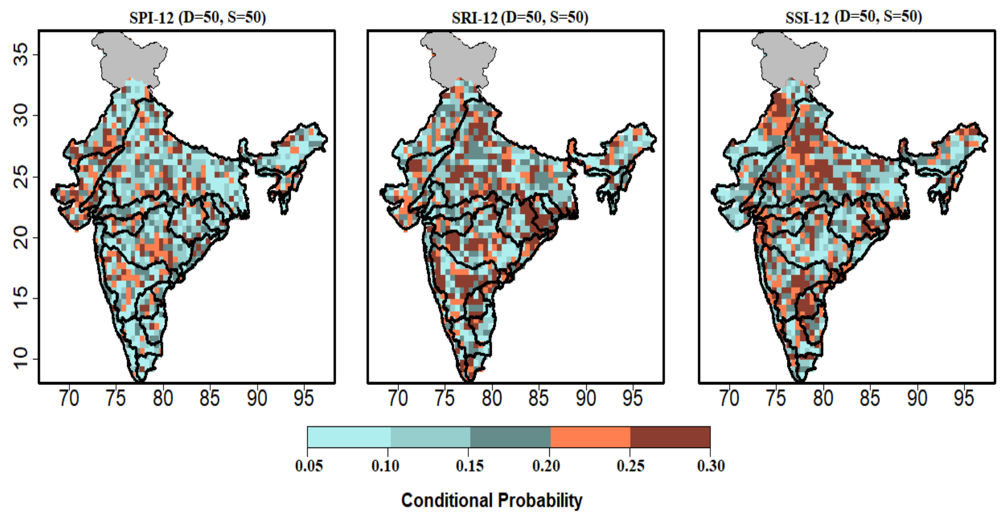

Figure 4.7 (a) Conditional probability at 50^{th} percentile of drought duration where drought severity passing a particular threshold of 50^{th} percentile value for meteorological (SPI-12), hydrological (SRI-12) and soil moisture drought (SSI-12).

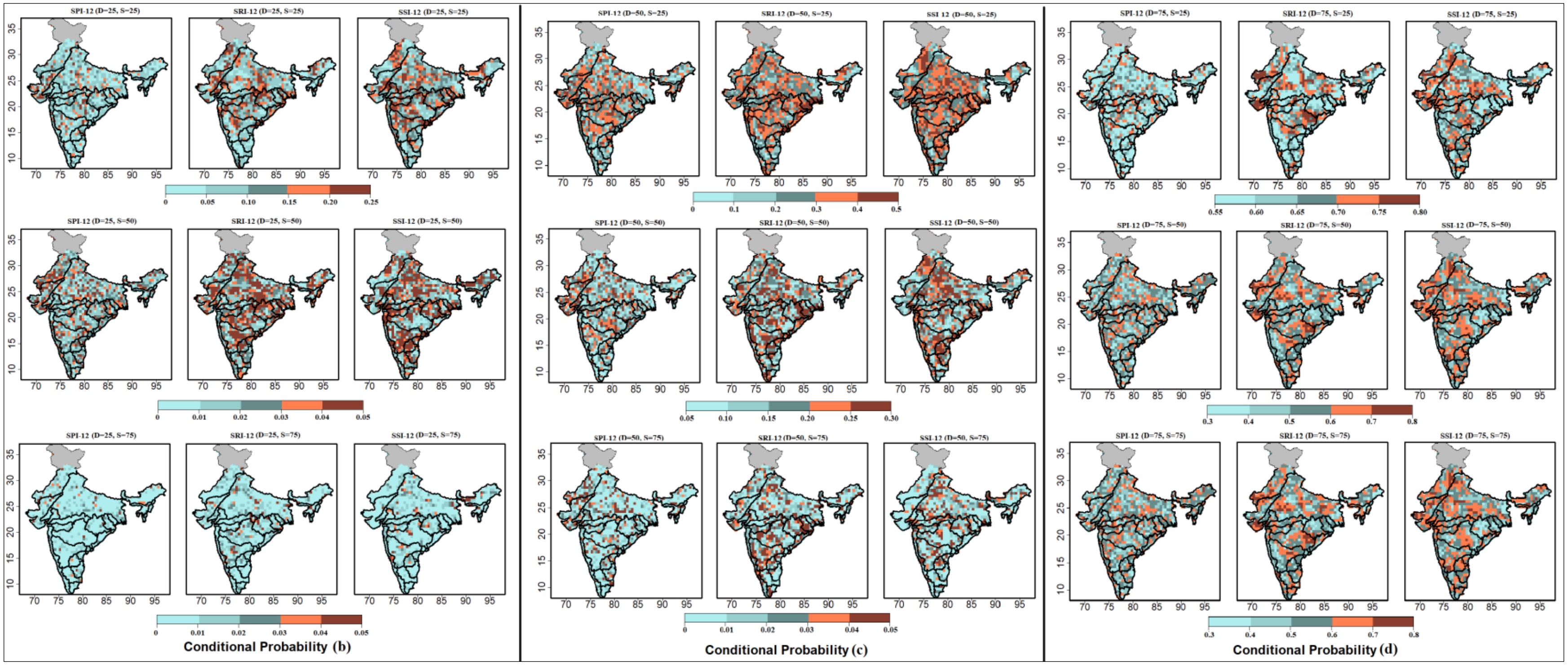

Figure 4.7 (b-d) Conditional probability at 25^{th}, 50^{th} and 75^{th} percentile of drought duration where drought severity passing a particular threshold of 25^{th},50^{th} and 75^{th} percentile values for meteorological (SPI-12), hydrological (SRI-12) and soil moisture drought (SSI-12).

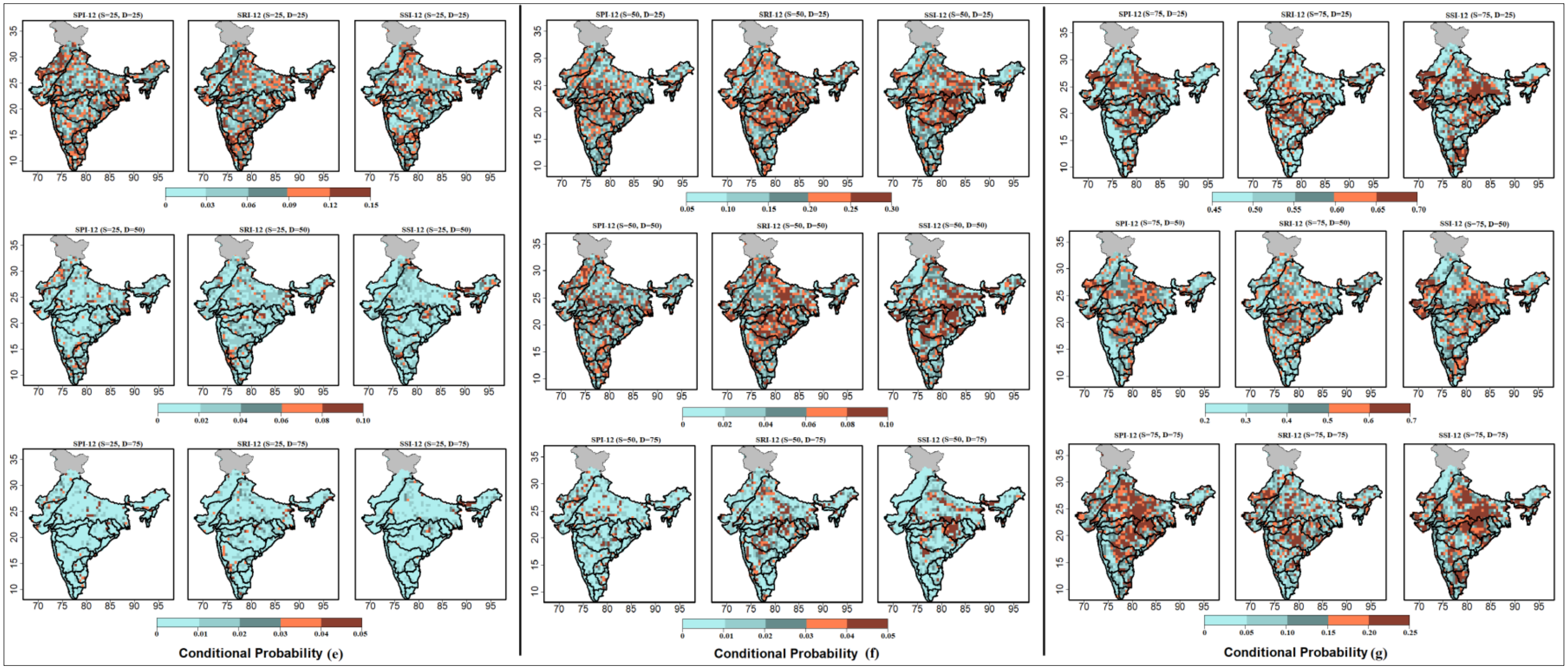

Figure 4.7 (e-g) Conditional probability at 25^{th}, 50^{th} and 75^{th} percentile of drought severity where drought duration passing a particular threshold of 25^{th},50^{th} and 75^{th} percentile values for meteorological (SPI-12), hydrological (SRI-12) and soil moisture drought (SSI-12).

4.3.4 Joint return period

This segment deals with the computation of the return period using the 'AND' and 'OR' criteria. Figure 4.8a presents the AND joint return period at 50^{th} thresholds of severity and duration. Figure 4.8b presents the AND joint return period at various thresholds (25^{th}, 75^{th} and 95^{th} percentile values) of severity and duration. Whereas OR return period is shown in Figure 4.8c. Results indicate that Eastern India (Brahmaputra, Barak, MRBB) and Western regions of India such as Tapi, Sabarmati, Mahi, Luni demonstrate the maximum return period in case of all percentile values for meteorological, hydrological, and soil moisture drought. However, in the case of meteorological drought, Indus, Narmada, and the Western Ghats also show the highest return period. A longer return period prevails in the Western Ghats because it receives the highest rainfall, one of the ecologically rich regions, and presence of evergreen forest. Moreover, this region is known to be resilient to hydroclimatic disturbances (Sharma and Goyal 2018b; Jha et al. 2019). Whereas the southern river basins of the country (Cauveri, EFRPCB, Krishna), Sabarmati, BB basins show smaller joint return periods in case of meteorological drought. This indicates that droughts are very common in southern India but with a lower return period. Moreover, hydrological and soil moisture droughts also show a smaller return period in southern river basins such as EFRGKB, EFRKPB, EFRPCB, EFRSCB, Pennar, Cauveri. The shorter return period in Southern India is also validated by Amrit et al., (2018), where they conclude frequent drought occurrence once in every 5-6 years in a larger part of Southern India. Outcomes of the joint return period will enable the stakeholders and policymakers to formulate better guidelines related to drought management and also helpful in managing and designing the water resource systems in drought conditions, especially in drought-prone areas.

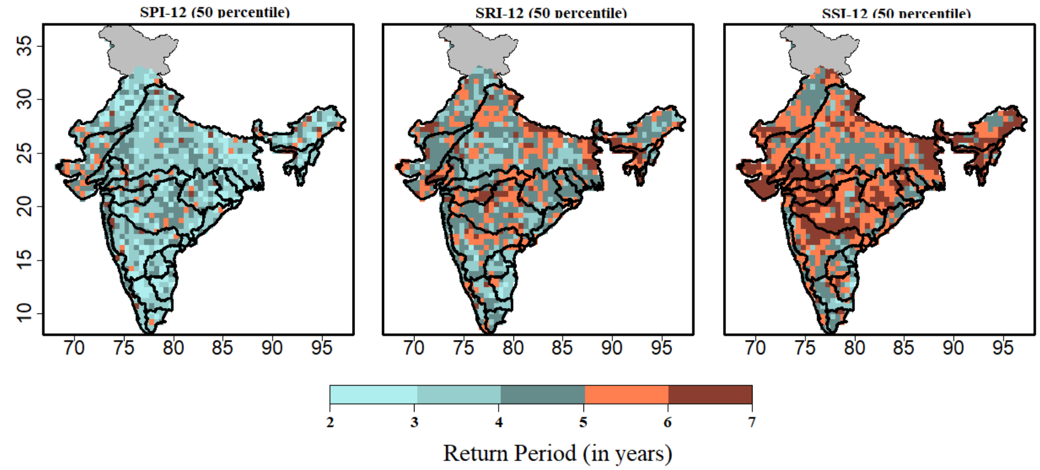

Figure 4.8a AND return period of drought characteristics exceeding their 50^{th} percentile value for meteorological (SPI-12), hydrological (SRI-12) and soil moisture drought (SSI-12).

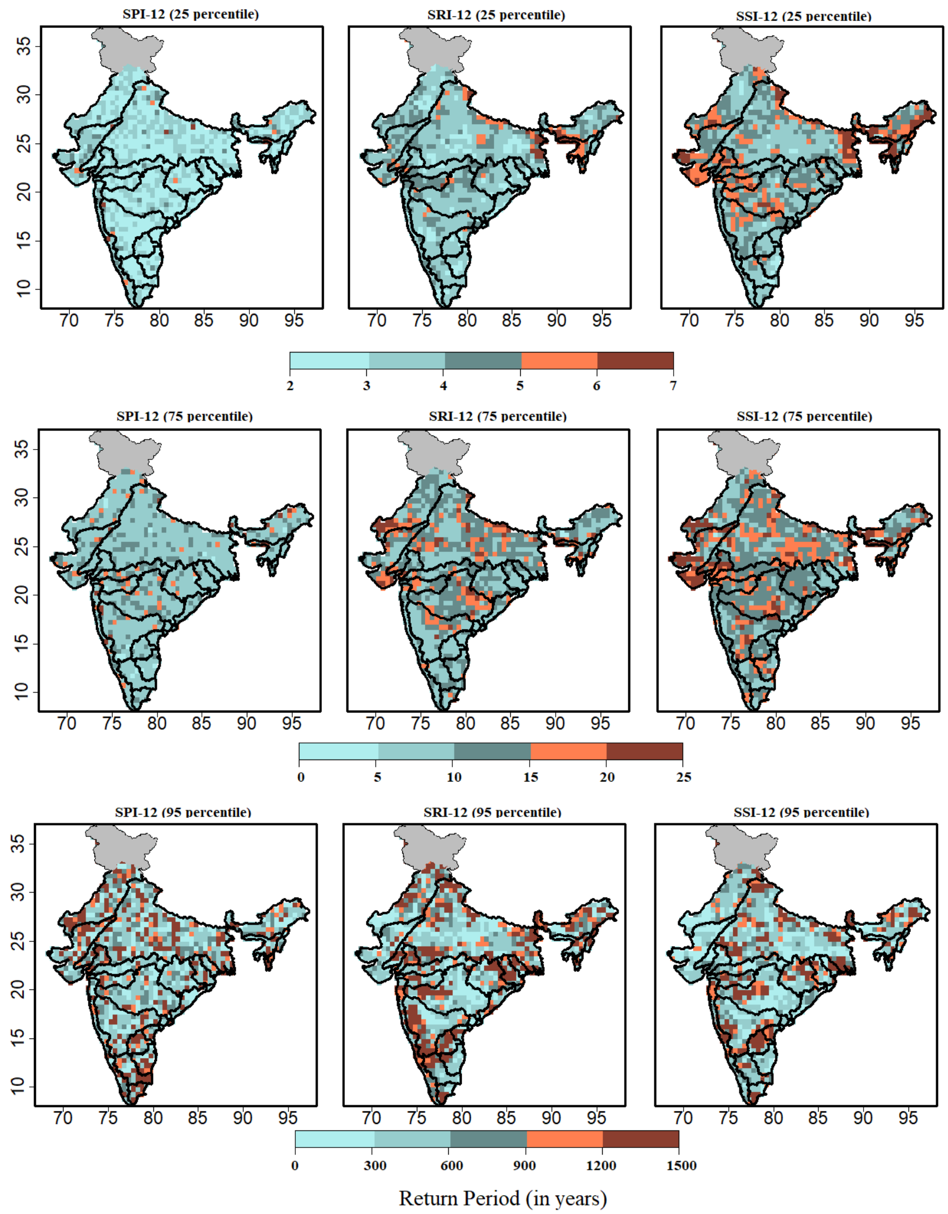

Figure 4.8b AND return period of drought characteristics surpassing their 25^{th}, 75^{th} and 95^{th} percentile values for meteorological (SPI-12), hydrological (SRI-12) and soil moisture drought (SSI-12).

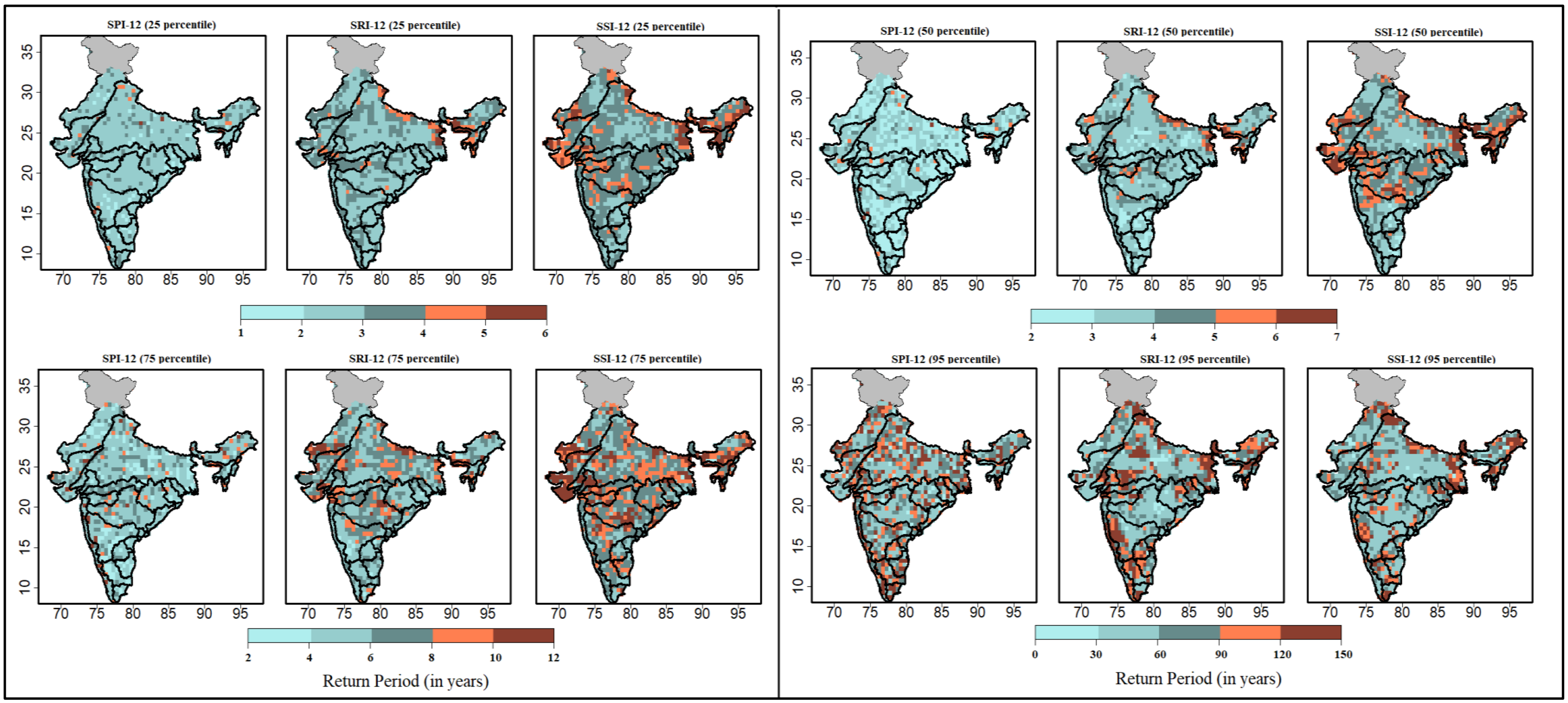

Figure 4.8c OR return period of drought characteristics passing their 25^{th}, 50^{th}, 75^{th} and 95^{th} percentile values for meteorological (SPI-12), hydrological (SRI-12) and soil moisture drought (SSI-12).

4.3.5 Conditional joint return period

Finally, the conditional return period of drought duration with a threshold at 25^{th}, 50^{th} and 75^{th} percentile was evaluated at each grid point using Eq. 4.13 where the severity exceeding several thresholds (25^{th}, 50^{th} and 75^{th} percentile). Figure 4.9a illustrates the conditional return period at 50^{th} percentile of drought duration where drought severity exceeding thresholds of 50^{th} percentile values respectively. However, the conditional return period at 25^{th}, $50^{th}$and 75^{th} percentile of drought duration where severity exceeding several thresholds of 25^{th},50^{th} and 75^{th} percentile values are shown in Figure 4.9(b-d), respectively. In the case of meteorological droughts (Figure 4.9a), almost all the river basins in India showed a lower conditional return period i.e., frequent occurrence of meteorological droughts at a threshold of 50^{th} percentile. Mallya et al., (2015) also suggest an increasing trend of drought frequency during recent decades. However, in the case of hydrological and soil moisture droughts, southern India such as Krishna, Cauveri, EFRPCB, and BB basins showed smaller conditional return periods. Moreover, the western part of the country (Luni, Mahi, Sabarmati), Eastern India, and Central India like Tapi river basin in southern India such as Krishna, Cauveri, EFRPCB, and BB basins show smaller conditional return periods in case of meteorological drought whereas EFRKPB, EFRPCB, EFRSCB, EFRGKB, Cauveri, and Pennar river basins show smaller conditional return periods in case of hydrological and soil moisture drought. The shorter return period in the southern region for all drought types might be due to their geographical location as well as less rainfall. These results clearly indicate that drought events are frequent in Southern river basins of India but with a lower return period as compared to other parts of India. Similar results were found in Amrit et al., (2018), where they conclude frequent droughts occurrence once in every 5-6 years in a larger part of Southern India.

Results of conditional return period using bivariate drought distribution provide a deep understanding of the drought persistence in India for given thresholds of drought duration and severity rather than univariate analysis. However, the conditional probability at 25^{th}, $50^{th}$and 75^{th} percentile of drought severity where duration exceeding several thresholds of 25^{th},50^{th} and 75^{th} percentile values are shown in Figure 4.9 (e-g), respectively.

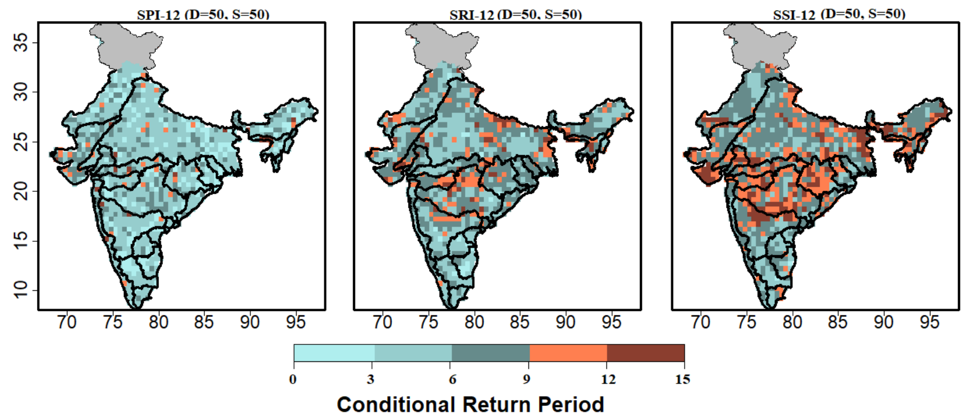

Figure 4.9 (a) Conditional joint return period at 50^{th} percentile of drought duration where drought severity passing a particular threshold of 50^{th} percentile value for meteorological (SPI-12), hydrological (SRI-12) and soil moisture drought (SSI-12).

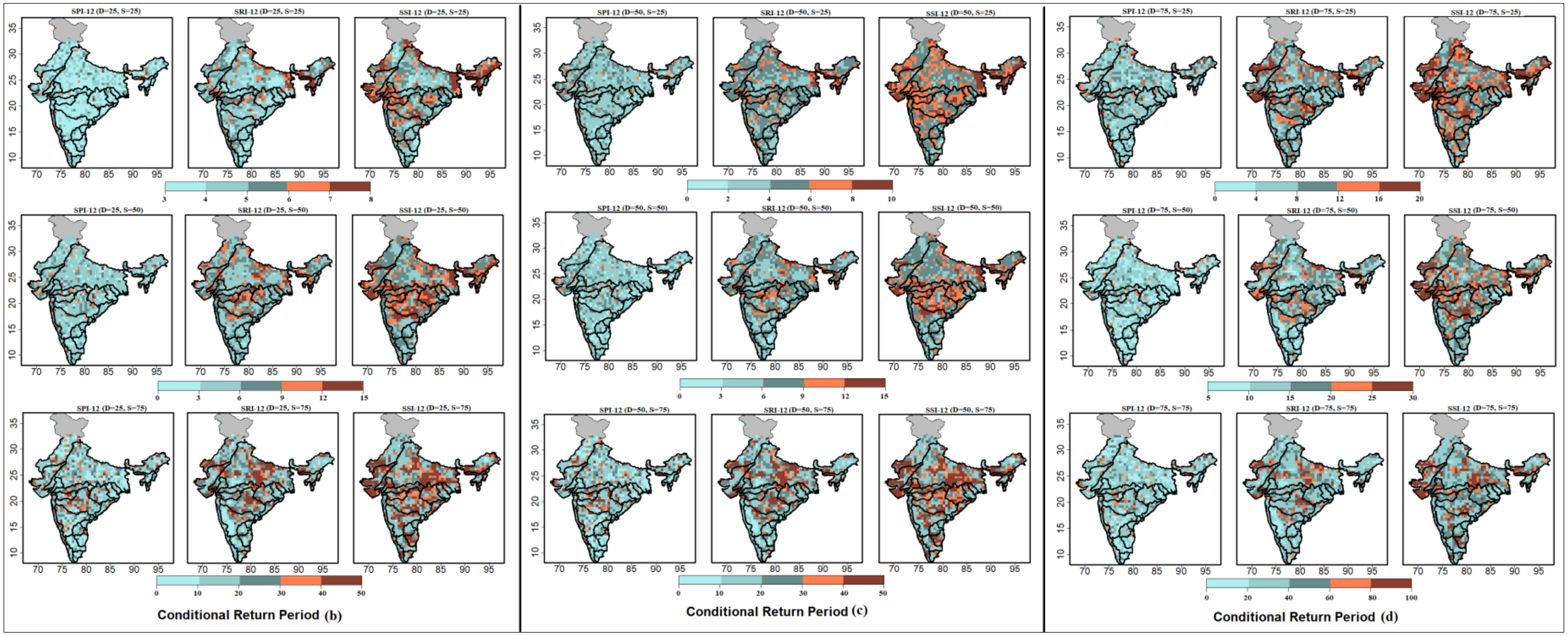

Figure 4.9(b-d) Conditional return period at 25^{th}, 50^{th} and 75^{th} percentile of drought duration where drought severity passing a particular threshold of 25^{th},50^{th} and 75^{th} percentile values for meteorological (SPI-12), hydrological (SRI-12) and soil moisture drought (SSI-12).

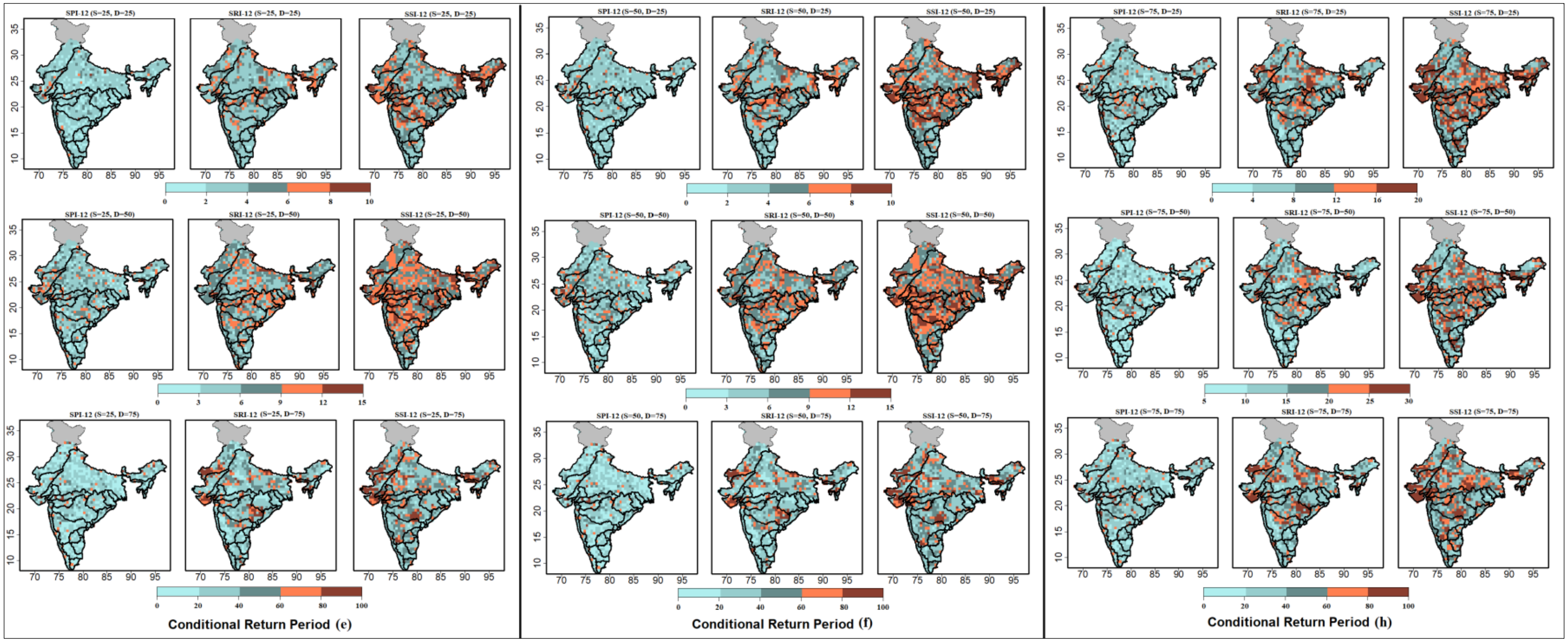

Figure 4.9(e-g) Conditional return period at 25^{th}, 50^{th} and 75^{th} percentile of drought severity where drought duration passing a particular threshold of 25^{th},50^{th} and 75^{th} percentile values for meteorological (SPI-12), hydrological (SRI-12) and soil moisture drought (SSI-12).

4.4 Conclusions

The present study is carried out to determine the joint dependence of drought characteristics (at the river basin scale) using the copula-based approach. For this purpose, different copulas are used to determine the dependence structure between drought characteristics using the goodness of fit tests. Based on the joint probability distribution, joint return period and exceedance probability were computed at various thresholds of drought characteristics (25^{th}, 50^{th}, 75^{th} and 95^{th} percentile values) over 24 major river basins of India. Exceedance probability and return period analysis can provide a better idea regarding drought existence. Further, the conditional approach is also used to compute conditional probability and conditional return period at three thresholds of drought characteristics (25^{th}, 50^{th}, and 75^{th} percentile values). Initially, it was observed that severity and duration need to be modeled for each grid point of different river basins with different distributions. Moreover, a single copula is unable to model the joint probability at bigger scales. Therefore, three different copulas were selected to construct a joint dependence structure among drought characteristics over 1162 grid points in India.

From the results, it was found that Southern India has a higher lower return period and higher exceedance probability as compared to Western river basins of India. Moreover, similar results were also obtained for the conditional return periods and conditional probability. Such results indicates that the drought events in Western and Central India are longer and more severe while the drought events in the southern river basins of the country are more frequent but less severe.

Arid regions of India, for example, EFRKPB, mahi, Luni, Sabarmati witness high severe droughts. This is supported by the fact that these arid regions of India receive the minimum annual mean precipitation (Subash and Sikka, 2014). This might be due to the inability of the river basins to attain the required soil moisture conditions for vegetation re-expansion, similar was found by Jha et al., (2019). Moreover, arid areas of southern river basins are as also witnessing frequent droughts. In the concluding remark, we can say that there is a remarkable impact of drought in India, especially over Southern as well as Western regions of the country.

However, the present analysis has been carried out at a 12-month time scale with a zero-threshold value of drought index for recognizing drought events. The change in the threshold value for the different river basins will result in a more rigorous analysis. Further, this can improve the joint return period values and be helpful in comparing the probabilities of different drought classes such as moderate, severe, extreme, and exceptional droughts. With the limited dataset, the copula-based methodology results in remarkable outcomes. Additionally, the analysis of hydrological and agricultural drought is carried out using reanalysis datasets. It should be noted that for understanding the exact physical behavior of the above-mentioned droughts, one should consider comparing the results with observational data sets. In this context, although reanalysis datasets have been utilized for a variety of climate studies, there might be minor inconsistencies in representing the drought indices if compared to observational data indices (Lin et al., 2014). Such comparisons for different regions could help in understanding the variability arising due to data sources and can be pursued in future studies. Additionally, the present analysis employs bivariate methodology among drought characteristics which may be insufficient in incorporating interaction among all drought characteristics. Therefore, it is suggested that the trivariate copula technique may perform better in future studies (Xu et al., 2015). The present study provides valuable information regarding the severe and longer drought events for risk management at a national scale and thus helpful to develop drought mitigation policies at a larger scale.

Chapter 5

Terrestrial ecosystem response to flash droughts over India

5.1 Introduction

Conventional drought is defined as a slowly growing climate phenomenon, taking few months or more to attain its spatial extent and maximum intensity (Otkin et al. 2013; Yuan et al. 2017a). However, recent findings have revealed a new kind of rapidly growing drought termed as "flash drought". It is a recently identified extreme event characterized by its rapid intensification and sudden onset (Otkin et al., 2018). Due to rapid intensification and high evapotranspiration (ET), flash drought causes quick soil moisture depletion, which results in vegetation stress (Otkin et al., 2018). Recently, flash droughts have occurred frequently, for example, northern USA in 2017 (Gerken et al., 2018), southern Africa in 2015 (Yuan et al., 2018), southern China in 2013 (Yuan et al., 2015), central USA in 2012 (Hoerling et al., 2014), etc. Moreover, a study by Yuan et al., (2019) also found significant increasing trends of flash droughts over China in the warming and changing climate. The increasing frequency may impose a higher risk on the ecosystem, crop production, water security, and environmental sustainability (Vazifehkhah et al., 2019).

Therefore, it is the need of the hour to understand that how ecosystem indicators (GPP, WUE, uWUE) respond to flash drought. In this regard, few studies have been carried out across the world (Guo et al., 2019; Xie et al., 2016; Zhang and Yuan, 2020), however, how the regional terrestrial carbon dynamics respond to flash droughts in India remains unknown. As we know that, India is a developing country, where agricultural sector provides livelihood to a large section of the population (Gadgil and Gadgil, 2006). Therefore, it is important to examine the flash drought and its impact on the ecosystem over India. Moreover, understanding the seasonal variability of flash drought occurrence is also important, especially in the rainfed-based agricultural regions of India (Asoka et al., 2017).

In this work, we present a novel approach, integrating remote sensing observations (GPP, WUE, uWUE) and climate data to quantify the ecosystem response to flash droughts in a finer and systematic view over India. The objectives of this study can be summarized as follows: (i) to perform Triple Collocation (TC) technique to assess the accuracy of soil moisture datasets; (ii) investigate the seasonal distribution of flash droughts and the associated hydrometeorological characteristics during different stages of flash droughts; (iii) investigate the seasonal response of ecosystem indicators (GPP, WUE, uWUE) to flash droughts over India. The present analysis is performed using high-resolution ($0.25^0 \times 0.25^0$) precipitation, temperature, soil moisture datasets over 24 major river basins of India. Moreover, satellite dataset i.e., terrestrial GPP product (MOD17A2) from the MODIS is used for spatiotemporal assessment of WUE and uWUE from 2000 to 2014.

5.2 Data and methodology

5.2.1 Study area

India is the 7th largest country across the world covering an area of approximately 3.28 million sq. km. According to India-WRIS [2014] classification, India is divided into 24 major river basins based on different climatic variability. For the present analysis, 24 major river basins of India (as per India-WRIS (2014) classification) are selected as study area to quantify the occurrence of flash droughts. Figure 5.1 describes the river basin ID, location, and nomenclature. In India, precipitation and temperature conditions substantially varies on spatio-temporal scale, therefore, all 24 major river basins are important for the flash drought investigation. For example, the western part of the country receives very less precipitation (<500 mm/year), whereas the Western Ghats and the northeastern part of India receive high precipitation (>2000 mm/year).

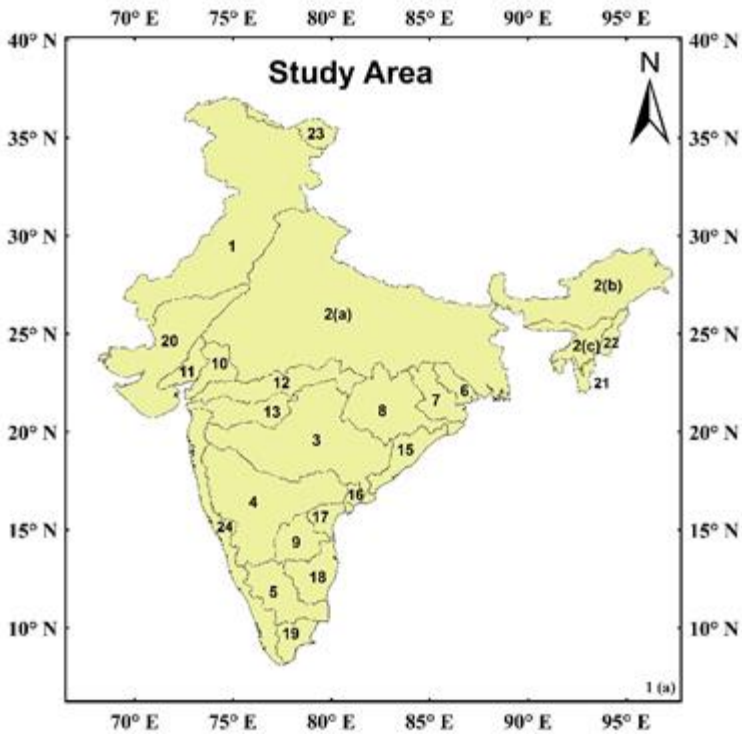

Figure 5.1. Major river basins in India. Source: Watershed Atlas of India (India-WRIS 2012).

5.2.2 Meteorological data

For the present study, daily gridded precipitation dataset was obtained from IMD during 1981-2014 at a grid resolution of 0.25° Latitude × 0.25° Longitude. The IMD precipitation dataset is available from 1901 to 2015, and the readers are suggested to refer Pai et al., (2014) for more details. IMD datasets are realistic in nature and utilized in several studies (Shivam et al. 2019). The mean annual precipitation (mm/year) was computed from daily precipitation values. Temperature data from 1981 to 2014 was also acquired from IMD at a grid resolution of 1° Latitude ×1° Longitude. The relative humidity data was downloaded from the NCEP/NCAR re-analysis dataset and the wind speed datasets are derived from the Terrestrial

Hydrology Research Group, Princeton University ($0.5^0 \times 0.5^0$). The evapotranspiration (ET) was computed using FAO Penman-Monteith equation (Liu and Yang, 2010). Further, vapour pressure deficit (VPD) is computed as the difference between saturated and actual vapour pressures. Further, the temperature, wind speed, and relative humidity datasets are regridded to $0.25^0 \times 0.25^0$ resolution using bilinear interpolation approach.

5.2.3 Soil moisture data

The soil moisture datasets used are: (i) European Space Agency's soil moisture dataset (ESA CCI_SM; https://www.esa-soilmoisture-cci.org/, accessed on 10th May 2021), (ii) European Centre for Medium-Range Weather Forecasts (ECMWF) interim reanalysis (ERA_SM; https://apps.ecmwf.int/datasets/data/interim-full-daily/levtype=sfc/, accessed on 10th May 2021), (iii) Modern-Era Retrospective analysis for Research and Applications-2 soil moisture (MERRA-2-SM; https://gmao.gsfc.nasa.gov/reanalysis/MERRA-2/data_access/, accessed on 10th May 2021), (iv) Global Land Data Assimilation System version 2 Noah soil moisture (GLDAS-2/Noah-SM; https://ldas.gsfc.nasa.gov/gldas/, accessed on 10th May 2021), and (v) Indian Monsoon Data Assimilation and Analysis reanalysis soil moisture dataset (IMDAA-SM; https://rds.ncmrwf.gov.in/, accessed on 10th May 2021). Soil moisture datasets are regridded to 0.25-degree resolution (if required) using the bilinear interpolation approach. Moreover, 8-day soil moisture datasets were computed from daily soil moisture datasets.

5.2.4 MODIS GPP

We used the global 8-day GPP dataset derived from MODIS (MOD17A2 product) starting from 2000 to 2014 at a spatial resolution of 500 m. The global annual GPP dataset is derived from MODIS (MOD17A3 product) from 2000 to 2014. These datasets were obtained from the NASA-EOS program. These products have been utilized in several past studies (Huang et al., 2017; Reichstein et al., 2007; Zhang and Yuan, 2020). The GPP dataset is finally aggregated to $0.25^0 \times 0.25^0$ resolution.

5.2.5 Triple Collocation

Availability of in situ based soil moisture data is scarce and application of satellite or model-based products requires large scale validation. Considering the high uncertainty associated with soil moisture products and unavailability of in situ information, various available products were evaluated against unknown truth based on triple collocation on all the possible triplets. The triplets were derived by arbitrarily selecting three products from a collection of 5 soil moisture datasets (IMDAA SM, GLDAS-2Noah SM, MERRA-2 SM, ERA-Interim SM, and ESA CCI SM). All the available products were firstly pre-processed by resampling to 0.25° grids and converting them into 8-day products (this was done to remove the influence of missing days) and then various triplets were derived to obtain correlation and RMSE values. Triple collocation was first developed to obtain error variance of wind dataset (Stoffelen, 1998) which was later applied to soil moisture (F. Chen et al., 2016; Gruber et al., 2016) and precipitation. The equations used to derive the correlation and RMSE values from triple collocation can be obtained from McColl et al., 2014.

5.2.6 Flash drought identification

Initially, daily gridded datasets (soil moisture, precipitation, temperature) were converted to 8-days called octads. Daily precipitation was added for the eight days while daily temperature and soil moisture were averaged for the eight days. Hence, a total of 46 octads were achieved for each year, where 16 octads represent the monsoon season (i.e., 19th to 34th octads in a year) while the remaining octads represent the non-monsoon season(from 1st to 18th and 35th to 46th octads). In the present analysis, soil moisture octads were used to identify flash droughts and their characteristics (frequency and duration). Flash drought occurs due to a quick reduction in soil moisture caused by either increased temperature or rainfall scarcity or both (Ford and Labosier, 2017). Flash drought was defined when the 8-day mean soil moisture percentile reduces to 20th (or less) percentile from above 40th percentile, with a mean rate of decline no less than 5 percentile per 8-day period (for example, June 21–July 15 in Figure 5.2), which is termed as the "onset" stage. The reduction from 40th percentile to 20th percentile indicates the development of flash drought. Once the soil moisture starts to either decrease slowly or increase, then the recovery stage of flash drought was considered. Once the soil moisture percentile rises to 20 (or more) percentile again, then the drought ends (e.g., July 31 in Figure 5.2). Moreover, the minimum duration of 24 days was considered for flash droughts in order to avoid short dry spells that have a small impact on the ecosystem. The 20th percentile was considered as the drought threshold to avoid persistent long-term (traditional) droughts (Yuan et al., 2019). Hence, flash droughts that transformed into traditional droughts were eliminated from the investigation. Readers are suggested to refer Figure 5.2 for more details.

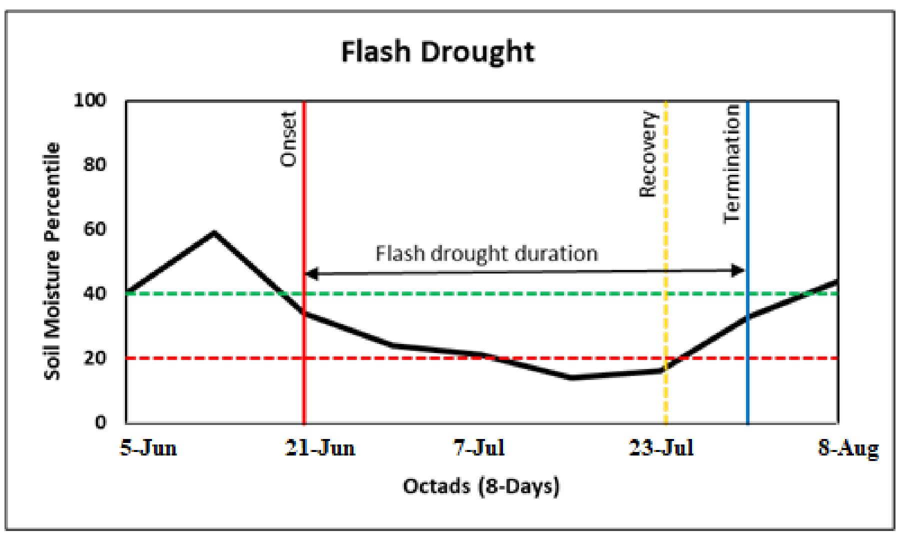

Figure 5.2 Schematic description of flash drought identification.

5.2.7 Ecosystem response to flash drought

It is important to note that droughts have great impact on ecosystem productivity by changing ecosystem respiration and plant photosynthesis (Stocker et al., 2018). GPP is the total photosynthetic CO_2 fixation at the ecosystem level and impacts all of the carbon cycle variables (Beer et al., 2010). Photosynthetic CO_2 assimilation is affected by leaf area index, rubisco activity, and stomatal conductance (Grossiord et al., 2020). The negative anomalies of ecological metric i.e., GPP indicates the commencement of ecological response. The standardized anomalies are computed as:

$$GPP_{SA} = \frac{GPP - \mu_{GPP}}{\sigma_{GPP}} \tag{5.1}$$

Where GPP_{SA} are standardized anomalies of GPP, σ_{GPP} and μ_{GPP} are standard deviation and mean of GPP time series. For example, all Jan 1-8 during 2000-2014 would have a μ_{GPP} and σ_{GPP}, and Jan 9-16 would have another μ_{GPP} and σ_{GPP}, and so on. In this study, response time index and response frequency are used to examine the interaction between ecological response and flash drought (Niu et al., 2018). For each grid, response frequency was obtained by dividing the flash drought events with negative GPP_{SA} by the total number of flash droughts. A lower response frequency indicates lower risk to the ecosystem and vice-versa. The response time index is described as the count of the positive standardized anomaly (GPP_{SA}) till the occurrence of first negative value during flash droughts. WUE is computed as the ratio of GPP to evapotranspiration (Song et al., 2017). In the present analysis, daily potential evapotranspiration (mm/day) is computed using FAO Penman-Monteith equation (Eq. 5.2) which is described as:

$$ET_o = \frac{0.408\Delta(R_n - G) + \gamma \times \frac{900}{T+273} \times U_2(VPD)}{\Delta + \gamma(1 + 0.34U_2)} \tag{5.2}$$

where, Δ is the slope of vapour pressure curve (Kpa/^oC); G is ground heat flux (MJ/m^2/day); R_n is the net radiation at the surface (MJ/m^2/day); γ is psychrometric constant (KPa/^oC); VPD is vapour pressure deficit, which is computed as the difference between saturated and actual vapour pressures; U_2 is the wind speed at 2-m height (m/sec).

The carbon cycle and water are linked via stomata, and the vegetation will adopt some mitigation measures to deal with drought conditions, for example, increasing its water use efficiency (Xu et al., 2019). Besides drought, WUE is also sensitive to the vapour pressure deficit (VPD). Therefore, underlying water use efficiency (uWUE) proposed by Zhou et al., (2014) would be a better alternative as it incorporates the effects of VPD. Underlying water use efficiencies are computed as ratio of the (GPP$\times \sqrt{VPD}$) to the ET, in order to reflect the non-linear interaction between ET, VPD, and GPP. The variations of underlying water use efficiency are supposed to be strongly associated with drought conditions. The average annual WUE (g C m^{-2} mm^{-1} yr^{-1}) and uWUE (g C $Pa^{0.5}$ m^{-2} mm^{-1} yr^{-1}) were computed from daily WUE and uWUE values. The standardized anomalies of WUE as well as uWUE are computed using Eq. (5.1).

5.3 Results

5.3.1 Triple Collocation

Figure 5.3 (a & b) represents the correlation coefficient values and figure 5.3 (c & d) represent the RMSE values obtained for various products by the application of triple collocation. Each row in these figure represent a triplet which was used to assess the performance of these products against the unknown truth (Gruber et al., 2016; McColl et al., 2014; Stoffelen, 1998), these figures suggest that GLDAS-2/Noah SM and ERA-interim SM outperformed the other products, whereas the performance of these two products were similar. Zonal statistics of different river basins suggested that GLDAS-2/Noah SM was slightly better than ERA-interim SM and therefore the data obtained from the GLDAS-2/Noah SM was further used for the analysis of flash drought.

5.3.2 Meteorological and ecological conditions over India

Figure 5.4 presents the annual mean climatological and ecological characteristics over India based on 2000-2014 datasets. The annual mean precipitation showed significant spatial variations over India, ranges from less than 100 mm/yr to 4000 mm/yr (Figure 5.4a). The western part of the country receives the lowest precipitation (<500 mm/year), whereas the Western Ghats and the northeastern parts of India receive the highest precipitation (>2000 mm/year). The mean annual soil moisture also showed considerable variation across the country (Figure 5.4b), with very dry soil characteristics over western India. Besides accumulated precipitation, soil moisture is also related to the changes in evapotranspiration. Similarly, the mean annual MODIS GPP also shows significant spatial variation over India (Figure 5.4c), with maximum GPP spread across the Western Ghats and Northeastern regions (>1400 g C/m^2), whereas the minimum GPP distributed across the arid regions of Western India (<400 g C/m^2). One-fourth of the forest area of the country lies in Northeastern India, whereas western India consists of grasslands with comparatively low vegetation productivity. Like precipitation and GPP, mean annual WUE and uWUE also varies significantly over India (Figure 5.4 (d & e)) due to different soil, climate, and vegetation types. WUE is higher for northeastern parts of the country followed by eastern, northern, and southern regions, respectively. Whereas lower WUE is observed over western parts of the country due to low vegetation productivity. The spatial variation in WUE is strongly associated with the variations in the mean annual precipitation and GPP.

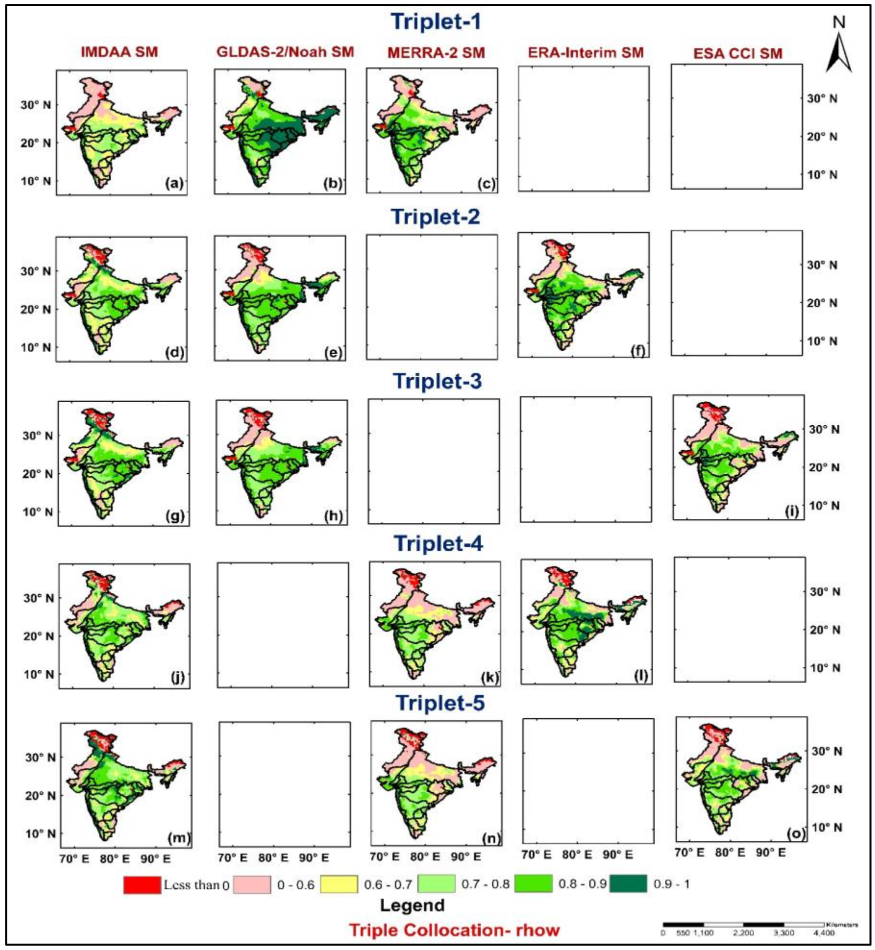

Figure 5.3a Correlation coefficient obtained for various products by applying triple collocation on different triplets (represented by datasets on various rows). The datasets used to derive these triplets include IMDAA SM, GLDAS-2Noah SM, MERRA-2 SM, ERA-Interim SM and ESA CCI SM.

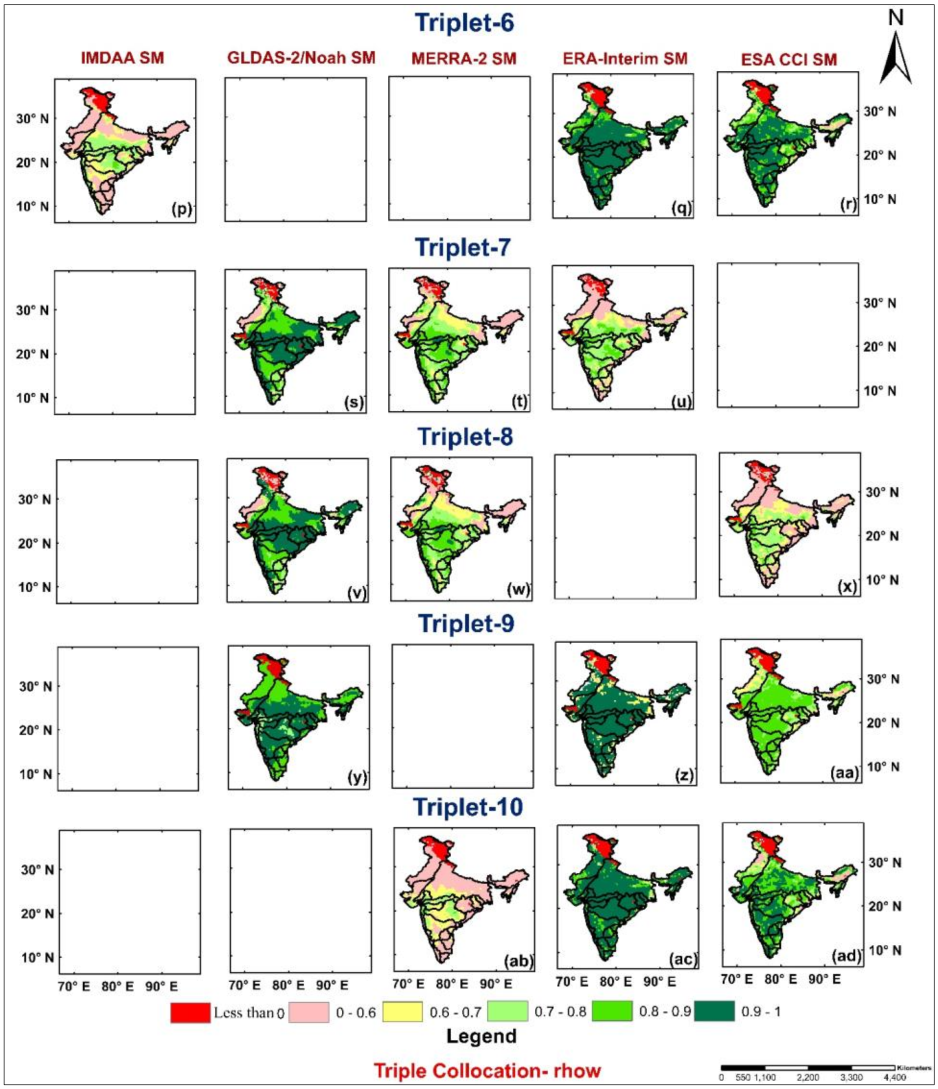

Figure 5.3b Correlation coefficient obtained for various products by applying triple collocation on different triplets (represented by datasets on various rows). The datasets used to derive these triplets include IMDAA SM, GLDAS-2Noah SM, MERRA-2 SM, ERA-Interim SM and ESA CCI SM.

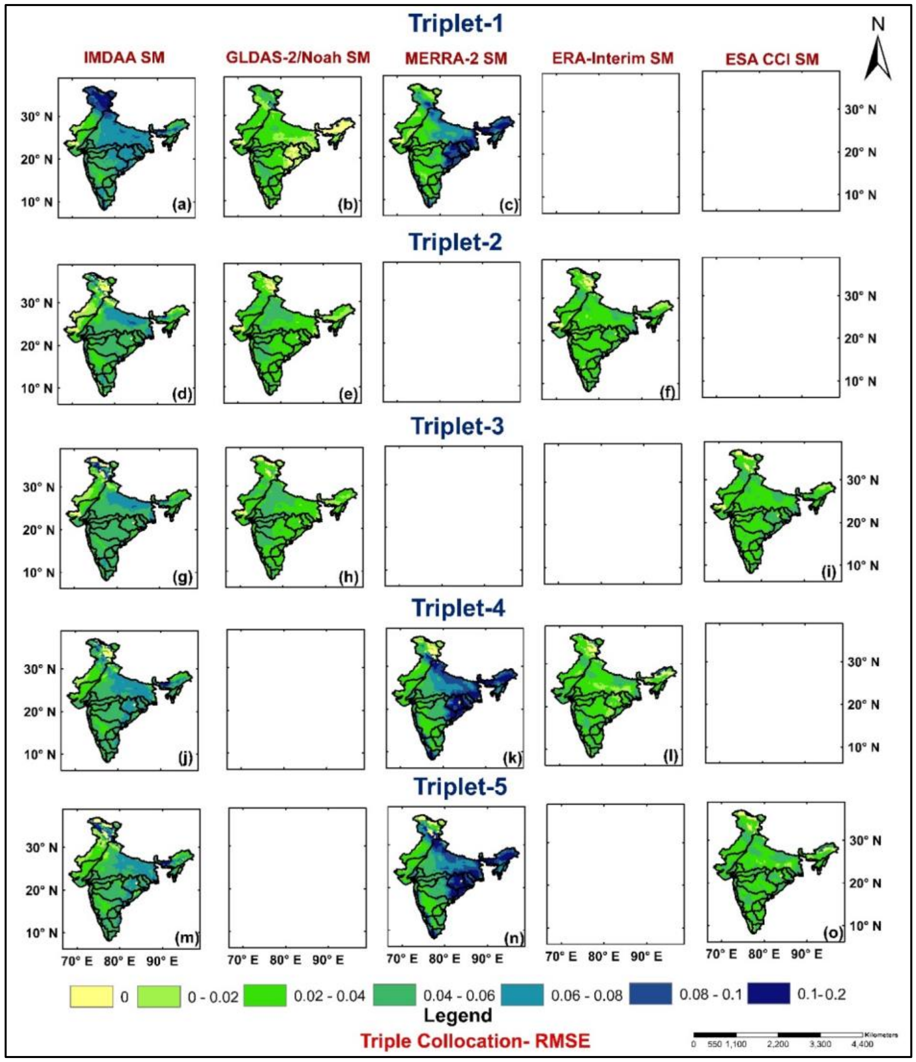

Figure 5.3c RMSE obtained for various products by applying triple collocation on different triplets (represented by datasets on various rows). The datasets used to derive these triplets include IMDAA SM, GLDAS-2Noah SM, MERRA-2 SM, ERA-Interim SM and ESA CCI SM.

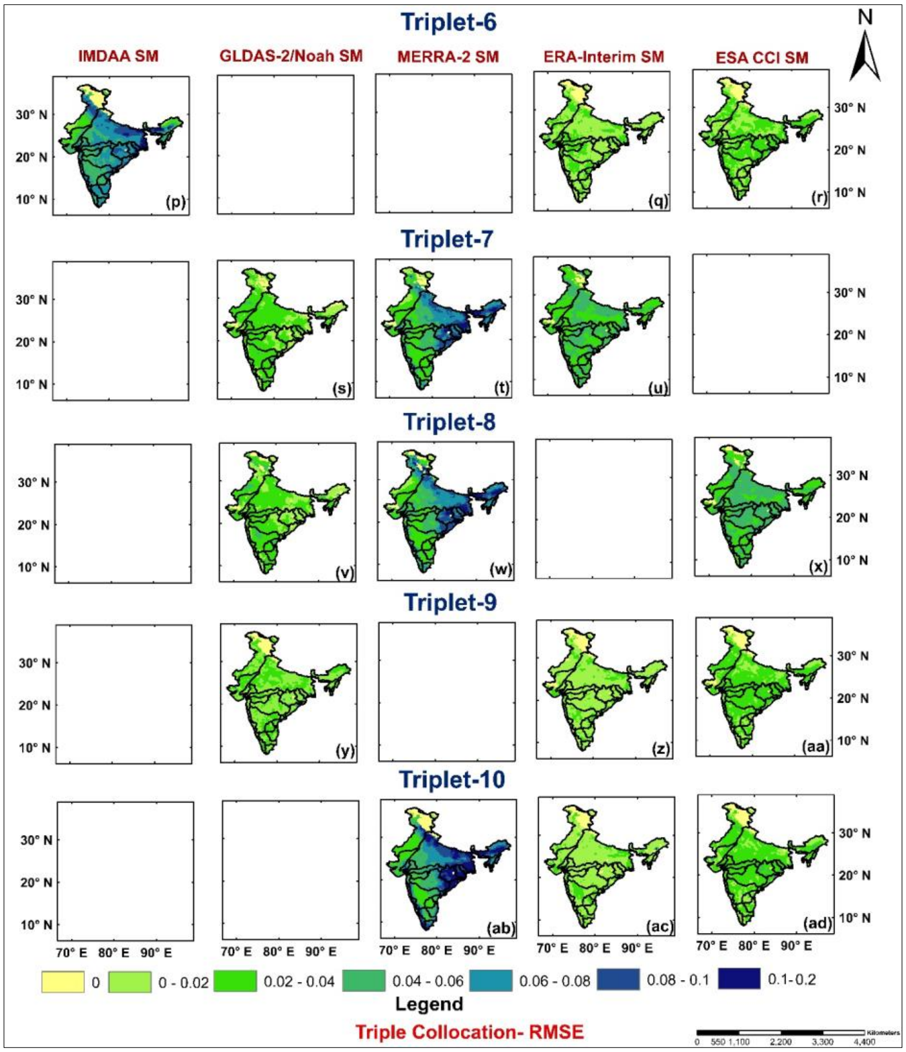

Figure 5.3d RMSE obtained for various products by applying triple collocation on different triplets (represented by datasets on various rows). The datasets used to derive these triplets include IMDAA SM, GLDAS-2Noah SM, MERRA-2 SM, ERA-Interim SM and ESA CCI SM.

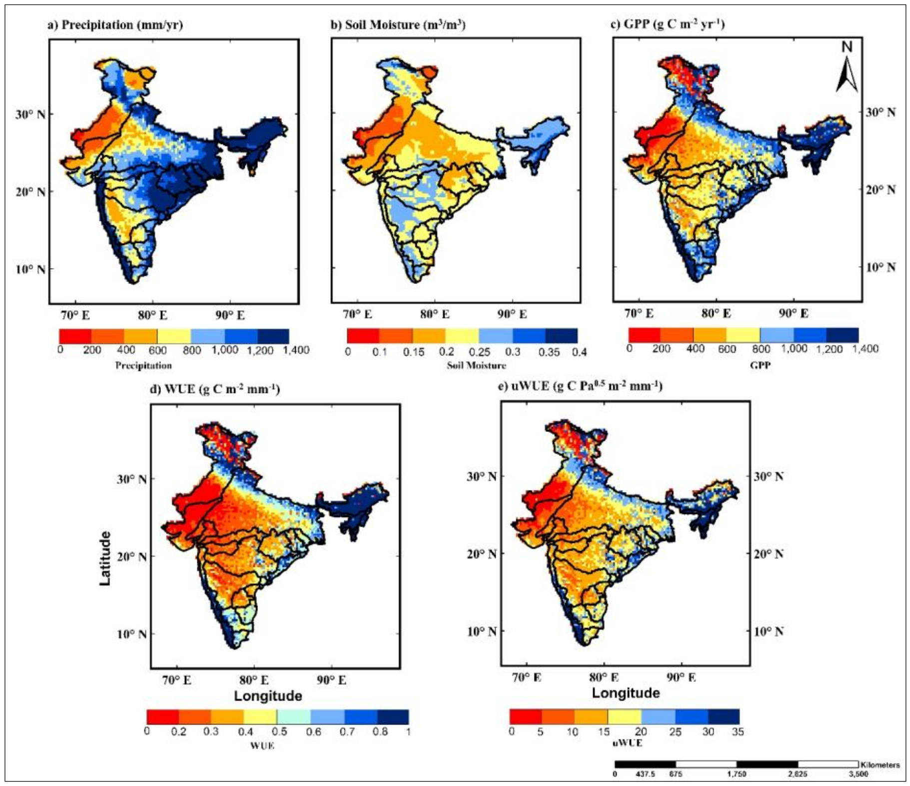

Figure 5.4 Mean annual (a) precipitation, (b) soil moisture, (c) GPP, (d) WUE, and (e) uWUE over India during 2000-2014.

5.3.3 Flash drought and associated hydrometeorological characteristics across India

The computation of flash drought duration and frequency are the same as those of traditional droughts (Mo, 2011), however, computed at a higher temporal scale. The mean duration was computed by dividing the total flash drought duration by the total number of flash droughts and the frequency was defined as the total number of flash drought events per decade (or any specific time period). Initially, we investigate the seasonal distribution of flash droughts based on the frequency and mean duration that occurred during the 1981-2014 period in India (Figure 5.5). In case of monsoon season, the mean frequency averaged over India is 2.6 events for 34 years (1981-2014), including some hotspots over Northwestern India (Figure 5.5a). Moreover, the mean duration of flash drought events is 37 days across all of India, with the longest mean durations detected over western and northern parts of the country (Figure 5.5c). Particularly, the Luni river basin experience frequent flash drought events with longer durations. This might be due to the minimum annual mean precipitation over Luni river basin (Subash and Sikka, 2014). Regions in the country like the Western Ghats, Northeast showed low likelihood of drought events in monsoon season. This suggests that vegetation cover of such river basins can tolerate extreme changes in soil moisture conditions in monsoon.

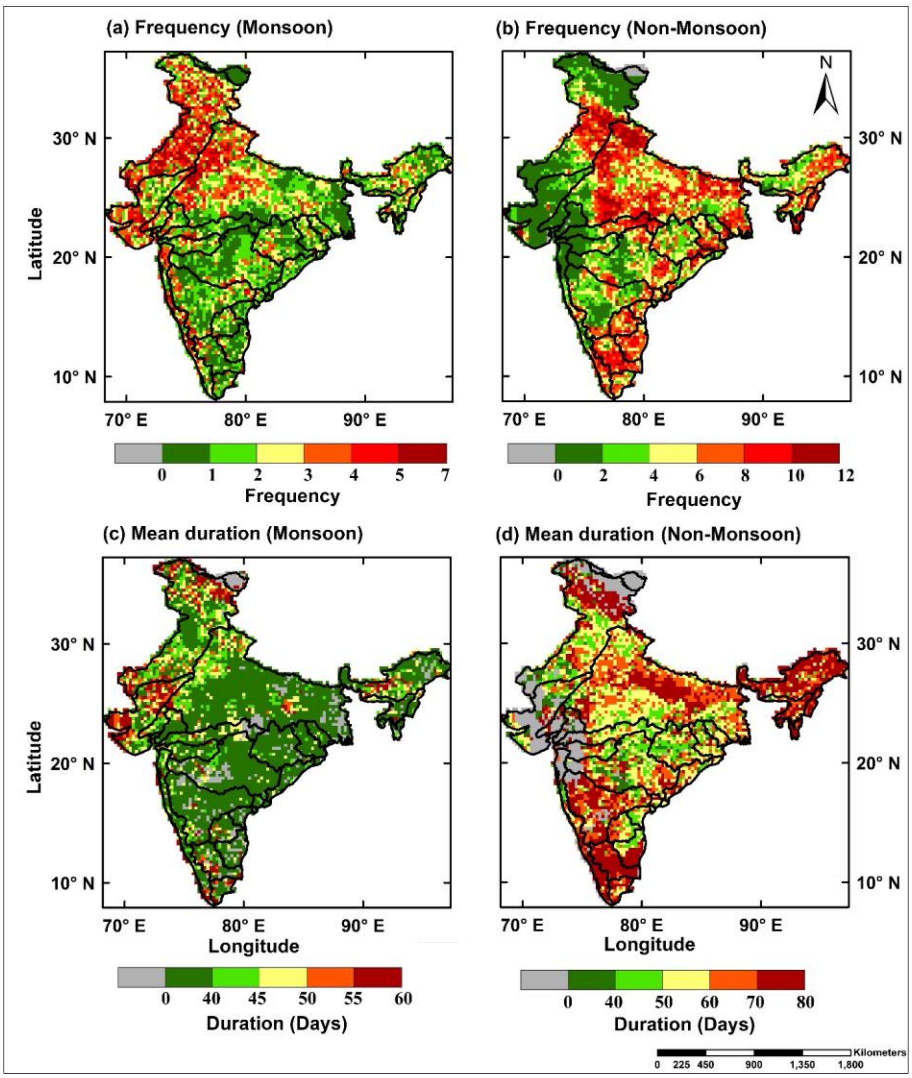

Figure 5.5 Mean duration and frequency of flash drought events for monsoon and non-monsoon seasons during 1981-2014 across India.

However, in the non-monsoon season, the majority of river basins of the country experience frequent and longer flash droughts during 1981-2014 (Figure 5.5 (b & d)). Long dry spells with negative precipitation anomalies in the non-monsoon rapidly reduce soil moisture which triggers flash droughts. The mean frequency averaged over India is 5.3 events for 34 years whereas, the mean duration is 54 days across all of India during the non-monsoon season. Particularly, southern and northeastern India were found to be more susceptible to flash droughts with high frequency and longer durations. Interestingly, arid or semi-arid parts of western India which were mostly suffer from drought risks experienced the lowest frequency and duration of flash droughts during non-monsoon season. This suggests that these regions are more susceptible to seasonal or long-term droughts rather than flash droughts in the non-monsoon.

Further, we determined the seasonal distribution of mean duration of onset and recovery stages of flash drought events that occurred during 1981-2014 across India (Figure 5.6). During the monsoon season, onset duration shows no substantial variation for distinct climate regions, though the duration changes significantly at different grids in some regions (i.e., ranges from zero to above 35) (Figure 5.6a). However, the recovery duration is slightly longer in some parts of the country (Figure 5.6c). Interestingly, it was observed that at least two-third area of the Ganga basin is witnessing zero onset duration, however, the recovery duration is longer (more than 30 days) due to lowered soil moisture level. The mean duration of the onset as well as recovery stages are 19.9 days and 27.7 days, respectively. During the non-monsoon season, northeastern India, southern India, and some parts of the Ganga basin were witnessing longer onset as well as recovery duration during 1981-2014 (Figure 5.6 (b & d)). This is primarily due to the precipitation deficit over a longer period. The mean duration of the onset as well as recovery stages are 24.7 days and 29.2 days, respectively.

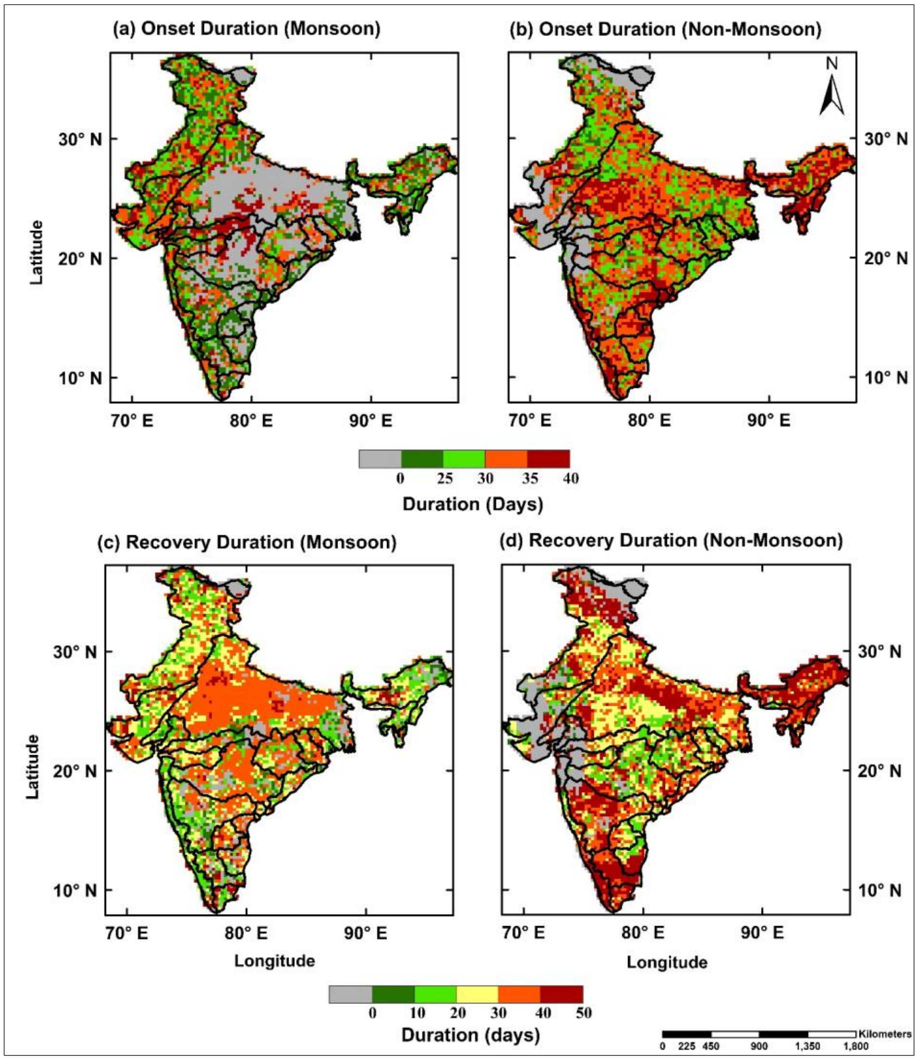

Figure 5.6 Seasonal distribution of mean duration of onset as well as recovery stages of flash droughts occurred during 1981-2014 across India.

Figure 5.7 describes the soil moisture percentiles and associated meteorological conditions throughout different stages of flash drought in the non-monsoon season. Only the pixels with at least three drought events detected are shown during the 1981-2014 period. Before the onset of drought, the soil moisture percentile is close to 45 percentiles across all of the selected grid points (Figure 5.7a). However, during the onset of flash drought, the soil moisture percentile falls from above 40 percentiles to 32 percentiles (Figure 5.7b). As soon as the flash drought enters into the recovery stage, there is a quick transition from high soil moisture condition to much drier condition (approximately 15 percentile) (Figure 5.7c). Further, the soil moisture recovers quickly to 41 percentiles after the termination of flash drought (Figure 5.7d). Regarding the onset stage, the standardized negative anomaly of precipitation and positive anomalies of temperature, and VPD suggest that flash drought events are characterized by elevated evaporative demand and precipitation deficit (Figure 5.7(e-p)). The quick-drying of soil moisture is usually related to anomalously high temperature, large rainfall deficits, and high VPD (Wang et al., 2016), which continue till the recovery stage of drought. The decrease in VPD and increased rainfall relieves the soil moisture once the drought terminates. Readers are suggested to refer Figure 5.8 for soil moisture percentiles and associated meteorological conditions during different stages of flash drought in the monsoon season.

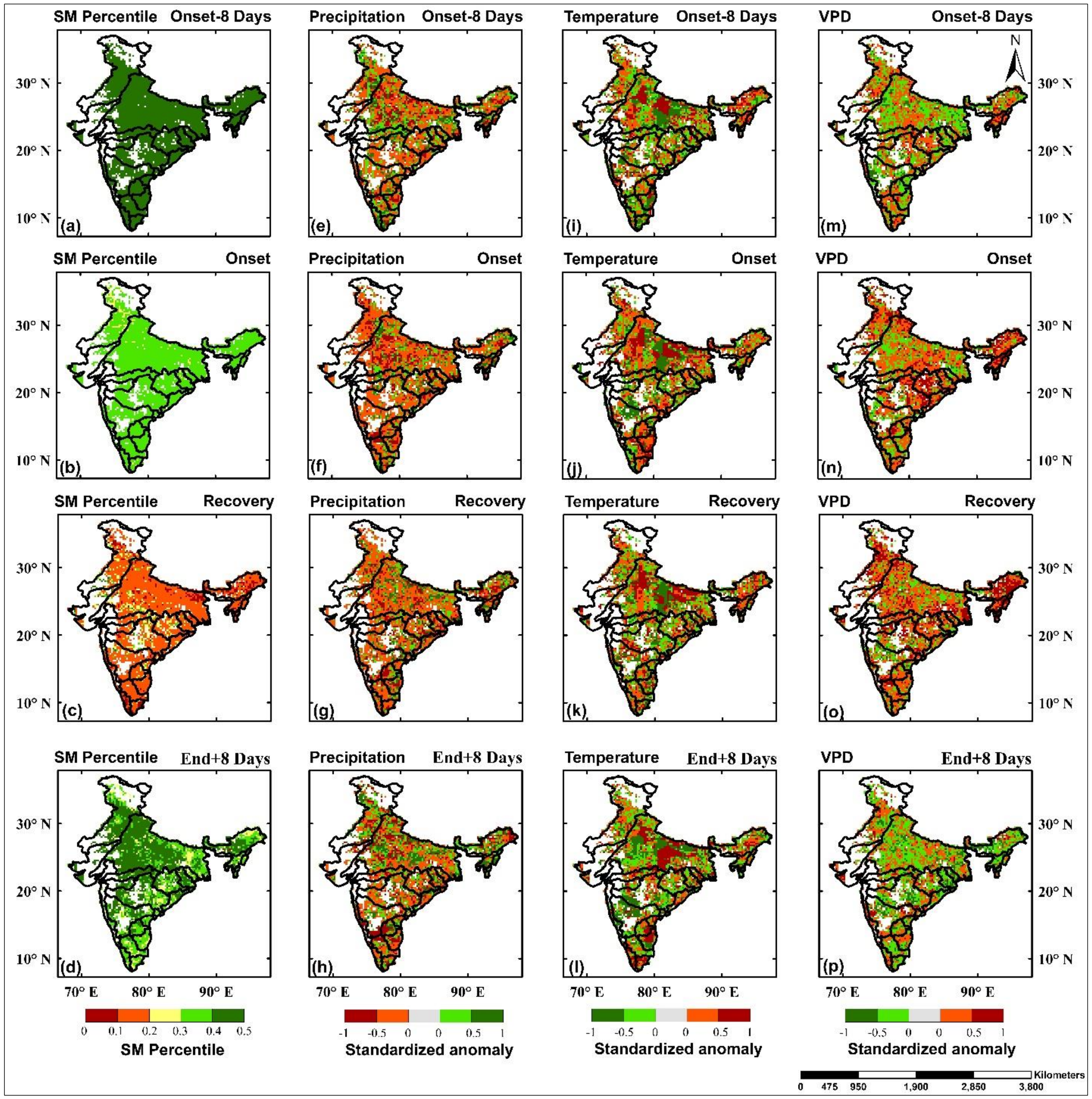

Figure 5.7 Hydrometeorological characteristics during different stages of flash drought in non-monsoon season.

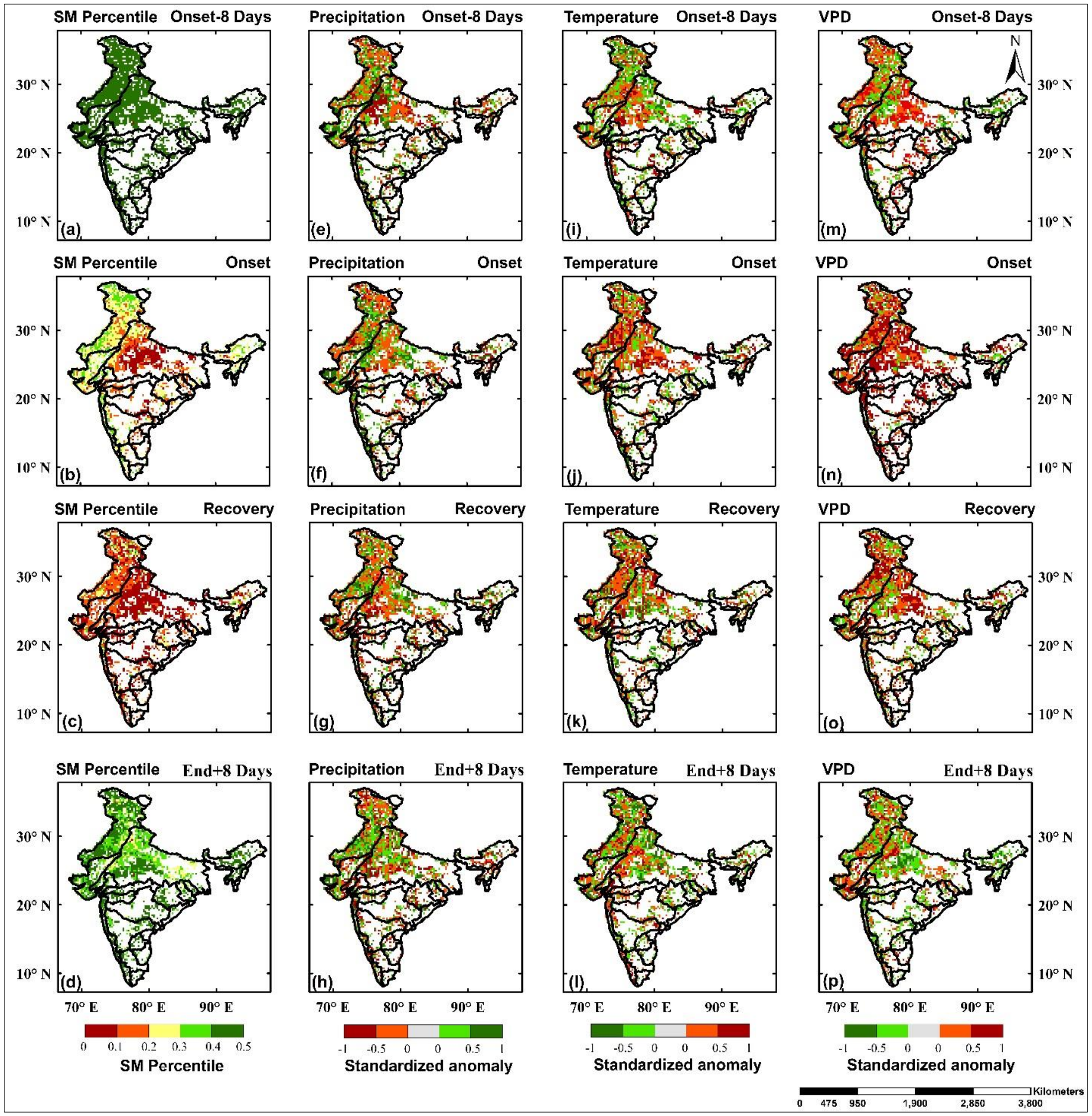

Figure 5.8 Hydrometeorological characteristics during different stages of flash drought in monsoon season.

5.3.4 Response of GPP to flash droughts across India

Figure 5.9 shows the response frequency and response time of gross primary productivity (GPP) to flash drought events during monsoon and non-monsoon seasons across India. In case of response frequency, no substantial discrepancy was observed across different climate regions of the country during monsoon as well as non-monsoon seasons (Figure 5.9 (a & b)). The mean response frequency is around 97% averaged over India during both seasons. In case of monsoon season, response time also shows no substantial difference (approximately 8 days or less) for different climate regions, however, some regions of the Brahmaputra, Godavari, and Krishna river basins exhibit longer response time (more than 20 days) (Figure 5.9c) which is primarily due to the presence of forests in these basins. In case of non-monsoon season, a longer response time is observed, especially in the Indo-Gangetic plain, northeastern India, and some parts of southern India (Figure 5.9d). A longer response time in Northeastern India and Indo-Gangetic plain indicates lower risk to the ecosystem (GPP). Moreover, the mean response time is about 10 days and 19 days averaged over India for monsoon and non-monsoon, respectively.

5.3.5 Response of WUE and uWUE to flash droughts across India

The positive standardized anomalies of underlying WUE are higher as compared to WUE over the onset as well as recovery stages of flash drought for both monsoon and non-monsoon seasons (Figure 5.10). This is majorly attributed to the influence of elevated vapour pressure deficit as higher VPD could rise evapotranspiration which in turn increases water loss. During the onset stage, the negative anomalies of WUE and uWUE indicate the non-resilient vegetation to flash droughts (Figure 5.10 (a-d)), however, this is further decreased during recovery stages (Figure 5.10 (e-h)). This reduction suggests that the vegetation adaptation to flash drought declines with the increasing drought duration. In terms of WUE and uWUE, the Ganga basin was observed to be the most badly affected river basin to flash droughts, especially in the monsoon season. This might be due to deforestation in the Ganga basin, which reduces 1-2 mm rainfall per day during the monsoon season (Paul et al., 2016). As we know that the recycled component is very high in the Ganga basin, therefore, a small change in vegetation cover may cause a significant change in precipitation which further result in drought conditions. Higher positive anomalies of WUE and uWUE were observed in non-monsoon season which suggests that GPP responds quicker to flash drought events in monsoon season as compared to non-monsoon season.

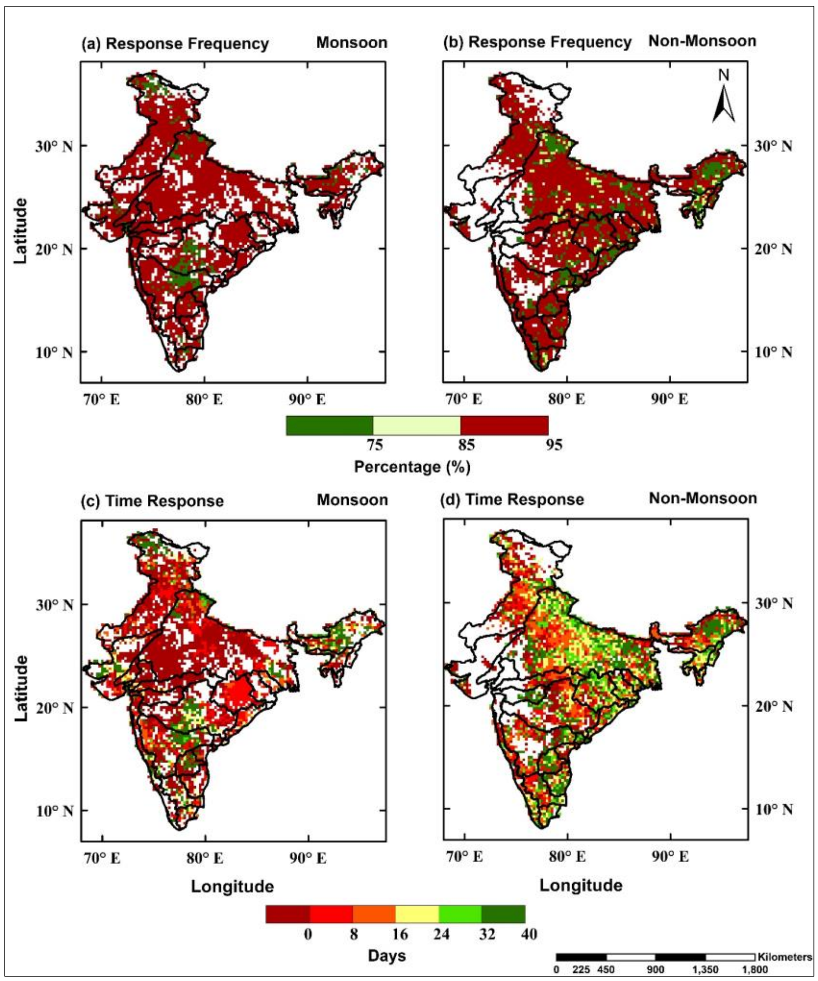

Figure 5.9 Response frequency and response time of gross primary productivity (GPP) to flash droughts across India.

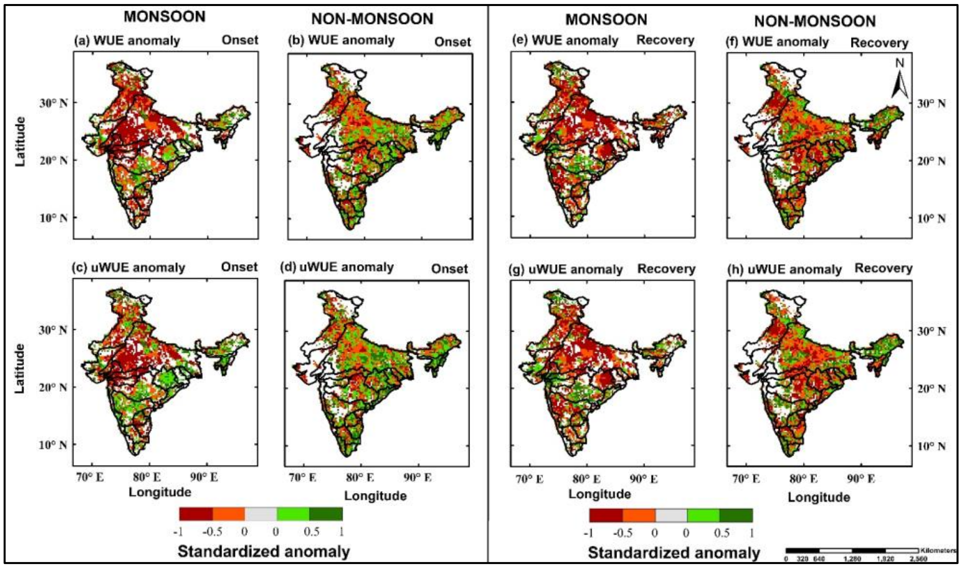

Figure 5.10 Seasonal distribution of standardized anomalies of WUE and uWUE.

5.4 Discussions

Despite growing concerns and challenges to flash droughts, their occurrence and impact on the terrestrial ecosystem are least addressed at the pan-India scale. It was observed that the quick transition of soil moisture is caused by large rainfall deficits and high vapour pressure deficit (VPD). The sudden onset of flash drought gives limited time for planning and preparation and poses a great challenge for early warning (Gerken et al., 2018; Otkin et al., 2015). As we know that plants rely mainly on soil moisture to extract water, which further regulates the transpiration losses, stomatal control, and stem-water dynamics (Daly et al., 2004). The decline in soil moisture would reduce stomatal conductance in order to prevent extra water loss. Moreover, the deficit in atmospheric humidity further decreases stomatal conductance. Meanwhile, the diffusion of carbon dioxide into the plant's leaf is also decreased. During droughts, the combined soil moisture and atmospheric conditions have synergistic impacts on transpiration and photosynthesis processes, and hence changing the coupling among water and carbon fluxes.

In addition to soil moisture droughts, the response of ecosystem respiration is also sensitive to higher temperatures (Johnston et al., 2021).

The ecosystem response of GPP occurs over 95% of identified flash droughts, which indicates that GPP is highly sensitive to flash droughts across the country. For Ganga and southern river basins of India, GPP response occurs during 97% of drought events, which was significantly higher than 75% for northeastern river basins of the country. This was mainly attributed to different vegetation resilience conditions across different parts of the country. Jha et al., (2019) suggest that southern river basins of the country were observed to be susceptible and non-resilient to droughts. The non-resilient vegetation characteristics of these basins basically show their incompetence to attain the required soil moisture conditions for vegetation redevelopment once the dry period ends. However, Northeastern India and Indo-Gangetic plain show less ecological response to flash droughts as they were considered as one of the most ecological rich regions of the country (Sankarganesh et al., 2017) where vegetation can tolerate extreme deviations in soil moisture conditions. A lower response frequency in Northeastern India and Indo-Gangetic plain indicates a lower risk to the ecosystem (GPP).

The mean response time is about 10 days and 19 days averaged across India for monsoon and non-monsoon, respectively. In case of monsoon season, the ecological response of GPP occurs only within 8 days for more than 50% of flash drought events in Ganga and Indus river basin, which was too prior to those for northeastern India. The quicker response time indicates that the vegetation cover of these river basins cannot tolerate extreme changes in soil moisture for a longer duration. In terms of vegetation drought, Indus and Ganga basins are found to be non-adaptable river basins (Jha et al. 2019). The response of GPP increases rapidly during 17 to 32 days of drought event for northeastern river basins of India, which suggests that vegetation adaptation would decrease with increasing drought duration.

The seasonal dependency was also observed in the time response. We found that vegetation cover of the Ganga basin experienced quicker time response to flash droughts in monsoon season however, it increases in case of non-monsoon season. The longer response time in Northeastern India and Indo-Gangetic plain indicates lower risk to the ecosystem (GPP) in non-monsoon. Therefore, it is important to examine flash drought characteristics, for example, drought duration and severity as they play a crucial role in influencing the ecosystem (Wu et al., 2016; Zhao et al., 2020). For example, longer and severe flash droughts could cause high carbon loss in terrestrial ecology.

Higher WUE and uWUE during drought events indicate the ecosystem's resilience to flash drought. Our results showed that the Brahmaputra and Godavari river basins have the maximum WUE and uWUE in both seasons, which can mainly be attributed to the presence of forests in these basins, as the forest land cover has higher WUE as compared to others (Sharma and Goyal, 2018a). Northeastern river basins have the largest forest cover among all river basins over India. In contrast, the Mahi and Sabarmati basins have the least WUE among all river basins, which is primarily due to the absence of forest areas (Sharma and Goyal, 2018b). It is interesting to note that the Mahi basin receives the lowest annual mean rainfall, whereas the Brahmaputra basin receives the highest annual mean rainfall (Figure 5.4a), which indicates the dependence of water use efficiency over precipitation. Moreover, the Ganga basin also experienced the least water use efficiency. Due to lowered soil moisture, about 2/3rd area of the Ganga basin comes under least water use efficiency. However, the WUE and uWUE are further decreased in the recovery stage with the increasing drought duration. This reduction suggests that the vegetation adaptation to flash drought declines with the increasing drought duration (Kapoor et al., 2020). The standardized anomalies of underlying WUE are higher as compared to WUE over the onset as well as recovery stages of flash drought. This is majorly attributed to the influence of elevated vapour pressure deficit as higher VPD could rise evapotranspiration which in turn increases water loss (Massmann et al., 2019). Regarding the recovery stage, no substantial difference in WUE and underlying WUE was observed across the study areas, especially in the Ganga, and Mahanadi river basins of India, signifying a more vulnerable grassland ecosystem in Ganga and Mahanadi river basin than forests in northeastern India.

5.5 Conclusions

The present analysis is carried out to demonstrates the quick response of terrestrial ecosystems to flash drought events using gross primary productivity (GPP). Our results showed that GPP was highly sensitive to the flash drought occurrence, especially over Ganga river basin and southern India containing semiarid climate rather than northeastern India i.e., humid part of the country. The results of the present analysis are fascinating as it highlights that ecosystems in majority of the river basins are non-resilient to flash droughts, as observed through the non-resilient nature of most of the basins to vegetation drought over India (Jha et al. 2019). The incompetence of ecosystems to tolerate the flash drought events may cause severe challenges in terms of food security, food production, and carbon sequestration. As we know that India is a developing country, where agricultural sector provides livelihood to a large section of the population, therefore, flash drought risk is frightening situation for the nation. To the best of the author's knowledge, this study is the first to relate the response of ecosystem metrics (GPP, WUE, and uWUE) to flash droughts in India. Moreover, our results provide information about the hotspots for drought management and ecosystem policymaking. However, the present study used satellite-based soil moisture datasets which may be insufficient in incorporating real-time conditions, therefore, it is suggested to perform hydrological modeling to simulate soil moisture datasets in order to obtain better results in future studies.

Chapter 6

Impact of climate change on crop water requirements and productivity of major crop in Sikkim, Himalayan region of northeast India

6.1 Introduction

It is well established that the adverse impact of climate change is going to affect every aspect of the ecosystem in the hilly terrain of the Himalayan region. According to FAO (2008), it is expected that global agricultural production is likely to decrease with an annual rate of 1.5% by 2030 and an additional reduction of 0.9% till 2050 as compared to the growth rate since 1961. Hence, researchers from all corners of the globe have attempted to investigate the climate change impact using crop simulation models on different crop productivity and irrigation requirement. However, there exists substantial debate in the recent literature that climate change and global warming both have some negative and positive effects on agricultural crops in different regions of the world. For instance, Lobell and Gourdji, (2012) stated that with the increase in the CO_2 concentration, the global yield is expected to increase roughly by 1.8% per decade, and simultaneously, the crop yield may decrease without any effective adaptation roughly by 1.5% per decade. These conflicting conclusions about linkage of climate change and agricultural crops in current research point out the necessity of a comprehensive understanding of climate change and its impact on crop yield, crop water requirement (CWR), and crop irrigation requirement (CIR), especially at a regional scale.

To overcome the conflicting conclusion, the present study tries to understand the linkage amid climate change and crop water requirement as well as crop yield using crop models (CROPWAT and AquaCrop) along with the uncertainty analysis based on the recently developed representative concentration pathways (RCP) scenarios of three major crops (maize, wheat, and rice). Daily climatic datasets such as maximum temperature, minimum temperature, rainfall, wind speed, sunshine hours, and relative humidity are used for this analysis along with crop and soil data. For future period (2021-2099), climatic datasets are collected from the four climate models (ACCESS1-0, CCSM4, CNRM-CM5, and MPI-ESM-LR) of CORDEX under two different scenarios RCP 4.5 and 8.5. This study facilitates the water and agricultural manager for considering proper and robust adaptation measures to ensure sustainability.

6.2 Data and methodology

6.2.1 Study area

The selected study site, Sikkim (Figure 6.1), lies in the northeast part of Himalaya which is landlocked by Bhutan, Nepal, and China. The study is conducted on three major areas in Sikkim namely, Gangtok (East Sikkim), Geyzing (West Sikkim), and Namchi (South Sikkim). The location map of Sikkim and digital elevation map of Sikkim is shown in figure 6.1(a), & 6.1(c). Figure 6.1(b) represents three chosen reference locations of east, west and south Sikkim, respectively. Geographical latitudes of the study area are 27˚07'N and 28˚13' N and longitudes 88˚01'E and 88˚92' E. The altitude of Sikkim ranges from 192 m and 7403 m above mean sea level (msl). Rainfall mainly occurs in monsoon season (May-September) with average annual rainfall of 3300-3600 mm. Absolute maximum temperature (Tmax) and minimum temperature (Tmin) ranges from 17–24°C and 9–13 °C, respectively (Deb et al., 2015).

The undulated geology and rough, rock-bounded topography of Sikkim make it difficult for agricultural practice. Yet, in spite of such impediments, farming practices are done by changing rocky and undulated topography to agrarian land by means of terraces. Major crops grown in Sikkim are maize, rice, and wheat. Although Sikkim's economy is largely dependent on agriculture, most of cultivation is rainfed with traditional system and low-level inputs. Due to lack of adequate harnessing techniques, the total area under agriculture is not more than 11% in Sikkim. However, about 70 % of Sikkim's population depends on agricultural activity for their income.

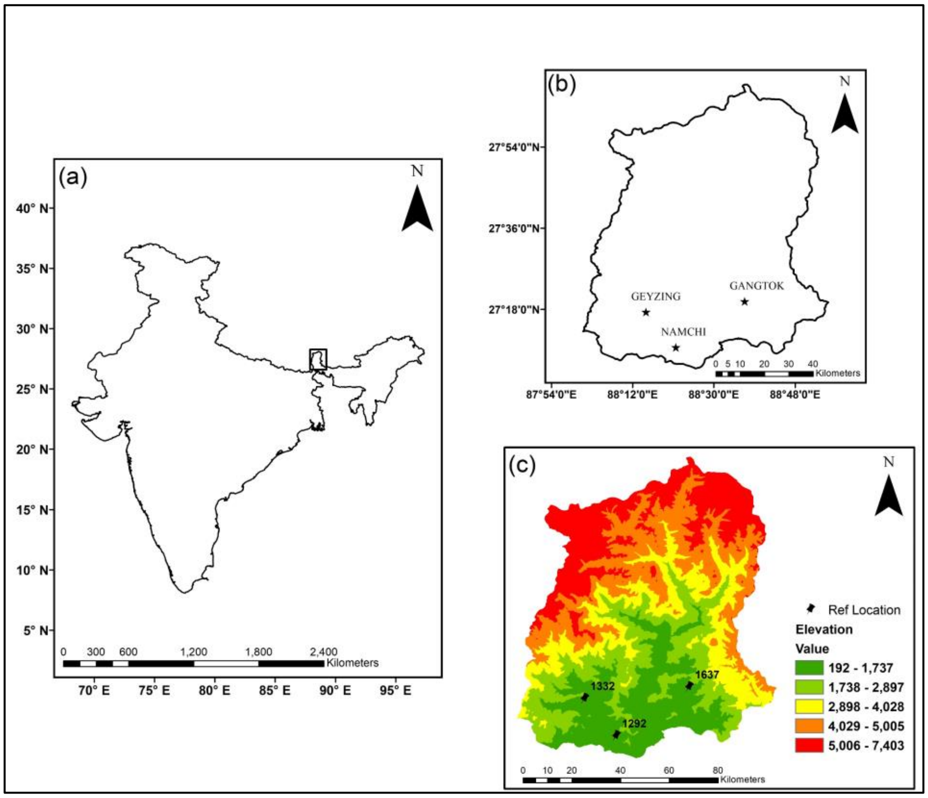

Figure 6.1 (a) Location map of Sikkim over India (red box); (b) map of Sikkim with selected locations; (c) digital elevation map (DEM) of Sikkim and elevation of the selected locations.

6.2.2 Meteorological data (historical and future)

High resolution (0.5°x0.5°) gridded precipitation and temperature data were obtained from India Meteorological Department (IMD). The wind speed data were obtained from the Terrestrial Hydrology Research Group, Princeton University website and were available at 0.5°x 0.5° resolution and the relative humidity data were obtained from the National Center for

Environmental Prediction/ National Center for Atmospheric Research (NCEP/ NCAR) re-analysis dataset. All the datasets were obtained for three different locations. The high-resolution future projection datasets were obtained from CORDEX under RCP4.5 and 8.5 scenarios. Under the CORDEX experiment, the coarser-resolution outputs from the Global Climate Models (GCMs) were downscaled to the finer resolution (0.5° x 0.5°) dynamically. To incorporate ensemble projections of GCMs, we have considered outputs from the four different climate models, namely, Australian Community Climate and Earth-System Simulator version 1.0 (ACCESS1.0), Community Climate System Model, version 4 (CCSM4), Centre National de Recherches Météorologiques Coupled Global Climate Model, version 5 (CNRM-CM5), Max Planck Institute for Meteorology Earth System Model LR (MPI-ESM-LR). It should be noted that the historical datasets were obtained for the period 1970-2005, and the future projected datasets were downloaded during 2006-2099 under different scenarios. The overlapping period during 1970-2005 was considered to perform the bias correction in the GCM simulated climate data with respect to measured data.

6.2.3 Crop, soil and management data

Three major crops such as (rice, wheat, and maize) were chosen to investigate the climate change impact on crop productivity under different climate scenarios. In case of rice, dry and wet field seeding methods were adopted; however, commonly the watered field direct seeding method was adopted to transplant the paddy seedlings. Hence, the total rice yield is assumed to come from the wetland rice grown area. Hence, the historical yields of these crops were obtained for east, south, and west Sikkim. The historical yields for different crops under different regions were collected during 1998-2015 and plotted as boxplot in Figure 6.2. The crop data was collected from *https://data.gov.in/resources/district-wise-season-wise-crop-production-statistics-1997* (accessed on 5th May 2018). The datasets were provided by the Ministry of Agriculture and Farmers Welfare and Department of Agriculture, Cooperation and Farmers Welfare Directorate of Economics and Statistics under National Data Sharing and Accessibility Policy. The datasets were meant to use to study and analyse the crop production, crop growing pattern and diversification, performance according to agro-climatic zone, etc. The annual yield datasets for different crops were provided according to district-wise across India.

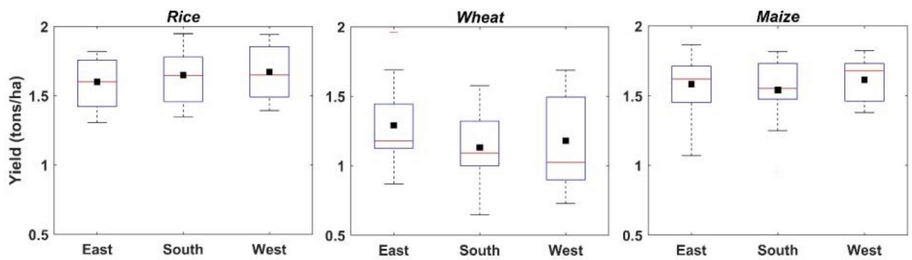

Figure 6.2 Boxplot of crop yield for different crops and regions during 1998-2015.

The black square in Figure 6.2 denotes the mean yield value during 1998-2015. It is shown by Figure 6.2 that the variability in the yield of wheat for all regions and maize for the east region is highest. There is no substantial change in the mean yield between rice and maize for all the regions during 1998-2015. However, the mean yield of wheat in east Sikkim was higher than the south and west Sikkim. The sowing dates for maize (pre-kharif), rice (Kharif), and wheat (rabi) were considered from April-May, June-July, and November-December, respectively. The length of the crop development stage (in days) for maize, rice, and wheat were taken as 35, 40 and 25 days, respectively. The typical local growing seasons for different crops were chosen based on the previous relevant literature (Basnet et al., 2003; Deb et al., 2015; Government of Sikkim, 2013). The cropping pattern over Sikkim varies with altitudes (above 1200m, between 800 to 1200m, and below 800m). As a main crop, for rice irrigation is mostly required. The tank irrigation system helps in collecting and conserving the water and using the sprinkler irrigation system the irrigation is performed from the water tank using networks of pipes under high pressure and is forced through nozzles of small diameter. The farm mechanization is almost nonexistent due to very steep slopes. The soil type is mostly loamy based on the FAO soil classification.

6.2.4 Methods

6.2.4.1 Bias correction

The outputs from the GCMs are generally biased and are rarely used directly. In particular, spatial averaging, imperfect conceptualization, and discretization within the grids can be attributed as the reasons for inherent biases in the outputs (Teutschbein and Seibert, 2012). Therefore, it is essential to bias-correct the GCM outputs so that it effectively denotes the real patterns. In the present analysis, distribution mapping is used as a bias-correction technique for precipitation and temperature profile. The motive of the method is to correct the probability distribution function of the model simulated series to match the distribution of the observed series. This method is also known as quantile-quantile mapping (Johnson and Sharma, 2011), histogram equalization (Rojas et al., 2011), probability mapping (Block et al., 2009). Generally, gamma and gaussian distributions are used in case of precipitation and temperature profiles, respectively. The readers are advised to follow Teutschbein and Seibert (2012) for the detailed explanation of the bias-correction methodology. The equations used to correct precipitation and temperature series are presented in Eqs. 6.1 and 6.2. Based on these corrections, the future projected datasets of multiple GCMs are corrected before analyzing the impact of climate change on crop water requirement and irrigation requirement (Teutschbein and Seibert, 2012).

$$P_{con}{}^{*}(d) = F_{\gamma}^{-1}(F_{\gamma}(P_{con}(d)|\alpha_{con,m}, \beta_{con,m})|\alpha_{obs,m}, \beta_{obs,m})$$

$$P_{fut}{}^{*}(d) = F_{\gamma}^{-1}(F_{\gamma}(P_{fut}(d)|\alpha_{con,m}, \beta_{con,m})|\alpha_{obs,m}, \beta_{obs,m}) \qquad (6.1)$$

$$T_{con}{}^{*}(d) = F_N^{-1}(F_N(P_{con}(d)|\mu_{con,m}, \sigma_{con,m}^2)|\mu_{obs,m}, \sigma^2{}_{obs,m})$$

$$T_{fut}{}^{*}(d) = F_N^{-1}(F_N(P_{fut}(d)|\mu_{con,m}, \sigma_{con,m}^2)|\mu_{obs,m}, \sigma^2{}_{obs,m}) \quad (6.2)$$

Different symbols and notation used in Eqs. 6.1 & 6.2: con- control period (GCM simulated under baseline period i.e., 1970-2005); fut- future; obs- observed; (d)- daily; m- monthly interval; P- precipitation; T- temperature; γ - Gamma distribution; N- Normal distribution; α and β - shape and scale parameter of the Gamma distribution; μ and σ - location and scale parameters of the Gaussian distribution; * - denotes bias-corrected. In this study, the 1970-2005 period is selected as observed reference period, and the bias correction is carried out up to the end of the twenty-first century for all the GCMs under both RCP 4.5 and 8.5 scenarios. For example, before and after bias correction of precipitation, maximum and minimum temperature during the baseline period for the reference location over South Sikkim (Namchi) is presented in Figure 6.3 as quantile-quantile plot for MPI-ESM-LR model. In can be noted from the figure that different meteorological series has been significantly improved as compared to the observed dataset after removal of the bias.

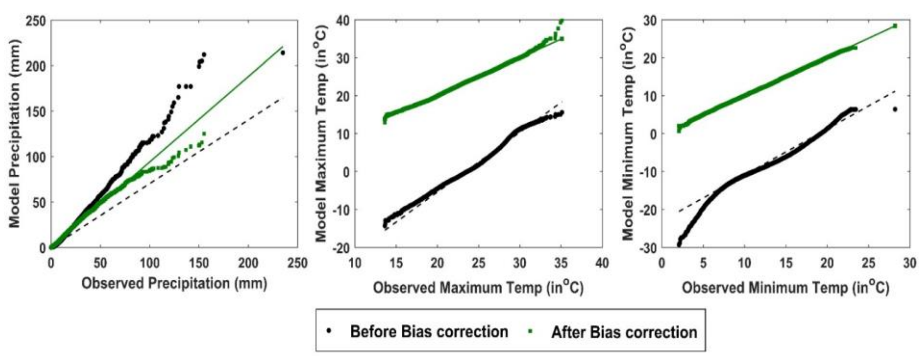

Figure 6.3 Before and after bias-correction of precipitation, maximum and minimum temperature over South Sikkim for MPI-ESM-LR.

6.2.4.2 Crop modelling using AquaCrop model

AquaCrop is a user-friendly model developed by the Food and Agriculture Organizations (FAO). It incorporates several modules viz., atmosphere, crop, soil, management practices to simulate the yield of major herbaceous crops. The model involves a lesser number of input datasets in comparison to the radiation-driven and carbon-driven models and has been proven its applicability to simulate the crop yield with reasonably good accuracy over the globe. AquaCrop considers water as a key limiting factor for crop production, where evapotranspiration (ET) is essential for computing the yield (Y). AquaCrop divides ET into two components, namely, crop transpiration (Tr) and soil evaporation (E). Based on separated Tr value, it develops a easy canopy growth model. AquaCrop computes the above-ground biomass (B) as a product of normalized water productivity (WP^*) and the ratio of crop transpiration and reference evapotranspiration (ET_o). The weather input variables for example, reference evapotranspiration (ET_o) and precipitation are responsible for the water balance in the soil root zone, temperature plays an essential role in phenology, and water productivity (WP) and leaf growth are controlled by the CO_2 concentration (Steduto et al., 2009). The stepwise procedures of crop yield simulation by AquaCrop are as follows:

I. Simulation of crop development: The green canopy cover is expressed by the fraction of soil covered by the canopy and can be varied between 0 (before emergence) and 100% (maximum CC) depending on the planting density and crop type. The canopy's expansion, ageing, conductance, and senescence determine the amount of water transmitted and subsequently control the biomass productivity (Steduto et al., 2009).

II. Modelling of crop transpiration (Tr): The Tr is computed by multiplying the ET_o with the crop coefficient Kc_{Tr}. The ET_o is calculated by means of Penman-Monteith equation (Fooladmand

and Ahmadi, 2009). The shortage of water and logging of water cause stomatal closure, and under such conditions, the Tr is simulated with Ks as Ks_{sto} for shortage and Ks as Ks_{aer} for logging.

III. Computation of above-ground biomass production (B): AquaCrop accumulates daily biomass production by means of Tr, ET_o and WP^*. The WP^* includes two environmental parameters such as ET_o and CO_2 concentration. The normalization of WP as WP^* increases its applicability to diverse locations and seasons. It is found through the experiment that the lower temperature has decremental effect on the WP^*. A stress indicator of cold temperature for biomass (Ks_b) with GDD is used to decrease biomass production. Therefore, the above-ground biomass production (B) can be defined as:

$$B = Ks_b WP^* \sum \left(\frac{Tr}{ET_o}\right) \tag{6.3}$$

IV. Crop yield (Y) simulation: The crop yield (Y) is computed by multiplying B with the harvest index (HI). The actual HI is evaluated by modifying reference harvest index (HIo) with an adjustment factor (f_{HI}) for stress effects. Thus, Y is computed as:

$$Y = f_{HI} HI_o B \tag{6.4}$$

For more details on AquaCrop, readers are advised to follow Raes et al. (2009), Steduto et al. (2009). For the successful running of the model, AquaCrop needs climate, soil, irrigation, field management, and crop development data.

AquaCrop model parameters: In general, to establish the relationship among the environmental conditions, including different management practices and crop growth, models are used as suitable tools. However, the mathematical representation of actual natural processes leads to parameterization, which inevitably entails simplifications and assumptions and hence imposes uncertainty and inaccuracy (Saltelli et al., 2000).

Therefore, sensitivity analysis of the model parameters is inevitable to quantify the influence of the parameters on the model output (Confalonieri et al., 2010). In this sense, Vanuytrecht et al. (2014b) conducted a global sensitivity analysis of the AquaCrop parameters through multi-crop simulation under various environmental conditions. Also, they examined the crop and soil parameters for maize, rice, and wheat under various meteorological conditions. Based on the sensitivity analysis by Vanuytrecht et al. (2014b) and from the literature review of other research papers, the selected crop and soil parameters are presented in Table 6.1. It should be noted that only the sensitive parameters for crop modelling were considered from the study by Vanuytrecht et al. (2014b). However, the optimum parameters values were obtained based on the calibration and validation processes in the present study.

Calibration and Validation of AquaCrop: The calibration of the AquaCrop model is carried out by changing the sensitive parameters to simulate the crop yield for the historical period, i.e., 1998-2007. The whole period (1998-2015) is divided into calibration (1998-2007) and the validation period (2008-2015). In other words, first 10 years were considered as calibration and the remaining 8 years as validation of the crop model. Due to a smaller number of datasets, the datasets were divided keeping in mind to minimize the chance of getting overfitted or underfitted. Statistically, the average yield during the calibration period is slightly lower than the validation period in case of maize and rice over different regions. Conversely, for wheat the mean yield during validation period is slightly more than calibration period. The optimum parameter set was obtained through the trial-and-error method for all the crops over different districts. In trial and error, one parameter is taken as reference parameter at a time and arrange other parameters that affect the reference parameter as most. This method is done until the closest match between observed and predicted yield achieved. To evaluate the efficiency of the model, the Mean Bias Error

(MBE), Root Mean Square Error (RMSE), and coefficient of determination (R^2) are used as evaluation criteria. The evaluation criteria are calculated as in Eqs. 6.6, 6.7, and 6.8.

$$R^2 = \frac{\sum Y_{S(i)} \times Y_{O(i)} - \sum Y_{S(i)} \times \sum Y_{O(i)}}{\sqrt{\sum Y_{S(i)}^2 - (\sum Y_{S(i)})^2 \times \sqrt{\sum Y_{O(i)}^2 - (\sum Y_{O(i)})^2}}} \tag{6.6}$$

$$RMSE = \sqrt{\frac{\sum_{i=1}^{n} (Y_{S(i)} - Y_{O(i)})^2}{n}} \times \frac{100}{\bar{Y}_O} \tag{6.7}$$

$$MBE = \frac{1}{n} \sum_{i=1}^{n} (Y_{S(i)} - Y_{O(i)}) \tag{6.8}$$

where $Y_{S(i)}$ refers to the model simulated yield during i^{th} period, $Y_{O(i)}$ denotes to the observed yield during i^{th} period, $\bar{Y}_O$ represents the mean observed yield. As proposed by Jamieson et al. (1991) and adopted by Andarzian et al. (2015), based on the RMSE value the model accuracy can be categorized into different groups viz., poor (>30%), fair (20-30%), good (10-20%), and excellent (< 10%). The calibrated parameters and the model efficiency values for different crops and different regions are presented under the results and discussion section.

Table 6.1 The selected crop parameters used in AquaCrop model.

CROP PARAMETERS	Units
Time from sowing to emergence	Days
Maximum effective rooting depth	M
Time from sowing to start senescence	Days
Time from sowing to maximum rooting depth	Days
Time from sowing to maturity	Days
Length of the flowering stage	Days
Time from sowing to flowering	Days
Building up of the Harvest index	Days
Reference Harvest Index	%
Soil surface covered by an individual seedling	cm2/plant
Number of plants per hectare	--
Canopy growth coefficient	% /day
Maximum canopy cover	%
Canopy decline coefficient	%/day
Shape factor for water stress limiting stomatal conductance	--
Shape factor describing root zone expansion	--
Upper threshold of soil water depletion inducing early canopy senescence	Fraction TAW
SOIL PARAMETERS	
Number of soil layers, their texture and thickness	--, --, m
Soil water retention in the fine soil fraction in % (PWP, FC)	% vol
Hydraulic conductivity, root zoon expansion rate, gravel mass	mm/day, %, %
Curve number and readily evaporable water	--, mm

Weather data inputs for AquaCrop: The details of the daily climatic data such as precipitation, temperature (maximum and minimum), wind speed are presented under Section 6.2.2. The ET_o is computed using the inbuilt ET_o calculator through the Penman-Monteith equation. The mean CO_2 concentration measured at Mauna Loa at Hawaii is considered for the observed period, and the future CO_2 concentration opts under RCP4.5 and 8.5 scenarios. It should be noted that the CO_2 concentration for the observed as well as the future scenarios (RCP4.5 and 8.5) are obtained from the AquaCrop model itself. Under the RCP4.5 scenario, the radiative forcing is stabilized before 2100 with the equivalent CO_2 concentration of ~ 650 ppm

(Thomson et al., 2011). However, RCP85 is characterized by an increase in the CO_2 concentration of ~ 1370 ppm by 2100 (Riahi et al., 2011).

Crop data inputs for AquaCrop: The crop data for different districts of Sikkim were described in Section 6.2.3. Here, the crop characteristics and development stage for rice, maize, and wheat are presented in a tabular form (Table 6.2). In addition, 17 different crop parameters were used in AquaCrop model. However, the critical parameters namely, reference harvest index (HI_o), maximum effective rooting depth, CGC, CDC, maximum canopy cover, time from sowing to flowering and sowing to maturity are identified during the model calibration for all the selected crops. CGC determines the time required to reach the maximum canopy and CDC presents the declination rate of green canopy in late season. The HI_o denotes the ratio between dry yield mass to the total dry above ground biomass at maturity under non-stressed conditions. The minimum and maximum temperatures at which pollination starts to fail are known as cold stress and heat stress, respectively. For rice, maize and wheat the cold and heat stress temperature were found to be 8 ^oC and 35 ^oC, 10 ^oC and 40 ^oC, and 5 ^oC and 35 ^oC, respectively. Table 6.3 presents the different parameters and their associated values over different districts.

Table 6.2 Different crops and their development stages.

Crop & it's Characteristics	**Initial**	**Crop Development**	**Mid-Season**	**Late**	**Total**	**Sowing Date**
Maize						
Stage length days	20	35	40	30	125	April-May
Crop Coefficient	0.4	--	1.2	0.5	--	
Root depth	0.3	>>	>>	1		
Yield Response factor	0.4	0.4	1.3	0.5	1.25	
Rice						
Stage length days	30	40	35	20	125	June-July
Root depth	0.1	>>	>>	0.6		
Crop Coefficient wet	1.7	--	1.7	0.4	--	
Crop Coefficient dry	0.5	--	1.05	0.7	--	
Yield Response factor	1	1.09	1.32	0.5	1.1	
Wheat						
Stage length days	15	25	50	30	120	Nov-Dec
Crop Coefficient	0.3	--	1.15	0.4	--	
Root depth	0.3	>>	>>	1.2		
Yield Response factor	0.2	0.65	0.55	0.1	1.05	

Table 6.3 Calibrated parameters of different crops over different districts.

Parameters	Unit	Rice			Maize			Wheat		
		ES*	**WS***	**SS***	**ES**	**WS**	**SS**	**ES**	**WS**	**SS**
Canopy Growth Coefficient (CGC)	Per day	0.11	0.1	0.1	0.11	0.11	0.09	0.11	0.1	0.1
Canopy Decline Coefficient (CDC)	Per day	0.09	0.1	0.1	0.09	0.08	0.08	0.09	0.1	0.1
Reference Harvest Index (%)	%	43	41	42	39	38	36	43	41	42
Maximum Effective Rooting Depth	M	0.68	0.7	0.7	0.91	0.9	0.87	0.68	0.7	0.7
Maximum Canopy Cover (CCx)	%	0.95	0.9	1	0.94	0.91	0.89	0.95	0.9	1
Time from Sowing to Flowering	Calendar day	61	59	60	68	63	63	61	59	60
Time from Sowing to Maturity	Calendar day	111	110	111	113	109	107	111	110	111
Air Temperature Stress (cold stress)	in degree Celsius	8			10			5		
Air Temperature Stress (hot stress)	in degree Celsius	35			40			35		

* ES-East Sikkim, WS-West Sikkim, SS- South Sikkim

Soil data inputs used for AquaCrop: AquaCrop needs a number of inputs such as number of soil horizon, and their respective thickness (m), saturated hydraulic conductivity (mm/day), field capacity (% vol), bulk density (gm/cc), total available water (mm/m), permanent wilting point (% vol) and curve number. These inputs are used by AquaCrop to project water content in the root zone of the crop. Curve number helps in the estimation of surface runoff occurred on the site. In general, the present study area is dominated by loamy soil. The type of soil was extracted from FAO soil map (raster image) by superimposing the boundary file of Sikkim. For loamy soil the saturated hydraulic conductivity (K_{sat}) was considered between 100 to 750 mm/day. The soil water content (%) at permanent wilting point, field capacity, and saturation 6-20%, 23-42%, and 42-55%, respectively. The curve number was considered based on the K_{sat} of type of soil of the top horizon. Hence, considering loamy soil as topsoil with K_{sat} > 250, the curve number value was considered as 65. The maximum effective rooting depth for rice, maize and wheat was obtained in the range of 0.68-0.7m, 0.87-0.91m, and 0.68-0.7m, respectively across different districts. These values are presented in Table 6.3. In the present study, four soil horizons were selected and different soil characteristics for each horizon are shown in Table 6.4.

Table 6.4 Different soil properties at different soil depth/horizon.

Parameters	**Soil Depth (cm)**			
	0-20	**21-60**	**61-76**	**77-120**
FC (%)	39	46	52	42
PWP (%)	24	15	18	16
SAT (%)	45	50	55	52
K (mm/day)	15	2	2.4	3
Bulk density (g cm^{-3})	1.36	1.24	1.22	1.09

Crop management inputs used for AquaCrop: The management inputs for the AquaCrop modelling incorporates irrigation and field management files. However, due to the unavailability of the field management data, the field management was not considered. In the present study, the irrigation scheduling (i.e., irrigation timing and net application depth) was computed using Cropwat software using climate, crop, and soil data for the rice crop only and provided as an input to AquaCrop as an irrigation management file. The percentage of soil surface wetted by the irrigation was considered as 100%. For maize and wheat rainfed irrigation technique was used.

To accomplish the AquaCrop modelling, the methodology is summarized in the form of a flowchart and presented in Figure 6.4.

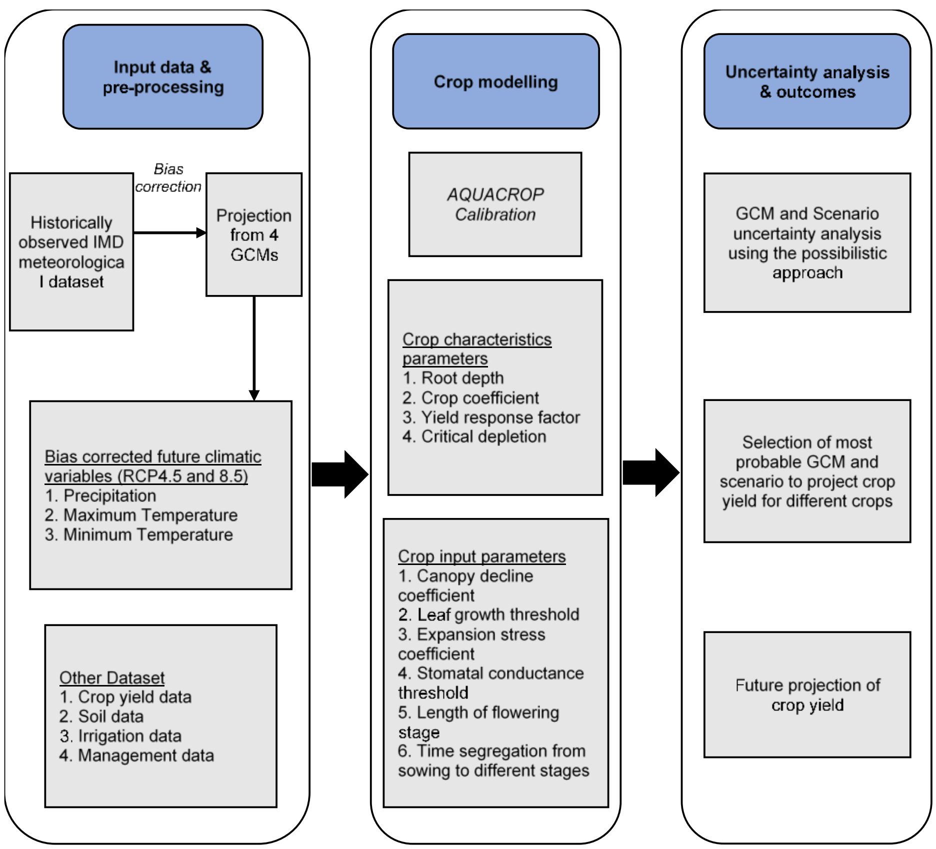

Figure 6.4 Flow chart of the AquaCrop methodology.

6.2.4.3 CROPWAT modelling

The crop water requirement varies extensively and is affected by types of crops, properties of soil, weather conditions, etc. The amount of water lost by the crop represents by the crop evapotranspiration (ET_c) and CWR represents the extra amount of water that has to be supplied for growth of crop. In the present study, CROPWAT model is used to compute the CWR for different major crops over Sikkim. According to Smith et al. (2002), the model requires less number of input datasets as compared to the other models. The model uses Penman-Monteith method (Eq. 6.9) to compute ET_o, crop evapotranspiration and irrigation requirement (Allen et al., 1998; Smith, 1991). At present, there are different methods are being used to compute the CWR in water resources research. For instance, the Blaney-Criddle, Penman-Monteith, radiation, and pan evaporation methods are commonly used to compute CWR for different crops. Moreover, the choice of methods is based on the precision required to compute the water needs and availability of climatic datasets. Due to the excellent performance and inclusion of physical theory in computation, Penman-Monteith method is widely used (Pereira et al., 2015). In addition, this method offers minimum percentage of error as compared to the other method, i.e. ±10% in summer and up to 20% under low evaporative condition (Doorenbos and Pruitt, 1977). Therefore, we have used Penman-Monteith method to analyse spatio-temporal variability of CWR for different major crops. To do so, CROPWAT, which has been highly recommended by FAO to better estimate of CWR under different climate change scenarios (Smith, 1992), is used.

$$ET_o\left(\frac{mm}{day}\right) = \frac{0.408\Delta(R_n - G) + \gamma \times \frac{900}{T+273} \times U_2(e_s - e_a)}{\Delta + \gamma(1 + 0.34U_2)} \tag{6.9}$$

where, Δ is the slope of the saturation vapor pressure temperature relationship (KPa/^{o}C); R_n is the net radiation at the crop surface (MJ/m^2/day); G is soil heat flux density (MJ/m^2/day); γ is psychrometric constant (KPa/^{o}C), U_2 is the measured wind speed at 2-meter height (m/sec); e_s and e_a are saturation and actual vapor pressure in KPa, respectively; T is the mean daily air temperature (in ^{o}C).

The model requires different input data modules, namely, climate data, crop data, soil data, and crop pattern data. The climate data includes precipitation, temperature (minimum and maximum), windspeed, relative humidity, sunshine hours, etc. Similar to the climate data, the crop data such as maximum rooting depth, crop description, crop factor, rooting depth, growing days, etc. are needed. The crop development stages with different crop properties are mentioned in Table 6.2. The soil properties, namely, soil moisture availability, initial soil moisture depletion, maximum rooting depth, and maximum infiltration rate are given as inputs to CROPWAT model. Loamy soil is more dominated in the study area. The soil and crop data are collected from the literature (Deb et al., 2015; Dubey and Sharma, 2018) and (Allen et al., 1998). The CWR is computed using Eq. 6.10.

$$ET_c = K_c \times ET_o \tag{6.10}$$

where, K_c is the crop coefficient that depends on various factors like soil, crop height, albedo, wind speed and its direction, etc. Moreover, K_c varies for the types of crop and growing stages of crop.

To compute the crop irrigation requirement (CIR), effective rainfall ($P_{effective}$) is computed based on the fixed percentage method. In Indian condition, it is advised to consider 50-80% of the total rainfall as effective (Dastane, 1974). In the present study, we have chosen 65% as effective precipitation considering the undulated topography of the study area. The amount of irrigation requirement is calculated by subtracting estimated effective rainfall from calculated crop water requirement (Eq. 6.11).

$$CIR = CWR - P_{effective} \tag{6.11}$$

To accomplish the CROPWAT modelling, the methodology is summarized in the form of a flowchart and shown in Figure 6.5.

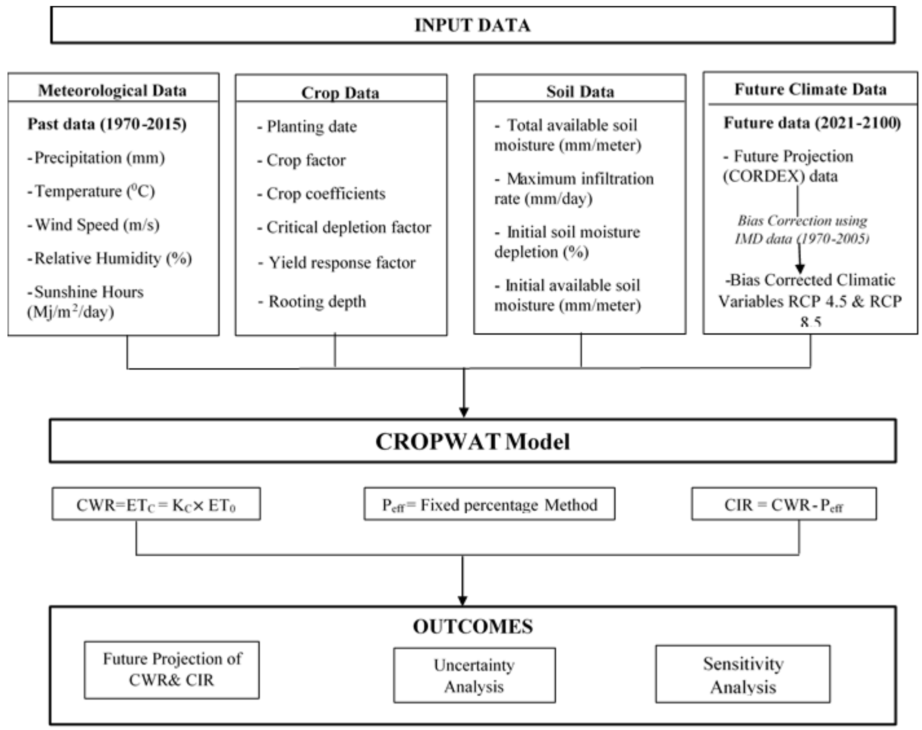

Figure 6.5 Flow chart of the CROPWAT methodology.

6.2.4.4 Linear trend analysis

To identify the linear trend in the CWR and CIR time series, we have used a non-parametric method named as Sen's slope estimator proposed by Sen (1968). Sen's slope method computes the slope of the trend and the corresponding intercept of the time series. The slope of the time series is computed by using Eq. 6.12.

$$S = \frac{y_j - y_k}{j-k}, \text{for } j = 1, \ldots\ldots, n-1, n;\ k = 1, \ldots\ldots, j-1 \tag{6.12}$$

where, S is the slope, y_j and y_k are the data points at time j and k where (j>k). With total number of data points n, the possible slope estimates can be n(n-1)/2 (Zaifoğlu et al., 2017). After computing all the possible slope values, the values of S are ranked in an increasing order. If the total count of slope is an odd number, then the middle value of will be the median of slope otherwise the median value will be the mean of the two values at the center.

6.2.4.5 Uncertainty analysis using possibility theory

As we know that outputs from the GCMs under the possible future scenarios are associated with the large uncertainties. In the context of agricultural practices and its management, it is indispensable to assess the uncertainties for effective planning and adaptation strategies. Moreover, the assumption of giving equal weight to all the projections from GCMs under different scenarios will induce more uncertainties and difficulties in agricultural management. In this sense, it is necessary to examine which scenario and GCM represent the current climate situation. Therefore, possibility theory is used to analyze the emission scenario and GCM uncertainty through possibilistic analysis concerning the capability in simulating the present climate conditions. Zadeh (1999) used the possibility theory to ascertain uncertainty due to incomplete or partial knowledge. For instance, the theory of probability can be applied to a dataset with complete information. However, the applicability of probabilistic theory for the dataset with partial knowledge is not possible. In the present situation, outputs from the GCMs and future climate scenarios can be considered as the dataset with partial information. In such cases, possibility theory can be assigned and the mathematical expression as in Eq. 6.11.

$$\prod_X(x): \Omega \rightarrow [0,1] \tag{6.11}$$

Where x is the degree of possibility that X can be assigned. Therefore, x=0 denotes that X=x is not possible, and x=1 denotes X=x is possible without any constraint. According to the property of normalization in possibilistic approach, there must be one $\tilde{x}$ such that $\prod_X(\tilde{x}) = 1$(Spott, 1999). For details of the possibility theory, readers are advised to follow Das et al. (2018). The hypothesis to perform the uncertainty analysis is as follows:

Step 1: It is assumed that during the early historical period (1998-2005) climate change forcing is lower than for the later period of 2006-2015. Hence a possibility approach is applied to assess for the second period the fit of the selected climate scenarios. It should be noticed that the period for the possibility analysis is purely based on the available dataset.

Step2: In this step, the climate scenario based simulated crop yields are compared with the observed yields for the period 2006-2015 in order to estimate the simulation performance, the performance index (C) evaluates the deviation of the simulated yield or CWR or CIR from the observed yield or CWR or CIR as presented in Eq. 6.12.

$$C = 1 - \frac{\sum_t (X_{obs(t)} - X_{sim(t)})^2}{\sum_t (X_{obs(t)} - \bar{X}_{obs})^2} \tag{6.12}$$

Where, $X_{obs(t)}$ and $X_{sim(t)}$refer to the observed and crop model simulated yield or CWR or CIR for the particular year (t) respectively and $\bar{X}_{obs}$denotes the mean observed yield or CWR or CIR.

Step 3: Based on the normalization property, the computed C values from a particular emission scenario and GCM is divided by the largest value of C of that climate scenario and the computed GCM and the computed value is treated as the possibility value.

6.3 Results and discussion

6.3.1 Future projection of precipitation and temperature

As discussed in the methodology section, distribution mapping is carried out to minimize the inherent bias in the meteorological outputs from the GCMs and significant improvement in the outcomes is noticed after the bias-correction. The annual variation in the precipitation, maximum and minimum temperature for east, south, and west Sikkim is presented in a graphical form (Figure 6.6).

The red and blue shadows denote the ensemble projection of all the GCMs under RCP8.5 and 4.5 respectively. The solid red and blue line presents the ensemble mean. It can be noted from the figure that there is an increasing trend in the minimum and maximum temperature under both the scenarios and the change is significantly higher in the case of RCP8.5 than 4.5. The highest variation in the maximum temperature is noticed over South Sikkim, whereas minimum variation is observed over East Sikkim. However, the variability in the increase in minimum temperature has no significant difference with respect to the baseline period temperature for the different regions. In line with the present study, other studies also reported an increase in warming trends over Sikkim (Deb et al., 2015; Goswami et al., 2018a; Telwala et al., 2013). The annual precipitation pattern is likely to decrease over South and West Sikkim, while there is no significant change in the annual precipitation over East Sikkim under both the climate forcing scenarios.

6.3.2 AQUACROP results

6.3.2.1 Evaluation of model performance

The calibration and validation of the AquaCrop model was carried out using the observed yield data during 1998-2015. Based on the model performance results, the best fit model is used to project the crop yield for future scenarios. It should be noted that the model parameters were used to simulate the yield for the future period while changing the meteorological parameters. AquaCrop was calibrated for rice, maize, and wheat for three different districts of Sikkim. The calibrated parameters for rice, wheat, and maize are presented as the tabular form in Table 6.3 (section 6.2.4.2). Moreover, the calibration and validation plots for different crops are presented in Figure 6.7(a & b), respectively. Table 6.5 presents the model evaluation criteria for different crops for the different regions. Based on the classification of RSME (as discussed in section 6.2.4.2), the model accuracy during calibration and validation resulted in excellent and good categories in simulating the maize, rice, and wheat. Moreover, in most of the cases, AquaCrop is capable of capturing more than 70% of the variance of the observed yield during the calibration and validation period.

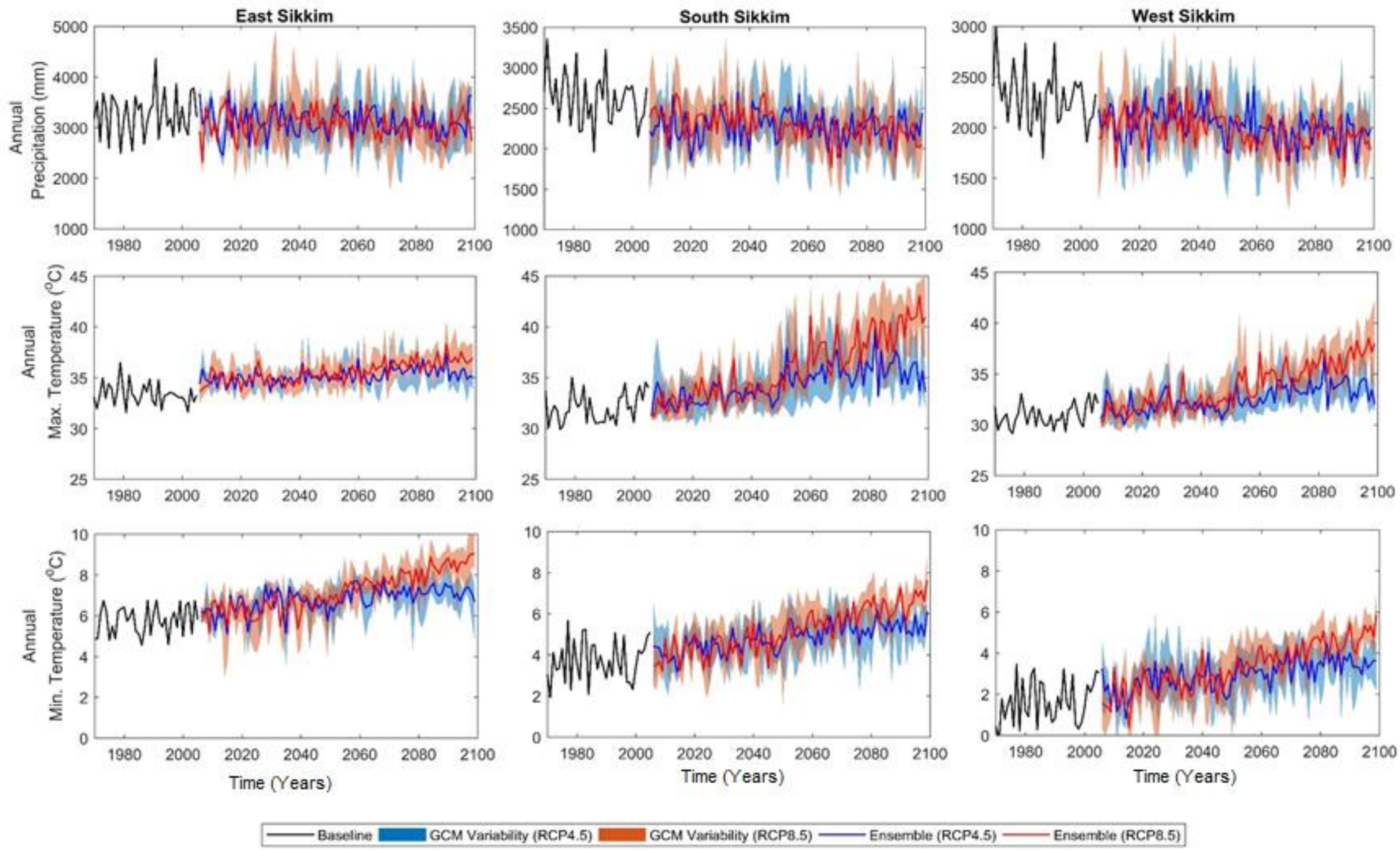

Figure 6.6 Annual variability of meteorological data for different districts of Sikkim.

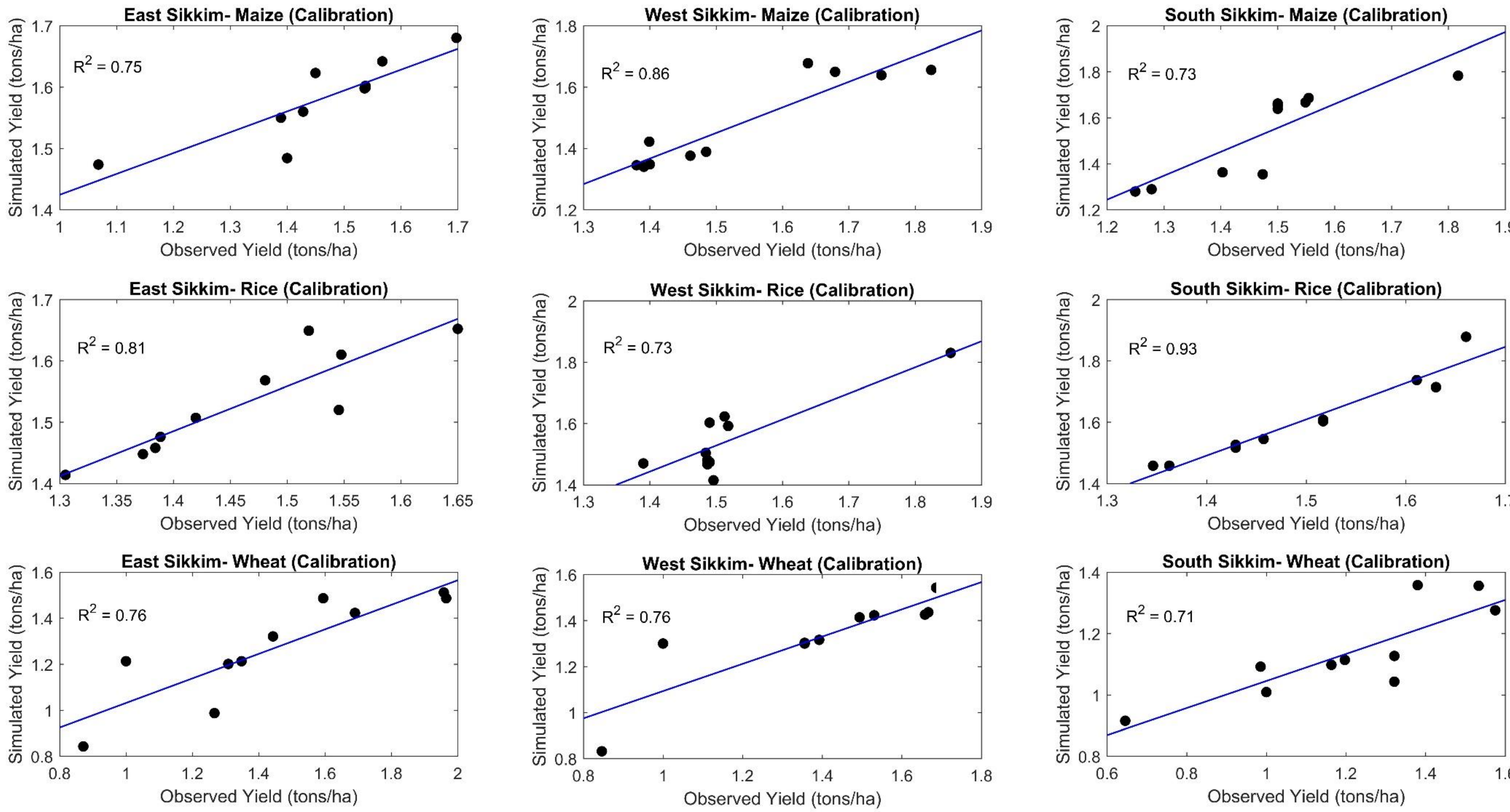

Figure 6.7a Calibration results of three major crops over three different districts.

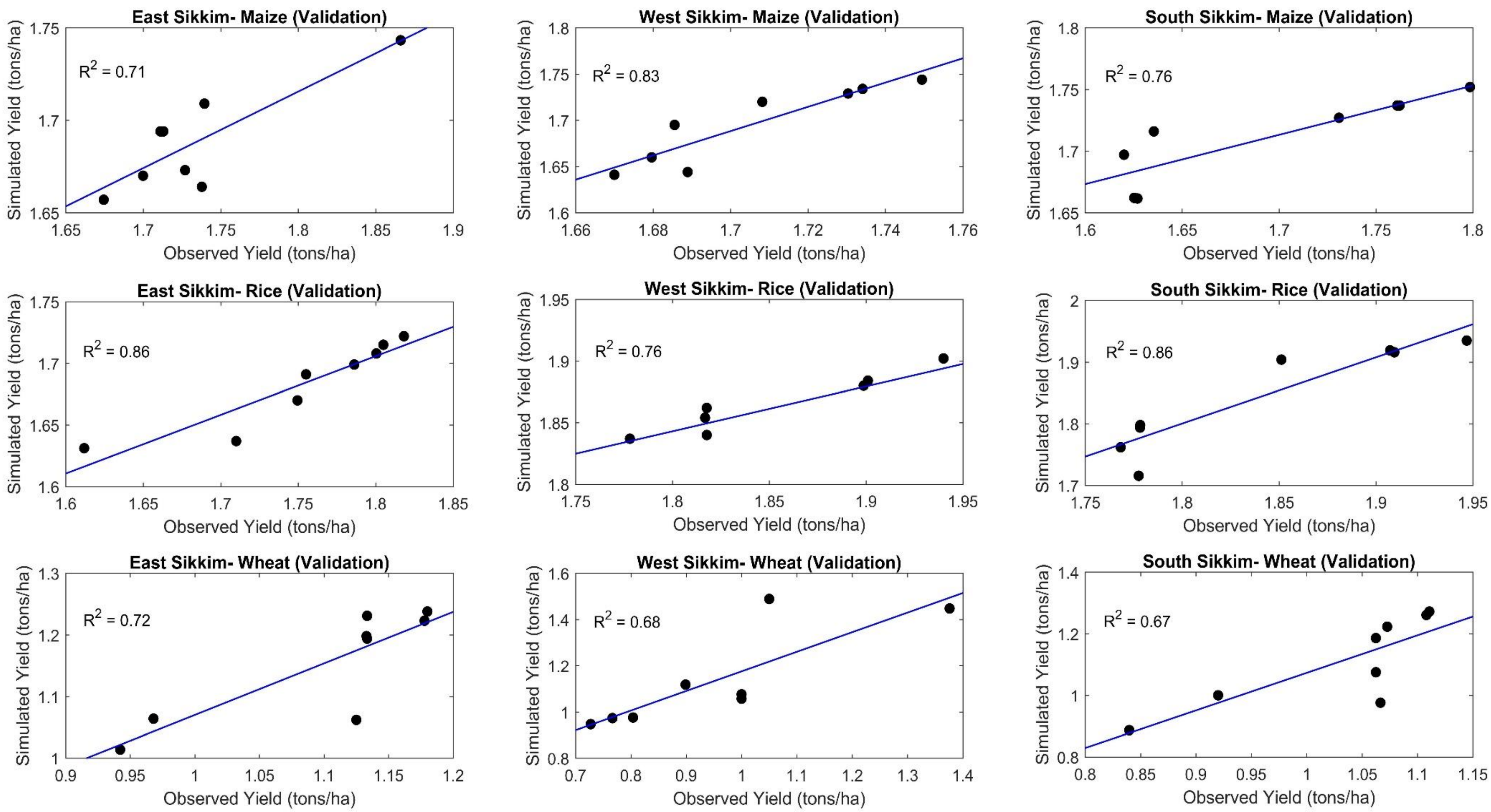

Figure 6.7b Validation results of three major crops over three different districts.

Table 6.5 Computed model efficiency for the calibration and validation period of different crops over different regions.

Period	Stations	Maize			Rice			Wheat		
		R^2	RMSE (kg/ha)	MBE (kg/ha)	R^2	RMSE (kg/ha)	MBE (kg/ha)	R^2	RMSE (kg/ha)	MBE (kg/ha)
Calibration	East Sikkim	0.75	10.56	109.10	0.81	5.35	62.50	0.76	17.20	-159.80
	West Sikkim	0.86	5.04	-51.30	0.73	4.77	22.68	0.76	10.72	-62.96
	South Sikkim	0.73	7.01	50.13	0.93	7.32	98.40	0.71	14.33	-66.77
Validation	East Sikkim	0.71	2.81	-45.50	0.86	3.82	-70.30	0.72	5.56	53.94
	West Sikkim	0.83	1.04	-9.90	0.76	1.64	7.57	0.68	19.38	182.60
	South Sikkim	0.76	2.41	16.36	0.86	1.42	3.36	0.67	9.44	79.62

6.3.2.2 Future projection of yield from all the GCMs

For the future projection of yield, the two emission scenarios, namely, RCP4.5 and 8.5, are used to predict the yields of rice, maize, and wheat over three districts of Sikkim. For analysis the future period, i.e. 2021-2099 is divided into 4 divisions (2021-2040, 2041-2060, 2061-2080, and 2081-2099). The outcomes are presented as boxplot (Figure 6.8a for Maize, Figure 6.8b for Rice, Figure 6.8c for wheat). It can be noted from Figure 6.8a that there is a significant increase in the maize yield for all the models under both the scenarios. Additionally, the yield variability is reduced significantly as compared to the historical period. The future rice yield (i.e., Figure 6.8b) projections show similar outcomes as maize. However, the variability in most of the projections especially over South and West Sikkim is higher in comparison with the observed period. Similarly, the projection of mean yield for wheat (Figure 6.8c) indicates an overall increase for the three districts. It has to be mentioned that the uncertainty analysis of GCM and emission scenarios was not carried out for the future projection of yield. The future projection with uncertainty analysis is discussed in the next section.

6.3.2.3 Future projection of yield after uncertainty analysis

The assumption, which is considered to perform the possibility theory-based uncertainty analysis, is that climate change has minimal impact on the baseline period. Incorporating the possibility theory, possible value for different GCMs and scenarios are calculated. For instance, from a group of GCMs (G_1, G_2, ….., G_n) and scenarios (S_1, S_2, ….., S_n) it is required to compute the possibility value for G_1 and S_1. Subsequently, according to the possibility distribution, the possibility values of G_1 and S_1 are provided in Eq. 6.13 and 6.14.

$$\prod(G1) = \prod((G_1, S_1) \cup \prod(G_1, S_2) \cup \ldots\ldots\ldots \cup \prod(G_1, S_n)) = sup(\prod(G_1, S_1), \prod(G_1, S_2), \ldots\ldots\ldots, \prod(G_1, S_n)) \quad (6.13)$$

$$\prod(S_1) = \prod((G_1, S_1) \cup \prod(G_2, S_1) \cup \ldots\ldots\ldots \cup \prod(G_n, S_1)) =$$
$$sup(\prod(G_1, S_1), \prod(G_2, S_1), \ldots\ldots\ldots, \prod(G_n, S_1)) \quad (6.14)$$

The ‘sup’ operator symbolizes maximum. In order to analyse the associated uncertainty, it has to be checked whether the observed trend of crop yield over the years were due to the improvements in production technology and/or due to the climatic influence. Therefore, the yield over the observed period 2006-2015 was simulated using the calibrated model and observed weather data. Then the comparison between the observed and simulated yield time series was carried out to check whether the trendlines were similar or different. In the case of dissimilarity, the uncertainty analysis should be carried out after de-trend the observed yield during 2006-2015. Conversely, it can be assumed that the yield trend was due to the influence of climatic factor and can be used directly in the uncertainty analysis. In the present study, the dissimilarity of temporal trend was not observed for all the crops and hence, the observed yield was directly used to assess the uncertainty. To evaluate the possibility value, performance index (C) is calculated and presented in Table 6.6a based on Eq. 6.11. The C value was computed for the duration between 2006 and 2015 for the GCM and emission scenarios in comparison to the observed yields for that period. The maximum C values for different crops over different districts for all the GCMs and scenarios are estimated and marked as superscripted star mark in the Table 6.6a. Based on the normalization property, the maximum C value is divided with other C values for a particular crop under a particular district. The possibility values are presented under Table 6.6b.

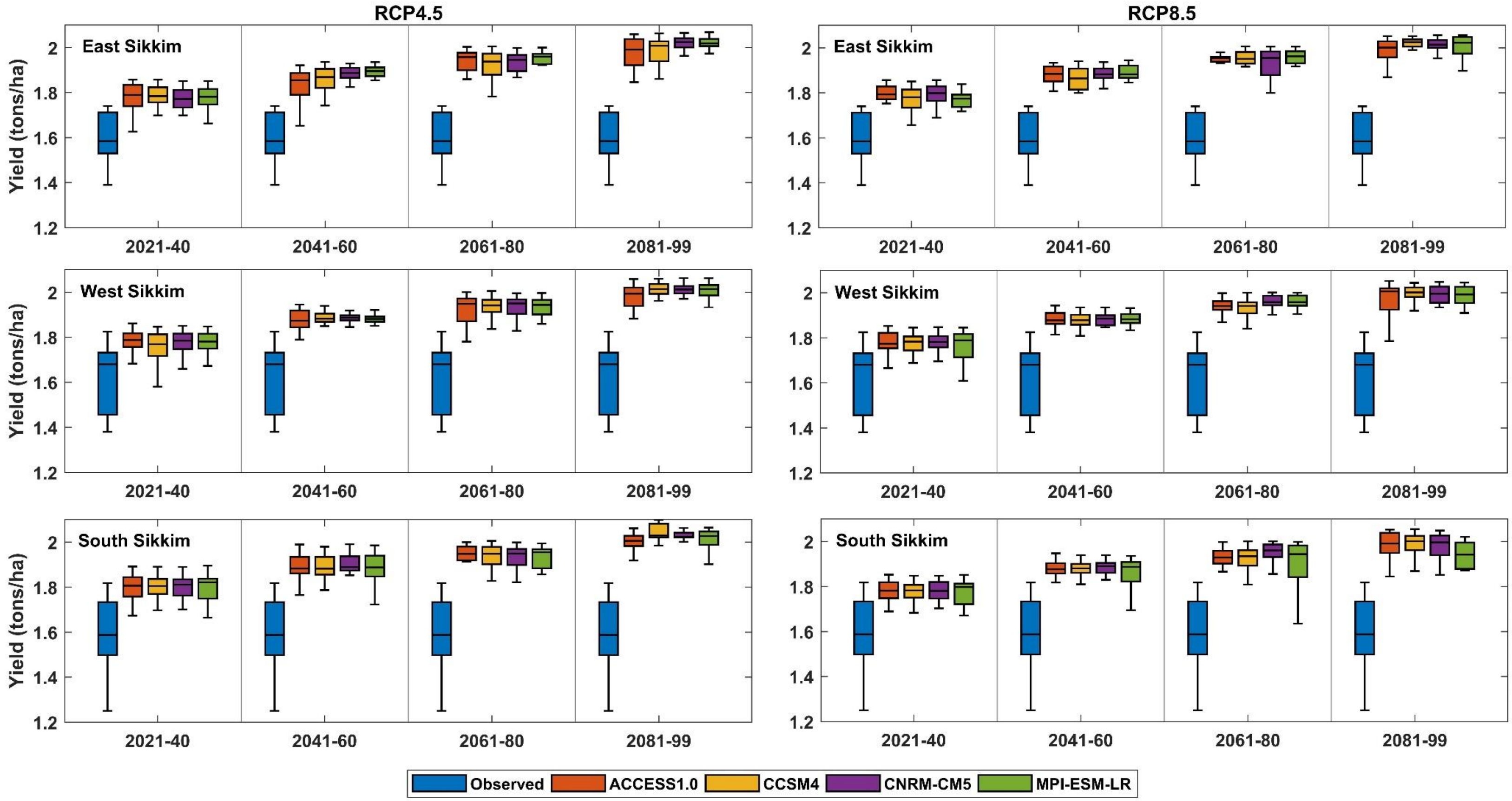

Figure 6.8a Future projection of Maize yield from all the GCMs and their scenarios.

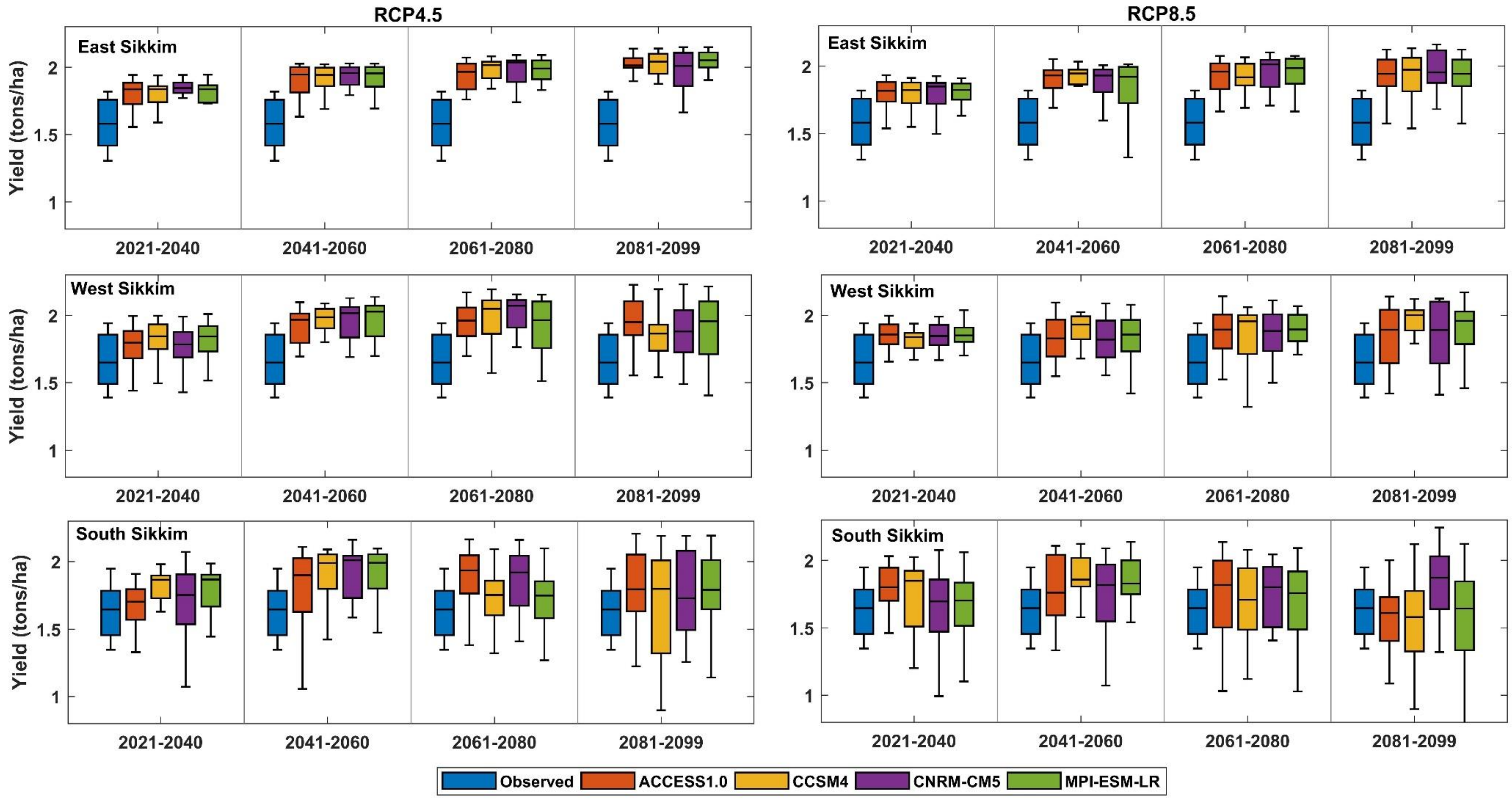

Figure 6.8b Future projection of Rice yield from all the selected GCMs and their scenarios.

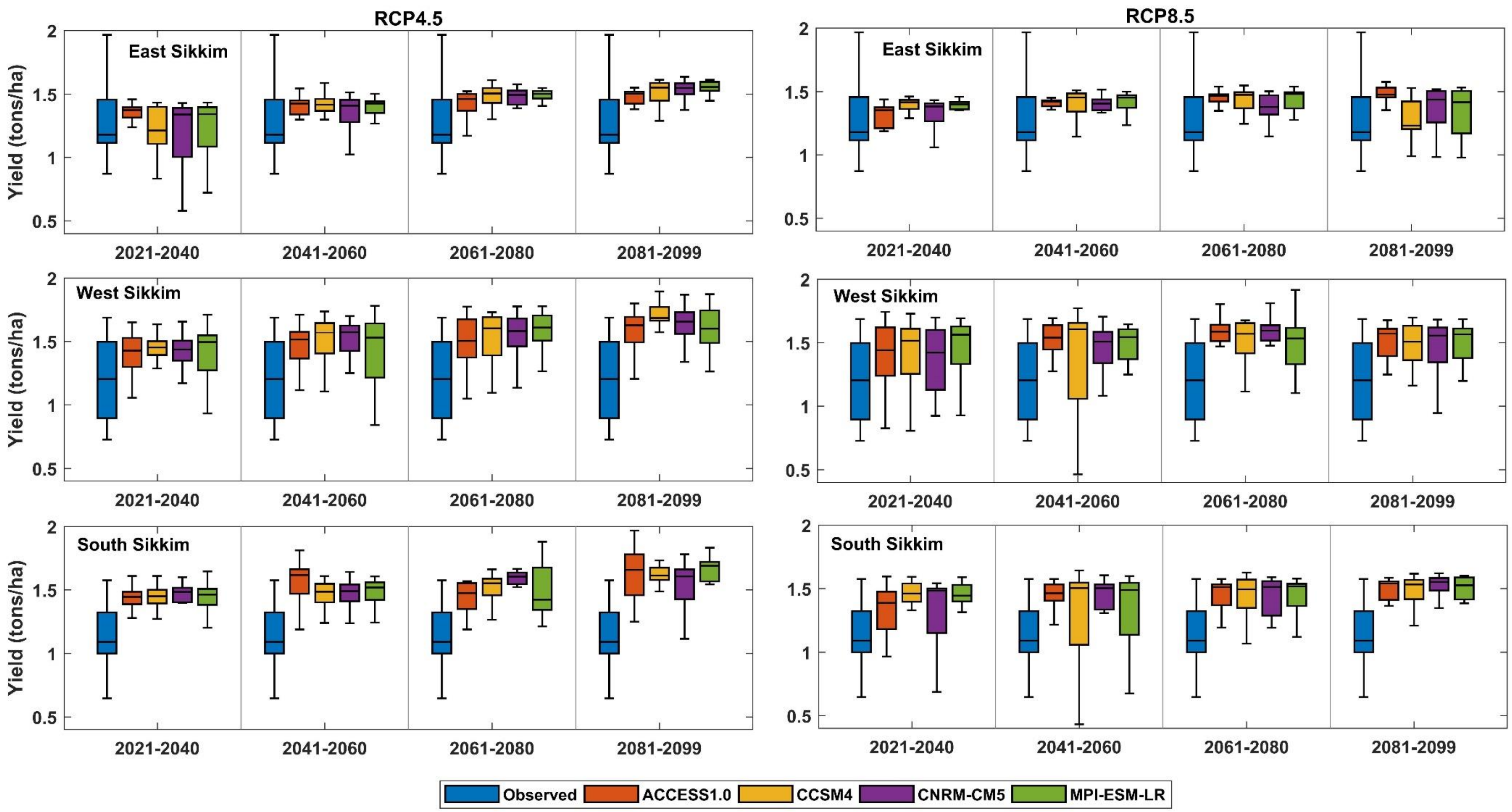

Figure 6.8c Future projection of Wheat yield from all the selected GCMs and their scenarios.

Table 6.6a The computed C values for different crops under different GCMs and scenarios during 2006-2015

Crop	**GCM/ Scenarios**	**ACCESS1.0**		**CCSM4**		**CNRM-CM5**		**MPI-ESM-LR**	
		RCP4.5	**RCP8.5**	**RCP4.5**	**RCP8.5**	**RCP4.5**	**RCP8.5**	**RCP4.5**	**RCP8.5**
Maize	East Sikkim	0.39	0.37	0.49*	0.40	0.44	0.48	0.45	0.43
	West Sikkim	0.77*	0.70	0.56	0.29	0.50	0.31	0.37	0.37
	South Sikkim	0.65	0.70*	0.69	0.69	0.65	0.69	0.63	0.68
Rice	East Sikkim	0.65	0.54	0.38	0.57	0.69	0.53	0.68	0.87*
	West Sikkim	0.92*	0.66	0.73	0.63	0.72	0.73	0.70	0.62
	South Sikkim	0.66*	0.52	0.59	0.39	0.61	0.42	0.49	0.39
Wheat	East Sikkim	0.31	0.37	0.32	0.35	0.31	0.41*	0.39	0.39
	West Sikkim	0.80	0.57	0.81*	0.52	0.80	0.60	0.78	0.57
	South Sikkim	0.38	0.31	0.39	0.32	0.41	0.33	0.42*	0.41

Table 6.6b Possibility value for different crops under different GCMs and scenarios during 2006-2015.

Crop	**GCM/ Scenarios**	**ACCESS1.0**		**CCSM4**		**CNRM-CM5**		**MPI-ESM-LR**	
		RCP4.5	**RCP8.5**	**RCP4.5**	**RCP8.5**	**RCP4.5**	**RCP8.5**	**RCP4.5**	**RCP8.5**
Maize	East Sikkim	0.79	0.75	***1.00***	0.82	0.89	0.98	0.92	0.87
	West Sikkim	***1.00***	0.91	0.73	0.37	0.65	0.40	0.48	0.48
	South Sikkim	0.93	***1.00***	0.98	0.98	0.93	0.98	0.90	0.96
Rice	East Sikkim	0.75	0.62	0.43	0.66	0.80	0.61	0.78	***1.00***
	West Sikkim	***1.00***	0.71	0.79	0.68	0.78	0.80	0.76	0.68
	South Sikkim	***1.00***	0.79	0.90	0.60	0.92	0.63	0.73	0.59
Wheat	East Sikkim	0.77	0.91	0.79	0.87	0.76	***1.00***	0.96	0.97
	West Sikkim	0.98	0.70	***1.00***	0.64	0.98	0.74	0.96	0.70
	South Sikkim	0.89	0.74	0.91	0.76	0.96	0.79	***1.00***	0.98

It can be noted from Table 6.6b that 6 out of 9 cases the highest possibility is given to the RCP4.5 scenarios, which signifies that climate forcings over the study area follow the stabilized scenario pathways than high emission pathways. It should be noted that the possibility values are given concerning the climate change impact during the recent past. Moreover, the present climate forcings will continue to impact the climate of the study area for the next few decades. In this sense, this may be the possible reason that the difference between the possibility values of RCP4.5 and 8.5 are not significant. However, considering the long-run impact of climate change with prominent climate forcings, the significance of possibility theory will increase. It is important to note that any GCM and scenario with one value is not imply that the particular GCM and scenario capture the climate of the recent past over the region and that local climate drivers can change in the future. Though, it infers that nonexistence of ant other better GCM and scenario to represent the recent past climate of the study area. Figure 6.9 presents the future projection of major crops yield over the different district in Sikkim for the most possible GCM as well as scenario.

The mean percentage yield increase in the future projection of maize over East Sikkim varies from 11% to 25%; West Sikkim varies from 10% to 21%, and over South Sikkim varies from 12% to 24% during 2021-2099 as compared to the historical yield. Similarly, the mean future yield of rice is likely to increase between 11% and 20% over East Sikkim, over West Sikkim it varies from 5% to 17%, and 0.5% to 14% increase over South Sikkim during 2021-2099. The increase in the mean wheat yield in future varies from 2% to 5% over East Sikkim, 21% to 41% over West Sikkim, and 26% to 44% over South Sikkim during 2021-2099.

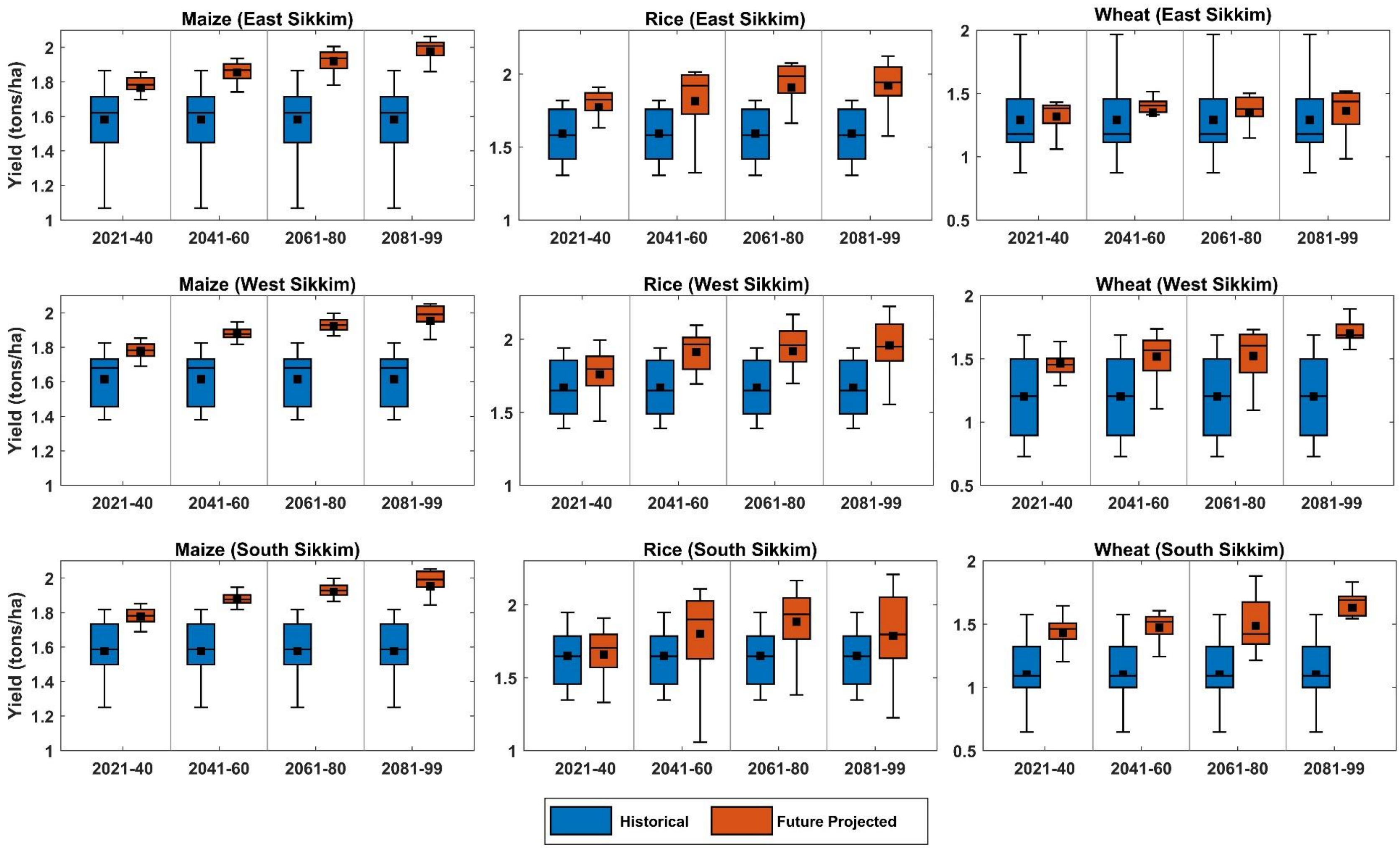

Figure 6.9 Future (2021-2099) projected crop yield for different crops after the uncertainty analysis.

6.3.2.4 Crop yield response to the weather variability

In this investigation, the growing periods/seasons for rice (July to November), wheat (September to December), and maize (April to July) are considered. As discussed, the crop yield is projected based on the change in the weather parameters only; thus, it is important to understand relationship between the weather/meteorological variability during the growing seasons of different crops and their yield. In addition, cultivar and fertilization effects, irrigation options, and other changes in future production technologies were not considered in the present study.

The weather variability during the growing seasons for rice, wheat, and maize is presented in Figure 6.10 a, b, and c, respectively. The future average yield of rice (Figure 6.9), after uncertainty analysis, has shown an increment during 2021-2099. From the previous studies, it is known that the impact on the local yield is affected mainly by the temperature conditions rather than precipitation (Bhatt et al., 2014; Lobell et al., 2011). The reason may be due to the temporal variability of temperature and precipitation. It can be seen from Figure 6.10a, b, and c that the temperature (maximum and minimum) variability is larger than the precipitation variability. In case of rice, through various experiments, the temperature threshold for rice yield is found to be 29^{o}C for maximum, and 19^{o}C for minimum temperature (Baker and Allen, 1993; Boote et al., 2005). From Figure 6.10a, it can be noted that the daily average precipitation during 2021-2099 doesn't show any significant change with respect to the observed period. However, the temperature (maximum and minimum) profile exhibits an increasing trend. Moreover, the warming trend at high-elevation area may have positive impact on the crop yields provided other conditions like soil fertility, water availability, etc., are favorable (Bhatt et al., 2014) as temperature controls the rate of photosynthesis, grain filling, and respiration (Lobell and Gourdji 2012). Similarly, the elevated CO_2 concentration tends to rise the growth and yield through enhanced photosynthesis (Kimball, 1983; Tubiello and

Ewert, 2002). Therefore, temperature reaching to the favourable temperature threshold, elevated CO_2 concentration, and the high elevation of the study area, are responsible for the increase in the mean rice yield over different parts of the Sikkim.

In case of wheat, the favourable temperature threshold is around 24^o for maximum, 19^o for minimum temperature (Bhatt et al., 2014; Prasad et al., 2008) and optimum mean temperature in the range of 17-23^{o}C (Porter and Gawith, 1999). It can be noted from Figure 6.10b that the maximum temperature in case of East Sikkim is quite high as compared to the observed period (nearly 4^{o}C increase towards the end of the twenty-first century). However, the maximum temperature over South and West Sikkim approaches the favourable threshold during 2021-2099. With the projected minimum and maximum temperature, the mean temperature during the growing periods of wheat over South and West Sikkim is likely to fall in the optimum range. Therefore, the average yield of the wheat over South and West is going to be increased during 2021-2099. Similarly, in case of maize, the optimum mean temperature for maize yield is recorded as 27-33^{o}C (Sánchez et al., 2014). The strong increase of maize yields under climate change scenarios only by the much higher temperature optimum for maize than wheat (and rice is between). Moreover, the daily average precipitation shows no significant change as compared to the observed. Therefore, under the favourable climatic conditions, the average yield of maize has shown an incremental trend.

Moreover, in order to analyze the crop yield response to the water and temperature stress, the normalized water productivity (WP^*) for the best possible scenario and GCM was computed and presented Table 6.7. The WP^* has the applicability to the diver locations, seasons, and even future climates (Steduto et al., 2009). The water stress has minimal effect on the WP^* and therefore, the impact of biomass (B) is completely controlled by means of Tr. From Eqs. 6.4 and 6.5, it can be noted that the WP* is directly proportional to the B and B is directly proportional to crop yield. The WP^* varies with crop type. The cold temperature stress has minimal effect on the crop yield. However, in the present study such condition is not observed with respect to the cold stress temperature of different crops. From the Table 6.7 it can be noted that WP^* increases with increasing in time as compared to the baseline period and possibly the increase in the WP^* resulted in increasing crop yield.

Using only one crop model is one of the major limitations of the present investigation and hence, the uncertainty stemmed from the crop models is ignored in the present study. On the other hand, the present study simulates future yield projection of rice, maize, and wheat over three different districts over Sikkim encompassing the GCM and scenario uncertainty. However, encompassing crop management practices viz., cropping pattern, changing the fertilizer doses, changing the irrigation depths and methods, altering the planting dates, and change in the cultivar in the crop modelling will provide future direction to pursue the study in the context of climate change.

Table 6.7 The normalised WP for different crops and different time periods after the uncertainty analysis.

MAIZE: WP* (g/m2)			
	East	**West**	**South**
Observed	32.3	31.8	32.2
2020-40	33.6	33.7	33.7
2041-60	34.5	34.7	34.7
2061-80	35.2	34.8	35.2
2081-99	35.7	35.7	35.4
WHEAT: WP* (g/m2)			
	East	**West**	**South**
Observed	16.5	16.8	15.7
2020-40	17.1	18.5	18.2
2041-60	17.4	19.0	18.6
2061-80	17.5	19.1	18.6
2081-99	17.7	20.5	20.1
RICE: WP* (g/m2)			
	East	**West**	**South**
Observed	16.4	17.2	17.4
2020-40	17.7	17.7	17.1
2041-60	18.5	19.0	18.4
2061-80	19.3	19.2	18.8
2081-99	19.2	19.5	18.2

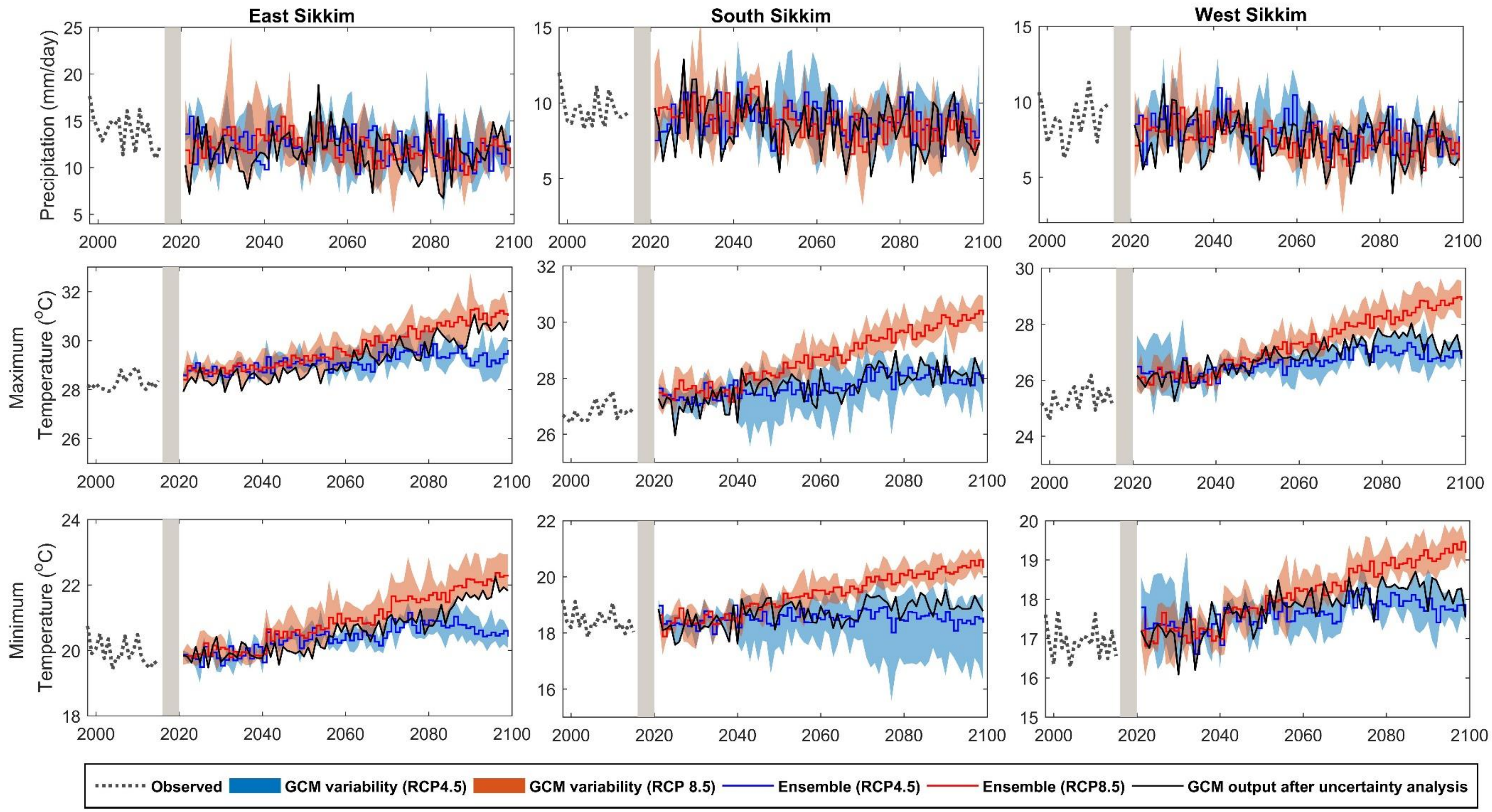

Figure 6.10a Precipitation, and temperature variability during the growing period of rice during historical and future projections for East, South, and West Sikkim.

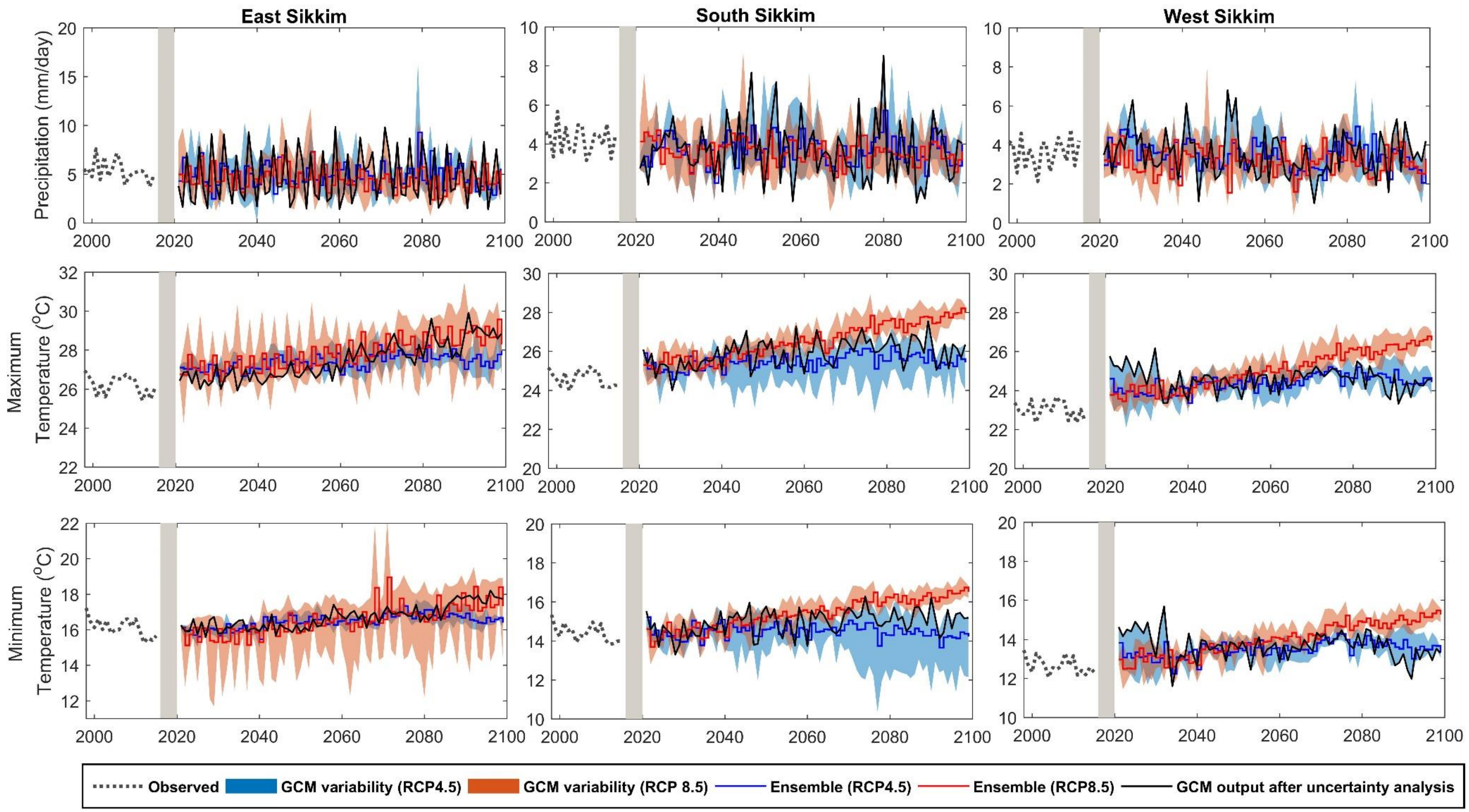

Figure 6.10b Precipitation, and temperature variability during the growing period of wheat during historical and future projections for East, South, and West Sikkim.

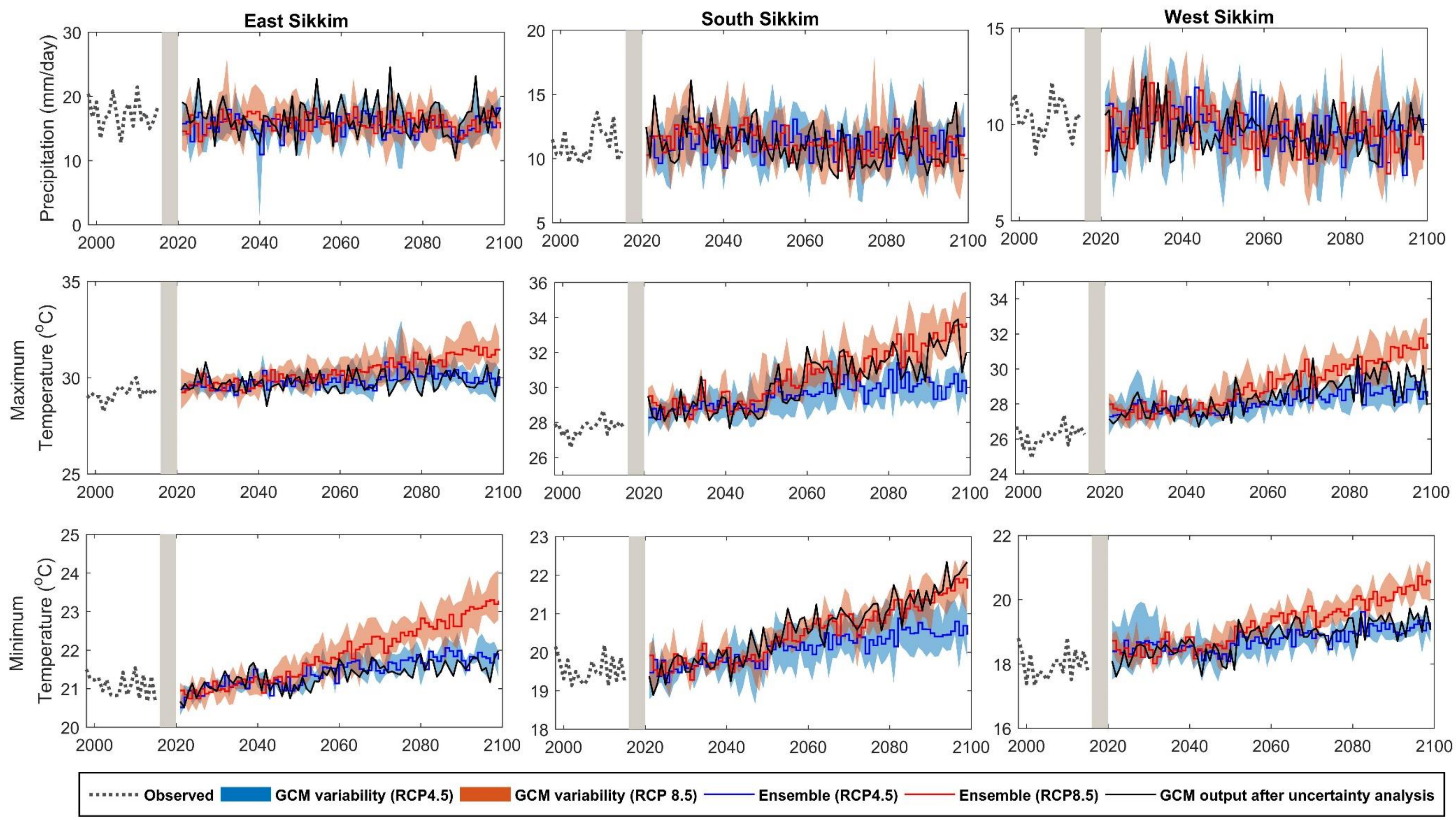

Figure 6.10c Precipitation, and temperature variability during the growing period of maize during historical and future projections for East, South, and West Sikkim.

6.3.3 CROPWAT results

6.3.3.1 Past and future trend of CWR

This section deals with the CWR of three major crops, namely, maize, wheat, and rice over three different locations of Sikkim. The historical CWR is computed based on the observed meteorological datasets and the future projections are obtained using the bias corrected outputs from the four selected GCMs under RCP 4.5 and 8.5 scenarios. The CWR of maize, wheat, and rice during their growth period for the baseline and future projected period for all three parts of Sikkim is presented in Figure 6.11a for Maize, 6.11b for Wheat and 6.11c for Rice. Moreover, the linear trend magnitude obtained from Sen's slope analysis of CWR of different crops is depicted in Figure 6.12.

An increasing trend of CWR for maize from 1998-2015 is observed for all the three parts of Sikkim and can be noted from Figure 6.11a. Further, the findings can be supported by the positive linear magnitude of slope in Figure 6.12a. In future projection, a significant decreasing trend is observed for all the models under both scenarios. However, a higher decreasing trend (-0.19 to -0.35 mm/year) is observed in case of RCP 4.5 than 8.5. More interestingly, the CWR trend is likely to increase under both the scenarios for all the models over West (0.29 to 0.5 mm/year for RCP 4.5) and South (0.32 to 0.61 mm/year for RCP 4.5) Sikkim. In case of RCP 8.5 scenario, the highest change in the CWR is observed in CNRM-CM5 (1.52 mm/year) over West Sikkim and in MPI-ESM-LR (1.96 mm/year) over South Sikkim. The decrease in CWR over East Sikkim can be attributed to the future changes in the precipitation and temperature. Over East Sikkim, there is no significant change in the precipitation from the historical period as compared to the West and South. Furthermore, the temperature has not significantly increased under the climate change scenarios with respect to the past records and as compared to the other two locations.

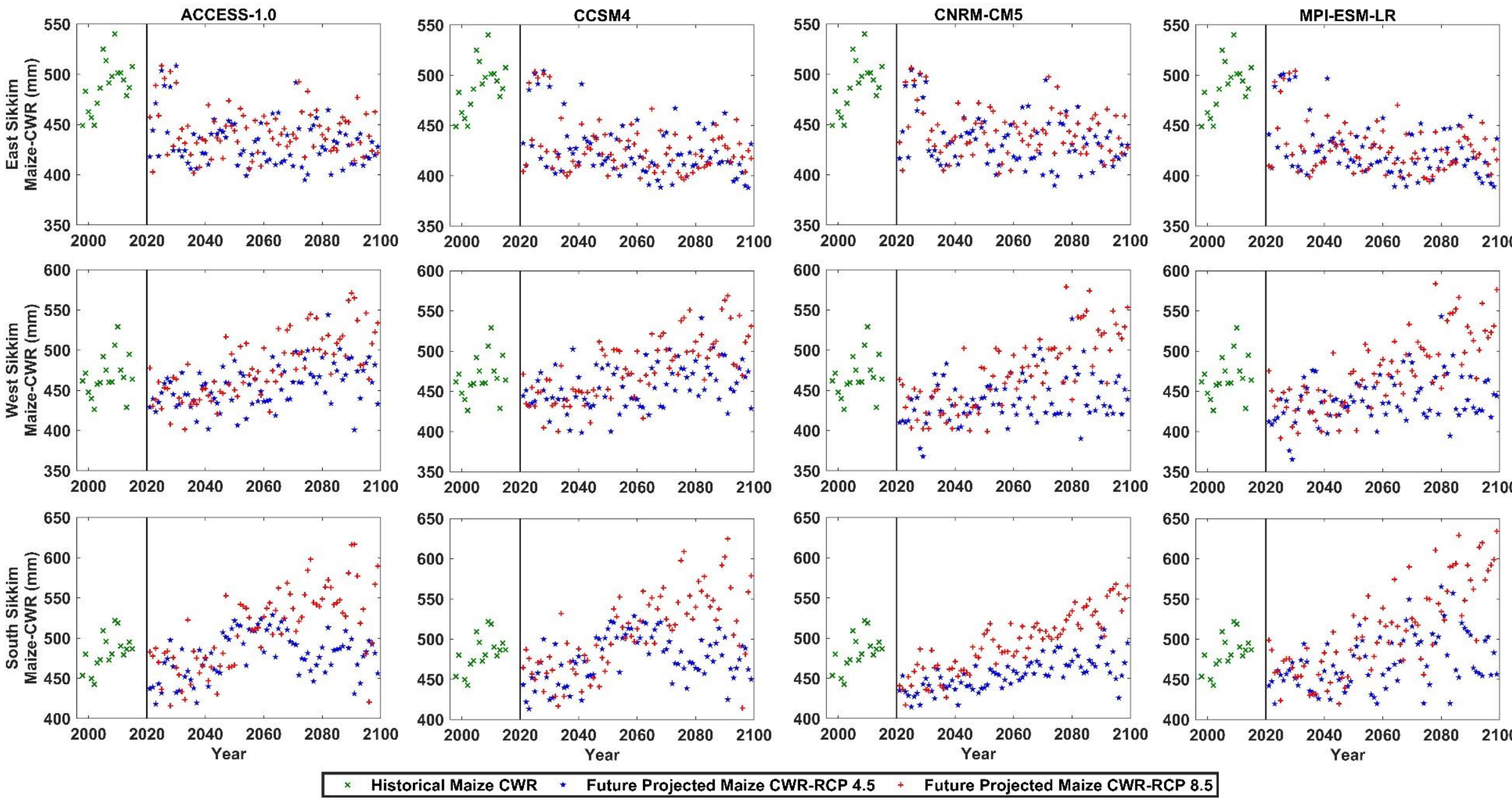

Figure 6.11a CWRs in the total growth stages of Maize for historical (1998-2015) and the ones future projected (2021-2100) by multiple GCMs under two scenarios in East, West, and South Sikkim, respectively.

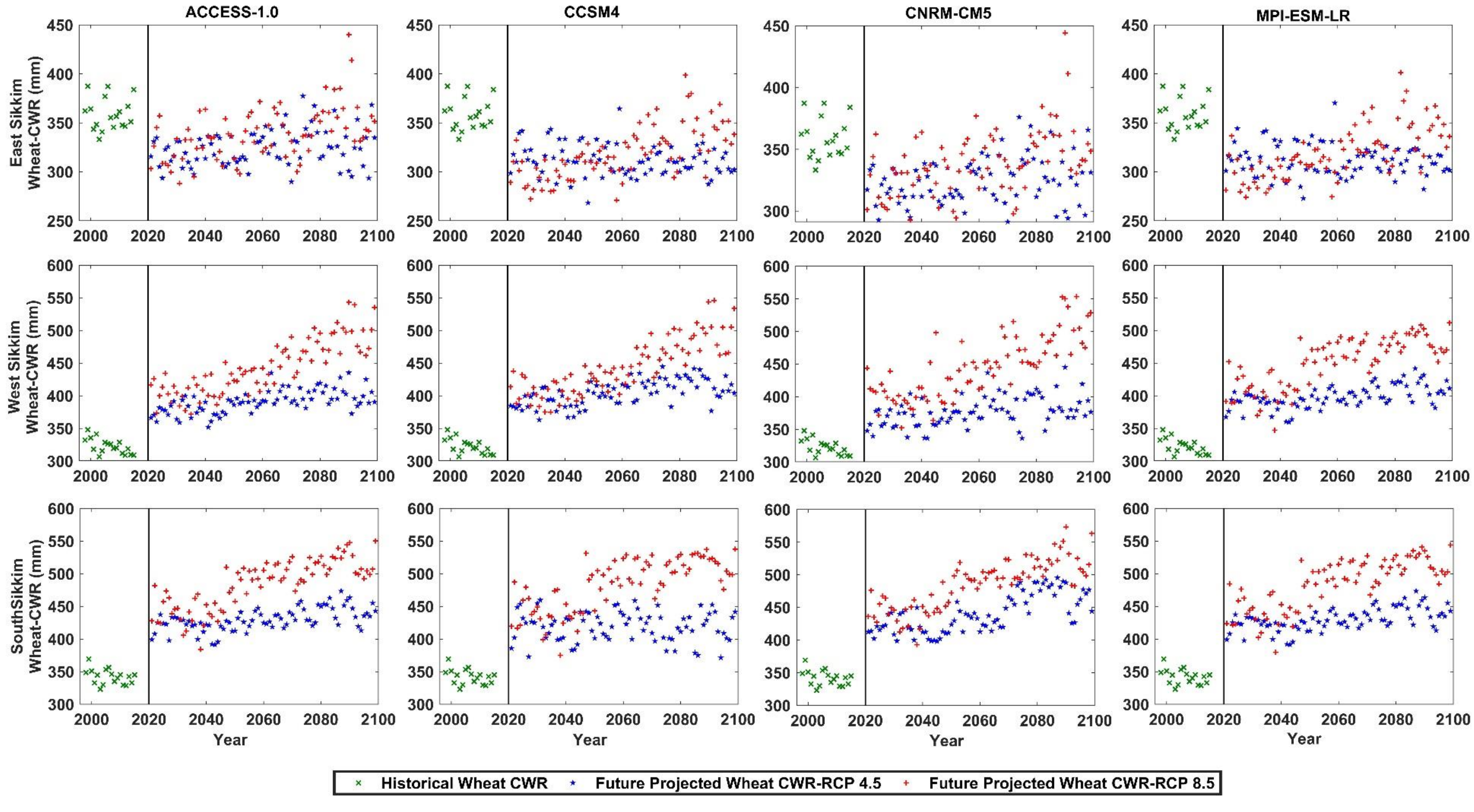

Figure 6.11b CWRs in the total growth stages of Wheat for historical (1998-2015) and the ones future projected (2021-2100) by multiple GCMs under two scenarios in East, West, and South Sikkim, respectively.

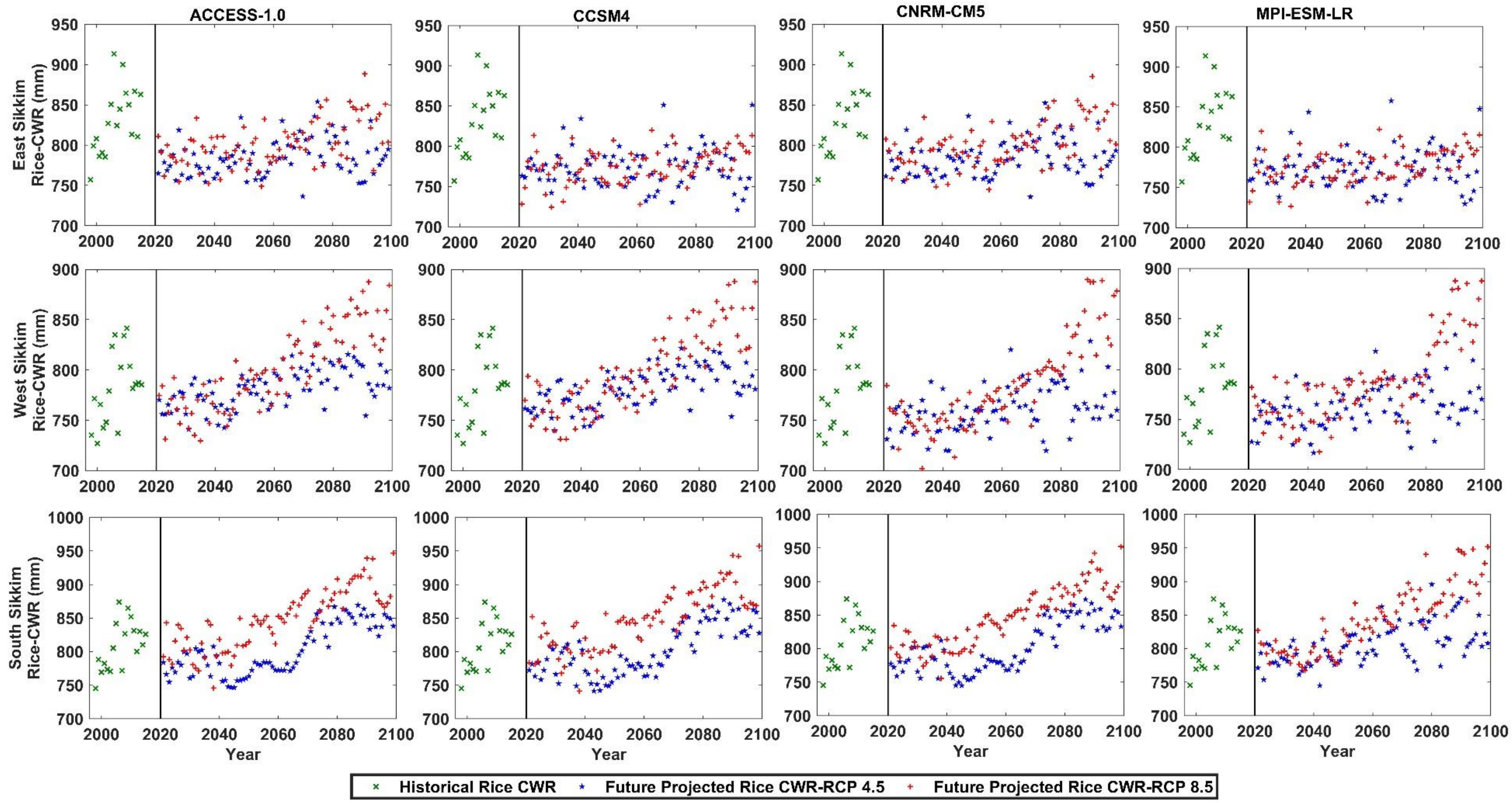

Figure 6.11c CWRs in the total growth stages of Rice for historical (1998-2015) and the ones future projected (2021-2100) by multiple GCMs under two scenarios in East, West, and South Sikkim, respectively.

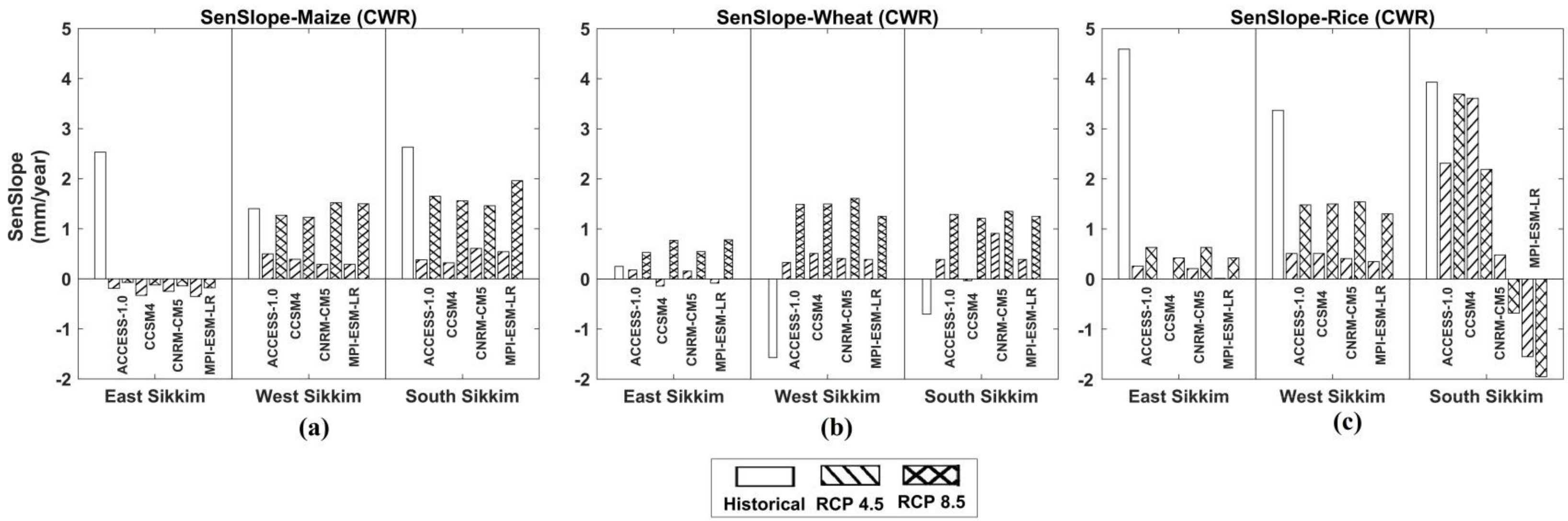

Figure 6.12 Sen's slope of CWRs in the total growth stages of maize, wheat and rice for historical (1998-2015) and future projected (2021-2100) by multiple GCMs under two scenarios in East, West and South Sikkim.

Therefore, the ET_o is not going to increase more significantly over East Sikkim resulting in less CWR.

In case of Wheat, a significant decreasing trend is noticed over West and South Sikkim for the baseline period. However, an insignificant increasing trend is observed over East Sikkim. In most of the cases, the future projections of CWR have shown an increasing trend under both the scenarios with maximum increase in case of RCP 8.5. The highest increasing rates are 0.78, 1.61, and 1.35 mm/year for East, West and South Sikkim, respectively. All the above-said results can be noticed under the Figure 6.11b and Figure 6.12b. It can be noted from Figure 6.11c and 6.12c that there is an increase in the CWR of rice during the baseline period. Similar to the wheat, the CWR of rice during the 2021-2099 has increased under both the scenarios for most of the cases. The highest increasing rates are 0.63, 1.54, and 3.69 mm/year for East, West and South Sikkim, respectively.

6.3.3.2 Past and future trend of CIR

The CIR of wheat and rice during the baseline and future period over three regions of Sikkim are shown in Figure 6.13a for wheat and 6.13b for rice. The Sen Slope results of a crop irrigation requirement are also shown in Figure 6.14. It should be noted that maize crop is considered as rainfed and hence CIR is not computed for the same.

Figure 6.13a demonstrates the decreasing trend in CIR for wheat crop during 1998-2015 in West and South Sikkim while the increasing trend is observed over East Sikkim. A similar trend can also be observed in Fig 6.14(a). An increasing trend is observed for East and West Sikkim under RCP 4.5 and 8.5 scenarios for most of the GCMs. On the other hand, in South Sikkim although the CIR is likely to increase in future, there is no visible difference observed between RCP 4.5 and 8.5 for all GCMs except MPI-ESM-LR. The highest increasing rates are notices as 0.77, 1.51, and 0.74 mm/year for East, West and South Sikkim, respectively.

The future projection and its linear trend are presented in Figure 6.13b and 6.14b. An increasing trend with magnitude 0.35 to 1.54 mm/year and 0.73 to 1.84 mm/year is observed over West and South Sikkim, respectively under both scenarios. However, an insignificant linear trend of -0.06 to 0.15 mm/year is noticed over East Sikkim under RCP 4.5 and 0.42 to 0.85 under RCP 8.5. The highest positive rates are obtained from ACCESS-1.0, CNRM-CM5, and MPI-ESM-LR models for East, West and South Sikkim, respectively. The decrease in CIR over East Sikkim can be attributed to the insignificant changes in the future CWR. Over East Sikkim, there is no significant change in the CWR of Rice as compared to the West and South. Therefore, the CWR is not going to increase more significantly over East Sikkim resulting in less CIR.

6.3.3.3 Uncertainty analysis of future CWR & CIR

Results discussed in Sections 6.3.3.1 and 6.3.3.2 are not analysed for the uncertainty. As uncertainty analysis in the climate change impact study is essential to minimize the errors, in the present section we are presenting the future outcomes of CWR and CIR after the uncertainty analysis using possibilistic approach.

The performance measure C is calculated for multiple GCMs under both scenarios based on their simulation during 2006 to 2015. Table 6.8a presents the unnormalized C value to assess both GCM and scenario uncertainty. The highest C values are marked as bold in Table 6.8a for three major crops and districts of Sikkim. The possibility value after normalization for both scenario and GCM uncertainty is presented in Table 6.8b.

It can be found from Table 6.8b that the RCP 4.5 scenario exhibits the highest possibility value (11 out of 15 cases) which implies that stabilized scenario pathway is identified as the most possible scenario for regional climate change impact assessment in our study areas for CWR and CIR.

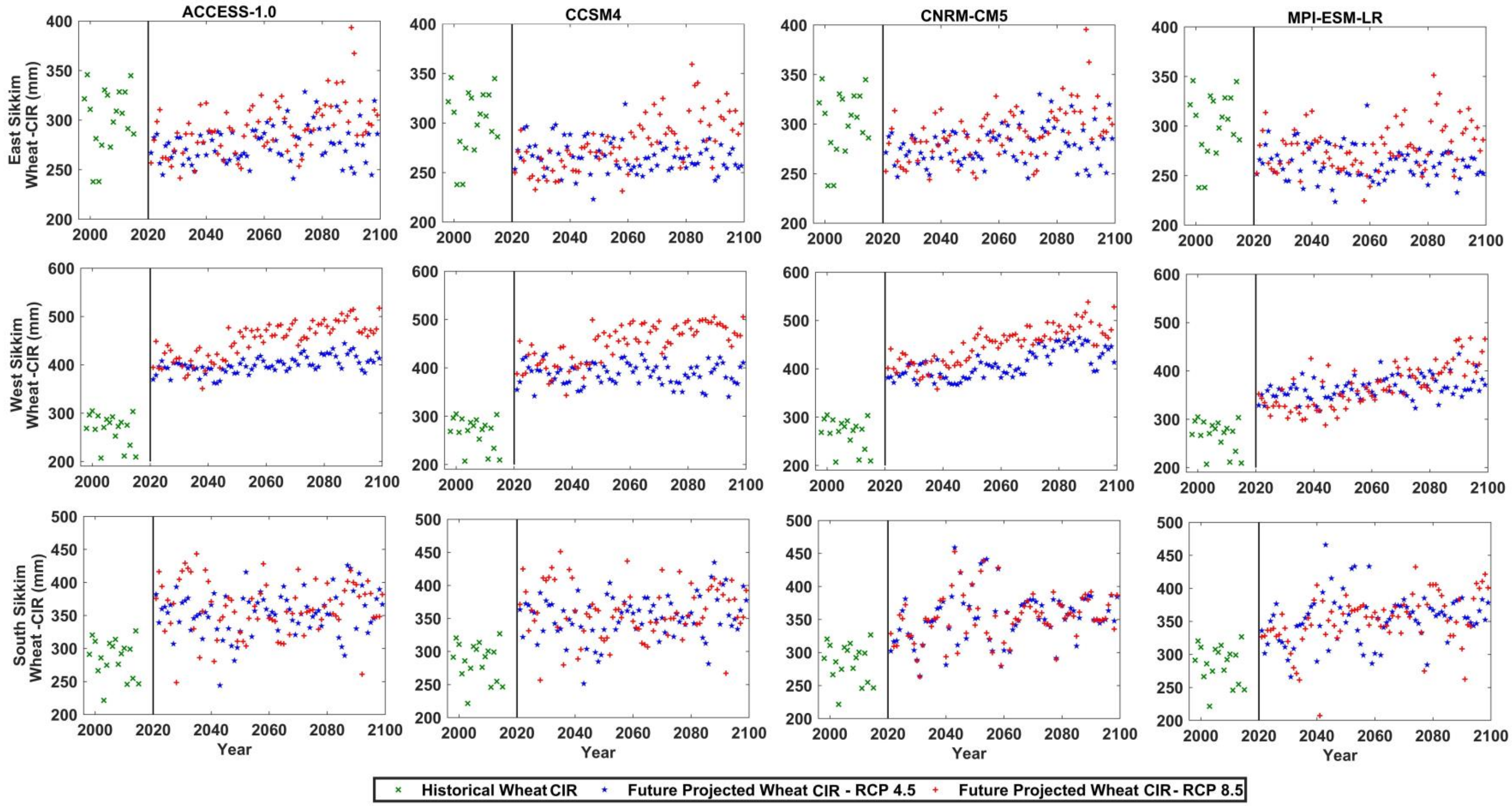

Figure 6.13a CIRs in the total growth stages of Wheat for historical (1998-2015) and the ones future projected (2021-2100) by multiple GCMs under two scenarios in East, West, and South Sikkim, respectively.

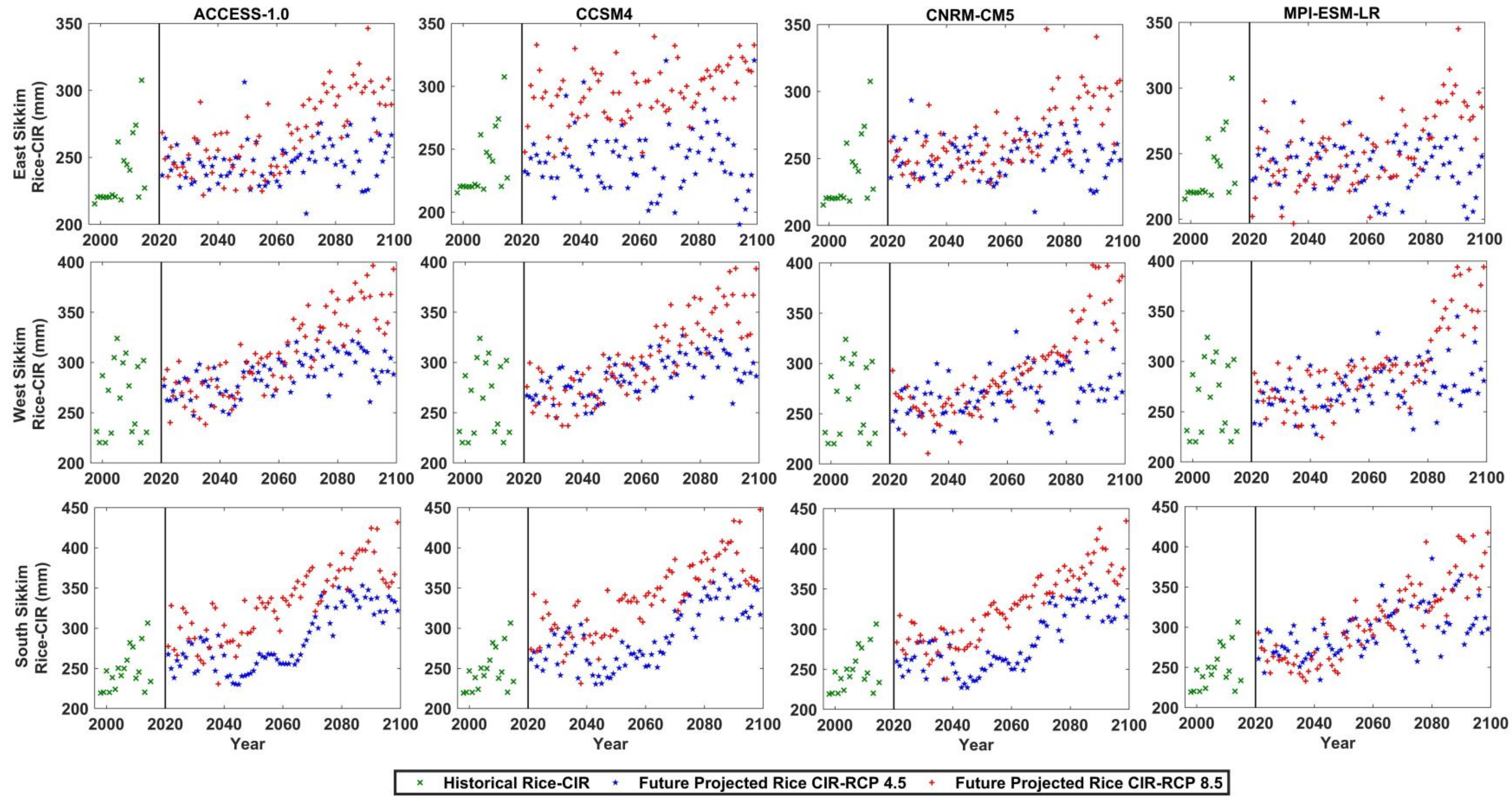

Figure 6.13b CIRs in the total growth stages of Rice for historical (1998-2015) and the ones future projected (2021-2100) by multiple GCMs under two scenarios in East, West and South Sikkim, respectively.

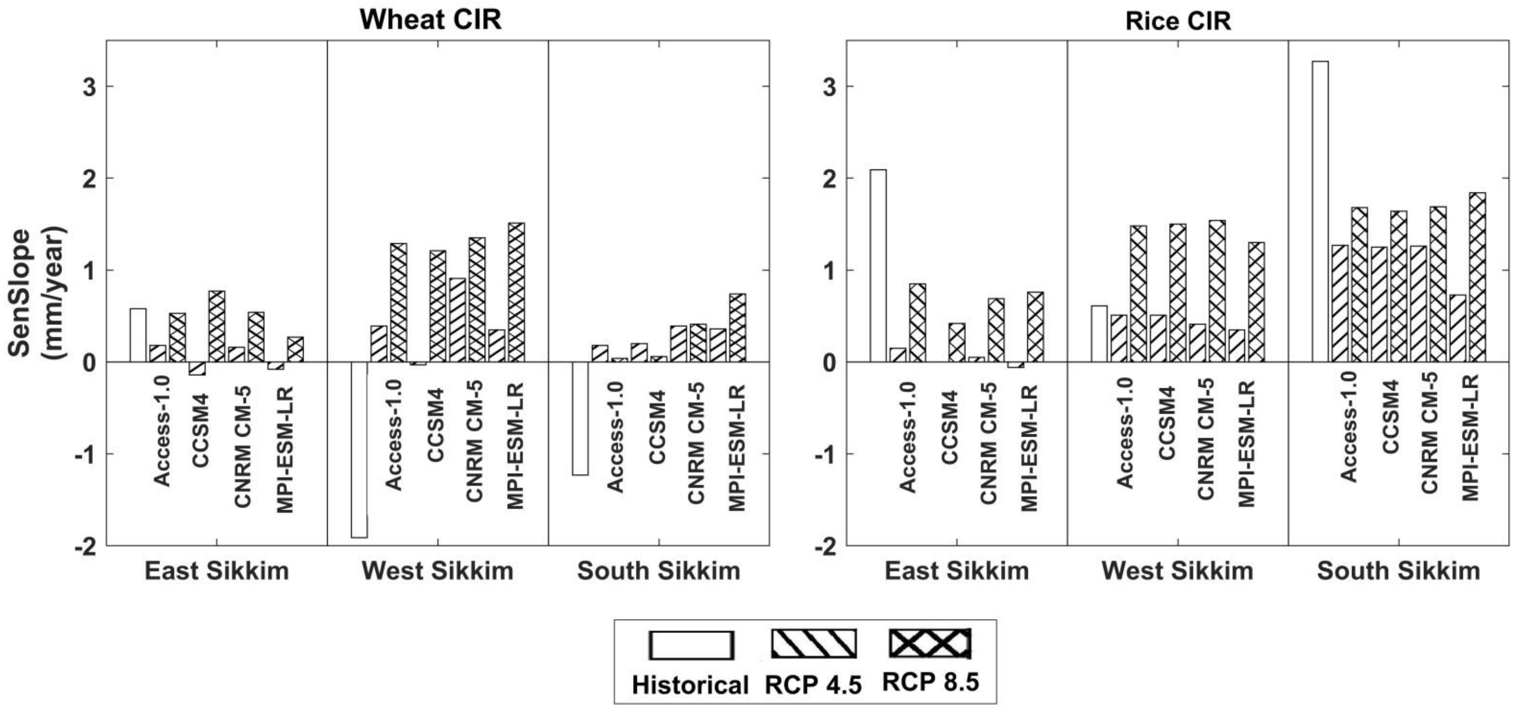

Figure 6.14 Sen's slope of CIRs in the total growth stages of maize, wheat and rice for historical (1998-2015) and future projected (2021-2100) by multiple GCMs under two scenarios in East, West and South Sikkim.

Table 6.8a Performance measure C for maize, wheat and rice for multiple GCMs and two scenarios during 2006-2015 (Maximum value is marked in bold).

Crop	GCM/	ACCESS1.0		CCSM4		CNRM-CM5		MPI-ESM-LR	
	Scenarios	RCP4.5	RCP8.5	RCP4.5	RCP8.5	RCP4.5	RCP8.5	RCP4.5	RCP8.5
Maize	East Sikkim	0.42	0.29	0.23	0.44	0.27	0.43	**0.50**	0.31
	West Sikkim	0.59	0.31	0.40	0.38	0.65	0.42	**0.68**	0.49
	South Sikkim	**0.72**	0.36	0.59	0.65	0.70	0.54	0.34	0.52
Rice	East Sikkim	0.38	0.43	0.35	0.27	**0.51**	0.42	0.39	0.24
	West Sikkim	0.30	**0.53**	0.33	0.34	0.23	0.29	0.29	0.24
	South Sikkim	0.32	0.40	0.50	**0.54**	0.43	0.29	0.30	0.26
Wheat	East Sikkim	**0.42**	0.25	0.30	0.29	0.36	0.34	0.26	0.27
	West Sikkim	0.58	0.41	0.53	0.42	**0.76**	0.43	0.51	0.39
	South Sikkim	0.22	0.33	0.39	0.27	**0.40**	0.20	0.39	0.28
Rice CIR	East Sikkim	**0.71**	0.38	0.68	0.65	0.52	0.50	0.69	0.48
	West Sikkim	0.51	**0.61**	0.38	0.55	0.49	0.38	0.36	0.34
	South Sikkim	0.65	0.49	**0.67**	0.48	0.43	0.46	0.38	0.35
Wheat CIR	East Sikkim	**0.28**	0.21	0.24	0.14	0.23	0.27	0.25	0.20
	West Sikkim	0.36	0.59	0.35	0.47	0.50	0.34	0.54	**0.64**
	South Sikkim	**0.71**	0.42	0.52	0.58	0.52	0.44	0.41	0.39

Table 6.8b Possibility values after normalization for different crops over different regions.

Crop	GCM/ Scenarios	ACCESS1.0		CCSM4		CNRM-CM5		MPI-ESM-LR	
		RCP4.5	**RCP8.5**	**RCP4.5**	**RCP8.5**	**RCP4.5**	**RCP8.5**	**RCP4.5**	**RCP8.5**
Maize	East Sikkim	0.86	0.59	0.47	0.89	0.55	0.89	**1.00**	0.63
	West Sikkim	0.87	0.46	0.59	0.56	0.96	0.62	**1.00**	0.73
	South Sikkim	**1.00**	0.50	0.81	0.90	0.97	0.75	0.46	0.72
Rice	East Sikkim	0.75	0.85	0.69	0.54	**1.00**	0.83	0.77	0.48
	West Sikkim	0.56	**1.00**	0.62	0.65	0.43	0.56	0.55	0.45
	South Sikkim	0.58	0.73	0.92	**1.00**	0.78	0.53	0.56	0.47
Wheat	East Sikkim	**1.00**	0.62	0.72	0.69	0.87	0.82	0.63	0.64
	West Sikkim	0.77	0.54	0.70	0.55	**1.00**	0.57	0.67	0.51
	South Sikkim	0.54	0.83	0.98	0.67	**1.00**	0.49	0.98	0.70
Rice CIR	East Sikkim	**1.00**	0.54	0.96	0.92	0.73	0.72	0.97	0.68
	West Sikkim	0.84	**1.00**	0.62	0.90	0.80	0.62	0.59	0.55
	South Sikkim	0.95	0.73	**1.00**	0.72	0.64	0.69	0.58	0.52
Wheat CIR	East Sikkim	**1.00**	0.75	0.86	0.51	0.83	0.96	0.88	0.71
	West Sikkim	0.53	0.92	0.55	0.73	0.78	0.53	0.84	**1.00**
	South Sikkim	**1.00**	0.58	0.73	0.82	0.73	0.62	0.58	0.55

It is important to note that for other agro-meteorological variables except CWR and CIR, the possibility distribution can be different for the same region. Since the climate forcing is not very significant during the recent past (2006-2015) and therefore significant difference in GCMs output is not found between RCP 4.5 & 8.5 scenarios. However, with the available GCM and scenario projections the particular selected GCM under the scenario is likely to prevail in the selected study area.

6.3.3.4 Future projection of CWR & CIR with uncertainty analysis

Future projection of CWR and CIR of different crops among three districts of Sikkim with best possible GCM and scenario is presented in Figure 6.15a & b, respectively.

The percentage change in CWR of wheat crop in the future increases from 32% to 39% and 23% to 37% over West and South Sikkim, respectively as compared to the baseline period. Whereas the percentage change is likely to decrease from -11% to -6% over East Sikkim during 2021-2099. In the case of maize, the CWR change is likely to decline between -15% to -9%, -8% to -4% and -5% to 3% over East, West and South Sikkim, respectively. Similarly, the percentage increase in the projected CIR ranges from 24% to 58% and 20% to 27% over West and South Sikkim while decreasing trend from -12% to -5% is observed over East Sikkim during 2021-2099. On the other hand, the percentage change in the CWR of rice ranges from -6% to -3%, -2% to 8%, and -0.5% to 11% over East, West, and South Sikkim, respectively. However, CIR of rice crop has shown an increasing trend among the three districts of Sikkim ranges from 4% to 25%, 2% to 35% and 2% to 36% over East, West and South Sikkim, respectively.

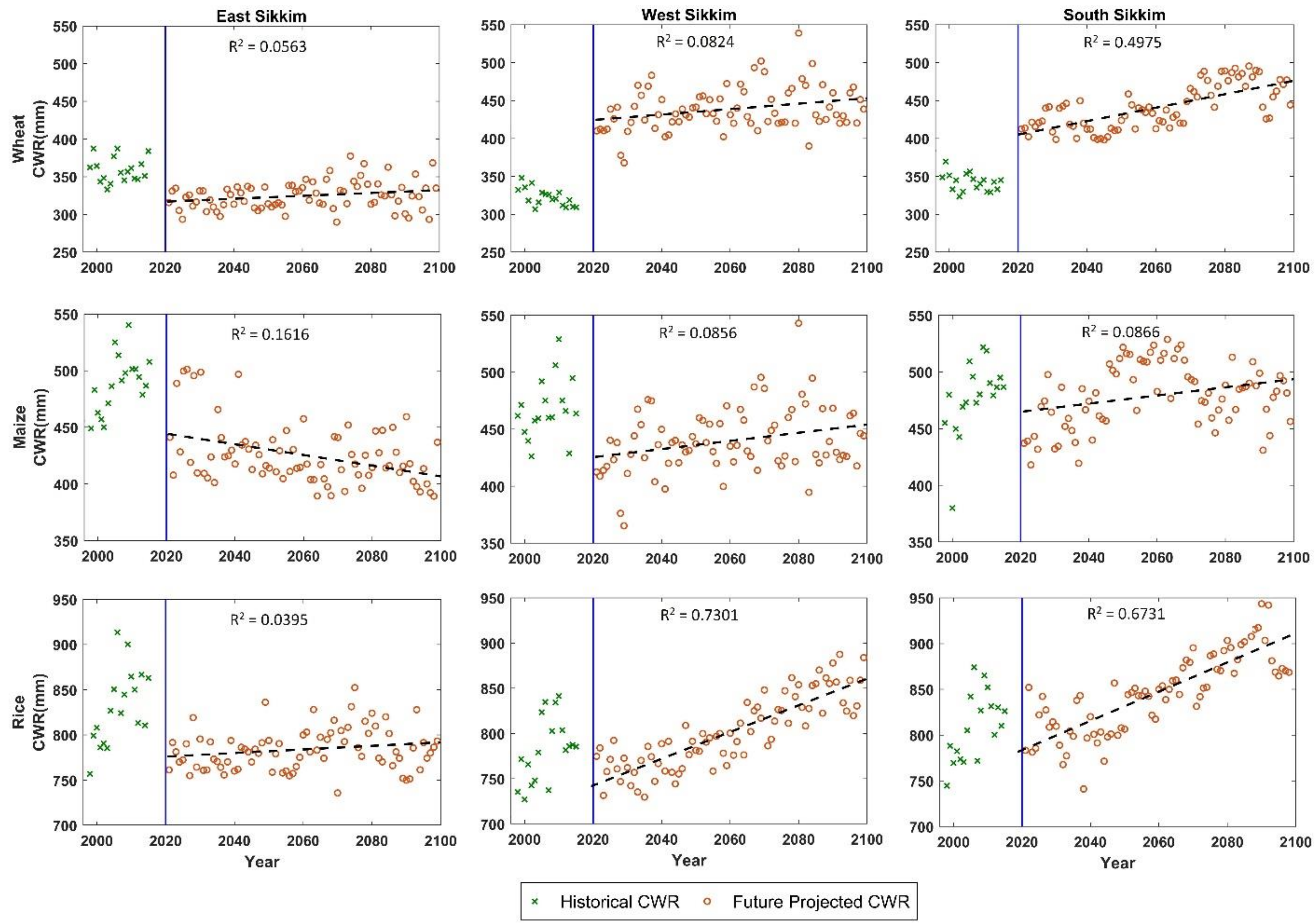

Figure 6.15a Observed and future projections of CWR for different crops over East, West, and South Sikkim after GCM and scenario uncertainty analysis.

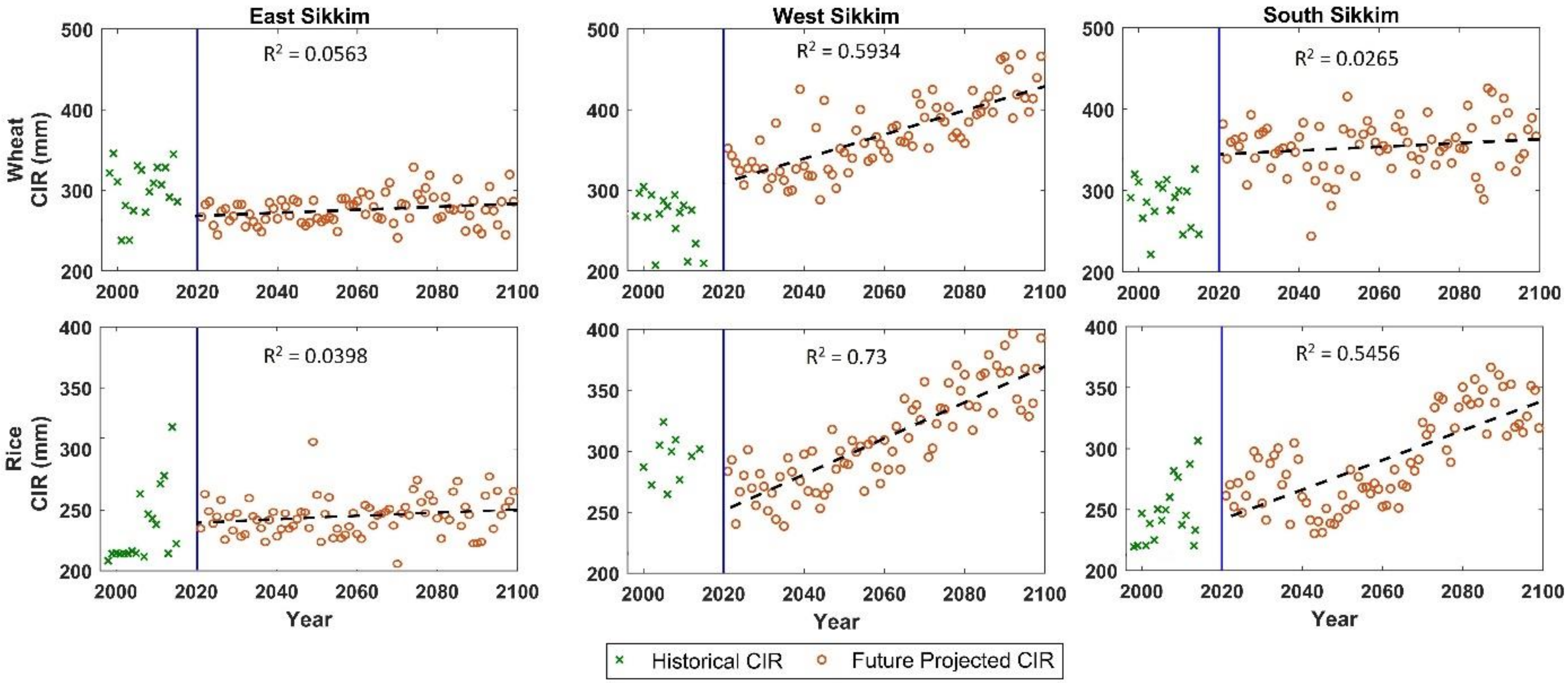

Figure 6.15b Observed and future projections of CIR for wheat and rice over East, West, and South Sikkim after GCM and scenario uncertainty analysis

6.3.3.5 Sensitivity analysis

With increasing in greenhouse gas emission and climate change forcings, it is necessary to find out the way for the opportunity to decrease CWR in terms of water conservation. Therefore, we have carried out sensitivity analysis through altering the growth period of different crops over three different districts of Sikkim. In Sikkim, the growing period of maize starts from April till the mid of June following earlier studies. A total of five additional scenarios were depicted based on the growth period of the crop are proposed such as Case I (30 March), Case II (30-April), Case III (15 May), Case IV (30 May) and Case V (15 June), i.e. growing period of maize is shifted from April to mid-June. Case I to Case IV is practiced in some parts of Sikkim, however, Case V is not practically practiced in Sikkim. For Case I, maize has shown an increasing trend in CWR whereas for other cases such as Case II to Case V, CWR is likely to decrease, under both RCP 4.5 and 8.5 scenarios for all 3 parts of Sikkim (Figure 6.16a, b, & c). A significant amount of water conservation is noticed from case II to case V whereas no conservation is observed in case I. Case V projects the lowest CWR and hence identified as highest level of water conservation. The growing seasons of Maize are shifted from April to June, indicating conservation of 10 to 60, 12 to 86, and 12 to 108 mm/year under both scenarios for East, West, and South Sikkim, respectively.

Also, the growing seasons of Wheat (Figure 6.17a) are shifted from 20 October to 5 December, i.e. Case I (5 October), Case II (20 October), Case III (5 November), Case IV (20 November) and Case V (5 December). For East and South Sikkim, case I, II & V clearly indicate increasing trend of CWR while a decrease is observed over case III & IV. However, for West Sikkim, CWR decreases over Case III, IV, & V. This clearly indicates that the wheat growth period is suitable to shift from 5th to 20th day of November from the current scenarios or else no water conservation is possible. The growing seasons of wheat are shifted from Oct to November, indicating conservation of 1 to 11, 18 to 29, and 3 to 95 mm/year for East, West, and South Sikkim, respectively.

Similarly, for the rice crop (see Figure 6.17b), in addition to current condition i.e., 1st week of July, 5 newly added growing periods are proposed viz., Case I (15 June), Case II (15 July), Case III (30 July), Case IV (15 August) and Case V (30 August). From Case II to Case V, CWR of rice shows a decreasing trend both scenarios over all three parts of Sikkim. After adopting the newly developed growing period from July to August, water conservation of 13 to 102, 4 to 102 and 11 to 88 mm/year under both RCP 4.5 & 8.5 scenarios for East, West and South Sikkim, respectively.

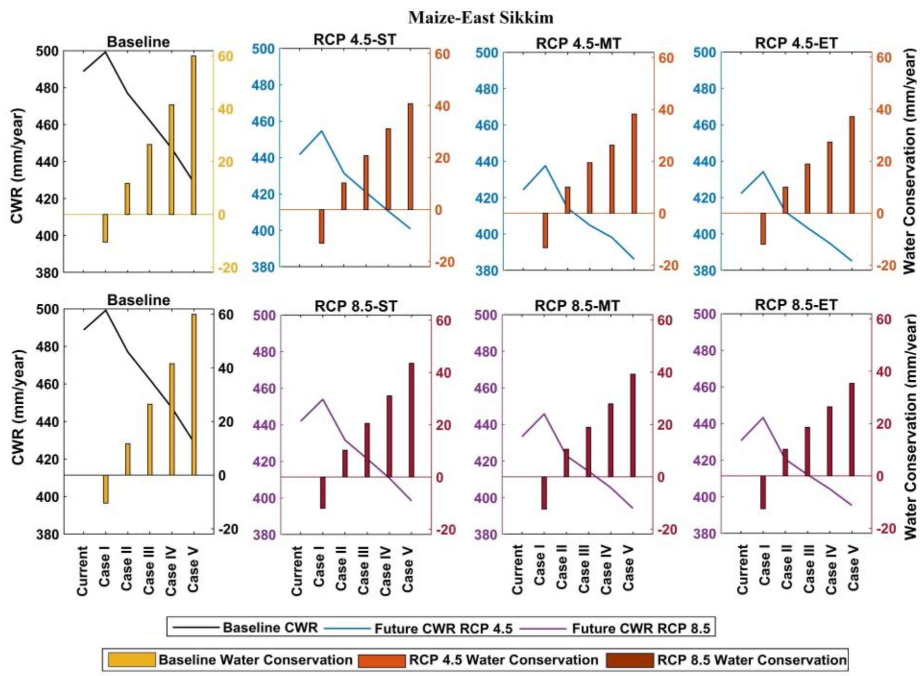

Figure 6.16a Sensitivity analysis on crop water requirement for different growing periods of Maize in East Sikkim.

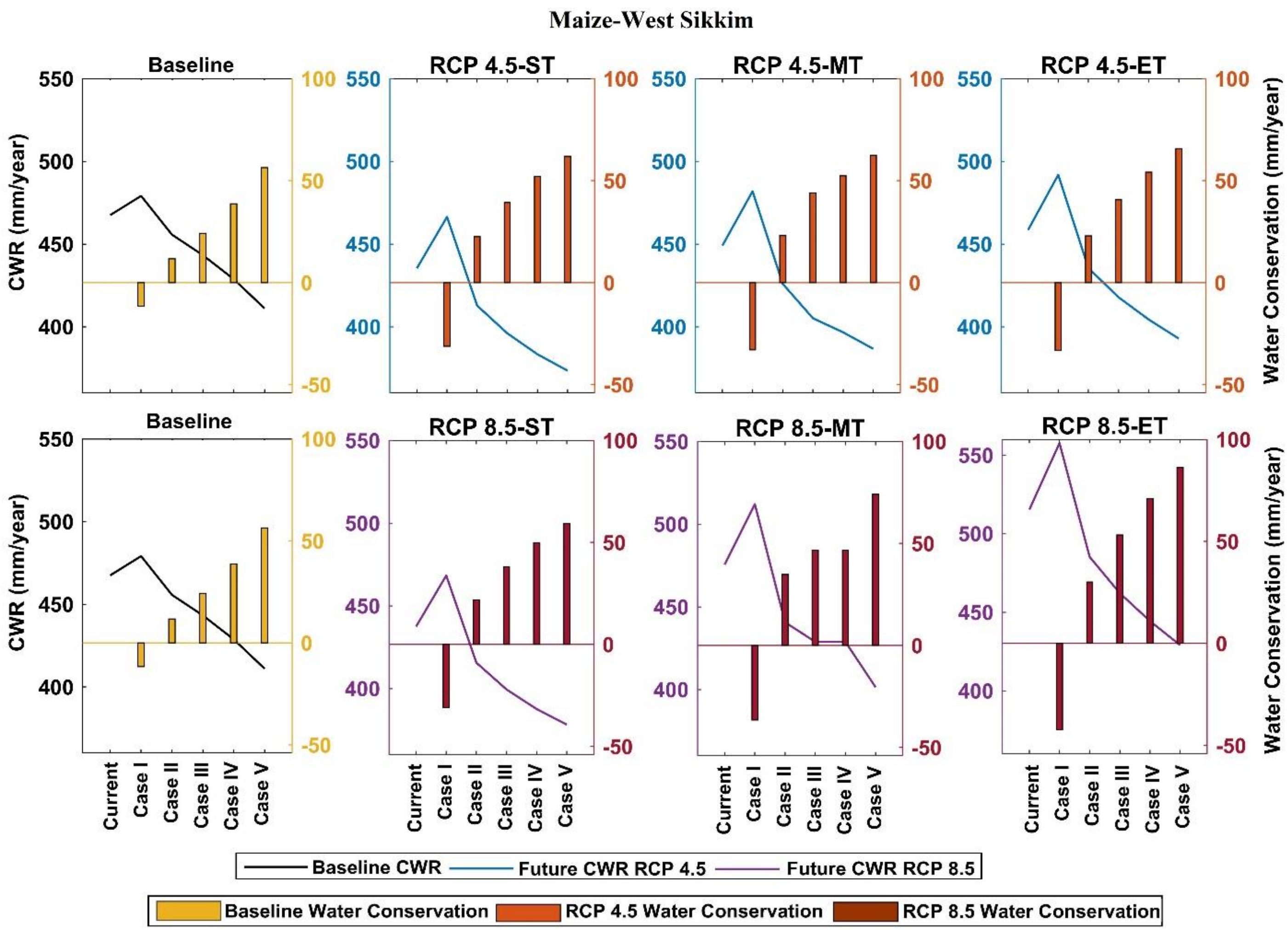

Figure 6.16b Sensitivity analysis on crop water requirement for different growing periods of Maize in West Sikkim.

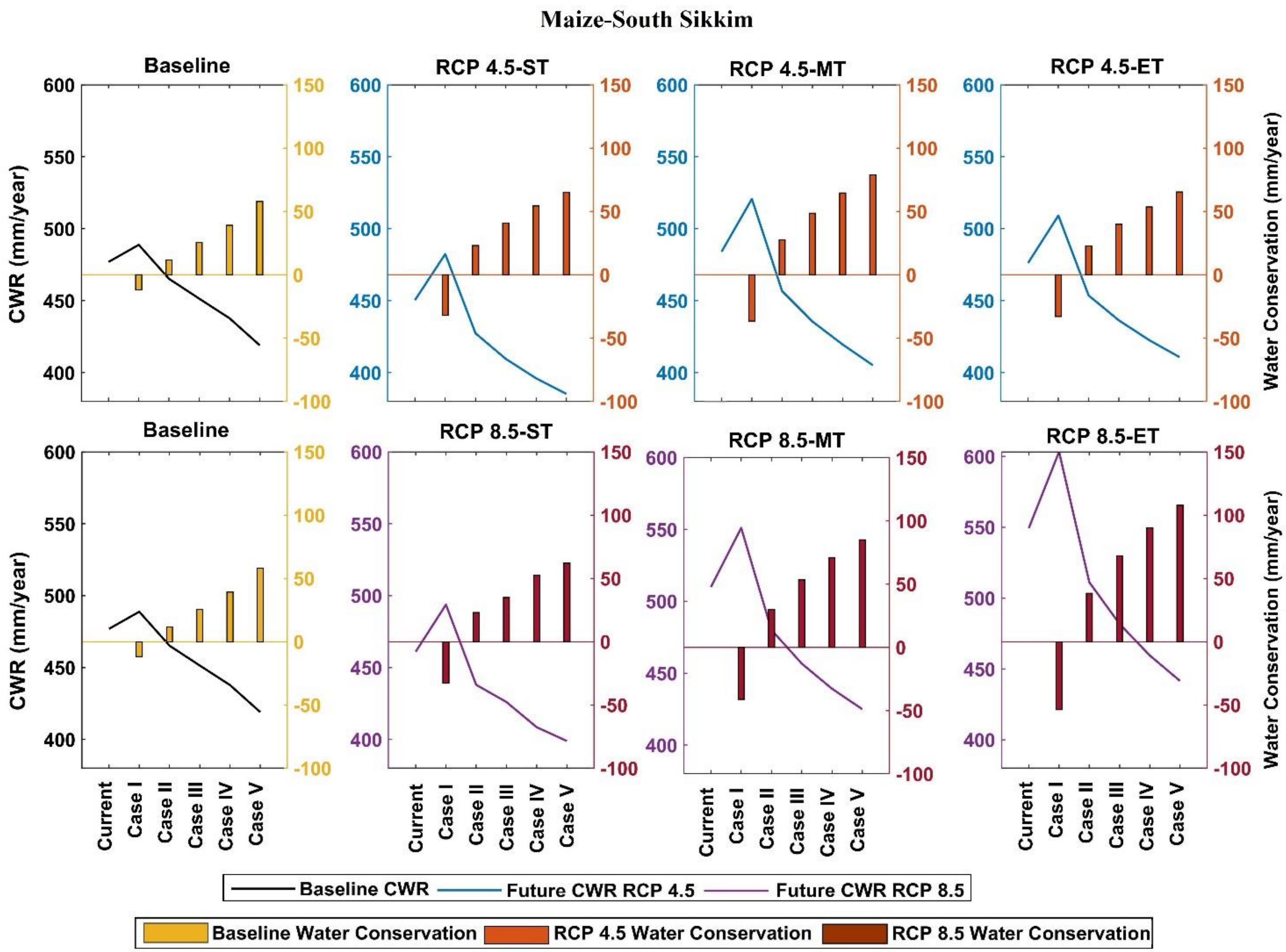

Figure 6.16c Sensitivity analysis on crop water requirement for different growing periods of Maize in South Sikkim.

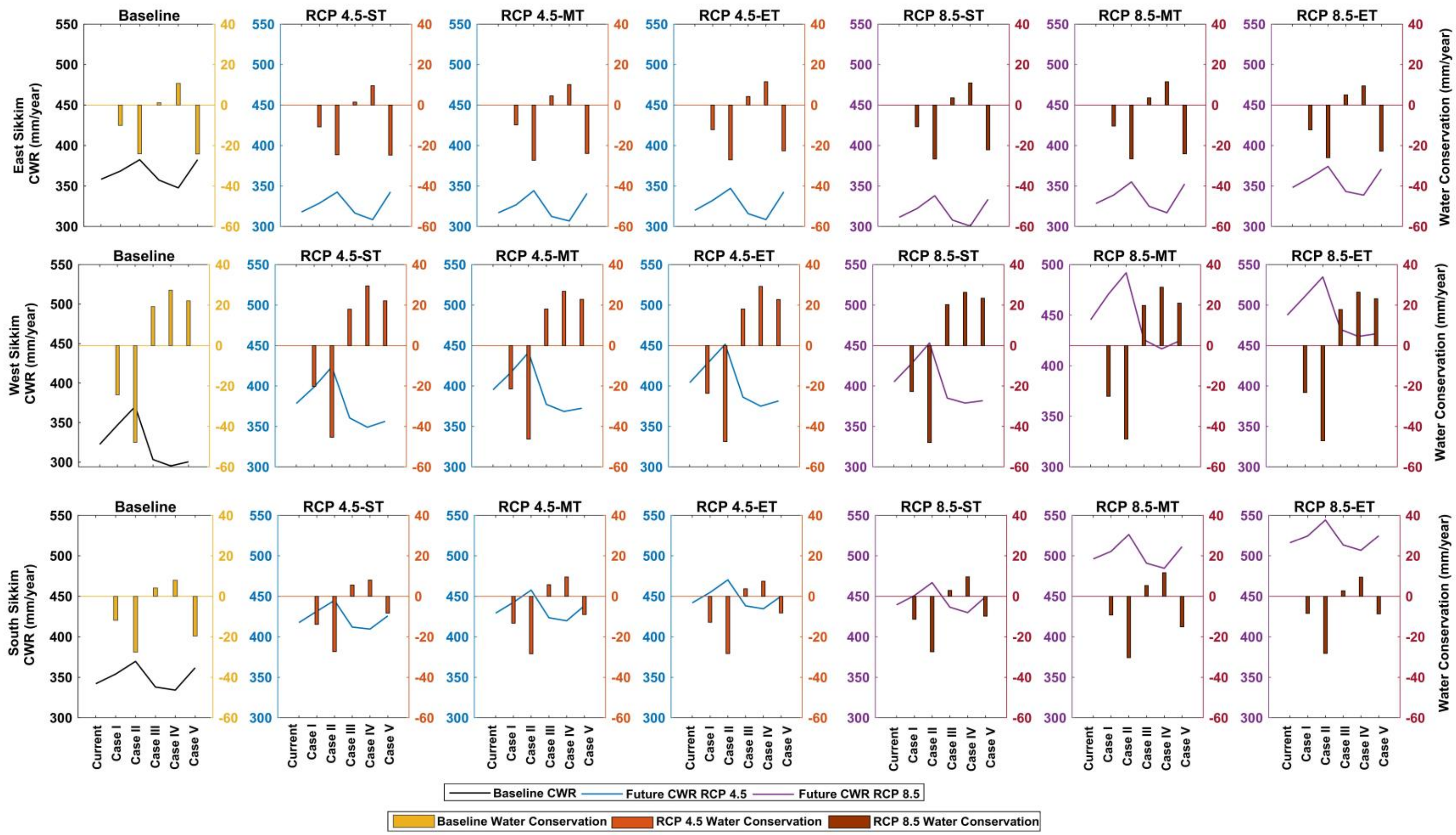

Figure 6.17a Sensitivity analysis on crop water requirement for different growing period of Wheat.

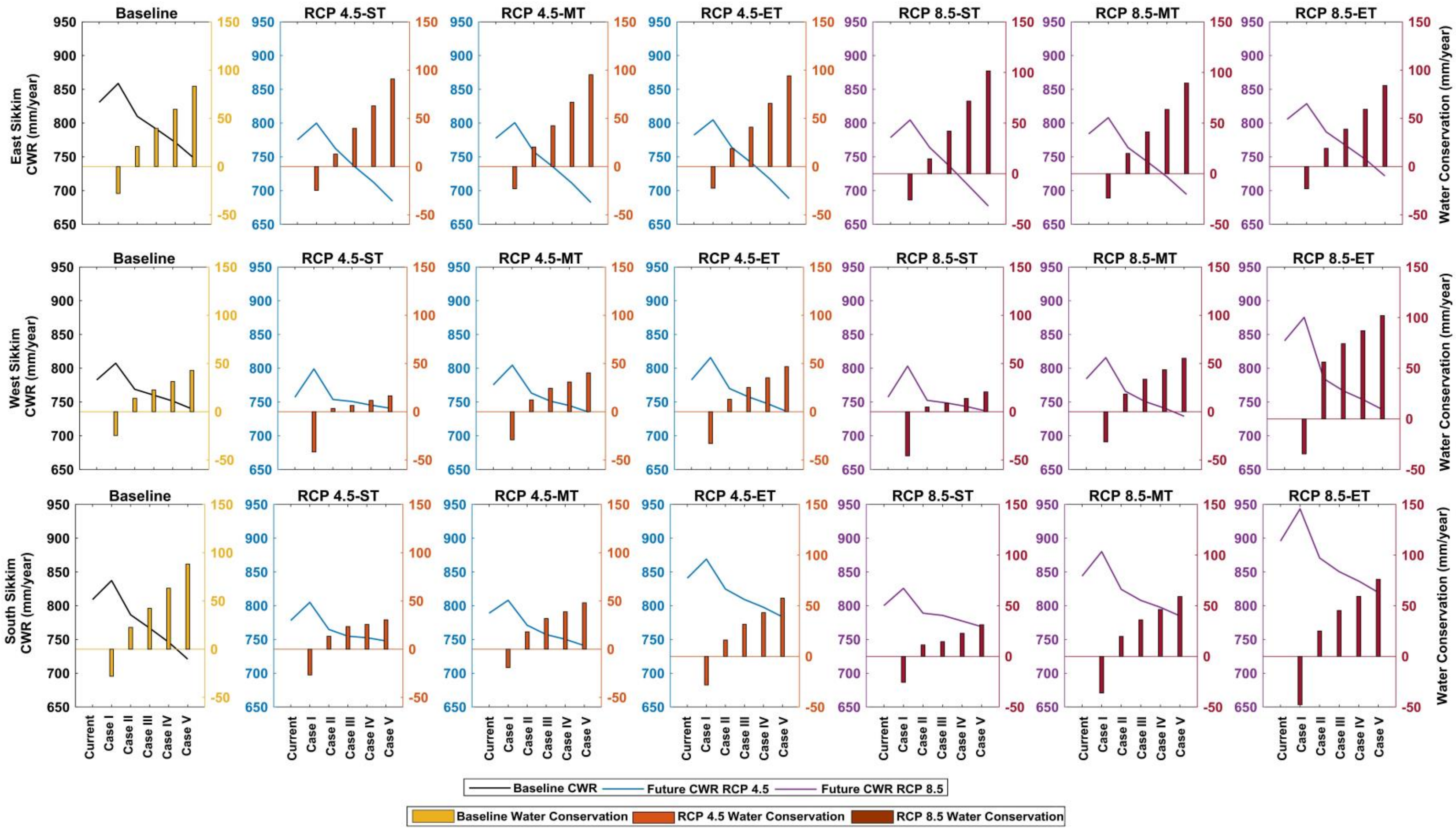

Figure 6.17b Sensitivity analysis on crop water requirement for different growing period of Rice.

6.4 Conclusion

The present study investigates the climate change implications on crop yield, CWR and CIR in three districts of Sikkim, namely East, West, and South Sikkim. Additionally, uncertainty analysis of both GCM as well as scenario is also carried by applying the possibility approach. The outcomes of the study are as follows:

- Significant increase in the crop yield for all the major crops for future scenarios.
- The reasons of the increase in the different crop yield can be attributed to the suitable temperature profile, increase in the CO_2 concentration, high elevation of the study area, and no significant water stress during the growing seasons of different crops.
- The future projection of regional CWR in the total growth stage of maize, wheat, and rice is likely to decrease over East Sikkim. On the other hand, CWR (except for maize in West Sikkim) over West and South Sikkim has shown an increasing trend during 2021-2099.
- The future trend of CIR of wheat and rice show a significant increasing trend in West and South Sikkim, whereas, over East Sikkim CIR is likely to decrease for wheat and increase for rice.
- It is noted that shifting growth period may reduce CWR in the study region.
- The uncertainty analysis reveals that the stabilized scenario pathway, i.e., RCP 4.5, is identified as the most possible scenario for the regional climate change impact assessment on CWR and CIR in our study area.

The outcomes from the study will provide a framework for the agricultural and water engineering over Sikkim for effective management of water resources for sustainable agriculture. Adaptation of different cropping pattern is necessary to combat climate change.

Chapter 7

Conclusions and scope for future work

7.1 Summary

The present study has been performed to deliver a comprehensive assessment of meteorological, hydrological, and agricultural drought conditions over India. In India, drought risk is greater due to unusually high temperatures, unfavorable meteorological conditions, and unfortunate monsoon. The complexity of the drought phenomenon, intricate ecosystem-drought interactions, and interdependence of the drought characteristics make the drought assessment a challenging task. In addition to traditional droughts, flash droughts are newly discovered extreme events that have rapid intensification without sufficient early warning. Such flash droughts pose a great threat to terrestrial ecosystems**.** The ecosystem resistance and adaptation to flash drought are significantly dependent upon the accurate estimation of flash drought events and their interaction with ecosystem metrics. Therefore, in context of climate change, a better understanding of the droughts in terms of their occurrence, trend, concurrence, evolution as well as joint dependence of drought characteristics is necessary to further evaluate the implications for the terrestrial ecosystem. The following paragraphs give a summary and conclusions of the study presented in the thesis.

Drought is a slowly growing, multivariate and complex phenomenon; therefore, it is important to recognize the drought from several perceptions such as severity, trends, distribution, duration as well as their complex interaction. In general, droughts are categorized into three categories i.e., meteorological, hydrological, and agricultural droughts. The present study further classified the agricultural drought into soil moisture drought and vegetation drought. The categorization is done because analyzing soil moisture and vegetation drought individually is better rather than a multivariate drought index, because the former gives a more detailed view on changes in environment variables than the latter one. The characterization of meteorological, hydrological, soil moisture, and vegetation droughts over different river basins of India using multi-perspectives such as occurrence, distribution, trend, concurrence, and evolution is investigated. The investigation is carried out using most widely used drought indices to monitor different drought types. The results show that hydrological and soil moisture droughts were observed to be more influential as compared to the meteorological and vegetation droughts in most of the river basins of India. Further, approximately 82% of concurrent droughts include soil moisture drought. This suggests that the soil moisture is more influencing rather than precipitation in the study area. This study facilitates to examine drought from various perspectives over all major river basins of India, and provides crucial inputs for local developing drought mitigation strategies and measures.

The above paragraph represents the outputs of the investigation based on univariate analysis of drought characteristics. As discussed in Chapter 4, the joint dependence of drought characteristics might not be suitably determined using the existing univariate approaches. Drought is a multivariate phenomenon, therefore, modeling the drought characteristics such as duration and severity through multivariate technique is more suitable. However, most of the multivariate techniques are derived from univariate ones and suffer from several disadvantages. To overcome such limitations, Copula is a useful tool to model multivariate distribution among random variables. In view of this, we used a bivariate copula-based approach to understand the joint dependence of drought characteristics for meteorological, hydrological, and agricultural droughts. It was observed that Southern India has a higher lower return period and higher exceedance probability as compared to Western river basins of India. Such results indicates that the drought events in Western and Central India are longer and more severe while the drought events in the southern river basins of the country are more frequent but less severe. This study provides information about the severe and longer drought event hotspots all over the study area and thus helpful for the policymakers in developing effective drought prevention and mitigation strategies.

The above two paragraphs present the outputs of the investigations based on conventional/traditional drought analysis. However, recent findings have revealed a new kind of rapidly growing drought termed as “flash drought”. It is a recently identified extreme event characterized by its sudden onset and rapid intensification. Due to rapid intensification and high evapotranspiration (ET), flash drought causes quick soil moisture depletion and poses a great threat to the terrestrial ecosystem. In view of this, the rapid intensification approach is employed to quantify the impact of flash droughts over terrestrial ecosystem in all 24 major river basins of India. Gross primary productivity (GPP) from MODIS was used to quantify the response of the ecosystem to flash droughts. It was observed that GPP responds to more than 95% of the flash droughts across India, with the highest response frequency occurring over Ganga basin and southern India while the lowest response across northeastern India. The discrepancies in the response frequency are majorly attributed to different vegetation resilience conditions across different parts of the country. Severe reduction in water use efficiency (WUE) was observed for the Ganga river basin and some parts of southern India, which highlighted the non-resilient nature of ecosystem towards rapid soil moisture variations. This study facilitates the identification of flash drought hotspots in the country and the ability of ecosystem to withstand such drastic conditions. These findings highlight the need to adopt essential drought mitigation measures to safeguard the sustainability of ecosystems.

Due to the climate change, the agricultural and socio-economical development over eastern Himalayan region of India is greatly affected. In view of this, the last chapter of the thesis presents a case study quantifying the impact of climate change on crop productivity and crop water requirement (CWR). Food and Agriculture Organization (FAO) developed Aquacrop model and Cropwat software are employed to investigate the climate change impact on regional crop yield, crop water requirement (CWR), and crop irrigation requirement (CIR) of major crops (maize, wheat, and rice) over a Himalayan state, i.e., Sikkim. The future projections of different crop yields and CWR are obtained by using bias-corrected climate scenarios from four different Global Climate Models (GCMs) under two different emission scenarios RCP 4.5 and RCP 8.5. From the investigation, an increase in the mean percentage change in the crop yield was observed over Sikkim during 2021 2099. This can be attributed to the suitable temperature profile, increase in the CO2 concentration, high elevation of the study area. The CWR and CIR investigation suggests an increase in the CWR towards the end of the twenty-first century for rice and wheat over West and South Sikkim with respect to the baseline period. This study facilitates the water and agricultural manager for considering suitable and robust adaptation measures to ensure sustainability.

7.2 Limitations of the study

The limitations of the study are as follows:

- The current study performed the characterization of major drought types, however, there is a lack of integration with crop production, which could be crucial for the food security of the country.
- Instead of the availability of multivariate copulas, the present study uses only bivariate copulas to estimate the joint dependence of drought characteristics. However, in the present analysis, we have considered only two major drought characteristics, which can be increased in future analysis, for example, drought frequency.
- Flash drought analysis is carried out using only soil moisture percentile datasets, however, evapotranspiration anomalies and

temperature anomalies datasets could also be crucial for comparative analysis.

- However, the present study used satellite-based soil moisture datasets which may be insufficient in incorporating real-time conditions, therefore, it is suggested to perform hydrological modeling to simulate soil moisture datasets in order to obtain better results in future studies.
- Also, the role of human influences such as changing cropping patterns, irrigation, and management activities has not been considered which can be incorporated.

7.3 Future scope of work

As discussed earlier, the present research is devoted to occurrence, distribution, concurrence, and evolution of droughts over India. However, there are many challenges that still exist in the field of drought assessment. Hence, the following would be possible future works.

- The drought evolution analysis is done to identify evolution of drought from one type to another type. A more comprehensive analysis of drought evolution may be carried out using the cross-correlation technique and find out the time lag in drought transformation. Further, it is suggested to use weekly or bi-weekly datasets instead of monthly datasets to have comprehensive view on drought evolution.

- The dependence structure of drought characteristics is estimated using bivariate Copula models. Instead of using bivariate, other multivariate Copulas may be utilised in future studies to model the joint dependence of more than two drought characteristics.

- Flash drought identification and its impact on the terrestrial ecosystems is investigated using gross primary productivity (GPP) as a terrestrial ecosystem indicator. However, the future study can use net primary productivity (NPP) and leaf area index (LAI) along with GPP for comparative analysis. Moreover, the future study can investigate flash drought risk and its underlying drivers in a changing climate.

- The simulation of crop yield is carried out using only changes in the climatic data and CO_2 concentration. Future studies can incorporate local experimental field data for more accurate yield simulations.

REFERENCES

AghaKouchak, A., 2015. A multivariate approach for persistence-based drought prediction: Application to the 2010-2011 East Africa drought. J. Hydrol. 526, 127–135. https://doi.org/10.1016/j.jhydrol.2014.09.063

AghaKouchak, A., Mirchi, A., Madani, K., Di Baldassarre, G., Nazemi, A., Alborzi, A., Anjileli, H., Azarderakhsh, M., Chiang, F., Hassanzadeh, E., Huning, L.S., Mallakpour, I., Martinez, A., Mazdiyasni, O., Moftakhari, H., Norouzi, H., Sadegh, M., Sadeqi, D., Van Loon, A.F., Wanders, N., 2021. Anthropogenic Drought: Definition, Challenges, and Opportunities. Rev. Geophys. 59. https://doi.org/10.1029/2019RG000683

Ahmed, K., Shahid, S., Nawaz, N., 2018. Impacts of climate variability and change on seasonal drought characteristics of Pakistan. Atmos. Res. 214, 364–374. https://doi.org/10.1016/j.atmosres.2018.08.020

Allen, R.G., Pereira, L.S., Raes, D., Smith, M., 1998. Crop evapotranspiration-Guidelines for computing crop water requirements-FAO Irrigation and drainage paper 56. Fao, Rome 300, D05109.

Amrit, K., Pandey, R.P., Mishra, S.K., Kumre, S.K., 2018. Long-Term Meteorological Drought Characteristics in Southern India, in: World Environmental and Water Resources Congress 2018. Minneapolis, Minnesota.

Anav, A., Friedlingstein, P., Beer, C., Ciais, P., Harper, A., Jones, C., Murray-Tortarolo, G., Papale, D., Parazoo, N.C., Peylin, P., Piao, S., Sitch, S., Viovy, N., Wiltshire, A., Zhao, M., 2015. Spatiotemporal patterns of terrestrial gross primary production: A review. Rev. Geophys. 53, 785–818. https://doi.org/10.1002/2015RG000483

Andarzian, Bahram, Hoogenboom, G., Bannayan, M., Shirali, M., Andarzian, Behnam, 2015. Determining optimum sowing date of wheat using CSM-CERES-Wheat model. J. Saudi Soc. Agric. Sci. 14, 189–199. https://doi.org/10.1016/j.jssas.2014.04.004

Annual-Report-2013-2014, 2016. Annual Report 2013-14, Ministry of Water Resources, River Development and Ganga Rejuvenation,.

Asoka, A., Gleeson, T., Wada, Y., Mishra, V., 2017. Relative contribution of monsoon precipitation and pumping to changes in groundwater storage in India. Nat. Geosci. 10, 109–117. https://doi.org/10.1038/ngeo2869

Ault, T.R., 2020. On the essentials of drought in a changing climate. Science (80-.). 368, 256–260. https://doi.org/10.1126/science.aaz5492

Baker, J.T., Allen, L.H., 1993. Contrasting crop species responses to CO2 and temperature: rice, soybean and citrus. Vegetatio 104–105, 239–260. https://doi.org/10.1007/BF00048156

Basara, J.B., Christian, J.I., Wakefield, R.A., Otkin, J.A., Hunt, E.H., Brown, D.P., 2019. The evolution, propagation, and spread of flash drought in the Central United States during 2012. Environ. Res. Lett. 14. https://doi.org/10.1088/1748-9326/ab2cc0

Basnet, B.., Avasthe, R.., Bhutia, K.., 2003. PRESENT STATUS OF MAIZE CULTIVATION IN SIKKIM AND FUTURE STRATEGIES. ENVIS Bull. Ecol. 11(1) 17–25.

Beer, C., Reichstein, M., Tomelleri, E., Ciais, P., Jung, M., Carvalhais, N., Rodenbeck, C., Arain, M.A., Baldocchi, D., Bonan, G.B., Bondeau, A., Cescatti, A., Lasslop, G., Lindroth, A., Lomas, M., Luyssaert, S., Margolis, H., Oleson, K.W., Roupsard, O., Veenendaal, E., Viovy, N., Williams, C., Woodward, F.I., Papale, D., 2010. Terrestrial Gross Carbon Dioxide Uptake: Global Distribution and Covariation with Climate. Science (80-.). 329, 834–838.

https://doi.org/10.1126/science.1184984

Beer, M., Ferson, S., Kreinovich, V., 2013. Imprecise probabilities in engineering analyses. Mech. Syst. Signal Process. 37, 4–29. https://doi.org/10.1016/j.ymssp.2013.01.024

Bergman, A., 1988. SRI International, in progress.

Bhatt, D., Maskey, S., Babel, M.S., Uhlenbrook, S., Prasad, K.C., 2014. Climate trends and impacts on crop production in the Koshi River basin of Nepal. Reg. Environ. Chang. 14, 1291–1301. https://doi.org/10.1007/s10113-013-0576-6

Bhuiyan, C., Singh, R.P., Kogan, F.N., 2006. Monitoring drought dynamics in the Aravalli region (India) using different indices based on ground and remote sensing data. Int. J. Appl. Earth Obs. Geoinf. 8, 289–302. https://doi.org/10.1016/j.jag.2006.03.002

Bisht, D.S., Sridhar, V., Mishra, A., Chatterjee, C., Raghuwanshi, N.S., 2019. Drought characterization over India under projected climate scenario. Int. J. Climatol. 39, 1889–1911. https://doi.org/10.1002/joc.5922

Block, P.J., Souza Filho, F.A., Sun, L., Kwon, H.-H., 2009. A Streamflow Forecasting Framework using Multiple Climate and Hydrological Models. JAWRA J. Am. Water Resour. Assoc. 45, 828–843. https://doi.org/10.1111/j.1752-1688.2009.00327.x

BOOTE, K.J., ALLEN, L.H., PRASAD, P.V. V., BAKER, J.T., GESCH, R.W., SNYDER, A.M., PAN, D., THOMAS, J.M.G., 2005. Elevated Temperature and CO_2 Impacts on Pollination, Reproductive Growth, and Yield of Several Globally Important Crops. J. Agric. Meteorol. 60, 469–474. https://doi.org/10.2480/agrmet.469

Bracken, C., Holman, K.D., Rajagopalan, B., Moradkhani, H., 2018. A Bayesian Hierarchical Approach to Multivariate Nonstationary Hydrologic Frequency Analysis. Water Resour. Res. 54, 243–255.

https://doi.org/10.1002/2017WR020403

Cao, M., Woodward, F.I., 1998. Dynamic responses of terrestrial ecosystem carbon cycling to global climate change. Nature 393, 249–252. https://doi.org/10.1038/30460

Chang, T.J., Stenson, J.R., 1990. Is It Realistic To Define a 100-Year Drought for Water Management? JAWRA J. Am. Water Resour. Assoc 26, 823–829.

Chen, F., Crow, W.T., Colliander, A., Cosh, M.H., Jackson, T.J., Bindlish, R., Reichle, R.H., Chan, S.K., Bosch, D.D., Starks, P.J., 2016. Application of triple collocation in ground-based validation of Soil Moisture Active/Passive (SMAP) level 2 data products. IEEE J. Sel. Top. Appl. Earth Obs. Remote Sens. 10, 489–502.

Chen, H., Sun, J., 2017. Characterizing present and future drought changes over eastern China. Int. J. Climatol. 37, 138–156. https://doi.org/10.1002/joc.4987

Chen, L., Singh, V.P., Guo, S., Mishra, A.K., Guo, J., 2013. Drought Analysis Using Copulas. J. Hydrol. Eng. 18, 797–808. https://doi.org/10.1061/(ASCE)HE.1943-5584.0000697

Chen, L.G., Gottschalck, J., Hartman, A., Miskus, D., Tinker, R., Artusa, A., 2019. Flash Drought Characteristics Based on U.S. Drought Monitor. Atmosphere (Basel). 10, 498. https://doi.org/10.3390/atmos10090498

Chen, Y.D., Zhang, Q., Xiao, M., Singh, V.P., Zhang, S., 2016. Probabilistic forecasting of seasonal droughts in the Pearl River basin, China. Stoch. Environ. Res. Risk Assess. 30, 2031–2040. https://doi.org/10.1007/s00477-015-1174-6

Cheng, L., Zhang, L., Wang, Y.-P., Canadell, J.G., Chiew, F.H.S., Beringer, J., Li, L., Miralles, D.G., Piao, S., Zhang, Y., 2017. Recent increases in terrestrial carbon uptake at little cost to the water cycle. Nat.

Commun. 8, 110. https://doi.org/10.1038/s41467-017-00114-5

Chiou, S.C., Tsay, R.S., 2008. A Copula-based Approach to Option Pricing and Risk Assessment. J. Data Sci. 6, 273–301.

Christian, J.I., Basara, J.B., Hunt, E.D., Otkin, J.A., Xiao, X., 2020. Flash drought development and cascading impacts associated with the 2010 Russian heatwave. Environ. Res. Lett. 15, 094078. https://doi.org/10.1088/1748-9326/ab9faf

Christian, J.I., Basara, J.B., Otkin, J.A., Hunt, E.D., 2019. Regional characteristics of flash droughts across the United States. Environ. Res. Commun. 1, 125004. https://doi.org/10.1088/2515-7620/ab50ca

Clark, M.P., Wilby, R.L., Gutmann, E.D., Vano, J.A., Gangopadhyay, S., Wood, A.W., Fowler, H.J., Prudhomme, C., Arnold, J.R., Brekke, L.D., 2016. Characterizing Uncertainty of the Hydrologic Impacts of Climate Change. Curr. Clim. Chang. Reports 2, 55–64. https://doi.org/10.1007/s40641-016-0034-x

Clausen, B., Pearson, C.P., 1995. Regional frequency analysis of annual maximum streamflow drought. J. Hydrol. 173, 111–130. https://doi.org/10.1016/0022-1694(95)02713-Y

Confalonieri, R., Bellocchi, G., Bregaglio, S., Donatelli, M., Acutis, M., 2010. Comparison of sensitivity analysis techniques: A case study with the rice model WARM. Ecol. Modell. 221, 1897–1906. https://doi.org/10.1016/j.ecolmodel.2010.04.021

Cong, R., Brady, M., 2012. The cientific WorldJOURNAL The Interdependence between Rainfall and Temperature : Copula Analyses 2012. https://doi.org/10.1100/2012/405675

Crausbay, S.D., Ramirez, A.R., Carter, S.L., Cross, M.S., Hall, K.R., Bathke, D.J., Betancourt, J.L., Colt, S., Cravens, A.E., Dalton, M.S., Dunham, J.B., Hay, L.E., Hayes, M.J., McEvoy, J., McNutt, C.A., Moritz, M.A., Nislow, K.H., Raheem, N., Sanford, T., 2017. Defining

Ecological Drought for the Twenty-First Century. Bull. Am. Meteorol. Soc. 98, 2543–2550. https://doi.org/10.1175/BAMS-D-16-0292.1

Crawford, A.J., McLachlan, D.H., Hetherington, A.M., Franklin, K.A., 2012. High temperature exposure increases plant cooling capacity. Curr. Biol. 22, R396–R397. https://doi.org/10.1016/j.cub.2012.03.044

Dai, A., 2013. Increasing drought under global warming in observations and models. Nat. Clim. Chang. 3, 52–58. https://doi.org/10.1038/nclimate1633

Dai, A., 2011. Drought under global warming: A review. Wiley Interdiscip. Rev. Clim. Chang. 2, 45–65. https://doi.org/10.1002/wcc.81

Daly, E., Porporato, A., Rodriguez-Iturbe, I., 2004. Coupled Dynamics of Photosynthesis, Transpiration, and Soil Water Balance. Part I: Upscaling from Hourly to Daily Level. J. Hydrometeorol. 5, 546–558. https://doi.org/10.1175/1525-7541(2004)005<0546:CDOPTA>2.0.CO;2

Das, J., Jha, S., Goyal, M.K., 2020a. Non-stationary and copula-based approach to assess the drought characteristics encompassing climate indices over the Himalayan states in India. J. Hydrol. 580, 124356. https://doi.org/10.1016/j.jhydrol.2019.124356

Das, J., Poonia, V., Jha, S., Goyal, M.K., 2020b. Understanding the climate change impact on crop yield over Eastern Himalayan Region: ascertaining GCM and scenario uncertainty. Theor. Appl. Climatol. 142, 467–482. https://doi.org/10.1007/s00704-020-03332-y

Das, J., Treesa, A., Umamahesh, N. V., 2018. Modelling Impacts of Climate Change on a River Basin: Analysis of Uncertainty Using REA & Possibilistic Approach. Water Resour. Manag. 32, 4833–4852. https://doi.org/10.1007/s11269-018-2046-x

Das, J., Umamahesh, N. V., 2018. Assessment of uncertainty in estimating future flood return levels under climate change. Nat. Hazards 1–16.

https://doi.org/10.1007/s11069-018-3291-2

Das, J., Umamahesh, N. V., 2017. Uncertainty and Nonstationarity in Streamflow Extremes under Climate Change Scenarios over a River Basin. J. Hydrol. Eng. 22, 04017042. https://doi.org/10.1061/(ASCE)HE.1943-5584.0001571

Das, R., Das, P.K., Bandyopadhyay, S., Raj, U., 2019. Trends and Vulnerability Assessment of Meteorological and Agricultural Drought Conditions Over Indian Region Using Time-Series (1982–2015) Satellite Data. ISPRS - Int. Arch. Photogramm. Remote Sens. Spat. Inf. Sci. XLII-3/W6, 453–459. https://doi.org/10.5194/isprs-archives-xlii-3-w6-453-2019

Dastane, N.G., 1974. Effective rainfall in irrigated agriculture. FAO.

De Michele, C., Salvadori, G., 2003. A Generalized Pareto intensity-duration model of storm rainfall exploiting 2-Copulas. J. Geophys. Res. D Atmos. 108, 1–11. https://doi.org/10.1029/2002jd002534

De Silva, C.S., Weatherhead, E.K., Knox, J.W., Rodriguez-Diaz, J.A., 2007. Predicting the impacts of climate change—A case study of paddy irrigation water requirements in Sri Lanka. Agric. Water Manag. 93, 19–29. https://doi.org/10.1016/j.agwat.2007.06.003

Deb, P., Shrestha, S., Babel, M.S., 2015. Forecasting climate change impacts and evaluation of adaptation options for maize cropping in the hilly terrain of Himalayas: Sikkim, India. Theor. Appl. Climatol. 121, 649–667. https://doi.org/10.1007/s00704-014-1262-4

Doorenbos, J., Pruitt, W.O., 1977. Crop water requirements. FAO irrigation and drainage paper 24. L. Water Dev. Div. FAO, Rome 144.

Dracup, J.A., Lee, K.S., Paulson, E.G., Jr., 1980. On the definition of droughts. Water Resour. Res. 16(2).

Droogers, P., 2004. Adaptation to climate change to enhance food security and preserve environmental quality: example for southern Sri Lanka. Agric. Water Manag. 66, 15–33. https://doi.org/10.1016/j.agwat.2003.09.005

Dubey, S.K., Sharma, D., 2018. Assessment of climate change impact on yield of major crops in the Banas River Basin, India. Sci. Total Environ. 635, 10–19. https://doi.org/10.1016/j.scitotenv.2018.03.343

Emura, T., Chen, Y.-H., 2018. Analysis of Survival Data with Dependent Censoring: Copula-based Approaches. Springer.

Eyshi Rezaei, E., Webber, H., Gaiser, T., Naab, J., Ewert, F., 2015. Heat stress in cereals: Mechanisms and modelling. Eur. J. Agron. 64, 98–113. https://doi.org/10.1016/j.eja.2014.10.003

FAO, 2016. The State of Food and Agriculture: Climate Change, Agriculture and Food Security.

FAO, 2008. The State of Food Insecurity in the World: High Food Prices and Food Security- Threats and Opportunities.

Favre, A.C., Adlouni, S. El, Perreault, L., Thiémonge, N., Bobée, B., 2004. Multivariate hydrological frequency analysis using copulas. Water Resour. Res. 40, 1–12. https://doi.org/10.1029/2003WR002456

Flack-Prain, S., Meir, P., Malhi, Y., Smallman, T.L., Williams, M., 2019. The importance of physiological, structural and trait responses to drought stress in driving spatial and temporal variation in GPP across Amazon forests. Biogeosciences 16, 4463–4484. https://doi.org/10.5194/bg-16-4463-2019

Fooladmand, H.R., Ahmadi, S.H., 2009. Monthly spatial calibration of Blaney-Criddle equation for calculating monthly ET o in south of Iran. Irrig. Drain. 58, 234–245. https://doi.org/10.1002/ird.409

Ford, T.W., Labosier, C.F., 2017. Meteorological conditions associated with the onset of flash drought in the Eastern United States. Agric. For.

Meteorol. 247, 414–423. https://doi.org/10.1016/j.agrformet.2017.08.031

Gadgil, Sulochana, Gadgil, Siddhartha, 2006. The Indian monsoon, GDP and agriculture. Econ. Polit. Wkly. 41, 4887–4895.

Gang, C., Wang, Z., Chen, Y., Yang, Y., Li, J., Cheng, J., Qi, J., Odeh, I., 2016. Drought-induced dynamics of carbon and water use efficiency of global grasslands from 2000 to 2011. Ecol. Indic. 67, 788–797. https://doi.org/10.1016/j.ecolind.2016.03.049

Ganguli, P., Reddy, M.J., 2014. Evaluation of trends and multivariate frequency analysis of droughts in three meteorological subdivisions of western India. Int. J. Climatol. 34, 911–928. https://doi.org/10.1002/joc.3742

Ganguli, P., Reddy, M.J., 2012. Risk Assessment of Droughts in Gujarat Using Bivariate Copulas. Water Resour. Manag. 26, 3301–3327. https://doi.org/10.1007/s11269-012-0073-6

Gerken, T., Bromley, G.T., Ruddell, B.L., Williams, S., Stoy, P.C., 2018. Convective suppression before and during the United States Northern Great Plains flash drought of 2017. Hydrol. Earth Syst. Sci. 22, 4155–4163. https://doi.org/10.5194/hess-22-4155-2018

Goldstein, J., Mirza, M., Etkin, D., Milton, J., 2003. J2. 6 hydrologic assessment: Application of extreme value theory for climate extremes scenarios construction, in: 14th Symposium on Global Change and Climate Variations, American Meteorological Society 83rd Annual Meeting.

Gómez, M., Concepción Ausín, M., Carmen Domínguez, M., 2017. Seasonal copula models for the analysis of glacier discharge at King George Island, Antarctica. Stoch. Environ. Res. Risk Assess. 31, 1107–1121. https://doi.org/10.1007/s00477-016-1217-7

Goswami, U.P., Bhargav, K., Hazra, B., Goyal, M.K., 2018a.

Spatiotemporal and joint probability behavior of temperature extremes over the Himalayan region under changing climate. Theor. Appl. Climatol. 134, 477–498. https://doi.org/10.1007/s00704-017-2288-1

Goswami, U.P., Hazra, B., Goyal, M.K., 2018b. Copula-based probabilistic characterization of precipitation extremes over North Sikkim Himalaya. Atmos. Res. 212, 273–284. https://doi.org/10.1016/j.atmosres.2018.05.019

Government of Sikkim, 2013. Annual Progress Report.

Goyal, M.K., Gupta, V., Eslamian, S., 2017. Hydrological drought: Water surface and duration curve indices. Handb. Drought Water Scarcity Princ. Drought Water Scarcity 45–72. https://doi.org/10.1201/9781315404219

Goyal, M.K., Sharma, A., 2016. A fuzzy c-means approach regionalization for analysis of meteorological drought homogeneous regions in western India. Nat. Hazards 84, 1831–1847. https://doi.org/10.1007/s11069-016-2520-9

Grimaldi, S., Serinaldi, F., 2006. Asymmetric copula in multivariate flood frequency analysis. Adv. Water Resour. 29, 1155–1167. https://doi.org/10.1016/j.advwatres.2005.09.005

Grossiord, C., Buckley, T.N., Cernusak, L.A., Novick, K.A., Poulter, B., Siegwolf, R.T.W., Sperry, J.S., McDowell, N.G., 2020. Plant responses to rising vapor pressure deficit. New Phytol. 226, 1550–1566. https://doi.org/10.1111/nph.16485

Gruber, A., Su, C.-H., Zwieback, S., Crow, W., Dorigo, W., Wagner, W., 2016. Recent advances in (soil moisture) triple collocation analysis. Int. J. Appl. Earth Obs. Geoinf. 45, 200–211.

Guo, L., Sun, F., Liu, W., Zhang, Y., Wang, Hong, Cui, H., Wang, Hongquan, Zhang, J., Du, B., 2019. Response of Ecosystem Water Use Efficiency to Drought over China during 1982–2015: Spatiotemporal

Variability and Resilience. Forests 10, 598. https://doi.org/10.3390/f10070598

Hagman, G., Wijkman, A., Bendz, M., Beer, H., 1984. Prevention Better Than Cure: Report on Human and Environmental Disasters in the Third World. Swedish Red Cross.

Hao, Z., AghaKouchak, A., 2013. Multivariate Standardized Drought Index: A parametric multi-index model. Adv. Water Resour. 57, 12–18. https://doi.org/10.1016/j.advwatres.2013.03.009

Hao, Z., AghaKouchak, A., Nakhjiri, N., Farahmand, A., 2014. Global integrated drought monitoring and prediction system. Sci. data 1, 140001. https://doi.org/10.1038/sdata.2014.1

Hayes, M.J., 2006. Drought Indices. Van Nostrand's Sci. Encycl. 1–13. https://doi.org/10.1002/0471743984.vse8593

Hayes, M.J., Svoboda, M.D., Wardlow, B.D., Anderson, M.C., Kogan, F., 2012. Drought monitoring: Historical and current perspectives. Remote Sens. Drought Innov. Monit. Approaches 1–19. https://doi.org/10.1201/b11863

Hisdal, H., Tallaksen, L.M., 2000. Assessment of the Regional Impact of Droughts in Europe. Assess. Reg. Impact Droughts Eurrope 41.

Hobaek, H., Frigessi, A., Maraun, D., 2015. How well do regional climate models simulate the spatial dependence of precipitation? An application of pair-copula constructions. J. Geophys. Res. Atmos. 120, 2624–2646.

Hodges, K.I., Lee, R.W., Bengtsson, L., 2011. A comparison of extratropical cyclones in recent reanalyses ERA-Interim, NASA MERRA, NCEP CFSR, and JRA-25. J. Clim. 24, 4888–4906. https://doi.org/10.1175/2011JCLI4097.1

Hoerling, M., Eischeid, J., Kumar, A., Leung, R., Mariotti, A., Mo, K., Schubert, S., Seager, R., 2014. Causes and Predictability of the 2012 Great Plains Drought. Bull. Am. Meteorol. Soc. 95, 269–282. https://doi.org/10.1175/BAMS-D-13-00055.1

Hofer, E., 1999. Sensitivity analysis in the context of uncertainty analysis for computationally intensive models. Comput. Phys. Commun. 117, 21–34. https://doi.org/10.1016/S0010-4655(98)00153-2

Höllermann, B., Evers, M., 2017. Perception and handling of uncertainties in water management—A study of practitioners' and scientists' perspectives on uncertainty in their daily decision-making. Environ. Sci. Policy 71, 9–18. https://doi.org/10.1016/j.envsci.2017.02.003

Huang, L., He, B., Han, L., Liu, J., Wang, H., Chen, Z., 2017. A global examination of the response of ecosystem water-use efficiency to drought based on MODIS data. Sci. Total Environ. 601–602, 1097–1107. https://doi.org/10.1016/j.scitotenv.2017.05.084

IPCC, 2014. Climate Change 2014 Synthesis Report Summary Chapter for Policymakers. Cambridge Univ Press.

IPCC, 2013. Climate Change 2013 - The Physical Science Basis. Contribution of Working Group I to the Fifth Assessment Report of the Intergovernmental Panel on Climate Change. Cambridge University Press, Cambridge. https://doi.org/10.1017/CBO9781107415324

Island, G., 2016. Seasonal copula models for the analysis of glacier discharge. https://doi.org/10.1007/s00477-016-1217-7

Iyengar, S.G., Varshney, P.K., Damarla, T., 2009. A parametric copula based framework for multimodal signal processing, in: Acoustics, Speech and Signal Processing, 2009. ICASSP 2009. IEEE International Conference On. IEEE, pp. 1893–1896.

Jain, V.K., Pandey, R.P., Jain, M.K., Byun, H.R., 2015. Comparison of drought indices for appraisal of drought characteristics in the Ken

River Basin. Weather Clim. Extrem. 8, 1–11. https://doi.org/10.1016/j.wace.2015.05.002

Jamieson, P.D., Porter, J.R., Wilson, D.R., 1991. A test of the computer simulation model ARCWHEAT1 on wheat crops grown in New Zealand. F. Crop. Res. 27, 337–350. https://doi.org/10.1016/0378-4290(91)90040-3

Jha, S., Das, J., Sharma, A., Hazra, B., Goyal, M.K., 2019a. Probabilistic evaluation of vegetation drought likelihood and its implications to resilience across India. Glob. Planet. Change 176, 23–35. https://doi.org/10.1016/j.gloplacha.2019.01.014

Jhong, B.-C., Tung, C.-P., 2018. Evaluating Future Joint Probability of Precipitation Extremes with a Copula-Based Assessing Approach in Climate Change. Water Resour. Manag. 32, 4253–4274.

Johnson, F., Sharma, A., 2011. Accounting for interannual variability: A comparison of options for water resources climate change impact assessments. Water Resour. Res. 47. https://doi.org/10.1029/2010WR009272

Johnston, A.S.A., Meade, A., Ardö, J., Arriga, N., Black, A., Blanken, P.D., Bonal, D., Brümmer, C., Cescatti, A., Dušek, J., Graf, A., Gioli, B., Goded, I., Gough, C.M., Ikawa, H., Jassal, R., Kobayashi, H., Magliulo, V., Manca, G., Montagnani, L., Moyano, F.E., Olesen, J.E., Sachs, T., Shao, C., Tagesson, T., Wohlfahrt, G., Wolf, S., Woodgate, W., Varlagin, A., Venditti, C., 2021. Temperature thresholds of ecosystem respiration at a global scale. Nat. Ecol. Evol. 5, 487–494. https://doi.org/10.1038/s41559-021-01398-z

Joshi, N., Gupta, D., Suryavanshi, S., Adamowski, J., Madramootoo, C.A., 2016. Analysis of trends and dominant periodicities in drought variables in India: A wavelet transform based approach. Atmos. Res. 182, 200–220. https://doi.org/10.1016/j.atmosres.2016.07.030

Kao, S., Govindaraju, R.S., 2010. A copula-based joint deficit index for droughts. J. Hydrol. 380, 121–134.

Kapoor, D., Bhardwaj, S., Landi, M., Sharma, Arti, Ramakrishnan, M., Sharma, Anket, 2020. The Impact of Drought in Plant Metabolism: How to Exploit Tolerance Mechanisms to Increase Crop Production. Appl. Sci. 10, 5692. https://doi.org/10.3390/app10165692

Keyantash, J., Dracup, J.A., 2002. The quantification of drought: An evaluation of drought indices. Bull. Am. Meteorol. Soc. 83, 1167–1180. https://doi.org/10.1175/1520-0477(2002)083<1191:TQODAE>2.3.CO;2

Kimball, B.A., 1983. Carbon Dioxide and Agricultural Yield: An Assemblage and Analysis of 430 Prior Observations1. Agron. J. 75, 779. https://doi.org/10.2134/agronj1983.00021962007500050014x

Kogan, F.N., 1995. Application of vegetation index and brightness temperature for drought detection. Adv. Sp. Res. 15, 91–100. https://doi.org/10.1016/0273-1177(95)00079-T

Kumar, N., Poonia, V., Gupta, B.B., Goyal, M.K., 2021. A novel framework for risk assessment and resilience of critical infrastructure towards climate change. Technol. Forecast. Soc. Change 165, 120532. https://doi.org/10.1016/j.techfore.2020.120532

Lasmar, N., Berthoumieu, Y., 2014. Gaussian Copula Multivariate Modeling for Texture 23, 2246–2261.

Lee, J.-H., Park, S.-Y., Kim, J.-S., Sur, C., Chen, J., 2018. Extreme drought hotspot analysis for adaptation to a changing climate: Assessment of applicability to the five major river basins of the Korean Peninsula. Int. J. Climatol. 38, 4025–4032. https://doi.org/10.1002/joc.5532

Lee, T., Modarres, R., Ouarda, T.B.M.J., 2013. Data-based analysis of bivariate copula tail dependence for drought duration and severity. Hydrol. Process. 27, 1454–1463.

Leng, G.Y., Tang, Q.H., Huang, M.Y., Hong, Y., Ruby, L.L., 2015. Projected changes in mean and interannual variability of surface water over continental China. Sci. China Earth Sci. 58, 739–754. https://doi.org/10.1007/s11430-014-4987-0

Lin, B.B., 2011. Resilience in Agriculture through Crop Diversification: Adaptive Management for Environmental Change. Bioscience 61, 183–193. https://doi.org/10.1525/bio.2011.61.3.4

Lin, R., Zhou, T., Qian, Y., 2014. Evaluation of global monsoon precipitation changes based on five reanalysis datasets. J. Clim. 27, 1271–1289. https://doi.org/10.1175/JCLI-D-13-00215.1

Liu, Q., Yang, Z., 2010. Quantitative estimation of the impact of climate change on actual evapotranspiration in the Yellow River Basin, China. J. Hydrol. 395, 226–234. https://doi.org/10.1016/j.jhydrol.2010.10.031

Liu, Y., Xiao, J., Ju, W., Zhou, Y., Wang, S., Wu, X., 2015. Water use efficiency of China's terrestrial ecosystems and responses to drought. Sci. Rep. 5, 13799. https://doi.org/10.1038/srep13799

Liu, Y., Zhu, Y., Zhang, L., Ren, L., Yuan, F., Yang, X., Jiang, S., 2020. Flash droughts characterization over China: From a perspective of the rapid intensification rate. Sci. Total Environ. 704, 135373. https://doi.org/10.1016/j.scitotenv.2019.135373

Lloyd-Hughes, B., Saunders, M.A., 2002. A drought climatology for Europe. Int. J. Climatol. 22, 1571–1592. https://doi.org/10.1002/joc.846

Lobell, D.B., Burke, M.B., Tebaldi, C., Mastrandrea, M.D., Falcon, W.P., Naylor, R.L., 2008. Prioritizing Climate Change Adaptation Needs for Food Security in 2030. Science (80-.). 319, 607–610. https://doi.org/10.1126/science.1152339

Lobell, David B., Gourdji, S.M., 2012. The Influence of Climate Change on

Global Crop Productivity. Plant Physiol. 160, 1686–1697. https://doi.org/10.1104/pp.112.208298

Lobell, D. B., Gourdji, S.M., 2012. The Influence of Climate Change on Global Crop Productivity. Plant Physiol. 160, 1686–1697. https://doi.org/10.1104/pp.112.208298

Lobell, D.B., Schlenker, W., Costa-Roberts, J., 2011. Climate Trends and Global Crop Production Since 1980. Science (80-.). 333, 616–620. https://doi.org/10.1126/science.1204531

Ma, J., Jia, X., Zha, T., Bourque, C.P.-A., Tian, Y., Bai, Y., Liu, P., Yang, R., Li, Cheng, Li, Chunyi, Xie, J., Yu, H., Zhang, F., Zhou, C., 2019. Ecosystem water use efficiency in a young plantation in Northern China and its relationship to drought. Agric. For. Meteorol. 275, 1–10. https://doi.org/10.1016/j.agrformet.2019.05.004

Mall, R.K., Gupta, A., Sonkar, G., 2017. Effect of Climate Change on Agricultural Crops, in: Current Developments in Biotechnology and Bioengineering. Elsevier, pp. 23–46. https://doi.org/10.1016/B978-0-444-63661-4.00002-5

Mallya, G., Mishra, V., Niyogi, D., Tripathi, S., Govindaraju, R.S., 2015. Trends and variability of droughts over the Indian monsoon region. Weather Clim. Extrem. 12, 43–68. https://doi.org/10.1016/j.wace.2016.01.002

Mann, H.B., 1945. Non-Parametric Test Against Trend. Econometrica 13, 245–259.

Massmann, A., Gentine, P., Lin, C., 2019. When Does Vapor Pressure Deficit Drive or Reduce Evapotranspiration? J. Adv. Model. Earth Syst. 11, 3305–3320. https://doi.org/10.1029/2019MS001790

McColl, K.A., Vogelzang, J., Konings, A.G., Entekhabi, D., Piles, M., Stoffelen, A., 2014. Extended triple collocation: Estimating errors and correlation coefficients with respect to an unknown target. Geophys.

Res. Lett. 41, 6229–6236.

McKee, T.B., Doesken, N.J., Kleist, J., 1993. The relationship of drought frequency and duration to time scales, in: Proceedings of the 8th Conference on Applied Climatology,Vol. 17. American Meteorological Society, Boston, MA, USA. pp. 179–184.

Michele, C. De, Salvadori, G., 2003. A Generalized Pareto intensity-duration model of storm rainfall exploiting 2-Copulas 108, 1–11. https://doi.org/10.1029/2002JD002534

Mishra, A. & Liu, S.C., 2014. Changes in precipitation pattern and risk of drought over India in the context of global warming. J. Geophys. Res-Atmos.

Mishra, A., Singh, V., 2010. A Review of Drought Concepts. J. Hydrol. 391, 202–216. https://doi.org/10.1016/j.jhydrol.2010.07.012

Mishra, A.K., Desai, V.R., 2005. Drought forecasting using stochastic models. Stoch. Environ. Res. Risk Assess. 19, 326–339. https://doi.org/10.1007/s00477-005-0238-4

Mishra, A.K., Singh, V.P., 2011. Drought modeling – A review. J. Hydrol. 403, 157–175. https://doi.org/10.1016/j.jhydrol.2011.03.049

Mishra, A.K., Singh, V.P., Desai, V.R., 2009. Drought characterization: A probabilistic approach. Stoch. Environ. Res. Risk Assess. 23, 41–55. https://doi.org/10.1007/s00477-007-0194-2

Mishra, V., Aadhar, S., Asoka, A., Pai, S., Kumar, R., 2016. On the frequency of the 2015 monsoon season drought in the Indo-Gangetic Plain. Geophys. Res. Lett. 43, 12,102-12,112. https://doi.org/10.1002/2016GL071407

Mishra, V., Aadhar, S., Mahto, S.S., 2021. Anthropogenic warming and intraseasonal summer monsoon variability amplify the risk of future flash droughts in India. npj Clim. Atmos. Sci. 4, 1.

https://doi.org/10.1038/s41612-020-00158-3

Mishra, V., Cherkauer, K.A., 2010. Retrospective droughts in the crop growing season: Implications to corn and soybean yield in the Midwestern United States. Agric. For. Meteorol. 150, 1030–1045. https://doi.org/10.1016/j.agrformet.2010.04.002

Mishra, V., Shah, R., Thrasher, B., 2014. Soil moisture droughts under the retrospective and projected climate in India. J. Hydrometeorol. 15, 2267–2292. https://doi.org/10.1175/JHM-D-13-0177.1

Mo, K.C., 2011. Drought onset and recovery over the United States. J. Geophys. Res. 116, D20106. https://doi.org/10.1029/2011JD016168

Mo, K.C., Lettenmaier, D.P., 2016. Precipitation Deficit Flash Droughts over the United States. J. Hydrometeorol. 17, 1169–1184. https://doi.org/10.1175/JHM-D-15-0158.1

Mo, K.C., Lettenmaier, D.P., 2015. Heat wave flash droughts in decline. Geophys. Res. Lett. 42, 2823–2829. https://doi.org/10.1002/2015GL064018

Molod, A., Takacs, L., Suarez, M., Bacmeister, J., 2015. Development of the GEOS-5 atmospheric general circulation model: Evolution from MERRA to MERRA2. Geosci. Model Dev. 8, 1339–1356. https://doi.org/10.5194/gmd-8-1339-2015

Mu, Q., Zhao, M., Running, S.W., 2011. Evolution of hydrological and carbon cycles under a changing climate. Hydrol. Process. 25, 4093–4102. https://doi.org/10.1002/hyp.8367

Muhammad, W., Muhammad, S., Khan, N.M., Si, C., 2020. Hydrological drought indexing approach in response to climate and anthropogenic activities. Theor. Appl. Climatol. 141, 1401–1413. https://doi.org/10.1007/s00704-020-03227-y

Mujumdar, P.P., Ghosh, S., 2008. Modeling GCM and scenario uncertainty using a possibilistic approach: Application to the Mahanadi River, India. Water Resour. Res. 44. https://doi.org/10.1029/2007WR006137

Mundetia, N., Sharma, D., 2014. Analysis of rainfall and drought in Rajasthan state, India. Glob. Nest J. 17, 12–21. https://doi.org/10.30955/gnj.001379

Nabaei, S., Sharafati, A., Yaseen, Z.M., Shahid, S., 2019. Copula based assessment of meteorological drought characteristics: Regional investigation of Iran. Agric. For. Meteorol. 276–277, 107611. https://doi.org/10.1016/j.agrformet.2019.06.010

Nagarajan, R., 2003. Drought: Assessment, Monitoring, Management and Resources Conservation. Cap. Publ. Company, New Delhi.

Nam, W.-H., Hayes, M.J., Svoboda, M.D., Tadesse, T., Wilhite, D.A., 2015. Drought hazard assessment in the context of climate change for South Korea. Agric. Water Manag. 160, 106–117. https://doi.org/10.1016/j.agwat.2015.06.029

National Weather Service, 2006. Drought: Public Fact Sheet.

Naumann, G., Alfieri, L., Wyser, K., Mentaschi, L., Betts, R.A., Carrao, H., Spinoni, J., Vogt, J., Feyen, L., 2018. Global Changes in Drought Conditions Under Different Levels of Warming. Geophys. Res. Lett. 45, 3285–3296. https://doi.org/10.1002/2017GL076521

Naveau, P., Nogaj, M., Ammann, C., Yiou, P., Cooley, D., Jomelli, V., 2005. Statistical methods for the analysis of climate extremes. Comptes Rendus Geosci. 337, 1013–1022.

Ning, C., 2010. Dependence structure between the equity market and the foreign exchange market–a copula approach. J. Int. Money Financ. 29, 743–759.

Niranjan Kumar, K., Rajeevan, M., Pai, D.S., Srivastava, A.K., Preethi, B., 2013. On the observed variability of monsoon droughts over India.

Weather Clim. Extrem. 1, 42–50. https://doi.org/10.1016/j.wace.2013.07.006

Niu, J., Chen, J., Sun, L., Sivakumar, B., 2018. Time-lag effects of vegetation responses to soil moisture evolution: a case study in the Xijiang basin in South China. Stoch. Environ. Res. Risk Assess. 32, 2423–2432. https://doi.org/10.1007/s00477-017-1492-y

Otkin, J.A., Anderson, M.C., Hain, C., Mladenova, I.E., Basara, J.B., Svoboda, M., 2013. Examining rapid onset drought development using the thermal infrared-based evaporative stress index. J. Hydrometeorol. 14, 1057–1074. https://doi.org/10.1175/JHM-D-12-0144.1

Otkin, J.A., Anderson, M.C., Hain, C., Svoboda, M., Johnson, D., Mueller, R., Tadesse, T., Wardlow, B., Brown, J., 2016. Assessing the evolution of soil moisture and vegetation conditions during the 2012 United States flash drought. Agric. For. Meteorol. 218–219, 230–242. https://doi.org/10.1016/j.agrformet.2015.12.065

Otkin, J.A., Shafer, M., Svoboda, M., Wardlow, B., Anderson, M.C., Hain, C., Basara, J., 2015. Facilitating the Use of Drought Early Warning Information through Interactions with Agricultural Stakeholders. Bull. Am. Meteorol. Soc. 96, 1073–1078. https://doi.org/10.1175/BAMS-D-14-00219.1

Otkin, J.A., Svoboda, M., Hunt, E.D., Ford, T.W., Anderson, M.C., Hain, C., Basara, J.B., 2018. Flash droughts: A review and assessment of the challenges imposed by rapid-onset droughts in the United States. Bull. Am. Meteorol. Soc. 99, 911–919. https://doi.org/10.1175/BAMS-D-17-0149.1

Pai, D.S., Guhathakurta, P., Kulkarni, A., Rajeevan, M.N., 2017. Variability of Meteorological Droughts Over India. pp. 73–87. https://doi.org/10.1007/978-981-10-2531-0_5

Pai, D.S., Sridhar, L., Rajeevan, M., Sreejith, O.P., Satbhai, N.S., Mukhopadhyay, B., 2014. (1901-2010) daily gridded rainfall data set over India and its comparison with existing data sets over the region. Mausam 1, 1–18.

Panu, U.S., Sharma, T.C., 2009. Analysis of annual hydrological droughts: The case of northwest Ontario, Canada. Hydrol. Sci. J. 54, 29–42. https://doi.org/10.1623/hysj.54.1.29

Pathak, A.A., Dodamani, B.M., 2019. Trend Analysis of Groundwater Levels and Assessment of Regional Groundwater Drought: Ghataprabha River Basin, India. Nat. Resour. Res. 28, 631–643. https://doi.org/10.1007/s11053-018-9417-0

Paul, S., Ghosh, S., Oglesby, R., Pathak, A., Chandrasekharan, A., Ramsankaran, R., 2016. Weakening of Indian Summer Monsoon Rainfall due to Changes in Land Use Land Cover. Sci. Rep. 6, 32177. https://doi.org/10.1038/srep32177

Pendergrass, A.G., Meehl, G.A., Pulwarty, R., Hobbins, M., Hoell, A., AghaKouchak, A., Bonfils, C.J.W., Gallant, A.J.E., Hoerling, M., Hoffmann, D., Kaatz, L., Lehner, F., Llewellyn, D., Mote, P., Neale, R.B., Overpeck, J.T., Sheffield, A., Stahl, K., Svoboda, M., Wheeler, M.C., Wood, A.W., Woodhouse, C.A., 2020. Flash droughts present a new challenge for subseasonal-to-seasonal prediction. Nat. Clim. Chang. 10, 191–199. https://doi.org/10.1038/s41558-020-0709-0

Peng, S., Huang, J., Sheehy, J.E., Laza, R.C., Visperas, R.M., Zhong, X., Centeno, G.S., Khush, G.S., Cassman, K.G., 2004. Rice yields decline with higher night temperature from global warming. Proc. Natl. Acad. Sci. 101, 9971–9975. https://doi.org/10.1073/pnas.0403720101

Pereira, L.S., Allen, R.G., Smith, M., Raes, D., 2015. Crop evapotranspiration estimation with FAO56: Past and future. Agric. Water Manag. 147, 4–20. https://doi.org/10.1016/j.agwat.2014.07.031

Pingale, S.M., Khare, D., Jat, M.K., Adamowski, J., 2014. Spatial and temporal trends of mean and extreme rainfall and temperature for the 33 urban centers of the arid and semi-arid state of Rajasthan, India. Atmos. Res. 138, 73–90. https://doi.org/10.1016/j.atmosres.2013.10.024

Porter, J.R., Gawith, M., 1999. Temperatures and the growth and development of wheat: A review. Eur. J. Agron. 10, 23–36. https://doi.org/10.1016/S1161-0301(98)00047-1

Prasad, P.V. V., Pisipati, S.R., Ristic, Z., Bukovnik, U., Fritz, A.K., 2008. Impact of Nighttime Temperature on Physiology and Growth of Spring Wheat. Crop Sci. 48, 2372. https://doi.org/10.2135/cropsci2007.12.0717

Raes, D., Steduto, P., Hsiao, T.C., Fereres, E., 2009. AquaCropThe FAO Crop Model to Simulate Yield Response to Water: II. Main Algorithms and Software Description. Agron. J. 101, 438. https://doi.org/10.2134/agronj2008.0140s

Ray, D.K., Mueller, N.D., West, P.C., Foley, J.A., 2013. Yield Trends Are Insufficient to Double Global Crop Production by 2050. PLoS One 8, e66428. https://doi.org/10.1371/journal.pone.0066428

Reddy, M. Janga, Ganguli, P., 2013. Spatio-temporal analysis and derivation of copula-based intensity-area-frequency curves for droughts in western Rajasthan (India). Stoch. Environ. Res. Risk Assess. 27, 1975–1989. https://doi.org/10.1007/s00477-013-0732-z

Reichstein, M., Ciais, P., Papale, D., Valentini, R., Running, S., VIOVY, N., CRAMER, W., Granier, A., Ogee, J., Allard, V., Aubinet, M., Bernhofer, C., Buchmann, N., Carrara, A., Grunwald, T., Heimann, M., Heinesch, B., Knohl, A., Kutsch, W., Loustau, D., Manca, G., Matteucci, G., Miglietta, F., Ourcival, J.M., Pilegaard, K., Pumpanen, J., Rambal, S., Schaphoff, S., Seufert, G., Soussana, J.-F., Sanz, M.-J., Vesala, T., Zhao, M., 2007. Reduction of ecosystem productivity and respiration during the European summer 2003 climate anomaly: a joint flux tower, remote sensing and modelling analysis. Glob. Chang. Biol. 13, 634–651. https://doi.org/10.1111/j.1365-2486.2006.01224.x

Renard, B., Lang, M., 2007. Use of a Gaussian copula for multivariate extreme value analysis: Some case studies in hydrology. Adv. Water Resour. 30, 897–912. https://doi.org/10.1016/j.advwatres.2006.08.001

Riahi, K., Rao, S., Krey, V., Cho, C., Chirkov, V., Fischer, G., Kindermann, G., Nakicenovic, N., Rafaj, P., 2011. RCP 8.5—A scenario of comparatively high greenhouse gas emissions. Clim. Change 109, 33–57. https://doi.org/10.1007/s10584-011-0149-y

Ribeiro, A.F.S., Russo, A., Gouveia, C.M., Pires, C.A.L., 2020. Drought-related hot summers: A joint probability analysis in the Iberian Peninsula. Weather Clim. Extrem. 30. https://doi.org/10.1016/j.wace.2020.100279

Rojas, R., Feyen, L., Dosio, A., Bavera, D., 2011. Improving pan-European hydrological simulation of extreme events through statistical bias correction of RCM-driven climate simulations. Hydrol. Earth Syst. Sci. 15, 2599–2620. https://doi.org/10.5194/hess-15-2599-2011

Running, S.W., Nemani, R.R., Heinsch, F.A., Zhao, M., Reeves, M., Hashimoto, H., H., 2004. A continuous satellite-derived measure of global terrestrial primary production. Biosci. · 54, 547–560.

Russo, S., Sillmann, J., Fischer, E.M., 2015. Top ten European heatwaves since 1950 and their occurrence in the coming decades. Environ. Res. Lett. 10, 124003.

Sadegh, M., Ragno, E., AghaKouchak, A., 2017. Multivariate Copula Analysis Toolbox (MvCAT): Describing dependence and underlying uncertainty using a Bayesian framework. Water Resour. Res. 53, 5166–5183.

Sahana, V., Sreekumar, P., Mondal, A., Rajsekhar, D., 2020. On the rarity of the 2015 drought in India: A country-wide drought atlas using the multivariate standardized drought index and copula-based severity-duration-frequency curves. J. Hydrol. Reg. Stud. 31, 100727. https://doi.org/10.1016/j.ejrh.2020.100727

Saltelli, A., Tarantola, S., Campolongo, F., 2000. Sensitivity Anaysis as an Ingredient of Modeling. Stat. Sci. 15, 377–395. https://doi.org/10.1214/ss/1009213004

Salvadori, G., De Michele, C., 2004. Frequency analysis via copulas: Theoretical aspects and applications to hydrological events. Water Resour. Res. 40, 1–17. https://doi.org/10.1029/2004WR003133

Sánchez, B., Rasmussen, A., Porter, J.R., 2014. Temperatures and the growth and development of maize and rice: a review. Glob. Chang. Biol. 20, 408–417. https://doi.org/10.1111/gcb.12389

Sankarganesh, E., Firake, D.M., Sharma, B., Verma, V.K., Behere, G.T., 2017. Invasion of the South American Tomato Pinworm, Tuta absoluta, in northeastern India: a new challenge and biosecurity concerns. Entomol. Gen. 36, 335–345. https://doi.org/10.1127/entomologia/2017/0489

Schlenker, W., Roberts, M.J., 2009. Nonlinear temperature effects indicate severe damages to U.S. crop yields under climate change. Proc. Natl. Acad. Sci. 106, 15594–15598. https://doi.org/10.1073/pnas.0906865106

Sen, P.K., 1968. Estimates of the Regression Coefficient Based on Kendall’s Tau. J. Am. Stat. Assoc. 63, 1379–1389. https://doi.org/10.1080/01621459.1968.10480934

Shafer, B.A., Dezman, L.E., 1982. Development of a surface water supply index (SWSI) to assess the severity of drought conditions in snowpack runoff areas. Proc. West. Snow Conf. Fort Collins, CO Color. State Univ. 50, 164–175.

Shah, R., Mishra, V., 2014. Evaluation of the Reanalysis Products for the Monsoon Season Droughts in India. J. Hydrometeorol. 15, 1575–1591. https://doi.org/10.1175/jhm-d-13-0103.1

Sharma, A., Goyal, M.K., 2018a. Assessment of ecosystem resilience to hydroclimatic disturbances in India. Glob. Chang. Biol. 24, e432–e441. https://doi.org/10.1111/gcb.13874

Sharma, A., Goyal, M.K., 2018b. District-level assessment of the ecohydrological resilience to hydroclimatic disturbances and its controlling factors in India. J. Hydrol. 564, 1048–1057. https://doi.org/10.1016/j.jhydrol.2018.07.079

Shen, Y., Li, S., Chen, Y., Qi, Y., Zhang, S., 2013. Estimation of regional irrigation water requirement and water supply risk in the arid region of Northwestern China 1989–2010. Agric. Water Manag. 128, 55–64. https://doi.org/10.1016/j.agwat.2013.06.014

Shiau, J.T., 2006. Fitting drought duration and severity with two-dimensional copulas. Water Resour. Manag. 20, 795–815. https://doi.org/10.1007/s11269-005-9008-9

Shiau, J.T., Shen, H.W., 2001. Recurrence analysis of hydrologic droughts of differing severity. J Water Resour Plan Manag. ASCE 127(1), 30–40.

Shivam, G., Goyal, M.K., Sarma, A.K., 2019. Index-based study of future precipitation changes over subansiri river catchment under changing climate. J. Environ. Informatics 34, 1–14. https://doi.org/10.3808/jei.201700376

Shrestha, S., Gyawali, B., Bhattarai, U., 2013. Impacts of climate change on irrigation water requirements for rice–wheat cultivation in Bagmati River Basin, Nepal. J. Water Clim. Chang. 4, 422–439. https://doi.org/10.2166/wcc.2013.050

Shukla, S., Wood, A.W., 2008. Use of a standardized runoff index for characterizing hydrologic drought. Geophys. Res. Lett. 35, 1–7. https://doi.org/10.1029/2007GL032487

Sivakumar, M.V.K., 2013. Weather and Climate Extremes: Need for and importance of the journal. Weather Clim. Extrem. 1, 1–3. https://doi.org/10.1016/j.wace.2013.08.002

Sklar, A., 1959. Fonctions de reprtition a n dimensions et leursmarges. Publ. Inst. Stat. Univ. Paris 8, 229–231.

Smith, M., 1992. CROPWAT: A computer program for irrigation planning and management. Food & Agriculture Org.

Smith, M., 1991. CROPWAT: Manual and guidelines. FAO UN, Rome, Italy.

Smith, M., Kivumbi, D., Heng, L.K., 2002. Use of the FAO CROPWAT model in deficit irrigation studies, in: Deficit Irrigation Practices.

Soľáková, T., De Michele, C., Vezzoli, R., 2014. Comparison between Parametric and Nonparametric Approaches for the Calculation of Two Drought Indices: SPI and SSI. J. Hydrol. Eng. 19, 04014010. https://doi.org/10.1061/(asce)he.1943-5584.0000942

Song, Q.-H., Fei, X.-H., Zhang, Y.-P., Sha, L.-Q., Liu, Y.-T., Zhou, W.-J., Wu, C.-S., Lu, Z.-Y., Luo, K., Gao, J.-B., Liu, Y.-H., 2017. Water use efficiency in a primary subtropical evergreen forest in Southwest China. Sci. Rep. 7, 43031. https://doi.org/10.1038/srep43031

Song, X., Song, S., Li, Z., Liu, W., Li, J., Kang, Y., Sun, W., 2018. Past and future changes in regional crop water requirements in Northwest China. Theor. Appl. Climatol. 137, 2203–2215. https://doi.org/10.1007/s00704-018-2739-3

Spinoni, J., Vogt, J. V., Naumann, G., Barbosa, P., Dosio, A., 2018. Will drought events become more frequent and severe in Europe? Int. J. Climatol. 38, 1718–1736. https://doi.org/10.1002/joc.5291

Spott, M., 1999. A theory of possibility distributions. Fuzzy Sets Syst. 102, 135–155. https://doi.org/10.1016/S0165-0114(97)00102-4

Sraj, M., Bezak, N., Brilly, M., 2015. Bivariate flood frequency analysis using the copula function: A case study of the Litija station on the Sava River. Hydrol. Process. 29, 225–238. https://doi.org/10.1002/hyp.10145

Stagge, J.H., Kohn, I., Tallaksen, L.M., Stahl, K., 2015. Modeling drought impact occurrence based on meteorological drought indices in Europe. J. Hydrol. 530, 37–50. https://doi.org/10.1016/j.jhydrol.2015.09.039

Steduto, P., Hsiao, T.C., Raes, D., Fereres, E., 2009. AquaCrop—The FAO Crop Model to Simulate Yield Response to Water: I. Concepts and Underlying Principles. Agron. J. 101, 426. https://doi.org/10.2134/agronj2008.0139s

Stocker, B.D., Zscheischler, J., Keenan, T.F., Prentice, I.C., Peñuelas, J., Seneviratne, S.I., 2018. Quantifying soil moisture impacts on light use efficiency across biomes. New Phytol. 218, 1430–1449. https://doi.org/10.1111/nph.15123

Stoffelen, A., 1998. Toward the true near-surface wind speed: Error modeling and calibration using triple collocation. J. Geophys. Res. Ocean. 103, 7755–7766.

Subash, N., Ram Mohan, H.S., 2011. Trend detection in rainfall and evaluation of standardized precipitation index as a drought assessment index for rice-wheat productivity over IGR in India. Int. J. Climatol. 31, 1694–1709. https://doi.org/10.1002/joc.2188

Subash, N., Sikka, A.K., 2014. Trend analysis of rainfall and temperature and its relationship over India. Theor. Appl. Climatol. 117, 449–462. https://doi.org/10.1007/s00704-013-1015-9

Sumanta Das, M.R.C.N., 2013. Geospatial Assessment of Agricultural Drought. Ijasr 3, 1–28.

Svoboda, M., LeComte, D., Hayes, M., Heim, R., Gleason, K., Angel, J., Rippey, B., Tinker, R., Palecki, M., Stooksbury, D., Miskus, D., Stephens, S., 2002. The drought monitor. Bull. Am. Meteorol. Soc. 83, 1181–1190. https://doi.org/10.1175/1520-0477(2002)083<1181:TDM>2.3.CO;2

Tam, B.Y., Szeto, K., Bonsal, B., Flato, G., Cannon, A.J., Rong, R., 2019. CMIP5 drought projections in Canada based on the Standardized Precipitation Evapotranspiration Index. Can. Water Resour. J. / Rev. Can. des ressources hydriques 44, 90–107. https://doi.org/10.1080/07011784.2018.1537812

Tan, X., Gan, T.Y., 2015. Contribution of human and climate change impacts to changes in streamflow of Canada. Sci. Rep. 5, 1–10. https://doi.org/10.1038/srep17767

Tao, F., Yokozawa, M., Hayashi, Y., Lin, E., 2003. Future climate change, the agricultural water cycle, and agricultural production in China. Agric. Ecosyst. Environ. 95, 203–215. https://doi.org/10.1016/S0167-8809(02)00093-2

Telwala, Y., Brook, B.W., Manish, K., Pandit, M.K., 2013. Climate-Induced Elevational Range Shifts and Increase in Plant Species Richness in a Himalayan Biodiversity Epicentre. PLoS One 8, e57103. https://doi.org/10.1371/journal.pone.0057103

Teutschbein, C., Seibert, J., 2012. Bias correction of regional climate model simulations for hydrological climate-change impact studies: Review and evaluation of different methods. J. Hydrol. 456–457, 12–29. https://doi.org/10.1016/j.jhydrol.2012.05.052

Thilakarathne, M., Sridhar, V., 2017. Characterization of future drought conditions in the Lower Mekong River Basin. Weather Clim. Extrem. 17, 47–58. https://doi.org/10.1016/j.wace.2017.07.004

Thomas, T., Nayak, P.C., Ghosh, N.C., 2015. Spatiotemporal analysis of drought characteristics in the bundelkhand region of Central India using the standardized precipitation index. J. Hydrol. Eng 1943–5584.

Thomey, M.L., Collins, S.L., Vargas, R., Johnson, J.E., Brown, R.F., Natvig, D.O., Friggens, M.T., 2011. Effect of precipitation variability on net primary production and soil respiration in a Chihuahuan Desert grassland. Glob. Chang. Biol. 17, 1505–1515. https://doi.org/10.1111/j.1365-2486.2010.02363.x

Thomson, A.M., Calvin, K. V., Smith, S.J., Kyle, G.P., Volke, A., Patel, P., Delgado-Arias, S., Bond-Lamberty, B., Wise, M.A., Clarke, L.E., Edmonds, J.A., 2011. RCP4.5: a pathway for stabilization of radiative forcing by 2100. Clim. Change 109, 77–94. https://doi.org/10.1007/s10584-011-0151-4

Todisco, F., Vergni, L., 2008. Climatic changes in Central Italy and their potential effects on corn water consumption. Agric. For. Meteorol. 148, 1–11. https://doi.org/10.1016/j.agrformet.2007.08.014

Trenberth, K.E., Dai, A., Van Der Schrier, G., Jones, P.D., Barichivich, J., Briffa, K.R., Sheffield, J., 2014. Global warming and changes in drought. Nat. Clim. Chang. 4, 17–22. https://doi.org/10.1038/nclimate2067

Trenberth, K.E., Houghton, J.T., Meira Filho, L.G., Callander, B.A., Harris, N., Kattenberg, A., Maskell, K., 1996. The climate system: An overview 51–64.

Tsakiris, G., Pangalou, P., 2009. Drought characterization in the Mediterranean, coping with drought risk in agriculture and water supply systems., in: Springer, New York.

Tubiello, F.N., Donatelli, M., Rosenzweig, C., Stockle, C.O., 2000. Effects of climate change and elevated CO2 on cropping systems: model predictions at two Italian locations. Eur. J. Agron. 13, 179–189. https://doi.org/10.1016/S1161-0301(00)00073-3

Tubiello, F.N., Ewert, F., 2002. Simulating the effects of elevated CO_2 on crops: Approaches and applications for climate change. Eur. J. Agron. 18, 57–74. https://doi.org/10.1016/S1161-0301(02)00097-7

Uttarwar, S.B., Barma, S.D., Mahesha, A., 2020. Bivariate Modeling of Hydroclimatic Variables in Humid Tropical Coastal Region Using Archimedean Copulas. J. Hydrol. Eng. 25, 05020026. https://doi.org/10.1061/(ASCE)HE.1943-5584.0001981

van Oort, P.A.J., Zwart, S.J., 2018. Impacts of climate change on rice production in Africa and causes of simulated yield changes. Glob. Chang. Biol. 24, 1029–1045. https://doi.org/10.1111/gcb.13967

Vanuytrecht, E., Raes, D., Willems, P., 2014. Global sensitivity analysis of yield output from the water productivity model. Environ. Model. Softw. 51, 323–332. https://doi.org/10.1016/j.envsoft.2013.10.017

Vazifehkhah, S., Tosunoglu, F., Kahya, E., 2019. Bivariate Risk Analysis of Droughts Using a Nonparametric Multivariate Standardized Drought Index and Copulas. J. Hydrol. Eng. 24, 05019006. https://doi.org/10.1061/(asce)he.1943-5584.0001775

Vicente-Serrano, S.M., Gouveia, C., Camarero, J.J., Beguería, S., Trigo, R., López-Moreno, J.I., Azorín-Molina, C., Pasho, E., Lorenzo-Lacruz, J., Revuelto, J., Morán-Tejeda, E., Sanchez-Lorenzo, A., 2013. Response of vegetation to drought time-scales across global land biomes. Proc. Natl. Acad. Sci. U. S. A. 110, 52–57. https://doi.org/10.1073/pnas.1207068110

Vicente-Serrano, S.M., López-Moreno, J.I., Beguería, S., Lorenzo-Lacruz, J., Azorin-Molina, C., Morán-Tejeda, E., 2012. Accurate Computation of a Streamflow Drought Index. J. Hydrol. Eng. 17, 318–332. https://doi.org/10.1061/(asce)he.1943-5584.0000433

Wang, L., Yuan, X., Xie, Z., Wu, P., Li, Y., 2016. Increasing flash droughts over China during the recent global warming hiatus. Sci. Rep. 6, 30571. https://doi.org/10.1038/srep30571

Wang, X., Cai, J., Jiang, D., Liu, F., Dai, T., Cao, W., 2011. Pre-anthesis high-temperature acclimation alleviates damage to the flag leaf caused by post-anthesis heat stress in wheat. J. Plant Physiol. 168, 585–593. https://doi.org/10.1016/j.jplph.2010.09.016

Wilhite, D.A., 2000. Drought as a natural hazard: Concepts and definitions, in: Drought: A Global Assessment. pp. 3–18.

Winkelmann, R., 2012. Copula bivariate probit models: with an application to medical expenditures. Health Econ. 21, 1444–1455.

Wolf, S., Keenan, T.F., Fisher, J.B., Baldocchi, D.D., Desai, A.R., Richardson, A.D., Scott, R.L., Law, B.E., Litvak, M.E., Brunsell, N.A., Peters, W., van der Laan-Luijkx, I.T., 2016. Warm spring reduced carbon cycle impact of the 2012 US summer drought. Proc. Natl. Acad. Sci. 113, 5880–5885. https://doi.org/10.1073/pnas.1519620113

World Bank, 2003. Financing Rapid Onset Natural Disaster Losses in India : A Risk Management Approach. Rep. No. 26 844-IN 126.

Wu, Y., Liu, S., Qiu, L., Sun, Y., 2016. SWAT-DayCent coupler: An integration tool for simultaneous hydro-biogeochemical modeling using SWAT and DayCent. Environ. Model. Softw. 86, 81–90. https://doi.org/10.1016/j.envsoft.2016.09.015

Xiao, J., Sun, G., Chen, J., Chen, H., Chen, S., Dong, G., Gao, S., Guo, H., Guo, J., Han, S., Kato, T., Li, Y., Lin, G., Lu, W., Ma, M., McNulty, S., Shao, C., Wang, X., Xie, X., Zhang, X., Zhang, Z., Zhao, B., Zhou, G., Zhou, J., 2013. Carbon fluxes, evapotranspiration, and water use efficiency of terrestrial ecosystems in China. Agric. For. Meteorol. 182–183, 76–90. https://doi.org/10.1016/j.agrformet.2013.08.007

Xie, Z., Wang, L., Jia, B., Yuan, X., 2016. Measuring and modeling the impact of a severe drought on terrestrial ecosystem CO 2 and water fluxes in a subtropical forest. J. Geophys. Res. Biogeosciences 121, 2576–2587. https://doi.org/10.1002/2016JG003437

Xu, H., Wang, X., Zhao, C., Zhang, X., 2019. Responses of ecosystem water use efficiency to meteorological drought under different biomes and drought magnitudes in northern China. Agric. For. Meteorol. 278, 107660. https://doi.org/10.1016/j.agrformet.2019.107660

Xu, K., Yang, D., Xu, X., Lei, H., 2015. Copula based drought frequency analysis considering the spatio-temporal variability in Southwest China. J. Hydrol. 527, 630–640. https://doi.org/10.1016/j.jhydrol.2015.05.030

Yadav, R.R., Misra, K.G., Yadava, A.K., Kotlia, B.S., Misra, S., 2015. Tree-ring footprints of drought variability in last ~300 years over Kumaun Himalaya, India and its relationship with crop productivity. Quat. Sci. Rev. 117, 113–123. https://doi.org/10.1016/j.quascirev.2015.04.003

Yang, H., Wang, H., Fu, G., Yan, H., Zhao, P., Ma, M., 2017. A modified soil water deficit index (MSWDI) for agricultural drought monitoring: Case study of Songnen Plain, China. Agric. Water Manag. 194, 125–138. https://doi.org/10.1016/j.agwat.2017.07.022

Yao, N., Li, Y., Lei, T., Peng, L., 2018. Drought evolution, severity and trends in mainland China over 1961–2013. Sci. Total Environ. 616–617, 73–89. https://doi.org/10.1016/j.scitotenv.2017.10.327

Yevjevich, V., 1969. An objective approach to definitions and investigations of continental hydrologic droughts. J. Hydrol. 7, 353. https://doi.org/10.1016/0022-1694(69)90110-3

Yin, J., Guo, S., He, S., Guo, J., Hong, X., Liu, Z., 2018. A copula-based analysis of projected climate changes to bivariate flood quantiles. J. Hydrol. 566, 23–42.

Yuan, W., Cai, W., Chen, Y., Liu, Shuguang, Dong, W., Zhang, H., Yu, G., Chen, Z., He, H., Guo, W., Liu, D., Liu, Shaoming, Xiang, W., Xie, Z., Zhao, Z., Zhou, G., 2016. Severe summer heatwave and drought strongly reduced carbon uptake in Southern China. Sci. Rep. 6, 1–12. https://doi.org/10.1038/srep18813

Yuan, X., Ma, Z., Pan, M., Shi, C., 2015. Microwave remote sensing of short-term droughts during crop growing seasons. Geophys. Res. Lett. 42, 4394–4401. https://doi.org/10.1002/2015GL064125

Yuan, X., Wang, L., Wood, E.F., 2018. Anthropogenic intensification of southern African flash droughts as exemplified by the 2015/16 season. Bull. Am. Meteorol. Soc. 99, S86–S90. https://doi.org/10.1175/BAMS-D-17-0077.1

Yuan, X., Wang, L., Wu, P., Ji, P., Sheffield, J., Zhang, M., 2019. Anthropogenic shift towards higher risk of flash drought over China. Nat. Commun. 10, 1–8. https://doi.org/10.1038/s41467-019-12692-7

Yuan, X., Zhang, M., Wang, L., Zhou, T., 2017. Understanding and seasonal forecasting of hydrological drought in the Anthropocene. Hydrol. Earth Syst. Sci. 21, 5477–5492. https://doi.org/10.5194/hess-21-5477-2017

Yuan, X.C., Wei, Y.M., Wang, B., Mi, Z., 2017. Risk management of extreme events under climate change. J. Clean. Prod. 166, 1169–1174. https://doi.org/10.1016/j.jclepro.2017.07.209

Zadeh, L.A., 1999. Fuzzy sets as a basis for a theory of possibility. Fuzzy Sets Syst. 100, 9–34. https://doi.org/10.1016/S0165-0114(99)80004-9

Zaifoğlu, H., Akıntuğ, B., Yanmaz, A.M., 2017. Quality Control, Homogeneity Analysis, and Trends of Extreme Precipitation Indices in Northern Cyprus. J. Hydrol. Eng. 22, 05017024. https://doi.org/10.1061/(ASCE)HE.1943-5584.0001589

Zhang, L., Singh, V.P., 2007. Gumbel–Hougaard Copula for Trivariate Rainfall Frequency Analysis. J. Hydrol. Eng. 12, 409–419.

https://doi.org/10.1061/(ASCE)1084-0699(2007)12:4(409)

Zhang, M., Yuan, X., 2020. Rapid reduction in ecosystem productivity caused by flash droughts based on decade-long FLUXNET observations. Hydrol. Earth Syst. Sci. 24, 5579–5593. https://doi.org/10.5194/hess-24-5579-2020

Zhang, M., Yuan, X., Otkin, J.A., 2020. Remote sensing of the impact of flash drought events on terrestrial carbon dynamics over China. Carbon Balance Manag. 15, 20. https://doi.org/10.1186/s13021-020-00156-1

Zhang, Q., Li, J., Singh, V.P., Xu, C.Y., 2013. Copula-based spatio-temporal patterns of precipitation extremes in China. Int. J. Climatol. 33, 1140–1152. https://doi.org/10.1002/joc.3499

Zhang, Q., Singh, V.P., Li, J., Jiang, F., Bai, Y., 2012. Spatio-temporal variations of precipitation extremes in Xinjiang, China. J. Hydrol. 434–435, 7–18. https://doi.org/10.1016/j.jhydrol.2012.02.038

Zhang, Q., Zhang, J., 2016. Drought hazard assessment in typical corn cultivated areas of China at present and potential climate change. Nat. Hazards 81, 1323–1331. https://doi.org/10.1007/s11069-015-2137-4

Zhang, X., Obringer, R., Wei, C., Chen, N., Niyogi, D., 2017. Droughts in India from 1981 to 2013 and Implications to Wheat Production. Sci. Rep. 7, 1–12. https://doi.org/10.1038/srep44552

Zhao, A., Zhang, A., Cao, S., Liu, X., Liu, J., Cheng, D., 2018. Responses of vegetation productivity to multi-scale drought in Loess Plateau, China. Catena 163, 165–171. https://doi.org/10.1016/j.catena.2017.12.016

Zhao, C., Liu, B., Piao, S., Wang, X., Lobell, D.B., Huang, Y., Huang, M., Yao, Y., Bassu, S., Ciais, P., Durand, J.-L., Elliott, J., Ewert, F., Janssens, I.A., Li, T., Lin, E., Liu, Q., Martre, P., Müller, C., Peng, S., Peñuelas, J., Ruane, A.C., Wallach, D., Wang, T., Wu, D., Liu, Z., Zhu, Y., Zhu, Z., Asseng, S., 2017. Temperature increase reduces global yields of major crops in four independent estimates. Proc. Natl. Acad. Sci. 114, 9326–9331. https://doi.org/10.1073/pnas.1701762114

Zhao, F., Wu, Y., Yao, Y., Sun, K., Zhang, X., Winowiecki, L., Vågen, T.-G., Xu, J., Qiu, L., Sun, P., Sun, Y., 2020. Predicting the climate change impacts on water-carbon coupling cycles for a loess hilly-gully watershed. J. Hydrol. 581, 124388. https://doi.org/10.1016/j.jhydrol.2019.124388

Zhao, M., Huang, S., Huang, Q., Wang, H., Leng, G., Xie, Y., 2019. Assessing socio-economic drought evolution characteristics and their possible meteorological driving force. Geomatics, Nat. Hazards Risk 10, 1084–1101. https://doi.org/10.1080/19475705.2018.1564706

Zhao, M., Running, S.W., 2010. Drought-Induced Reduction in Global Terrestrial Net Primary Production from 2000 Through 2009. Science (80-.). 329, 940–943. https://doi.org/10.1126/science.1192666

Zhong, R., Chen, X., Lai, C., Wang, Z., Lian, Y., Yu, H., Wu, X., 2019. Drought monitoring utility of satellite-based precipitation products across mainland China. J. Hydrol. 568, 343–359. https://doi.org/10.1016/j.jhydrol.2018.10.072

Zhou, S., Yu, B., Huang, Y., Wang, G., 2014. The effect of vapor pressure deficit on water use efficiency at the subdaily time scale. Geophys. Res. Lett. 41, 5005–5013. https://doi.org/10.1002/2014GL060741

Zhou, T., Wu, P., Sun, S., Li, X., Wang, Y., Luan, X., 2017. Impact of Future Climate Change on Regional Crop Water Requirement—A Case Study of Hetao Irrigation District, China. Water 9, 429. https://doi.org/10.3390/w9060429

Ziolkowska, J., 2016. Socio-Economic Implications of Drought in the Agricultural Sector and the State Economy. Economies 4, 19. https://doi.org/10.3390/economies4030019